

Lam, Jenny Ka-Wing (2006) Phosphorylcholine-based copolymer as synthetic vector for gene delivery. PhD thesis, University of Nottingham.

**Access from the University of Nottingham repository:**

<http://eprints.nottingham.ac.uk/13171/1/436729.pdf>

**Copyright and reuse:**

The Nottingham ePrints service makes this work by researchers of the University of Nottingham available open access under the following conditions.

This article is made available under the University of Nottingham End User licence and may be reused according to the conditions of the licence. For more details see:  
[http://eprints.nottingham.ac.uk/end\\_user\\_agreement.pdf](http://eprints.nottingham.ac.uk/end_user_agreement.pdf)

**A note on versions:**

The version presented here may differ from the published version or from the version of record. If you wish to cite this item you are advised to consult the publisher's version. Please see the repository url above for details on accessing the published version and note that access may require a subscription.

For more information, please contact [eprints@nottingham.ac.uk](mailto:eprints@nottingham.ac.uk)

**GEORGE GREEN LIBRARY OF  
SCIENCE AND ENGINEERING**

**PHOSPHORYLCHOLINE – BASED COPOLYMER  
AS SYNTHETIC VECTOR FOR GENE DELIVERY**

**Jenny Ka-Wing Lam MPharm (Hon), MRPharmS**



**The University of  
Nottingham**

**School of Pharmacy**

**The University of Nottingham**

**Thesis submitted to the University of Nottingham**

**For the degree of Doctor of Philosophy**

**2006**

---

## TABLES OF CONTENTS

Abstract	vii
Abbreviations	ix
Acknowledgements	xi
List of figures	xii
List of tables	xvii

## CHAPTER 1

### INTRODUCTION

<b>1.1</b>	<b>Basic Concepts of Gene Therapy</b>	<b>1</b>
<b>1.2</b>	<b>Gene Therapy Clinical Trials</b>	<b>3</b>
<b>1.3</b>	<b>Methods of Gene Delivery</b>	<b>5</b>
1.3.1	Viral Vectors	5
1.3.2	Non-viral Vectors	7
1.3.2.1	Naked DNA	8
1.3.2.2	Liposomes	9
1.3.2.3	Cationic Polymers	11
<b>1.4</b>	<b>Barriers to Non-viral Gene Delivery System</b>	<b>16</b>
1.4.1	Physical Stability	16
1.4.2	Extracellular Barrier	19
1.4.2.1	Degradation of DNA in Plasma	20
1.4.2.2	Reticuloendothelial System and Opsonisation	21
1.4.2.3	Specificity to target cells	23
1.4.3	Intracellular Barrier	24
1.4.3.1	Cellular Uptake	25
1.4.3.2	Endosomal Escape and Lysosomal Degradation	25
1.4.3.3	DNA unpacking	26
1.4.3.4	Nuclear Entry	27
<b>1.5</b>	<b>Strategies to Improve Polymer Based Gene Delivery System</b>	<b>30</b>
1.5.1	Design of Multifunctional Gene Delivery System	30
1.5.2	Hydrophilic Polymer	32
1.5.3	Cell Penetrating Peptides	34

---

1.5.4	Endosomolytic Agents	36
1.5.5	Targeting Ligands	37
1.5.6	Nuclear Localization Signals	39
<b>1.6</b>	<b>Phosphorylcholine-Based Gene Delivery System</b>	<b>40</b>
<b>1.7</b>	<b>Aims</b>	<b>42</b>

## **CHAPTER 2**

### **GENERAL MATERIALS AND METHODS**

<b>2.1</b>	<b>Materials</b>	<b>44</b>
2.1.1	DNA	44
2.1.2	Polymers	45
<b>2.2</b>	<b>General Methods</b>	<b>48</b>
2.2.1	Preparation of Polymer – DNA Complexes	48
2.2.2	Cell Lines and Routine Subculture	48
2.2.3	Statistical Analysis	49
<b>2.3</b>	<b>Instrumentation and Basic Theory</b>	<b>50</b>
2.3.1	Ethidium Bromide Displacement Assay	50
2.3.2	Gel Retardation Assay	50
2.3.3	Zeta Potential Theory	51
2.3.4	Photon Correlation Spectroscopy	53
2.3.5	Transmission Electron Microscopy	54
2.3.6	Atomic Force Microscopy	54
2.3.7	Flow Cytometry	55
2.3.8	Laser Scanning Confocal Microscopy	57

## **CHAPTER 3**

### **PHYSICOCHEMICAL ANALYSIS OF DMA-MPC DIBLOCK COPOLYMER – DNA COMPLEXES**

<b>3.1</b>	<b>Introduction</b>	<b>59</b>
3.1.1	Surface Charge	59
3.1.2	Particle Size	60
3.1.3	Long Term Stability	61

---

3.1.4	Aims	61
<b>3.2</b>	<b>Materials and Methods</b>	<b>63</b>
3.2.1	Materials	63
3.2.2	Ethidium Bromide Displacement Assay	63
3.2.3	Gel Retardation Assay	64
3.2.4	Zeta Potential Measurement	64
3.2.5	Particle Size Analysis	65
3.2.6	Long Term Stability of Polymer – DNA Complexes	65
3.2.6.1	Preparation of lyoprotectant – containing complexes	65
3.2.6.2	Freeze-drying of complexes and particle size measurements	66
<b>3.3</b>	<b>Results</b>	<b>67</b>
3.3.1	Ethidium Bromide Displacement Assay	67
3.3.2	Gel Retardation Assay	70
3.3.3	Zeta Potential Measurement	75
3.3.4	Particle Size Analysis	77
3.3.5	Long Term Stability of Polymer – DNA Complexes	81
<b>3.4</b>	<b>Discussion</b>	<b>85</b>
3.4.1	Characterisation of Polymer – DNA complexes	85
3.4.2	Freeze-dried Formulation to Enhance Long-Term Stability of DNA Complexes	89
<b>3.5</b>	<b>Conclusions</b>	<b>92</b>

## CHAPTER 4

### MORPHOLOGY STUDY OF DMA-MPC DIBLOCK COPOLYMER – DNA COMPLEXES

<b>4.1</b>	<b>Introduction</b>	<b>93</b>
4.1.1	Theoretical Aspects of DNA Condensation	93
4.1.2	Aims	95
<b>4.2</b>	<b>Materials and Methods</b>	<b>96</b>
4.2.1	Materials	96
4.2.2	Morphology Study Using TEM	96
4.2.3	Morphology Study Using AFM	96
<b>4.3</b>	<b>Results</b>	<b>98</b>

---

4.3.1	Morphology of DNA Complexes Under TEM	98
4.3.2	Morphology of DNA Complexes Under AFM	111
<b>4.4</b>	<b>Discussion</b>	119
4.4.1	Comparison of TEM and AFM Data	119
4.4.2	DNA Condensation	120
<b>4.5</b>	<b>Conclusions</b>	128

## CHAPTER 5

### BIOLOGICAL STUDY OF DMA-MPC DIBLOCK COPOLYMER – DNA COMPLEXES

<b>5.1</b>	<b>Introduction</b>	129
5.1.	Aims	129
5.2.	Principles of Enzymatic Degradation Study	130
5.3.	Principles of Model Membranes Interaction Study	131
<b>5.2</b>	<b>Materials and Methods</b>	133
5.2.1	Materials	133
5.2.2	Cell Lines and Routine Subculture	133
5.2.3	Enzymatic Degradation Assay	133
5.2.3.1	Fluorescence Study	133
5.2.3.2	Gel Electrophoresis	134
5.2.4	Model Membranes Interaction Study	135
5.2.4.1	Preparation of liposomes – model membrane	135
5.2.4.2	Fluorescence Study	136
5.2.5	Flow Cytometry Study	136
5.2.6	Transfection Study	137
5.2.6.1	Detection of Luciferase	137
5.2.6.2	Determination of Cellular Proteins	138
<b>5.3</b>	<b>Results</b>	139
5.3.1	Enzymatic Degradation Assay	139
5.3.2	Model Membranes Interaction Study	145
5.3.3	Flow Cytometry Study	150
5.3.4	Transfection Study	152
<b>5.4</b>	<b>Discussion</b>	155
<b>5.5</b>	<b>Conclusions</b>	161

---

## CHAPTER 6

### CELLULAR UPTAKE AND INTRACELLULAR TRAFFICKING STUDY OF DMA HOMOPOLYMER – DNA COMPLEXES

<b>6.1</b>	<b>Introduction</b>	162
6.1.1	Endocytosis	162
6.1.2	Clathrin – mediated Endocytosis	165
6.1.3	Caveolae – mediated Endocytosis	167
6.1.4	Involvement of microtubules and actin filaments in Endocytosis	169
6.1.5	Aims	170
<b>6.2</b>	<b>Materials and Methods</b>	171
6.2.1	Materials	171
6.2.2	Cell Lines and Routine Subculture	171
6.2.3	Transfection Study at Different Time Point	171
6.2.4	Transfection Study with Inhibitors	172
6.2.3	Confocal Microscopy Study	172
<b>6.3</b>	<b>Results</b>	174
6.3.1	Transfection Study at different time point	174
6.3.2	Transfection Study with Tubulin /Actin Inhibitors	175
6.3.3	Transfection Study with Clathrin/Caveolae Inhibitors	180
6.3.4	Confocal Microscopy Study	183
<b>6.4</b>	<b>Discussion</b>	190
<b>6.5</b>	<b>Conclusions</b>	202

## CHAPTER 7

### FOLATE CONJUGATED DMA-MPC GENE DELIVERY SYSTEM

<b>7.1</b>	<b>Introduction</b>	203
7.1.1	Folic Acid	203
7.1.2	Aims	205
<b>7.2</b>	<b>Materials and Methods</b>	207
7.2.1	Materials	207
7.2.2	Preparation of Polymer – DNA Complexes	208
7.2.3	Gel Retardation Assay	208

---

7.2.4	Particle Size Analysis	209
7.2.5	Morphology Study	209
7.2.6	Enzymatic Degradation Assay	209
7.2.7	Cell Lines and Routine Subculture	209
7.2.8	Flow Cytometry Study	210
7.2.9	Transfection Study	210
<b>7.3</b>	<b>Results</b>	211
7.3.1	Gel Retardation Assay	211
7.3.2	Particle Size Analysis	213
7.3.3	Morphology Study	214
7.3.4	Enzymatic Degradation Assay	221
7.3.5	Flow Cytometry Study	222
7.3.6	Transfection Study	225
<b>7.4</b>	<b>Discussion</b>	229
<b>7.5</b>	<b>Conclusions</b>	237
 <b>CHAPTER 8</b>		
<b>CONCLUSIONS AND FUTURE DIRECTION</b>		238
 <b>References</b>		244



---

## ABSTRACT

Gene therapy has a great potential for the treatment of a wide range of diseases. However, the development of a safe and efficient delivery vector is the major obstacle for gene therapy. Recently synthesized 2-(dimethylamino)ethyl methacrylate – 2-(methacryloxloxyethyl phosphorylcholine) (DMA-MPC) diblock copolymer was investigated in this work as a novel non-viral vector for gene delivery. It has been previously demonstrated that the cationic DMA block can condense DNA efficiently. The zwitterionic PC head groups are found naturally in the outer leaflet of biomembranes and are extremely biocompatible. It is thus proposed here that the MPC can act as a new steric stabilizer to the system.

Different compositions of DMA-MPC diblock copolymers were evaluated. The MPC block with minimum length 30 monomeric units can successfully provide steric stabilization to the system, and reduce non-specific cellular interaction by providing a steric barrier to the DNA complexes. However, long MPC chain can hinder the interaction between cationic DMA and DNA, leading to the formation of loosely condensed complexes which were more susceptible to enzymatic degradation. Therefore the composition of the copolymer must be carefully adjusted so that the DNA condensing and steric stabilization effect are well balanced.

In order to investigate the cellular uptake mechanism DMA homopolymer - DNA complexes, the effect of different endocytosis inhibitors was examined. Microtubules and actin filaments were involved in the uptake of DNA complexes, suggesting that the complexes were internalised by endocytosis. Both the clathrin- and caveolae- mediated pathway were responsible for the uptake of DNA complexes, and the former appeared to be the main route of entry.

---

Finally, folic acid ligand was incorporated into the DMA-MPC copolymer in order to improve the specific targeting. Initial data showed that there was selective uptake of the folate conjugated system in folate receptor expressing cells possibly *via* receptor mediated endocytosis. However, parameters such as the optimum length of MPC component, number of ligands per DNA complex and the composition of the system need to be further investigated in order to maximize the specificity and transfection efficiency.

---

## Abbreviations

ADA	Adenosine deaminase
AFM	Atomic force microscopy
bp	Base pair
conA	Concanavalin A
CPP	Cell penetrating peptide
DC-Chol	3 $\beta$ -(( <i>N,N</i> -dimethylaminoethane) carbamoyl) cholesterol
DMA	(2-dimethylamino)ethyl methacrylate
DNA	Deoxyribonucleic Acid
DNase	Deoxyribonuclease
DOPE	Dioleoylphosphatidyl ethanolamine
DOTAP	1,2-bis(oleoyloxy)-3(trimethylammonio) propane
DOTMA	Dioleoyl propyl trimethylammonium chloride
DPH	1,6-diphenyl-1,3,5-hexatriene
DPI	Dual Polarisation Interferometry
EDTA	Ethylenediaminetetraacetic acid
EGF	Epidermal growth factor
EtBr	Ethidium Bromide
FA	Folic acid
FCS	Foetal calf serum
FR	Folate receptors
GFP	Green fluorescent protein
HPMA	<i>N</i> -(2-hydroxypropyl)methacrylamide
KCps	Kilo-counts per second
K <sub>d</sub>	Dissociation constant
M	Molar
MAP	Model amphipathic peptide
MDR	Multi-drug resistance
MPC	2-(methacryloyloxyethyl phosphorylcholine)
MgCl <sub>2</sub>	Magnesium Chloride
M <sub>w</sub>	Molecular weight

---

NaCl	Sodium Chloride
NiCl <sub>2</sub>	Nickel Chloride
NLS	Nuclear localization signal
NPC	Nuclear pore complex
OTC	Ornithine transcarbamylase
PAMAM	Polyamidoamine
pAsp	Poly-L-aspartic acid
PBS	Phosphate buffer saline
PC	Phosphorylcholine
PCS	Photon correlation spectroscopy
PEC	Polyelectrolyte complex
PEG	Polyethylene glycol
PEI	Poly(ethylenimine)
PGP	P- glycoprotein
PLL	Poly(L-lysine)
PTD	Protein transduction domain
RES	Reticuloendothelial system
RFC	Reduced folate carrier
RNase	Ribonuclease
RPMI	Rowell Park Memorial Institute
sd	Standard deviation
SDS	Sodium dodecyl sulphate
SPR	Surface plasmon resonance
SV40	Simian virus 40
TAE	Tris acetate EDTA
TAT	Trans-activating transcriptional activator
TMAEMA	2-(trimethylammonio)ethyl methacrylate
TEM	Transmission electron microscopy
T <sub>g</sub>	Glass transition temperature
v/v	Volume per unit volume
w/v	Weight per unit volume
X-SCID	X-linked severe combined immunodeficiency

---

---

## ACKNOWLEDGEMENTS

There are so many people I would like to thank throughout my PhD study. First, I would like to thank my supervisors, Dr. Snow Stolnik, for all her advice, guidance and support since I was an undergraduate, and Dr. Tom Baldwin for his valuable suggestions. Also to my industrial supervisor Dr. Andy Lewis for all his useful advice and comments.

I would also like to thank everyone in the Advanced Drug Delivery group, especially Dr. Paraskevi Kallintari and I-Lin Lee for their help and training during the first year of my PhD study, and Christy Grainger-Boulby for her excellent technical support throughout the course of my study.

Special thanks to Tissue Engineering Group for their help with my cell culture work, and Anne Chim (Laboratory of Biophysics and Surface Analysis) for conducting the atomic force microscopy experiments, and many hours of exciting and constructive discussions we had.

Other people I would like to acknowledge include Mr. Tim Self (Queens Medical Centre) for his tremendous help and advice on the confocal microscopy study, Mr Charlie Matthews for his help with the flow cytometry, Dr. Trevor Gray (Histopathology, Queens Medical Centre) for his training and assistance in transmission electron microscopy study, and Professor Steve Armes (University of Sheffield) for providing polymers for my study, as well as his useful suggestions.

I am extremely grateful to my family for their support, encouragement and love which is more than words can describe.

Last but not least, I would like to thank the University of Nottingham and Biocompatibles for their funding.

---

## List of Figures

<b>Figure 1.1</b>	Schematic diagram of major extracellular barriers to successful non-viral gene delivery	20
<b>Figure 1.2</b>	Schematic diagram of major intracellular barriers to successful non-viral gene delivery	24
<b>Figure 1.3</b>	Schematic diagram of a multifunctional non-viral gene delivery vector using cationic polymer	31
<b>Figure 2.1</b>	Chemical structures of DMA homopolymer, MPC homopolymer and DMA-MPC diblock copolymer	46
<b>Figure 2.2</b>	Diagram showing the zeta potential of a charged particle	52
<b>Figure 2.3</b>	Diagram showing the basic setup of a flow cytometry	56
<b>Figure 2.4</b>	Diagram showing the basic setup of a confocal microscope	58
<b>Figure 3.1</b>	EtBr displacement assay of DMA <sub>x</sub> MPC <sub>30</sub> copolymer series	68
<b>Figure 3.2</b>	EtBr displacement assay of DMA <sub>40</sub> MPC <sub>y</sub> copolymer series	69
<b>Figure 3.3</b>	Agarose gel retardation assay of DMA <sub>x</sub> MPC <sub>30</sub> copolymer series	73
<b>Figure 3.4</b>	Agarose gel retardation assay of DMA <sub>40</sub> MPC <sub>y</sub> copolymer series	74
<b>Figure 3.5</b>	Zeta potential measurements of DMA <sub>x</sub> MPC <sub>30</sub> – DNA complexes	76
<b>Figure 3.6</b>	Zeta potential measurements of DMA <sub>40</sub> MPC <sub>y</sub> – DNA complexes	76
<b>Figure 3.7</b>	Schematic diagram to show the charge distribution along the chain of DMA <sub>32</sub> at pH 8	86
<b>Figure 3.8</b>	Schematic diagram to show the charge distribution along the chain of DMA <sub>10</sub> MPC <sub>30</sub> at pH 7.4	86
<b>Figure 4.1</b>	TEM images of DMA homopolymer – DNA complexes at 2:1 monomeric unit: nucleotide ratio	99
<b>Figure 4.2</b>	TEM images of DMA <sub>40</sub> MPC <sub>10</sub> – DNA complexes at 2:1 monomeric unit: nucleotide ratio	101

---

<b>Figure 4.3</b>	TEM images of DMA <sub>40</sub> MPC <sub>20</sub> – DNA complexes at 2:1 monomeric unit: nucleotide ratio	102
<b>Figure 4.4</b>	TEM images of DMA <sub>40</sub> MPC <sub>30</sub> – DNA complexes at 2:1 monomeric unit: nucleotide ratio	103
<b>Figure 4.5</b>	TEM images of DMA <sub>40</sub> MPC <sub>40</sub> – DNA complexes at 2:1 monomeric unit: nucleotide ratio	104
<b>Figure 4.6</b>	TEM images of DMA <sub>40</sub> MPC <sub>50</sub> – DNA complexes at 2:1 monomeric unit: nucleotide ratio	105
<b>Figure 4.7</b>	TEM images of DMA <sub>10</sub> MPC <sub>30</sub> – DNA complexes at 2:1 monomeric unit: nucleotide ratio	107
<b>Figure 4.8</b>	TEM images of DMA <sub>20</sub> MPC <sub>30</sub> – DNA complexes at 2:1 monomeric unit: nucleotide ratio	108
<b>Figure 4.9</b>	TEM images of DMA <sub>60</sub> MPC <sub>30</sub> – DNA complexes at 2:1 monomeric unit: nucleotide ratio	109
<b>Figure 4.10</b>	TEM images of DMA <sub>100</sub> MPC <sub>30</sub> – DNA complexes at 2:1 monomeric unit: nucleotide ratio	110
<b>Figure 4.11</b>	AFM images of uncondensed luciferase plasmid	112
<b>Figure 4.12</b>	AFM images of DMA <sub>10</sub> MPC <sub>30</sub> – DNA complexes at 2:1 monomeric unit: nucleotide ratio	114
<b>Figure 4.13</b>	AFM images of DMA <sub>20</sub> MPC <sub>30</sub> – DNA complexes at 2:1 monomeric unit: nucleotide ratio	115
<b>Figure 4.14</b>	AFM images of DMA <sub>40</sub> MPC <sub>30</sub> – DNA complexes at 2:1 monomeric unit: nucleotide ratio	116
<b>Figure 4.15</b>	AFM images of DMA <sub>60</sub> MPC <sub>30</sub> – DNA complexes at 2:1 monomeric unit: nucleotide ratio	117
<b>Figure 4.16</b>	TEM images of intermediate DNA structures (between rods and toroids) formed with DMA <sub>20</sub> MPC <sub>30</sub> copolymer	124
<b>Figure 4.17</b>	TEM images of intermediate DNA structures (between rods and toroids) formed with DMA <sub>40</sub> MPC <sub>30</sub> copolymer	125
<b>Figure 5.1</b>	Location and orientation of DPH in a phospholipids bilayer	132
<b>Figure 5.2</b>	Enzymatic degradation study using fluorescent probe intercalation method	140
<b>Figure 5.3</b>	Gel electrophoresis of naked DNA in enzymatic degradation study	141

---

<b>Figure 5.4</b>	Gel electrophoresis of polymer – DNA complexes dissociated with pAsp	142
<b>Figure 5.5</b>	Gel electrophoresis of polymer – DNA complexes in enzymatic degradation study	144
<b>Figure 5.6</b>	The effect of DNA (250 µg /ml) on model membranes	146
<b>Figure 5.7</b>	The effect of polymer – DNA complexes prepared at 2:1 monomeric unit: nucleotide ratio on model membranes	148
<b>Figure 5.8</b>	The effect of polymer – DNA complexes prepared at 10:1 monomeric unit: nucleotide ratio on model membranes	149
<b>Figure 5.9</b>	Percentage of A549 cells exhibiting associated fluorescence at 180 min in flow cytometry study	151
<b>Figure 5.10</b>	The average fluorescence intensity associated with A549 cells at 180 min in flow cytometry study	152
<b>Figure 5.11</b>	Transfection efficiency of polymer – DNA complexes (2:1 monomeric unit: nucleotide ratio) on A549 cells	154
<b>Figure 6.1</b>	Schematic diagram of clathrin-mediated endocytosis	166
<b>Figure 6.2</b>	Schematic diagram of caveolae-mediated endocytosis	168
<b>Figure 6.3</b>	Transfection efficiency of DMA homopolymer – DNA complexes on A549 cells measured at different time post-transfection	174
<b>Figure 6.4</b>	Transfection efficiency of DMA homopolymer – DNA complexes on colchicine pre-treated A549 cells	176
<b>Figure 6.5</b>	Protein level of colchicine pre-treated A549 cells in the luciferase assay	176
<b>Figure 6.6</b>	Transfection efficiency of DMA homopolymer – DNA complexes on colchicine pre-treated A549 cells, with colchicine present during the entire experiment	177
<b>Figure 6.7</b>	Protein level of colchicine treated A549 cells in the luciferase assay	177
<b>Figure 6.8</b>	Transfection efficiency of DMA homopolymer – DNA complexes on cytochalasin D pre-treated A549 cells	179
<b>Figure 6.9</b>	Protein level of cytochalasin D pre-treated A549 cells in the luciferase assay	179



---

<b>Figure 6.10</b>	Transfection efficiency of DMA homopolymer – DNA complexes on con A pretreated A549 cells, with con A present during the entire experiment	181
<b>Figure 6.11</b>	Transfection efficiency of DMA homopolymer – DNA complexes on chlorpromazine pretreated A549 cells, with chlorpromazine present during the entire experiment	181
<b>Figure 6.12</b>	Transfection efficiency of DMA homopolymer – DNA complexes on filipin pre-treated A549 cells, with filipin present during the entire experiment	182
<b>Figure 6.13</b>	Transfection efficiency of DMA homopolymer – DNA complexes on nystatin pre-treated A549 cells, with nystatin present during the entire experiment	182
<b>Figure 6.14</b>	Confocal images showing intracellular trafficking of DMA homopolymer – DNA complexes on A549 cells at various time intervals	184
<b>Figure 6.15</b>	Trans-sectional confocal images of A549 cells at 240 min following the addition of DMA homopolymer – DNA complexes	185
<b>Figure 6.16</b>	Confocal images of conA treated A549 cells at 240 min following the addition of DMA homopolymer – DNA complexes (1)	187
<b>Figure 6.17</b>	Confocal images of conA treated A549 cells at 240 min following the addition of DMA homopolymer – DNA complexes (2)	188
<b>Figure 6.18</b>	Trans-sectional confocal images of nystatin treated A549 cells at 240 min following the addition of DMA homopolymer – DNA complexes	189
<b>Figure 6.19</b>	Confocal images of DMA homopolymer – DNA complexes that entered the cells appeared as discrete particles	197
<b>Figure 6.20</b>	Confocal images of DMA homopolymer – DNA complexes that remained outside the cells appeared as aggregates	198
<b>Figure 7.1</b>	Chemical structure of folic acid	204
<b>Figure 7.2</b>	Chemical structures of DMA-MPC-FA	208
<b>Figure 7.3</b>	Agarose gel retardation assay of folate conjugated systems	212
<b>Figure 7.4</b>	TEM images of DMA <sub>50</sub> MPC <sub>30</sub> -FA – DNA complexes at 1:1 monomeric unit: nucleotide ratio	216

---

---

<b>Figure 7.5</b>	TEM images of DMA <sub>50</sub> MPC <sub>30</sub> -FA – DNA complexes at 2:1 monomeric unit: nucleotide ratio	217
<b>Figure 7.6</b>	TEM images of DMA <sub>50</sub> MPC <sub>30</sub> -FA – DNA complexes at 5:1 monomeric unit: nucleotide ratio	218
<b>Figure 7.7</b>	TEM images of DMA <sub>50</sub> MPC <sub>30</sub> -FA/DMA binary polymer -DNA complexes at 2:1 monomeric unit: nucleotide ratio	219
<b>Figure 7.8</b>	TEM images of DMA <sub>50</sub> MPC <sub>30</sub> -FA/DMA binary polymer -DNA complexes at 5:1 monomeric unit: nucleotide ratio	220
<b>Figure 7.9</b>	Gel electrophoresis of folate conjugated system in enzyme degradation assay	222
<b>Figure 7.10</b>	Average fluorescent intensity associated with A549, MCF-7 and KB cells using folate conjugated system in flow cytometry study	224
<b>Figure 7.11</b>	Cellular association of DMA <sub>50</sub> MPC <sub>30</sub> -FA – DNA complexes On KB cells, with the presence or absence of free folic acid in flow cytometry study	225
<b>Figure 7.12</b>	Transfection efficiency of folate conjugated systems on A549, MCF-7 and KB cells.	227
<b>Figure 7.13</b>	Transfection efficiency of DMA <sub>50</sub> -MPC <sub>30</sub> -FA on (a) MCF-7 and (b) KB cells, in the presence or absence of free folic acid	228
<b>Figure 7.14</b>	Schematic diagram of the proposed structure of folate conjugated DNA	235

---

## List of Tables

<b>Table 2.1</b>	Summary of properties for DMA homopolymer, MPC homopolymer and DMA-MPC diblock copolymers	47
<b>Table 3.1</b>	Particle size, scattering intensity and polydispersity of DNA complexes with DMA homopolymer and DMA <sub>x</sub> MPC <sub>30</sub> measured by PCS	78
<b>Table 3.2</b>	Particle size, scattering intensity and polydispersity of DNA complexes with DMA homopolymer and DMA <sub>40</sub> MPC <sub>y</sub> measured by PCS	79
<b>Table 3.3</b>	The effect of sucrose as lyoprotectant on particle size, with sucrose added before complexes formation.	83
<b>Table 3.4</b>	The effect of sucrose as lyoprotectant on particle size, with sucrose added after complexes formation	83
<b>Table 3.5</b>	The effect of glucose as lyoprotectant, with glucose added before complexes formation	84
<b>Table 3.6</b>	The effect of glucose as lyoprotectant, with glucose added after complexes formation	84
<b>Table 4.1</b>	Measurements of rods and toroids structures formed with DMA <sub>40</sub> MPC <sub>30</sub> and DMA <sub>40</sub> MPC <sub>40</sub> under TEM	106
<b>Table 4.2</b>	Measurements of rods/linear and toroids structures formed with DMA <sub>10</sub> MPC <sub>30</sub> , DMA <sub>20</sub> MPC <sub>30</sub> , and DMA <sub>40</sub> MPC <sub>30</sub> under TEM	111
<b>Table 4.3</b>	Measurements of toroids or globular structures formed with DMA <sub>20</sub> MPC <sub>30</sub> , DMA <sub>40</sub> MPC <sub>30</sub> , DMA <sub>60</sub> MPC <sub>30</sub> and DMA <sub>100</sub> MPC <sub>30</sub> under TEM	111
<b>Table 4.4</b>	Measurements of contour length and dimensions of DNA condensates formed with DMA <sub>x</sub> MPC <sub>30</sub> under AFM	118
<b>Table 4.5</b>	Comparison of the relative populations (%) of toroids and rods under TEM	123
<b>Table 6.1</b>	Effect of different cell treatments on cellular uptake mechanism	164
<b>Table 7.1.</b>	Summary of molecular weight data and folic acid contents for DMA-MPC-FA functionalized diblock copolymers	207
<b>Table 7.2</b>	Average particle size, scattering intensity and polydispersity of DMA <sub>50</sub> MPC <sub>30</sub> -FA – DNA complexes measured by PCS	213

---

<b>Table 7.3</b>	Average particle size, scattering intensity and polydispersity of DMA <sub>50</sub> MPC <sub>30</sub> -FA/DMA binary polymer – DNA complexes measured by PCS	214
<b>Table 7.4</b>	Average particle size of DMA <sub>50</sub> MPC <sub>30</sub> – FA – DNA complexes and DMA <sub>50</sub> MPC <sub>30</sub> – FA/ DMA binary polymer – DNA complexes measured under the TEM.	215

## CHAPTER 1

### INTRODUCTION

#### 1.1 BASIC CONCEPTS OF GENE THERAPY

Since the discovery of the structure of deoxyribonucleic acid (DNA) by James Watson and Francis Crick over 50 years ago (Watson and Crick, 1953), the understanding of how DNA controls and affects our health has improved rapidly. The use of DNA as a therapeutic tool became theoretically possible after the successful identification and cloning of the gene responsible for inherited single genetic disorder, such as cystic fibrosis (Riordan *et al.*, 1989) and adenosine deaminase (ADA) deficiency (Orkin *et al.*, 1983). Gene therapy was introduced and initially regarded as an approach for treating the single genetic disorder by replacing the defective gene(s) with a normal healthy gene (Orkin, 1986).

However, very few diseases are caused by a single gene mutation, and thus the benefits of gene therapy are very limited. The potential of gene therapy was soon expanded to the treatment of a wide range of other genetic disorder, as well as diseases of non-genetic origin, such as cardiovascular diseases (Yla-Herttuala and Martin, 2000), infectious diseases (Bunnell and Morgan, 1998), neurological diseases (Suhr and Gage, 1993) and cancer (El-Aneed, 2004). The definition of gene therapy has become boarder and is no longer only restricted to the correction of defective genes. Other approaches, for example, the delivery of suicide genes to kill cancer and infected cells (Mullen, 1994), the delivery of oligonucleotides to block the expression of a particular protein (Stein and Cheng, 1993), or the use of DNA as vaccines by introducing DNA encoding for antigenic components in order to induce an

immunological response (Ulmer *et al.*, 1993), are all regarded as gene therapy. In recent years, gene therapy is broadly redefined as the transfer of genetic materials into human cells in order to generate a therapeutic effect.

A successful gene therapy requires the delivery and the expression of the therapeutic gene in the human target cells. With the completion of the human genome project in 2003 (Collins *et al.*, 2003), the identification and design of a suitable therapeutic gene for a particular disease is no longer a major obstacle. The biggest challenge for gene therapy nowadays is the development of a suitable vehicle (or vector), which is capable of delivering the therapeutic gene into the target cells safely and efficiently.

## 1.2 GENE THERAPY CLINICAL TRIALS

The first human gene therapy clinical trial was performed in 1989 by Rosenberg *et al.* (1990) who used retrovirus in the attempt to treat advanced melanoma. Since then, over 1000 clinical trials have been carried out worldwide (Edelstein *et al.*, 2004). Two-thirds of all trials have been conducted in the United States, whereas United Kingdom is the second leading country in gene therapy trials, accounting for 11% of the total number of trials in the world.

Like all other pharmaceutical clinical trials, gene therapy trials are conducted in phases. Phase I trials are the first stage of testing in human and are designed to assess the safety and tolerability of the new therapy. They are normally conducted in a small group (20 to 80) of healthy volunteers. Phase II trials are performed in larger groups of patients and volunteers (20 to 300) and are designed to evaluate the clinical efficacy as well as the safety of the therapy. Phase III trials involve a larger group of patients (100 to 3000) and are aimed at evaluating the efficacy of the new therapy, in comparison with current 'Gold Standard' treatment. Phase IV trials involve the post-marketing studies to provide additional information including long term effects of the treatment. Disappointingly, there has been limited clinical success in gene therapy over the last 15 years. The majority of clinical trials performed were stopped at early stage. Phase I or I/II represent 84% of all gene therapy trials (completed or ongoing); 13% are phase II trials, with less than 3% are phase II/III or III trials.

In terms of therapeutic indication, most of the clinical trials in gene therapy have been aimed at the treatment of various types of cancer (66% of all trials), followed by inherited monogenic diseases and cardiovascular diseases. Viral vectors are the most frequently used vectors to deliver genes into human cells. They have been used in about 70% of the trials performed to date. In non-viral system, 'naked DNA' is the most popular system which accounts for

14% of all trials, followed by lipofection (cationic lipid/DNA complexes) which have been involved in just over 9% of all trials.

The biggest breakthrough of gene therapy came in 2003 when a gene therapy product was approved to be used in human for the very first time (Peng 2005, Wilson 2005). China's State Food and Drug Administration approved Gendicine for the treatment of head and neck squamous cell carcinoma after it achieved promising results in clinical trial. Gendicine consists of an adenovirus designed to insert a p53 tumour suppressor gene. The results from the clinical trial studies showed there was complete regression of tumours in 64% of patients after eight weekly intratumoral injections of Gendicine in combination with radiotherapy, a rate three times higher than those in the radiotherapy only group (Peng 2005). As of July 2005, Gendicine has been used to treat over 2600 patients and the same product is currently in late-stage clinical trials for a variety of other cancer treatments (Wilson 2005). The result is very encouraging and marks an important milestone in gene therapy.



### 1.3 METHODS OF GENE DELIVERY

The success of gene therapy relies essentially on the development of safe and efficient vectors. Ideally, a gene delivery vector should be able to provide protection from gene degradation and deliver the therapeutic gene to the target cells only without triggering host immune response. In addition, it should be non-toxic, able to accommodate therapeutic DNA of any size, and easy to produce at an acceptable cost. Unfortunately at present, no single vector exhibits all of the above characteristics. Each vector currently being investigated has its own advantages and limitations.

There are several possible routes for administration of the therapeutic gene. The choice of administration routes depends on the type of delivery vector and the cells to be targeted. In general, two major approaches are studied, including *in vivo* and *ex vivo* (Hauser *et al.*, 2000). With the *in vivo* gene therapy, the therapeutic DNA is transferred directly into cells within a patient. The process is direct and involves less manipulation than that of the *ex vivo* approach, in which the target cells are removed from the patient, transfected *in vitro* and returned to the patient.

A number of gene delivery vectors have been developed and can be broadly divided into two categories – viral and non-viral vectors.

#### 1.3.1 Viral vectors

Viral vectors refer to the use of viruses as a tool for gene delivery. They are the vehicles of choice for gene delivery in clinical trials in the United Kingdom and worldwide. In March 2004, 74% of all ongoing gene therapy trials in the United Kingdom involved the use of viral vectors, most of these are for cancer treatment (Relph *et al.*, 2004). Viruses are extremely efficient vectors to deliver genes to target cells, as they have evolved to enter the host

cells and express their genes there. Therefore it is possible to take advantage of this by introducing a therapeutic gene into the viruses and using their properties to deliver the therapeutic gene with high efficiency into the target cells (Walther and Stein, 2000). Before viruses can be used to deliver the genes into human cells, they must be genetically modified with care so that the pathogenicity of the virus is eliminated and the uncontrolled replication of the engineered virus is prevented, while the efficiency of gene transfer and expression is retained.

In general, viral vectors are broadly divided into two groups, integrating and non-integrating vectors (Kootstra and Verma, 2003). Integrating viruses include retrovirus (Weber *et al.*, 2001) and adeno-associated virus (Rabinowitz and Samulski, 1998), which have the ability to integrate their viral genome into the chromosomal DNA of the host cell so that long-lasting gene expression could be achieved. The non-integrating viruses include adenovirus (McConnell and Imperiale 2004) and herpes simplex virus (Lachman, 2001), which deliver their genomes into the nucleus of the target cell where they remain episomal.

Each of the viral vectors has its own characteristics. The choice of viral vector in gene therapy approach depends largely on the types of cells to be targeted by the therapy, the size of therapeutic DNA and the desired duration of expression of the therapeutic gene.

Although viral vectors are currently the most efficient gene delivery system being investigated, several safety issues have led to a reconsideration of their use in human gene therapy. In 1999, 18-year old Jesse Gelsinger, who took part in a gene therapy clinical trial in United States, died from multi-organ failure only four days after the treatment (Lehrman, 1999, Thomas *et al.*, 2003). His death was directly attributed to the administration of the adenovirus which was used to treat ornithine transcarbamylase (OTC) deficiency, a rare metabolic disease that can cause a dangerous build up of ammonia in the body. An autopsy showed that although the viral vector had

been infused directly into the liver, substantial amounts of the virus had spread into the circulation and accumulated into the spleen, lymph nodes and bone marrow. The virus triggered a massive inflammatory response that led to intravascular coagulation, respiratory distress and multi-organ failure (Marshall, 1999).

The nightmare of adverse events caused by viral vector in gene therapy did not end there. In 2000, an 18 month-old boy with the fatal X-linked severe combined immunodeficiency (X-SCID), a rare immune disorder caused by a defective gene on the x chromosome, was the first patient saved by gene therapy using retrovirus (Cavazzana-Calvo *et al.*, 2000). The results appeared to be encouraging in the beginning. However, within a year, two out of 10 children treated in France for X-SCID had developed leukaemia-like disease (Hacein-Bey-Abina *et al.*, 2003). It was found that the retrovirus, which was used to carry a therapeutic genome into bone marrow stem cells, had inserted into the patients' DNA and activated an oncogene, triggering the cause of leukaemia.

The main concerns regarding the safety of viral vectors include the possibility of insertional mutations, high immune response and problems of toxicities. Furthermore, weakened viruses can conceivably change inside the patient's body and regain their pathogenic activity. In fact, the X-SCID and Gelsinger cases have brought the attention of the safety with the use of viral vectors, leading to the development of non-viral vectors as potentially safer alternative.

### **1.3.2 Non-viral vectors**

Non-viral delivery systems offer many advantages over viral vectors, including their relatively safe profile and potentially lower immune response. Furthermore, they can be produced in large quantities at a relatively low cost and provide virtually unlimited capacity to accommodate therapeutic DNA

(Schatzlein, 2001). However, the major drawback of non-viral methods is poor efficiency, which holds back their use in gene therapy. Improvements in the efficiency of non-viral DNA delivery systems are being studied intensively in order to make these systems competitive options over viral vectors in the near future. In general, non-viral gene delivery involves the use of naked DNA, liposomes and cationic polymers.

#### 1.3.2.1 Naked DNA

The direct transfer of naked DNA is the most straightforward mode of gene delivery. Naked DNA can be administered via two possible routes, *ex vivo* or *in vivo* delivery. The *ex vivo* delivery of naked DNA provides a precise but time consuming method to transfer therapeutic DNA to the target cells. Its reliance on the culture of harvested cells renders it unsuitable for many cell types.

*In vivo* delivery of naked DNA is the simplest way for administration of DNA to a patient (Herweijer and Wolff 2003). This method was used in several pre-clinical and clinical trials (Nishitani *et al.*, 2003). It was first described in 1990 and was demonstrated that direct injection of DNA into skeletal muscle could result in local transient gene expression (Wolff *et al.*, 1990). Gene expression was also detected when naked DNA was directly applied to liver (Hickeman *et al.*, 1994, Zhang *et al.*, 1997), solid tumours (Yang and Huang, 1996, Baque *et al.*, 2002), and epidermis (Yu *et al.*, 1999). The therapeutic DNA can be introduced through either intravascular or intramuscular injection, with the latter demonstrating better results (Gardlik *et al.*, 2005). However, the level of gene expression was low and short term in both cases. Nevertheless, the level of expression may be sufficient for use in DNA vaccination (Smith *et al.*, 1998, Youssef *et al.*, 1998).

Several methods have been employed to improve the level of gene expression with naked DNA. One of them is electroporation (Wong and Neumann, 1982.

Rols *et al.*, 1998, Tupin *et al.*, 2003). It involves the use of high voltage electrical pulses to temporarily permeabilise cell membranes, allowing the DNA to enter the cell easily. This can be done by injecting naked DNA followed by electric pulses from electrodes that are located *in situ* in the target tissues. Successful use of electroporation *in vivo* was observed in tissues such as muscle and skin (Rols *et al.*, 1998, Rizzuto *et al.*, 1999). However, a large percentage of cells may die following this technique, limiting its application *in vivo*.

Another technique to enhance the delivery of naked DNA is called 'the gene gun' (Fynan *et al.*, 1993, Kuriyama *et al.*, 2000). With this approach, the DNA is transferred by colloidal-sized particles of gold on which the DNA is bound. These particles are then shot directly into the cells under great pressure and high velocity, with the help of compressed helium. The gene gun was originally developed for gene transfer to plant cells. Its use was soon expanded to gene delivery in mammalian cells, and it has great potential for the delivery of DNA vaccines (Qiu *et al.*, 1996, Surman *et al.*, 1998).

#### 1.3.2.2 Liposomes

The idea with the use of liposomes to deliver DNA was based on the experience with liposomal delivery of conventional small molecule drugs (Nicolau and Cudd, 1989, Chonn and Cullis, 1995, 1998). Liposomes have been well studied in the last few decades for the controlled and site-specific delivery of drugs, peptides and proteins. Anionic or uncharged liposomes have been used to deliver encapsulated drugs, and are adapted to deliver genes in the same fashion. They act as closed vesicles, which separate the internal compartment from the external medium by the lipid bilayer, with the potential to protect the encapsulated DNA from enzymatic degradation. In early years, methods used to encapsulate DNA always yield relatively large multilamellar vesicles with low DNA encapsulating efficiencies, resulting in poor gene transfer capabilities (Nicolau *et al.*, 1983, Baru *et al.*, 1995). In the

last two decades, there have been significant advances in the formulation of plasmid DNA into relatively small, stable DNA-containing liposomes for gene delivery. The use of cationic liposomes to deliver DNA was introduced in the late 1980s (Felgner *et al.*, 1987). The ability of cationic liposomes to interact with DNA to form complexes (lipoplexes) is dependant on several physical conditions, such as pH and charge, as well as structural characteristics of the liposomes. Two processes are involved in lipoplex formation: a fast exothermic process is attributed to the electrostatic binding of DNA to the liposome surface (Felgner and Ringold, 1989, Pector *et al.*, 2000). A subsequent slower endothermic reaction is caused by fusion of the two components and their rearrangement into a new structure. During this process, the homogenous and physically stable suspensions are formed (Hong *et al.*, 1999).

Liposomes can be formed from a variety of cationic lipids. The best known is DOTMA (Dioleoyl propyl trimethylammonium chloride), which is often formulated with a neutral helper lipid such as DOPE (Dioleoylphosphatidyl ethanolamine). Liposomes formulated without neutral lipids always have poor transfection efficiency (Lasic and Pearlman, 1996). The role of the neutral helper lipid is to facilitate membrane fusion and improve transfection efficiency by assisting endosomal escape (Felgner *et al.*, 1987, Farhood *et al.*, 1995). In addition, these supporting lipids help to stabilise the cationic liposome suspension (Zuidam and Barenholz, 1998). Other commonly used cationic lipids include DOTAP (1,2-bis(oleoyloxy)-3(trimethylammonio) propane) (McLachalan *et al.*, 1994) and DC-Chol (3 $\beta$ -(*N,N*-dimethylaminoethane) carbamoyl) cholesterol) (Gao and Huang, 1991).

Liposomes are the most efficient non-viral gene delivery vector currently available and have become the standard for *in vitro* transfection of plasmid DNA. Many commercially available transfection kits, such as lipofectin (*N*-(1-(2,3-di-olyloxy) propyl)- *N, N, N*- trimethylammonium chloride, 1,2-dioleoylphosphatidylethanol-amine-DOPE, 1:1) and lipofectamine (*N*-(2-(2,5-bis((3-aminopropyl)amino)-1-oxpentyl)amino) ethyl)-*N,N*-dimethyl-2,3-

bis(9-octadecenyloxy)-1-propanaminium trifluoroacetate-DOPE 3:1) are developed from liposomes. To date, almost 50% of the non-viral gene therapy clinical trials worldwide involve the use of lipoplexes, which contribute to about 9% of all on going gene delivery clinical trails (Edelstein *et al.*, 2004). However, they are not without drawbacks. Their *in vivo* use is limited by their inherent instability, poor biodistribution, lack of cell specificity and cytotoxicity (Mahato *et al.*, 1997, Filion and Phillipsm 1998, Hope *et al.*, 1998, Tousignant *et al.*, 2000). Strategies such as introduction of ligands and alternations in the chemical composition of the liposomes are being investigated to tackle these problems (Lee and Huang, 1996, Martin and Boulikas, 1998, Kawakami *et al.*, 2000).

### 1.3.2.3 Cationic polymers

The interest in using cationic polymers as gene delivery vectors is growing in recent years due to their relatively safe profile and the flexible chemical design, which allows the incorporation of various functional components to overcome delivery barriers. In addition, they are relatively simple to manufacture at a low cost.

Cationic polymers typically contain protonable amines. The relative numbers and pK(a) of the protonable amines differ between polymers. Some of the cationic polymers have the positive charges on the backbone whereas some have the positive charge on the side groups. Cationic polymers are able to condense DNA to form polymer – DNA complexes (polyplexes) through electrostatic interaction between the positively charged amine groups of polycations and negatively charged phosphate groups of DNA. This can be explained by polyelectrolyte theory (Kabanov and Kabanov, 1995a, Kabanov *et al.*, 1995b).

According to the polyelectrolyte theory, when aqueous solutions of polycations and polyanions are mixed together, they spontaneously interact to

form a complex coacervate, which is also known as a polyelectrolyte complex (PEC). The composition of PEC can be defined by the charge ratio  $\phi$ , the ratio of the positive charge (amine groups of polycations) to the negative charge (phosphate bases of nucleic acid). At low values of  $\phi$  ( $<1$ ), soluble PEC with a net negative charge exist. Aggregates of PECs start to form when the concentration of polycations increased. The largest aggregates exist at a value of  $\phi$  close to 1. As the value of  $\phi$  further increases ( $>1$ ), the size of PEC reduces due to electric repulsion.

Several variables affect the formation mechanisms and the stability of PECs, such as the strength of the polyelectrolyte in terms of acid or base, the molecular weight of the polyions and the conditions of solvent (e.g. pH and ionic or salt condition) (Kabanov *et al.*, 1985, Dautzenberg and Karibyants, 1999, Dragan and Cristea, 2002, Leclercq *et al.*, 2003, Zintchenko *et al.*, 2003, Becheran-Maron *et al.*, 2004). For example, when PECs are formed at a very low salt concentration, there is repulsion between high concentration of ionic groups in the polyelectrolyte, resulting in bigger and less compact PECs. As salt concentration increases, it competes with polyelectrolyte binding, thus reducing interaction between polyelectrolyte, and allows salt bonds and polyelectrolyte to arrange more easily, leading to the formation of tighter and more compact PECs. Further increase of salt concentration leads to precipitation of PECs. When the salt concentration is high enough, the presence of salt shields the charge of polyelectrolyte, preventing the formation of PECs at all. Therefore, the properties of polymer – DNA complexes are heavily dependent on the types and properties of the cationic polymer, the ratio of each component as well as the conditions under which they are formed. It will be important to define the optimum compositions of the complexes, which will eventually affect their prospects as effective gene delivery system.

Commonly used cationic polymers for gene delivery include poly(L-lysine) (PLL), polyethylenimine (PEI), chitosan, dendrimers and poly(2-dimethylamino)ethyl methacrylate (DMA). each of them have its own



characteristics. PLL is one of the first polymers being studied in non-viral gene delivery. As a polypeptide, PLL is biodegradable. The epsilon amino group of lysine is positively charged at physiological pH 7.4, thus PLL is able to interact and form complexes with the negatively charged DNA through electrostatic interaction (Laemmli, 1975, Reich *et al.*, 1990, Wolfert and Seymour, 1996). The transfection efficiency of PLL – DNA complexes is relatively poor but strategies such as incorporation of targeting ligands (Wu and Wu, 1987, Mislick *et al.*, 1995, Zauner *et al.*, 1998) or endosomolytic agents (Kichler *et al.*, 1999) can improve its efficiency. However, the chain length heterogeneity of commercially available PLL preparations and the resulting variability in size distribution of the polyplexes has adversely affected the reproducibility of PLL mediated gene delivery (Wolfert and Seymour, 1996). In addition, PLL displays high to severe toxicity as the lysine homopolymers are not rapidly metabolized by the body, discouraging its use *in vivo* (Wolfert and Seymour, 1996, Anwer *et al.*, 2003).

With the lack of promising results and toxicity issues regarding the use of PLL, other cationic polymers are being investigated and developed as potential gene delivery vectors. PEI is one of the most extensively studied cationic polymers in gene delivery due to its excellent transfection efficiency against a wide selection of cells *in vitro* (Boussif *et al.*, 1996). Its use in gene delivery has been reviewed in many publications (Godbey *et al.*, 1999a, Kircheis *et al.*, 2001b, Neu *et al.*, 2005). The most attractive property regarding the use of PEI is the ability to act as an effective buffer through a wide pH range. This property, also known as ‘proton sponge’ property (Boussif *et al.*, 1995), facilitates the endosomal escape of PEI – DNA complexes and is in fact a crucial factor for the high transfection level obtained with this polymer. However, toxicity is still a major problem associated with the use of PEI (Godbey *et al.*, 2001).

Dendrimers are also popular in gene delivery area. A range of polyamidoamine (PAMAM) dendrimers have been widely studied (Haensler and Szoka, 1993, Kukowska-Latallo *et al.*, 1996, Hudde *et al.*, 1999,

Bielinska *et al.*, 2000, Brauen *et al.*, 2005). PAMAM dendrimers contain both tertiary amines at branch points as well as primary amines at the termini. The terminal amines are responsible for DNA condensation and complexation through electrostatic interaction, whereas the inner amines provide buffering capacity at low pH, allowing the complexes to escape from the endosomes / lysosomes through proton sponge mechanism (Tang *et al.*, 1996). There are two major types of dendrimers, the intact dendrimers, which bear two new polymers arms at each point of branching, and fractured dendrimers, in which either one or two arms originate or the polymer is terminated at this point. The fractured form of dendrimer is far more effective than the intact form, with transfection efficiency significantly enhanced by over 50-fold (Tang *et al.*, 1996). This is possibly due to the higher flexibility of the fractured dendrimers, which gives rise to better DNA condensation and more efficient endosomal escape. Although PAMAM was reported to be less toxic than PLL, toxicity remains an important issue with their *in vivo* application.

While most of the cationic polymers face the problem of toxicity, chitosan seems to be an attractive candidate compared to the others. Chitosan is a natural basic polysaccharide derived from the common biopolymer chitin. It is rapidly degraded in the body, non-toxic and of low immunogenicity (Brine *et al.*, 1992). It displays a significantly better biocompatibility than other cationic polymers such as PEI. With the optimum molecular weight, chitosan exhibits gene expression level that is comparable to PEI (Koping-Hoggard *et al.*, 2001). Interestingly, chitosan appears to control the release of DNA, prolonging its action *in vitro* (Erbacher *et al.*, 1998). However, chitosan lacks the buffering capacity at low pH, causing the endosomal escape to be a major limiting factor for this polymer. Approaches such as incorporation of endosomolytic agents into chitosan can enhance the transfection efficiency both *in vitro* and *in vivo* (MacLaughlin *et al.*, 1998).

2-(dimethylamino)ethyl methacrylate (DMA) is a water soluble cationic polymer that has also been extensively investigated in recent years as a gene

delivery vector (Cherng *et al.*, 1996, van de Wetering *et al.*, 1999, Zuidam *et al.*, 2000, Rungsardthong *et al.*, 2001, Deshpande *et al.*, 2002). DMA can efficiently bind and form complexes with DNA, and is able to transfect a variety of cell types *in vitro* (van de Wetering *et al.*, 1997). It is also found to be less toxic than PLL. One of the major problems associated with DMA is the formation of large insoluble aggregating DNA complexes (Varbaan *et al.*, 2003). Modification of the polymer by incorporating hydrophilic components such as poly(ethylene glycol) (PEG) has been investigated in order to improve colloidal stability (Rungsardthong *et al.*, 2001, Funhoff *et al.*, 2005).

Since DMA is only partially protonated at physiological pH, it has been proposed that DMA might possess buffering capacity and act as a proton sponge similar to PEI, facilitating the endosomal escape of the DNA complexes (Zuidam *et al.*, 2000). However, a recent study has suggested that DMA actually lacks the ability to escape from endosomes (Jones *et al.*, 2004), leading to a reconsideration of this hypothesis.

In general, a number of physicochemical characteristics such as the size, surface properties (hydrophobicity / hydrophilicity) and solubility of the polyplexes affect their efficiency as gene delivery vectors. All the polyplexes encounter similar barriers, either inside or outside the body, which are described in the following section. While each of the barriers affects different polymers to a different extent, the development of a successful gene delivery system requires the optimisation of the polymer accordingly. While a lot of research has been focused on the design and engineering of the polymeric vectors, it must be stressed that the toxicity of polymers must not be ignored.

## 1.4 BARRIERS TO NON-VIRAL GENE DELIVERY SYSTEM

Non-viral gene delivery systems have considerable advantages over viral vectors, such as low immunogenicity and a relatively safe profile. In order for the non-viral delivery systems to be developed into true therapeutic products for humans use, several major barriers are needed to be overcome. These barriers can be broadly divided into three classes: physical stability, extracellular barriers and intracellular barriers.

### 1.4.1 Physical stability

Once the polyplexes or lipoplexes are produced, either on a laboratory bench or clinical scale, their physical and chemical characteristics must be successfully preserved in order to maintain their maximum biological activity, i.e., the transfection efficiency. Since the formation of polycation – DNA complexes is due to electrostatic interaction between the polycations and the negatively charged DNA, aggregation of the complexes could be a potential problem. Although the complexes are usually prepared with an excess of positive charge, the local regions of charge neutrality may promote interaction between complexes, resulting in aggregation (Tang and Szoka, 1997). This problem may be aggravated when highly concentrated suspensions are required for clinical studies (Zelphati *et al.*, 1998). Structural alteration with DNA complexes that do not affect the size of the complexes may also affect biological activity (Anchordoquy *et al.*, 1998). In addition, the complexes must also be formulated to resist any chemical modification or degradation (Middaugh *et al.*, 1998), such as attack by free radicals and or singlet oxygen.

To avoid instability of lipid – DNA suspensions in early clinical trials, the lipoplexes were usually prepared at the bedside immediately prior to injection (Nabel *et al.*, 1992 and 1993). This is undesirable and impractical when it

comes to large scale manufacturing. In order to improve long term stability and extend the shelf life of the suspensions, one of the strategies is to employ sucrose gradients to isolate a stable fraction of complexes that could be stored at 4°C for 3 months (Gao and Huang, 1996, Hofland *et al.*, 1996). It has been demonstrated that these complexes can effectively deliver gene *in vivo* (Hofland *et al.*, 1997). However, it is uncertain whether this method of sucrose density gradient fractionation could be sufficiently scaled up for bulk manufacturing. Another approach is to incorporate a steric stabilizer such as PEG to the system (Hong *et al.*, 1997). Although the efficiency of the complexes can be preserved at 4°C for 2 months, it is unclear whether liquid formulations can be rendered sufficiently stable to withstand stresses associated with shipping and prolonged storage (Anchordoquy and Koe, 1999).

Due to the relatively low stability of liquid formulation, freeze drying, also referred to as lyophilization, is an alternative strategy to stabilize the complexes. Lyophilization is carried out using a simple principle of physics called sublimation, by which a substance is transitioned from solid to vapour state, without first passing through an intermediate liquid phase. Lyophilization is often used to stabilize various pharmaceutical products, including virus vaccines, protein and peptide formulations, liposome, and small-chemical drug formulations (Friede *et al.*, 1993, Wang 2000).

Studies have been carried out on both lipoplexes and polyplexes to evaluate the feasibilities of freeze-drying for providing long term stability of non-viral gene delivery systems (Molina *et al.*, 2001, Anchordoquy *et al.*, 1998, Li *et al.*, 2000, Cherng *et al.*, 1999, Kwok *et al.*, 2000, Seville *et al.*, 2002). The main concern with the freeze-dried complexes is whether they can retain the same properties as the freshly prepared complexes.

When the DNA is complexed with polycations, the transfection level of freeze-dried complexes is significantly reduced (Zelphati *et al.*, 1998, Anchordoquy *et al.*, 1998). Since the DNA is protected during complexation

by the polycations, the level of DNA damage during freeze-thawing would be too low to affect the transfection efficiency. Instead, the structural alterations within the complexes and / or aggregation are the main reasons for the reduction of transfection level. Several studies have shown that complex size increases dramatically following freeze-thawing, suggesting that aggregation of complexes are responsible for the reduction of transfection level (Cherng *et al.*, 1997, Anchordoquy *et al.*, 1998). During the freezing process, formation of ice crystals causes solutes and suspended particles to be concentrated in the unfrozen fraction. As the temperature is further reduced, the growth of ice crystals causes particles to be further concentrated in the unfrozen fraction, and aggregation is facilitated (Allison *et al.*, 2000).

In order to develop efficient freeze-dried formulations, it is essential to maintain the particle size throughout the freeze drying process. Many studies have demonstrated that sugars, including glucose, sucrose, trehalose and dextrose, can be used as effective lyoprotectants to preserve particle size of lipoplexes (Anchordoquy *et al.*, 1998, Molina *et al.*, 2001) and polyplexes (Cherng *et al.*, 1999), and hence their transfection efficiency *in vitro*. However, the mechanism by which a sugar preserves the complexes property is not clearly understood. Currently there are two hypotheses explaining the stabilizing effect of sugar, namely vitrification (glass formation) (Anchordoquy *et al.*, 2001) and particle isolation hypothesis (Allison *et al.*, 2000). In the vitrification hypothesis, it is suggested that the presence of sugar increases the volume of unfrozen fraction, and thereby reduces the concentrating effect of ice formation. As temperature decreases, the unfrozen solution will either crystallize or form an amorphous glass at  $T_g$  (glass transition temperature). The formation of viscous glass might have contributed to size preservation by immobilizing the complexes in a glassy matrix and thus preventing aggregation. However, some studies indicate that sugar (e.g. glucose) can preserve particle size effectively even in the lack of glass formation under certain conditions (Allison *et al.*, 2000).

In the second hypothesis, it is proposed that sugar isolates individual particles in the unfrozen fraction, thereby preventing aggregation during freezing (Allison *et al.*, 2000). According to this hypothesis, vitrification is not required to maintain particle size.

It has also been proposed that incorporating steric stabilizer such as PEG can prevent aggregation during freeze drying. This approach could potentially eliminate the need for sugar as lyoprotectant. However, the results observed by Armstrong *et al.* suggest that incorporation of PEG alone does not preserve complexes size following freeze drying. In contrast, when PEGylation is combined with the use of sucrose as lyoprotectant, transfection efficiency is fully preserved following freeze-drying (Armstrong *et al.*, 2002).

#### 1.4.2 Extracellular barriers

Extracellular barriers to the systemic delivery of DNA are referred to the obstacles that the delivery system encounters from the point of injection into the human body to the uptake of the system by the target cells, as demonstrated in figure 1.1. Blood contains many proteins, lipids and other molecules than can bind and destabilize the delivery system. Therefore, a successful delivery system must show ability to remain colloidally stable in the blood, evade the adaptive immune system, minimize interactions with plasma proteins (opsonisation) and non-targeted cell surfaces. The *in vivo* activity of the non-viral delivery system is still difficult to predict due to the lack of correlation between *in vitro* and *in vivo* results (Wells *et al.*, 2000). To allow the design of an efficient system, the underlying principle of each potential barrier must be clearly understood.

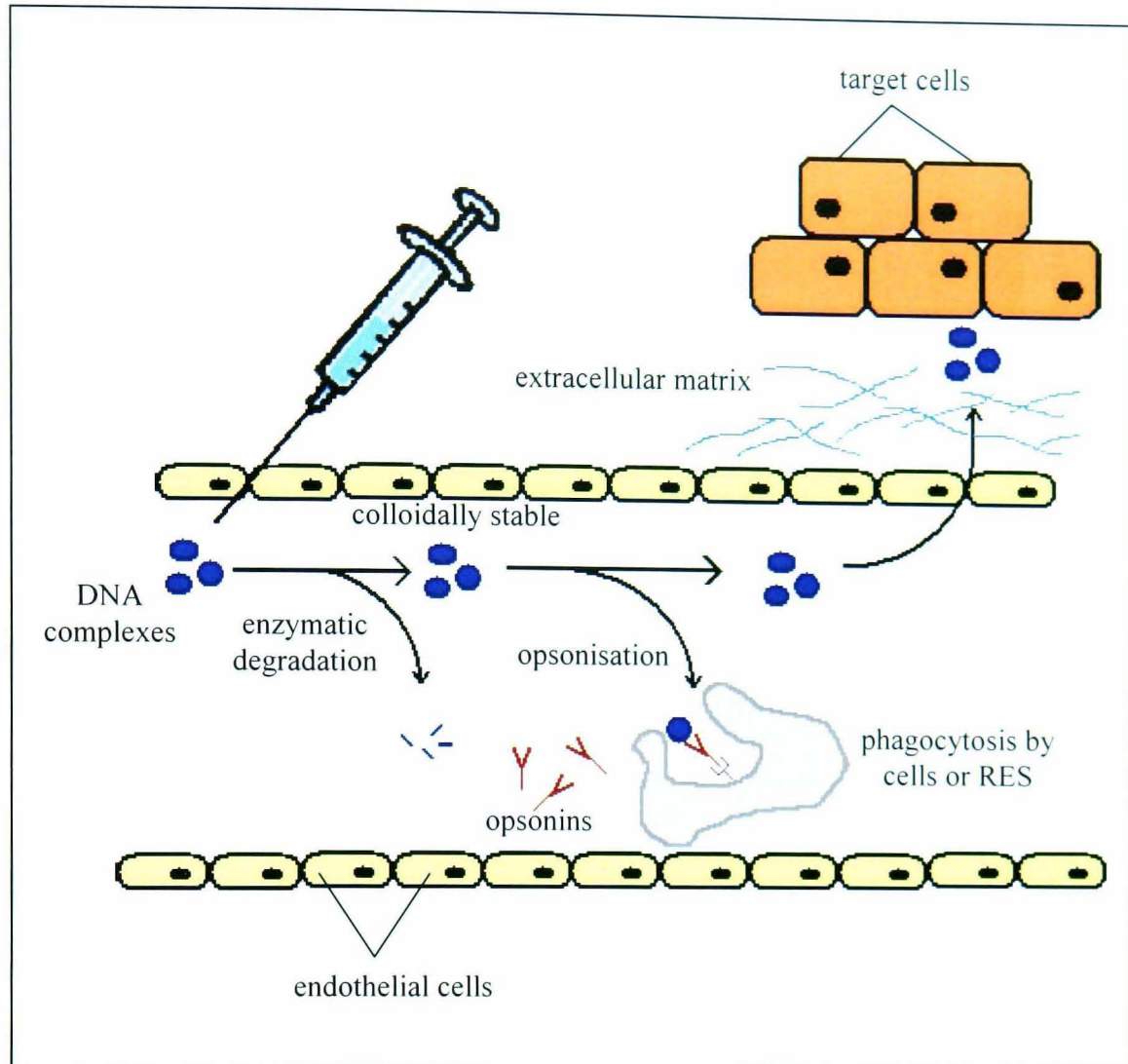


**Figure 1.1 Schematic diagram of major extracellular barriers to successful non-viral gene delivery.** After injection, the therapeutic DNA must be protected from the enzymatic activity in plasma. The DNA complexes have to remain colloidally stable in the blood, and escape from opsonisation and phagocytosis by the cells of the reticuloendothelial system (RES) in the circulation. The complexes must also be specific to and able to reach to target cells.

#### 1.4.2.1 Degradation of DNA in plasma

Once the lipoplexes or polyplexes are present inside the systemic circulation, they are intermediately exposed to enzymatic activities. Experiments using naked DNA *in vivo* have demonstrated that the fate of the DNA is affected by its rapid clearance from the blood via nuclease degradation (Lecocq *et al.*,



2003). Nuclease is an important biological enzyme that can be found in the serum (Cox and Gokcen, 1976, Wickstrom 1986, Eder *et al.* 1991, French-Anderson, 1998). It catalyses the hydrolysis of phosphodiester bonds in both RNA and DNA. Nucleases usually show chemical specificity and are either deoxyribonucleases (DNase) or ribonucleases (RNase). Introduction of a single break in DNA phosphodiester backbone leads to conversion of supercoiled to open circular and ultimately linear forms of DNA with further breakage (Middaugh *et al.*, 1998). Although the conversion of DNA from a supercoiled to an open circular form usually has a minor effect on transfection efficiency, the subsequent conversion to linear forms can substantially reduce the level of gene expression (Adami *et al.*, 1998). In order for successful transfection to take place, the therapeutic DNA must be effectively protected from any enzymatic degradation.

The ability of a delivery system to protect DNA from enzymatic degradation appears to be highly dependent on DNA condensation ability and the nature of the DNA complexes formed. With better DNA binding and condensation ability, and the subsequent formation of tighter structures of DNA complexes, it is expected that the system can offer better DNA protection capacity (Richardson *et al.*, 2001). No specific strategy is currently available to improve DNA protection from enzymatic degradation, apart from the choice of an effective DNA condensing agent as the delivery vector or optimizing the polycation to DNA ratios.

#### 1.4.2.2 Reticuloendothelial system and opsonisation

The human immune defence system provides an excellent protection against any foreign or potentially harmful substances. As part of the defence system, the cells of the reticuloendothelial system (RES) can rapidly remove intravenously administered particulate carriers from the systemic circulation (Davis *et al.*, 1984, Stolnik *et al.*, 1995). The RES is composed of monocytes and macrophages located in reticular connective tissues, e.g. the spleen, liver

and bone marrow. These cells are responsible for engulfing (phagocytosis) and removing cellular debris, old cells, pathogens, and foreign substances from the bloodstream. Before any foreign substances are engulfed by phagocytes, they are marked and differentiated by being coated with chemical mediators generated by the immune system. Such endogenous chemicals that make foreign substances more susceptible to phagocytosis are known as opsonins. Opsonins provide extrinsic ligands for specific receptors on the phagocyte membrane, which dramatically increases the rate of adherence and ingestion of the opsonised foreign substances (Horwitz, 1982). The most important opsonins are immunoglobulins and one of the activated components of complement system, C3b. Without opsonins, the foreign substances will not normally be removed by the RES. In order to prolong circulation of the non-viral gene delivery system, it must be able to escape from opsonisation effectively.

Several factors, such as surface charge and surface characteristics (hydrophilicity / hydrophobicity) are known to have a major influence on opsonin – lipoplex or polyplex interactions (Young *et al.*, 1988, Choun *et al.*, 1991, Stolnik *et al.*, 1995, Semple *et al.*, 1998). Several reports have suggested that overall positively charged polyplexes or lipoplexes show considerably more complement activation in an *in vitro* human complement assay when compared to their neutral counterparts (Senior *et al.*, 1991, Oku *et al.*, 1996). Generally, surfaces with negative or neutral charge are less likely to activate the complement system, as compared to positively charged surfaces (Freitas Jr., 2003). This is because the majority of plasma proteins carry a net negative charge at physiological pH. On the other hand, strong negative charge on the particle surface can cause scavenging by phagocytosis via the macrophage polyanion receptors, which recognise a wide range of anionic molecules, thus enhancing the clearance of the particles from the systemic circulation (Juliano and Stamp, 1975, Krieger *et al.*, 1993). Therefore, it is desirable for the complexes to have a surface charge that is close to neutral.

The hydrophilicity and hydrophobicity of the particle surface affects their attractive forces, therefore affecting the opsonisation process. Hydrophobic particles are usually opsonised and taken up by cells in the RES within a few minutes following intravenous administration (Patel, 1992). In general, higher protein adsorption is observed on hydrophobic surfaces than on hydrophilic surfaces, resulting in a higher uptake of hydrophobic particles by phagocytes *in vitro* and rapid removal *in vivo* (Illum and Davis, 1986, Golander and Pitt, 1990, Müller *et al.*, 1997, Gessner *et al.*, 2000). A hydrophilic component can be incorporated into the delivery system to create a hydrophilic corona on the surface of the complexes.

#### 1.4.2.3 Specificity to target cells

Lack of specificity is another obstacle to non-viral gene delivery. Specificity is based on the recognition and exploitation of differentials between the diseased or target site and the healthy tissues. It is an important factor in determining the efficacy and safety of a delivery system. In order to avoid any unwanted effects in healthy or non-target cells, it is necessary to address the delivery system to the specific cell types while minimizing any non-specific interaction.

Specificity targeting can be achieved by incorporating specific ligands which facilitate the exclusive uptake of the system in certain tissues or cell types (e.g. in receptors expressing tissues or cells). This strategy is described in further details in section 1.4.5. Another method to achieve gene expression in specific tissues involves the use of cell type specific promoters or enhancers, which can be activated by induction factors, such as hormones, growth factors and cytokins, via responsive elements. This strategy has been shown to successfully increase cell specific efficiency in several targets (Walther and Stein, 1996, Kurane *et al.*, 1998, Nettelbeck *et al.*, 2000, Shi *et al.*, 2001, Varda-Bloom *et al.*, 2001).

### 1.4.3 Intracellular barriers

Reaching the surface of the targeted cell is only half way to successful gene delivery. The therapeutic DNA has to overcome another series of barriers inside the cells to reach its site of action, the nucleus, in order to generate the desired therapeutic effect. These barriers include cellular uptake, escape from the endosomes / lysosomes, unpacking or dissociation of the DNA complexes and nuclear entry. The intracellular barriers that are needed to be overcome by the delivery system are demonstrated in figure 1.2.

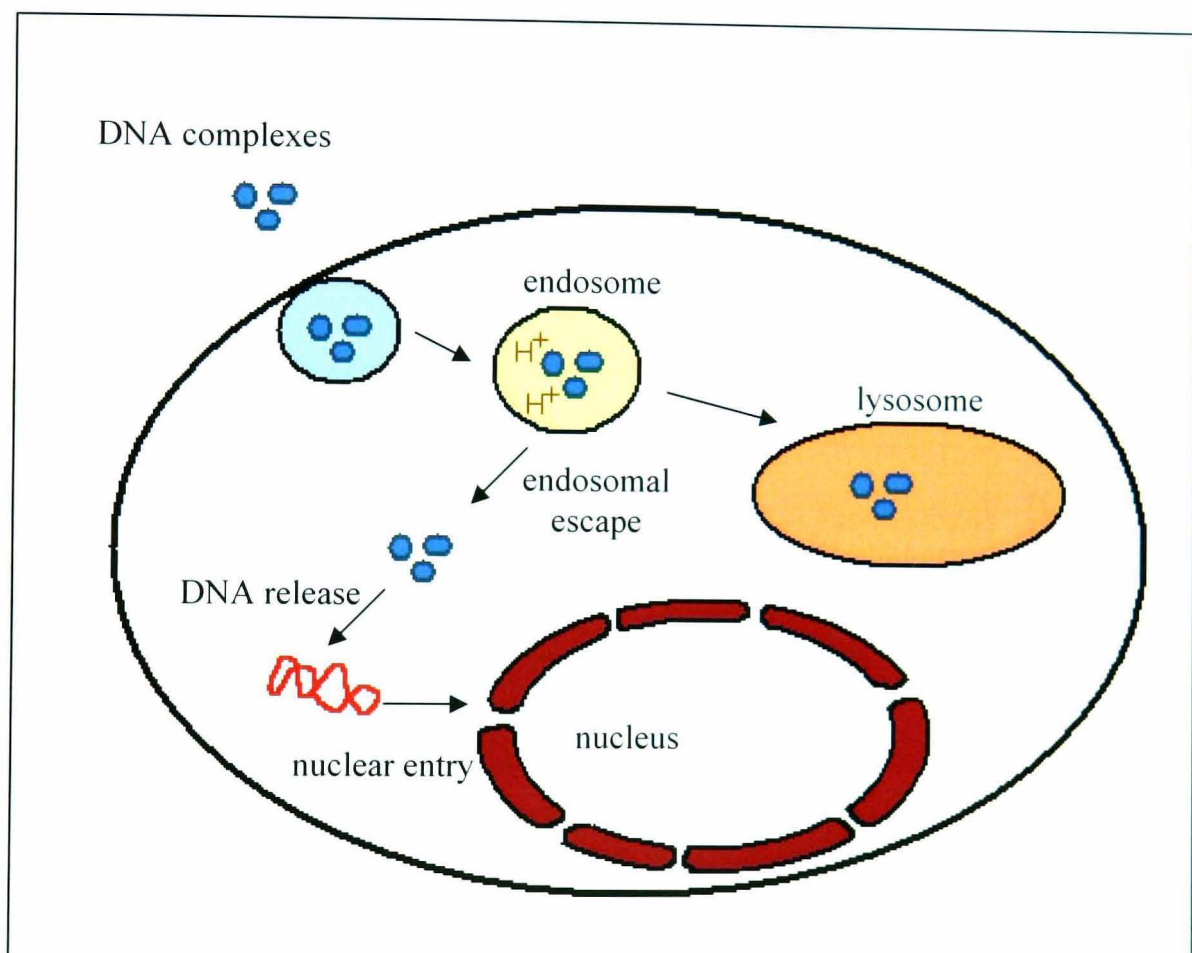


**Figure 1.2 Schematic diagram of the major intracellular barriers to successful non-viral gene delivery.** First, the DNA complexes must be able to enter the targeted cells by endocytosis. Inside the cells, the complexes are delivered into endosomes and subsequently into the lysosomes for degradation. For successful gene delivery, the DNA complexes must rapidly escape from the endosomes, followed by dissociation of the complexes to release DNA which must enter into the nucleus.

#### 1.4.3.1 Cellular Uptake

The plasma membrane is composed of a lipid bilayer and contains various integral proteins, which selectively screen all foreign substances entering the cell. Non-viral gene delivery systems are often too large and too polar for rapid passive diffusion into the cell, making cellular uptake a potential obstacle.

The mechanism of cellular uptake varies with the nature of the complexes and the types of cell into which they will be delivered. It is generally believed that the majority of the non-viral gene delivery systems enter the cells via endocytosis (Farhood, 1995, Klemm *et al.*, 1998, Kichler *et al.*, 2001). Cell surfaces are negatively charged due to their content of glycoproteins, proteoglycans and glycerolphosphates (Singh *et al.*, 1992). Adsorptive endocytosis is a plausible mechanism of entry for DNA complexes with positive surface charges (Godbey *et al.*, 1999c, Remy-Kristensen *et al.*, 2001). Alternatively, receptor – mediated endocytosis of the delivery system can be achieved by attachment of a ligand that binds to specific cell surface receptors.

#### 1.4.3.2 Endosomal escape and lysosomal degradation

Once within the cells through endocytosis, DNA complexes will follow the endosomal / lysosomal pathway, leading from the early to late endosomes, and eventually ending in the lysosomal compartment where the pH drops to approximately 5. With the presence of aggressive nucleases in the lysosomes, the DNA complexes are eventually degraded. Therefore, the DNA complexes must be able to escape from the endosomes rapidly and effectively in order to avoid destruction.

A few cationic polymers such as PEI have the ability to escape from the endosomes efficiently. PEI has buffering capacity at a pH range of 5-7

(Fischer *et al.*, 1999). The buffering capacity of the polymer allows the increased influx of protons and chloride ions during endosomal / lysosomal acidification, which results in an increase of osmotic pressure in the vesicle. As a consequence, the passive diffusion of water into the vesicle increases, leading to swelling and eventually rupture or leakage of the vesicle. This is known as the 'proton sponge' hypothesis (Boussif *et al.*, 1995). However, not all gene delivery systems have such buffering capacity. Strategies such as the employment of endosomolytic agents have been developed to enhance endosomal escape and / or prevent lysosomal degradation. These strategies are described in section 1.4.4.

#### 1.4.3.3 DNA unpacking

DNA unpacking or the dissociation of DNA complexes is essential in the transfection process, because only released and intact DNA can be transcribed into RNA. In fact, it is a critical step in the success of gene delivery (Arigita *et al.*, 1999, van de Wetering *et al.*, 1999, Schaffer *et al.*, 2000). This problem is often overlooked especially when the gene delivery system is designed to have good stability.

The release of therapeutic DNA from the delivery system could take place either in the cytosol or in the nucleus. The dissociation characteristic of non-viral vectors is directly related to the interaction between the polycations and DNA. When the strength of interaction is weak, the complexes may dissociate too easily at an early stage, exposing the therapeutic DNA to enzymatic degradation before they can reach the target cells. However, when the strength of interaction is too strong, the complexes may be incapable of dissociation, and the therapeutic gene will be unable to express. It is generally believed that the DNA is released from the DNA complexes *in vivo* by exchanging with anionic biological macromolecules such as sulphated glycosaminoglycans, hyaluronan and mRNA (Ruponen *et al.*, 1999). The

optimal complex dissociation rate or location are unclear and are currently being investigated (Schaffer *et al.*, 2000).

Recently, a strategy has emerged to assist the release of DNA by developing vectors with linear reducible polycations using PLL that can be cleaved (disulfide reduction) in the intracellular environment to facilitate the release of DNA (Read *et al.*, 2003). The initial results are very encouraging as the transfection level of the reducible system is increased by 187-fold compared to the non-reducible counterparts. A similar approach has been employed by Funhoff *et al.* who designed a novel polymeric delivery system that can be degraded within a few days at physiological pH and temperature, hence releasing the DNA in the cytosol of the cell (Funhoff *et al.*, 2004a). However, the design of such system has to be careful so as not to jeopardize the stability of the DNA complexes.

#### 1.4.3.4 Nuclear entry

In order for the therapeutic genes to be expressed, they must be efficiently delivered inside the nucleus of the target cells. However, nuclear uptake is one of the major limitations for successful gene delivery (Zabner *et al.*, 1995). Microinjection studies have demonstrated that gene expression can be achieved by direction injection of less than 100 plasmids into the nucleus. However, to achieve a comparable effect by microinjection of DNA into the cytoplasm, it is necessary to inject 100 to 1000 times more DNA (Pouton, 1998), showing that nuclear entry is an extremely inefficient process.

The nucleus is separated from the cytoplasm by two membranes, which form the nuclear envelope. Like the plasma membrane, each nuclear membrane consists of a water-impermeable phospholipid bilayer and various associated proteins. The nuclear envelope is perforated by nuclear pores. Nuclear pores are cylindrical channels formed by a protein structure called the 'nuclear pore complex' (NPC), which allows the passage of selected molecules between

cytosol and nucleus. There are two possible routes for the transport of DNA into the nucleus. The DNA can either pass into the nucleus through the nuclear pores, or it can become physically associated with chromatin during mitosis when the envelope breaks down.

Nuclear pores are embedded in the nuclear envelope at fairly high surface densities (3000-4000 / nucleus) (Walter, 1999). They exist in at least two conformation states. The closed state permits the passive diffusion of small molecules of less than 9 nm in diameter, such as ions and globular proteins (40-60 kDa). The open state facilitates the active transport of larger proteins or molecules which are less than 26 nm (Mattaj and Englmeier, 1998, Ryan and Wentz, 2000). All proteins that are actively imported through the nuclear pore contain a short polypeptide sequence called a nuclear localization signal (NLS) sequence.

NLS sequences were first discovered during the analysis of mutants of simian virus 40 (SV40) that produced an abnormal form of the early protein called large T-antigen (Jans and Hübner, 1996). The wild type form of this protein is localized in the nucleus in virus-infected cells, whereas mutated forms of large T-antigen accumulate in the cytoplasm. This suggests the existence of a peptide sequence that may govern the transportation across the nucleus. Numerous NLS sequences have been identified (Moroianu, 1999). The rate of NLS sequence – mediated transportation is likely to be directly proportional to the number of functional nuclear signals, and the NLS content determines nuclear targeting efficacy (Jans and Hübner, 1996).

Apart from the transport through the nuclear pore, DNA may also gain access to the nucleus by association with nuclear material on breakdown of the nuclear envelope during the process of mitosis. This association has been observed on numerous occasions on both lipoplexes and polyplexes by comparing transfection efficiencies for cells at various stages in the cell cycle (Wilke *et al.*, 1996, Tseng *et al.*, 1999, Mortimer *et al.*, 1999, Fasbender *et al.*, 1997, Brunner *et al.*, 2000, 2002, Brisson *et al.*, 1999, Tait *et al.*, 2004.



Parker *et al.*, 2005, Mannisto *et al.*, 2005). DNA is typically observed as localized in the perinuclear region of the cell where it presumably awaits the breakdown of nuclear membrane (Zabner *et al.*, 1995). However, this route of nuclear uptake is only effective when the target cells are rapidly dividing.

## 1.5 STRATEGIES TO IMPROVE POLYMER BASED GENE DELIVERY SYSTEMS

### 1.5.1 Design of a multifunctional delivery system

Successful gene delivery requires the efficient transport of therapeutic DNA into the nucleus of the target cells, overcoming all the barriers as discussed in the previous section. Unfortunately, most of the currently available non-viral gene delivery systems have very low efficiency. Poor stability, lack of specificity, inadequate cellular uptake, ineffective intracellular trafficking and limited nuclear import are all responsible for the poor performance. In fact, the *in vivo* gene delivery is too complex and multifaceted to be achieved successfully using a single carrier molecule in most instances. Nowadays, DNA complexes without any supplementary components are rarely used *in vivo*. A common strategy to improve the efficiency of non-viral delivery system is to design a multifunctional delivery system with various components, each of them serving one or two different specific roles. Figure 1.3 shows a schematic diagram of a proposed multifunctional gene delivery based on a cationic polymer as the non-viral vector. Each of the potential components of such a system is examined in greater details in the following section.

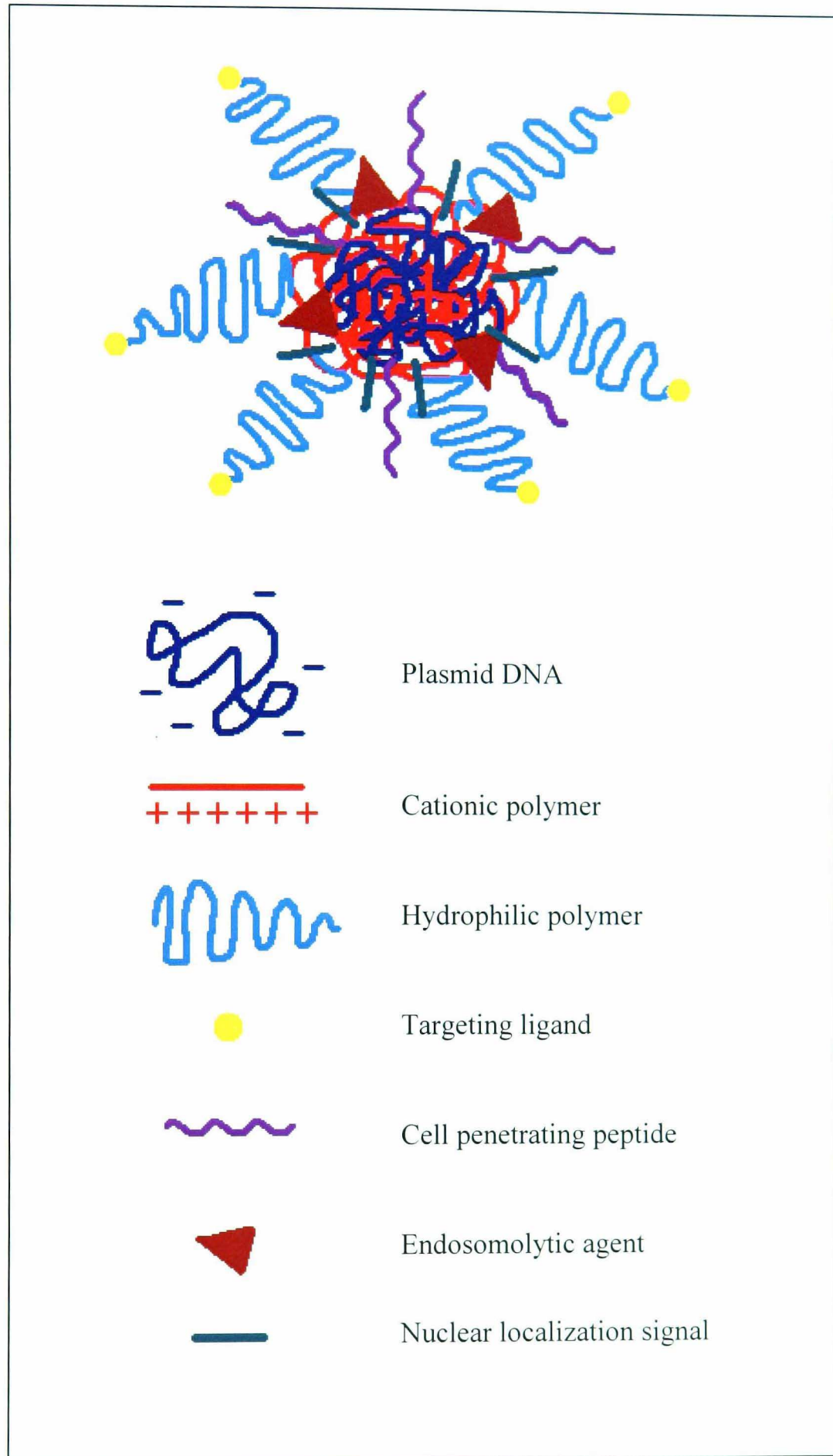


**Figure 1.3** Schematic diagram of a multifunctional non-viral gene delivery vector using cationic polymer.

### 1.5.2 Hydrophilic polymer

In order to improve stability and biocompatibility, as well as to prolong the circulation of the DNA complexes, hydrophilic polymers may be incorporated with the cationic polymer as a copolymer. The binding interaction between the copolymer and DNA occur in an orientated manner, allowing the hydrophilic block to displace from the polyelectrolyte interaction, forming a hydrophilic corona on the surface of the complexes, thereby providing steric stabilization to the delivery system, as well as decreasing potential adsorption of opsonins.

A number of polymers have been used in formulations of polyplexes to confer steric stabilization on the gene delivery system. Poly(ethylene glycol) (PEG) polymers are at present the most popular materials used to modify particulate surfaces in order to provide steric stabilization and to avoid recognition by cells from the RES. PEG is one of the few family at polymers that are approved by FDA for clinical use. They have been successfully grafted to surfaces of biomedical devices to increase biocompatibility and to reduce thrombogenicity (Holmberg *et al.*, 1993, Ista *et al.*, 1996, Deible *et al.*, 1998, Jo and Park, 2000, Otsuka *et al.*, 2001).

In gene delivery, PEG polymers are usually used to form either block or graft copolymers with the cationic polymers such as PLL, PEI and DMA (Wolfert *et al.*, 1996, Katayose and Kataoka, 1997, Choi *et al.*, 1998, Ogris *et al.*, 1999, Rungsardthong *et al.*, 2001, Petersen *et al.*, 2002,). Both types of copolymers (block or graft) form DNA complexes with similar properties. The PEG polymers normally form a hydrophilic corona surrounding the polyplexes. This flexible hydrophilic layer exhibit rapid chain motion in aqueous medium and has a large excluded volume. The steric repulsion resulting from a loss of conformational entropy of the bound PEG chains upon the approach of other substances and the low interfacial free energy of PEG in water contribute to the excellent biocompatibility properties of materials or particles covered with PEG (Gref *et al.*, 1994, Otsuka *et al.*, 2003). PEG

polymers not only effectively reduce the self aggregation of polyplexes, but also significantly reduce interactions between polyplexes and plasma proteins, hence prolonging circulation (Ogris *et al.*, 1999, Harada-Shiba *et al.*, 2002, Kichler *et al.*, 2002, Petersen *et al.*, 2002, Merdan *et al.*, 2005).

Despite its stabilization effect on the delivery system, PEG has been reported to affect DNA condensation, probably due to the local crowding effect (Wolfert *et al.*, 1996b, Erbacher *et al.*, 1999, Rungsardthong *et al.*, 2001). Therefore, an alternative method has emerged. Instead of using block copolymers, PEG can be coated on the surfaces of the polyplex after complex formation. This approach allows more efficient condensation of DNA with cationic polymers (Kircheis *et al.*, 1999, 2001, Blessing *et al.*, 2001, Lee *et al.*, 2001).

Another hydrophilic polymer, poly-*N*-(2-hydroxy)-propylmethacrylamide (HPMA) (Oupický *et al.*, 1999, Oupický *et al.*, 2000a,b, Carlisle *et al.*, 2004) has also been employed as a steric stabilizer in gene delivery. HPMA has long been used as a soluble polymeric drug carrier for peptide and other anticancer drugs (Duncan, 1992, Morgan *et al.*, 1996, Vasey *et al.*, 1999, Kopecek *et al.*, 2000). This polymer is water soluble and shows excellent biocompatibility. Since HPMA shares similar properties with PEG, including flexibility, hydrophilicity and low immunogenicity, it may also function as an efficient steric stabilizer and prolong circulation (Torchilin and Trubetskoy, 1995, Toncheva *et al.*, 1998).

HPMA has been incorporated on to the surface of liposomes in drug delivery. The HPMA-modified liposomes were able to provide strong steric protection for liposomes, increasing their circulation time and decreasing liver accumulation in experimental mice (Whiteman *et al.*, 2001). In polymer based gene delivery systems, HPMA can either form block or graft copolymers with a cationic polymer such as PLL (Toncheva *et al.*, 1998) and 2-(trimethylammonio)ethyl methacrylate (TMAEMA) (Oupický *et al.*, 1999, Howard *et al.*, 2000). The presence of HPMA in the copolymer appears to

have no significant effect on its ability to form complexes with DNA (Oupický, *et al.*, 1999, 2000). In addition, HPMA is able to provide steric stabilization to the DNA complexes and significantly reduce their association with phagocytic cells *in vitro* (Toncheva *et al.*, 1998). However, an *in vivo* study showed that DNA complexes with PLL – HPMA copolymer are cleared from the circulation in the mouse rapidly (Oupický, *et al.*, 2000a). Lateral stabilized multivalent polymers based on HPMA are a recent development and this modified gene delivery system can significantly prolong circulation in mice (Dash *et al.*, 2000, Oupický *et al.*, 2002). The HPMA polymer therefore remains an excellent alternative to PEG.

In recent years, dextran has also been introduced as a potential steric stabilizer in non-viral gene delivery. Dextran is a branched polymer consisting of repeating units of glucose. Because of its hydrophilic property and lack of toxicity to biological systems (Amiji, 1996), dextran is used in drug delivery systems to escape from the RES and consequently increase the circulation time of the drug (Patel, 1983). Its branched structure might provide better shielding effect than linear polymers, such as PEG, to minimize charge interactions with serum proteins (Tseng and Jong, 2003). Conjugation of dextran on a cationic polymer has been shown to improve the stability of DNA complexes in the presence of serum (Toncheva *et al.*, 1998, Erbacher *et al.*, 1999, Tseng and Jong, 2003). However, the experience with the use of dextran in gene delivery is still very limited. Various parameters such as the molecular weight of dextran and the optimum ratio of dextran to cationic polymer must be defined for further development of this system.

### **1.5.3 Cell penetrating peptides**

The lipophilic nature of biological membranes has prevented the direct entry of any large hydrophilic molecules. This is a particular problem when polyplexes are sterically stabilized by a hydrophilic polymer at the surface of the complexes. A novel approach to increase the cellular uptake of such

complexes involves the attachment of peptides that can translocate through the cellular membranes (Derossi *et al.*, 1998, Lindgren *et al.*, 2000, Deshayes *et al.*, 2005, Gupta *et al.*, 2005). These peptides are called cell penetrating peptides (CPPs). They are short peptides that are usually fewer than 30 residues. Many CPPs were designed from sequences of membrane interacting proteins, such as fusion proteins, signal peptides, transmembrane domains and antimicrobial peptides. These peptides sequences contain short sequences called protein transduction domains (PTD) which can efficiently cross the biological membranes without the need for receptor and deliver peptides or protein into intracellular compartments (Schwarze and Dowdy, 2000).

CPPs are divided into two classes, the amphipathic helical peptides, such as transportan and model amphipathic peptide (MAP) and arginine-rich peptides, such as trans-activating transcriptional activator (TAT) and penetratin (Hallbrink *et al.*, 2001). The mechanisms of CPPs entering the cells are currently poorly understood. Since CPPs can enter the cells at 4°C, it is first believed that they are internalized through an energy-independent pathway (Derossi *et al.*, 1994, Vives *et al.*, 1997, Pooga *et al.*, 1998). However, results from more recent studies have held back this assumption (Console *et al.*, 2003, Letoha *et al.*, 2003, Saalik *et al.*, 2004). It is currently believed that there is more than one mechanism for CPP-mediated cellular uptake. For example, TAT-mediated cellular uptake occurs via energy-dependent macropinocytosis (Snyder and Dowdy, 2004, Wadia *et al.*, 2004), whereas some other CPPs penetrate cells via electrostatic interactions and/or hydrogen bonding between CPPs and proteoglycans on the cell surface, and do not seem to require energy (Rothbard *et al.*, 2004, Shen *et al.*, 2004). In any case, the direct contact between the PTD and cell membrane or cell membrane interacting proteoglycans is required for successful intracellular delivery.

The employment of CPP to improve gene delivery has already been reported by linking PLL to TAT (Hashida *et al.*, 2004). The initial results are promising as the novel system promotes the delivery of DNA *in vitro* without

affecting DNA binding ability. However, the weakness of using CPPs to enhance gene delivery is the lack of specificity towards the target site as they tend to trigger internalization in many cell types. Modification of CPP sequences that can improve their specificity (Deshayes *et al.*, 2005) is therefore desirable in designing a targeting gene delivery system.

#### 1.5.4 Endosomolytic agent

Once the delivery systems have entered the cells through endocytosis, they are immediately transported to endosomes and then lysosomes for degradation. PEI is well known to be able to escape from the endosomes through the 'proton sponge' mechanism (Boussif *et al.*, 1995). However, not all the cationic polymers possess this beneficial characteristic. In order to enhance the endosomal release of these systems, an additional endosomolytic agent is required.

There are several types of endosomolytic agents. The most common agent employed is chloroquine, an anti-malarial drug. It prevents the acidification of endosomes, promotes swelling of endosomal vesicle and destabilizes endosomal membranes, thus enhancing endosomal release of the delivery system (Luthman and Magnusson, 1983, Erbacher *et al.*, 1996, Pouton *et al.*, 1998, Ciftci and Levy, 2001). However, due to toxicity problems with chloroquine *in vivo*, the applicability of this agent is limited to the enhancement of transfection *in vitro*.

Peptides with pH dependent membrane lytic activity have also been used to enhance endosomal escape of gene or drug delivery system (Wagner, 1998). This concept is based on the pore-forming proteins used by both viruses and bacteria to facilitate lysosomal escape of their contents to host cells in order to avoid destruction. Analogous peptides have been synthetically developed to exploit this pH dependent activity for endosomal / lysosomal escape. These peptides include GALA, KALA and JTS1 (Parente *et al.*, 1990.



Gottschalk *et al.*, 1996, Turk *et al.*, 2002). They are designed to exhibit random coil structures at physiological pH 7.4, transforming back to a membrane active, penetrating helix to prompt membrane leakage in the acidic environment. Disadvantages of using these peptides include low stability of the peptides, high costs for peptide synthesis and the immunogenic potential of these structures.

### 1.5.4 Targeting Ligand

Non-viral vectors generally lack specificity. One of the widely employed approaches to achieve specific targeting in the pharmaceuticals area is coupling of a targeting ligand to the therapeutic agent. The most frequently used pre-existing targeting ligands are based on endogenous molecules, which are already present in the body. Specific targeting not only can enhance the net uptake of genes to the target cells, but also reduces gene deposition into normal healthy cells, thereby minimising cytotoxicity.

The main criterion to be an efficient targeting ligand is that its receptor should only be highly expressed in the target tissues and no others. For that reason, the choice of ligand heavily depends on the types of tissues to be targeted. After coupling to the delivery vector, the ligand should retain full binding affinity for its receptor. In addition, the targeting ligand must be available on the surface of the delivery system for effective ligand – receptor interaction. Other desirable features of a targeting ligand include high affinity to the receptor with low immunogenicity (Schüzlein 2003, Marcucci and Lefoulon, 2004).

The use of targeting ligands is popular in the delivery of cancer therapy due to the high toxicity of anti-cancer agents. The development of gene delivery has adopted this approach to achieve specific delivery. This concept was first described over 20 years ago by Cheng *et al.* (Cheng *et al.*, 1983), who linked  $\alpha$ 2-macroglobulin directly to DNA for gene delivery. The use of targeting

ligand attached to a polycationic vector was developed later. Such a system was first reported with PLL conjugated with asialoglycoprotein for hepatocytes targeting (Wu and Wu, 1987, 1988). Since then, asialoglycoprotein (Stankovics *et al.*, 1994, Park. *et al.*, 2000, Kim *et al.*, 2005) and many other receptors have been targeted by gene delivery systems using different targeting ligands such as folic acid (Mislick *et al.*, 1995, Wang and Low, 1998), transferrin (Wagner *et al.*, 1990, Cotton *et al.*, 1996, Lee *et al.*, 2005), and epidermal growth factor (EGF) (Cristiano and Roth, 1996, Kloeckner *et al.*, 2004). Each of these ligands has its own advantages and limitations.

Asialoglycoprotein is useful in targeting hepatocytes as its receptor was found to be selectively expressed by these cells (Kawasaki and Ashwell 1976). However, Asialoglycoprotein – PLL – DNA complexes are immunogenic when repeatedly administered to mice (Stankovics *et al.*, 1994). A similar problem is faced by EGF, when incorporated in PLL and PEI (Cristiano and Roth, 1996, Kloeckner *et al.*, 2004). Transferrin is another commonly used ligand for gene delivery. Its receptors are upregulated in many tumours (Huebers and Finch, 1987) and are therefore suitable for targeting a variety of cells. Transferrin has been reported to conjugate with PLL (Cotton *et al.*, 1990), PEI (Kircheis *et al.*, 1997, Orgis *et al.*, 1999, Lee *et al.*, 2005) and chitosan (Mao *et al.*, 2001). However, the presence of transferrin receptors on various cell types has potentially limited the specificity of transferrin conjugated system, (Simoes *et al.*, 1999). Folic acid is also employed to target tumour tissues due to overexpression of folate receptors in most cancer cells (Ross *et al.*, 1994, Weitman *et al.*, 1994). It has been conjugated to polycations such as PEI (Guo and Lee, 1999, 2001) and PLL (Mislick *et al.*, 1995, Ward *et al.*, 2002).

The results from most of the *in vitro* studies of these ligand-conjugated polymer – DNA complexes appear to be promising. However, the experience with their use *in vivo* is still very limited. Further optimization of

these targeted delivery systems *in vivo* is required for the development of therapy in humans.

### 1.5.5 Nuclear localization signals

In order to be actively transported through the nuclear pores, DNA complexes must carry a NLS. Many NLS sequences have been discovered, with the most widely used being the sequence derived from the SV40 large T antigen (Boulikas, 1993, Christophe *et al.*, 2000, Hodel *et al.*, 2001). The sequence that is responsible for the transportation across the nucleus is a seven amino acid sequence: 'PKKKRKV' (Pro-Lys-Lys-Lys-Arg-Lys-Val) (Görlich and Mattaj, 1996, Jans and Hübner, 1996). This sequence has often been referred as the 'classical' NLS.

Attempts have been made to enhance nuclear entry by designing NLS peptide bearing vectors (Sebestyén *et al.*, 1998, Branden *et al.*, 1999, Ciolina *et al.*, 1999, Neves *et al.*, 1999). The size limit for active transport through the nuclear pore is about 25 nm. Unfortunately, polyplexes are generally far too large to cross the nuclear pore even when towed by the NLS sequences. Therefore, one has to assume that the polyplexes are (or at least partly) disassembled in the cytoplasm so that the NLS sequence containing DNA can be taken up through the nuclear pores.

Covalent modification of DNA for the attachment of NLS sequences has been demonstrated to increase nuclear translocation of DNA (Zanta *et al.*, 1999). In that study, the transfection level *in vitro* was enhanced from 10- to 1000- fold as a result of the NLS peptide. Interestingly, the degree of labelling with NLS to the DNA is found to be the major factor affecting the level of DNA uptake. A single NLS per reporter gene is sufficient to carry DNA into the nucleus, whereas too many signals per DNA would lead to the inhibition of nuclear entry by simultaneously interacting with multiple nuclear pores.

## 1.6 PHOSPHORYLCHOLINE BASED GENE DELIVERY SYSTEM

It is well understood that the major criteria of the use of biomaterials *in vivo* is to be biocompatible. They must be non-thrombogenic and show minimal interactions with plasma proteins. Introduction of phosphorylcholine (PC) containing materials has been suggested to enhance biocompatibility. PC is a zwitterionic head group that can be found naturally in the outer leaflet of biomembranes in the form of phospholipids. It has demonstrated an ability to resist adsorption of proteins (Lewis, 2000, Murphy *et al.*, 2000). This attractive property has led to the development of synthetic polymers bearing the PC group, such as 2-methacryloyloxyethyl phosphorylcholine (MPC) polymers (Lewis *et al.*, 2000, Konno *et al.*, 2001)

PC-based polymers have been shown to reduce the surface adsorption of many important proteins, e.g. albumin, immunoglobulins and fibrinogen etc., which are found in high concentrations in human blood plasma, by over 50% compare to relevant controls (Lewis, 2000). As a result, the body is less likely to detect these foreign materials and immune response may not be activated. The mechanism of how PC-based polymers reduce protein adsorption is not fully understood. It is suggested that the high water affinity of the polymer plays an important role (Ishihara *et al.*, 1998). Some studies show that the hydrophilic PC-based polymer has a large free water fraction when compared to other materials. With high level of free water fraction on the polymer surface, proteins are allowed to contact the surface reversibly without much conformational change (Ishihara and Iwasaki, 1998). Other factors, such as flexibility and mobility of PC group may also contribute to its resistance to protein adsorption (Lewis, 2000).

The biocompatible PC-based polymers have been employed in various biomedical applications, such as surface coatings for coronary stents (Lewis *et al.*, 2001a, 2002, Lewis and Stratford, 2002), thoracic drain catheters

(Hunter and Angellini, 1993), and vascular grafts (Chen *et al.*, 1997). There are data to support the safety uses of these materials. Recently, the PC-based polymers have been investigated in controlled drug delivery (Lewis *et al.*, 2001b, Salvage *et al.*, 2005). The initial results are very encouraging. Perhaps it is possible to extend its application to gene delivery systems. Due to its excellent biocompatibility and hydrophilic property, we propose here that the PC-based polymer can be used as a steric stabilizer to improve the stability and possibly prolong circulation of gene delivery systems.

## 1.7 AIMS

Cationic polymer – DNA complexes have been investigated by many researchers in recent years as potentially safer gene delivery systems compared to the viral system. However, the major obstacle faced by cationic polymer systems remains poor efficiency. The efficiency of these systems can be improved by designing a multifunctional gene delivery system based on a cationic polymer, with functional components that address system properties including colloidal stability (steric barrier), reduction of non-specific interaction and specific cellular targeting and entry.

The cationic 2-(dimethylamino)ethyl methacrylate (DMA) homopolymer has been shown previously to condense DNA efficiently. However, problems associated with colloidal instability of the homopolymer – DNA complexes and their non-specific cellular interactions have held back their *in vivo* use. The hydrophilic 2-(methacryloxyloxyethyl phosphorylcholine) (MPC) polymer, which has been successfully employed as a biocompatible coating of many biomedical applications, is currently proposed as a potential steric stabilizer for the delivery system, and to reduce any non-specific cellular interaction. Thus, a novel synthetic A-B type diblock copolymer, DMA-MPC, was introduced here as a candidate for gene delivery, with folic acid incorporated into the system as a targeting ligand to improve specificity.

The primary aim of this thesis was to evaluate the potential of this DMA-MPC diblock copolymer system in gene delivery. First of all, it is crucial to find out whether the hydrophilic MPC is indeed an effective steric barrier to prevent aggregation of the system. The characterisation of DNA complexes prepared from various diblock copolymer composition was needed, including DNA binding ability, particle size and morphology etc.. in order to determine the optimum composition at which both DNA condensation and steric stabilization could be achieved simultaneously. The next step was to assess the biological properties of the systems, including their ability to protect

DNA from enzymatic degradation, membrane and cellular interaction, and *in vitro* transfection efficiency. These results would also be valuable to reveal whether the hydrophilic MPC could successfully reduce any undesirable non-specific cellular interaction. In addition, the cellular uptake mechanism and the intracellular trafficking of the DNA complexes were examined to improve our understanding and to assist the design of a more efficient delivery system. Finally, in order to improve specific targeting and cellular entry, folic acid conjugated DMA-MPC system was introduced, and both physicochemical and biological properties of this system examined.

## CHAPTER 2

### GENERAL MATERIALS AND METHODS

#### 2.1 MATERIALS

Unless otherwise specified, all reagents and buffer salts were obtained from Sigma, UK. Water used was obtained from an ELGA purification system (resistivity 15M $\Omega$ cm, Maxima USF ELGA, High Wycombe, UK) while that used for cell culture was of tissue culture grade. Phosphate buffered saline (PBS), containing 0.14 M NaCl, 0.01 M phosphate at pH 7.4, was prepared from tablets, with any further dilutions for reduced strength buffers being made with ELGA water.

##### 2.1.1 DNA

gWiz<sup>TM</sup> luc plasmid (6732 bps) containing the luciferase reporter gene was purchased from Aldevron, Fargo, USA. The plasmid was supplied at a concentration of 5.6 mg/ml, which was diluted to 1 mg/ml with water before use. It was used for all experiments unless otherwise specified. gWiz<sup>TM</sup> GFP plasmid (5757 bps) containing the green fluorescent protein reporter gene was purchased from Aldevron, Fargo, USA. The plasmid was supplied at a concentration of 4.23 mg/ml, which was diluted to 1 mg/ml with water before use. gWiz<sup>TM</sup> GFP plasmid was used for enzymatic degradation assay. Calf thymus DNA was purchased from Sigma (Poole, UK) and was purified before use for the membrane models interaction study. Calf thymus DNA was purified by ethanol precipitation and reconstituted prior to use by using dry ice-cold ethanol / 3 M sodium acetate (90/10) to 1ml of DNA solution (1 mg/ml). Relative purity can be determined by calculating the ratios of absorbance at 260 and 280 nm using UV spectroscopy. Pure DNA has the



ratio of 1.8, therefore the purity of the calf thymus DNA can be determined from  $(A_{260}/A_{280})/1.8$ . The actual concentration of the calf thymus DNA solutions can be determined using the following equation (1):

$$\text{concentration} = (50 \times \frac{A_{260} / A_{280}}{1.8} \times A_{260}) \times \text{Dilution factor } (\mu\text{g/ml}) \quad (1)$$

### 2.1.2 Polymers

DMA homopolymers, MPC homopolymers and DMA-MPC diblock copolymers were all synthesised within the group of Professor S. Armes (Department of Chemistry, The University of Sheffield, UK) according to the methods described in literature (Armes *et al.*, 2001, Ma *et al.*, 2003). All polymers were supplied as freeze-dried solids which were subsequently dissolved in ELGA water (1-10 mg/ml) and stored at -20°C. The chemical structures of the polymers are shown in Figure 2.1. Their relevant physical and chemical properties are shown in Table 2.1.

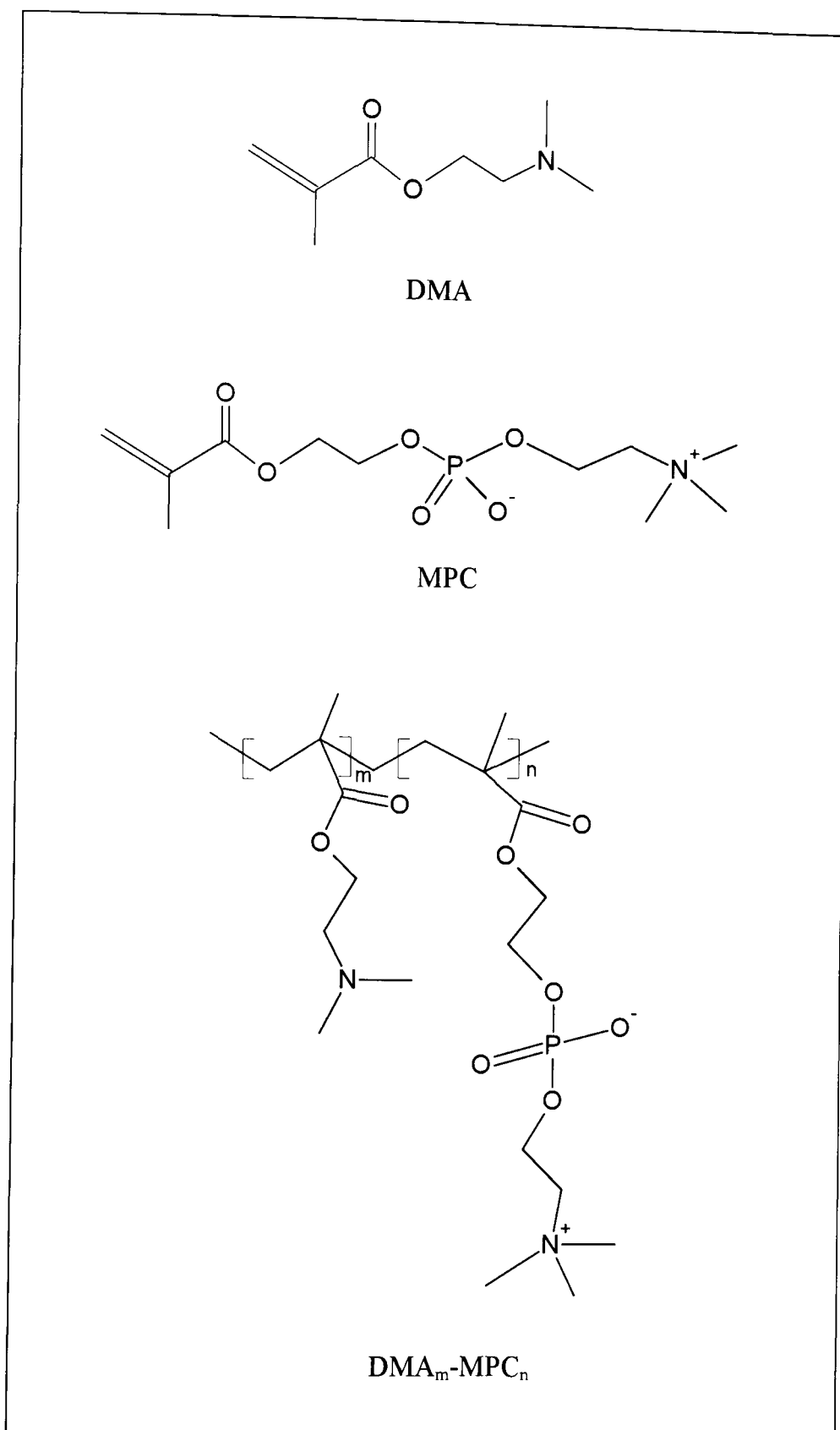


Figure 2.1 Chemical structures of 2-(dimethylamino)ethyl methacrylate (DMA), 2-(methacryloyloxyethyl phosphorylcholine) (MPC) and - (dimethylamino) ethyl methacrylate –(methacryloyloxyethyl phosphorylcholine) ( $\text{DMA}_m\text{-MPC}_n$ ) diblock copolymer.

**Table 2.1 Summary of properties for DMA homopolymer, MPC homopolymer and DMA-MPC diblock copolymers.**

Polymer	DMA (m)	MPC (n)	$M_n$	$M_w/M_n$	MPC % (wt %)
DMA homopolymer	81	-	12,700	1.07	0
MPC homopolymer	-	30	8,300	1.21	100
DMA <sub>40</sub> MPC <sub>10</sub>	40	10	9,000	1.21	32
DMA <sub>40</sub> MPC <sub>20</sub>	40	20	12,000	1.25	48
DMA <sub>40</sub> MPC <sub>40</sub>	40	40	18,000	1.26	65
DMA <sub>40</sub> MPC <sub>50</sub>	40	50	21,000	1.23	70
DMA <sub>10</sub> MPC <sub>30</sub>	10	30	10,000	1.28	85
DMA <sub>20</sub> MPC <sub>30</sub>	20	30	12,000	1.26	74
DMA <sub>40</sub> MPC <sub>30</sub>	40	30	15,000	1.26	58
DMA <sub>60</sub> MPC <sub>30</sub>	60	30	18,000	1.29	48
DMA <sub>100</sub> MPC <sub>30</sub>	100	30	24,000	1.32	36

## 2.2 GENERAL METHODS

### 2.2.1 Preparation of polymer – DNA complexes

Unless stated otherwise, all polymer – DNA complexes were prepared by the addition of a single aliquot of polymer solution to DNA in buffer solution, followed by vortexing of the mixture for 30 s. The amount of polymer required to produce complexes of a given monomeric unit: nucleotide ratio was calculated according to the equation below. It is noted that the monomeric unit of the polymer refers to the number of monomer of the cationic polymer, i.e. DMA polymer. In the case of DMA-MPC diblock copolymers, the proportion of MPC (by weight) has been taken into account of the calculation.

$$\text{Amount of polymer} = \frac{\text{Polymer monomer Mw} \times \text{ratio} \times \text{Amount of DNA}}{\text{DNA nucleotide Mw}} \quad (2)$$

The DNA nucleotide molecular weight was taken as 308.

### 2.2.2 Cell lines and routine subculture

A549 cells (human lung carcinoma) were provided by the Experimental Cancer Chemotherapy Group, University of Nottingham, UK. The cells were routinely cultured in RMPI-1640 medium supplemented with 10% newborn calf serum and antibiotic antimycotic solution (100 units/ml penicillin G, 0.1mg/ml streptomycin sulphate and 0.25µg/ml amphotericin B) at 37°C under 5% CO<sub>2</sub> in humidified air. The cells were sub-cultured twice a week at a 1:10 ratio, using Trypsin – EDTA as the dissociating agent.

### 2.2.3 Statistical analysis

Statistical analyses were performed to establish the significance of variation between sets of data using Prism Version 4 (GraphPad Software). Significance was set at  $P < 0.05$  using Unpaired Student's t test.

## 2.3 INSTRUMENTATION AND BASIC THEORY

### 2.3.1 Ethidium bromide displacement assay

Ethidium bromide (EtBr) displacement assay is frequently used to assess a compound's ability to bind with DNA by measuring the changes in the fluorescence of EtBr – DNA complexes (Le Pacq & Paoletti, 1967). EtBr is an intercalating agent commonly used as a nucleic acid stain in molecular biology. It is weakly fluorescent in water, but its intensity increases about 30-fold upon binding to DNA (Lokowicz, 1999). This is likely due to rigid stabilization of the phenyl moiety. EtBr binds with DNA by intercalation of the planar aromatic rings between the base pairs of DNA. When a cationic polymer is added to bind with DNA, the intercalated EtBr is displaced and the level of fluorescence decreases accordingly. The reduction of fluorescence therefore corresponds to the affinity of polymer – DNA binding.

### 2.3.2 Gel retardation assay

The gel retardation assay involves the use of electrophoresis technique to study the interaction between polymer and DNA. Electrophoresis refers to the movement of small ions and charged molecules in solution under the influence of an electric field. The rate of migrations depends on the size and charge of molecules. DNA has a negatively charged phosphate in every base in the sequence. It possesses a constant charge to size ratio. As a result, DNA molecules of all sizes migrate at a similar rate in liquid. Therefore, electrophoresis must be carried out in a medium with obstructive properties so that DNA molecules can be separated according to size. Agarose gel is a commonly used medium to perform electrophoresis of DNA. It consists of a solid matrix entrapping a buffer and exhibits a molecular sieving effect: smaller molecules experience fewer collisions with the matrix and pass through more rapidly.

When a cationic polymer is added to DNA, complexes are formed through electrostatic interaction. During electrophoresis, the negatively charged DNA migrates towards the positively charged anode whereas the positively charged polymer migrates towards the negatively charged cathode. EtBr is a commonly used fluorescent dye to visualize DNA bands in gel electrophoresis. It binds to free DNA so that DNA bands can be viewed under UV illumination. The polymer bands can also be viewed after being stained with the appropriate staining solution.

### **2.3.3 Zeta Potential Theory**

Zeta potential is a physical property exhibited by any particle in suspension. It is not the actual surface charge of the particle, but is closely related to it. Factors which alter zeta potential will affect surface charge; therefore the magnitude of the zeta potential can be used as a reliable indication of the surface charge of the particle. As shown in figure 2.2, the liquid layer surrounding a particle exists as two parts; an inner region, the Stern layer, where the ions are strongly bound, and an outer region, the diffuse layer, where they are loosely associated. Within the diffuse layer there is a notional boundary inside which the ions and particles form a stable entity. When a particle moves, ions within the boundary move with it. Those ions beyond the boundary stay with the bulk solution. The potential at this boundary is called the zeta potential (Lyklema 2000).

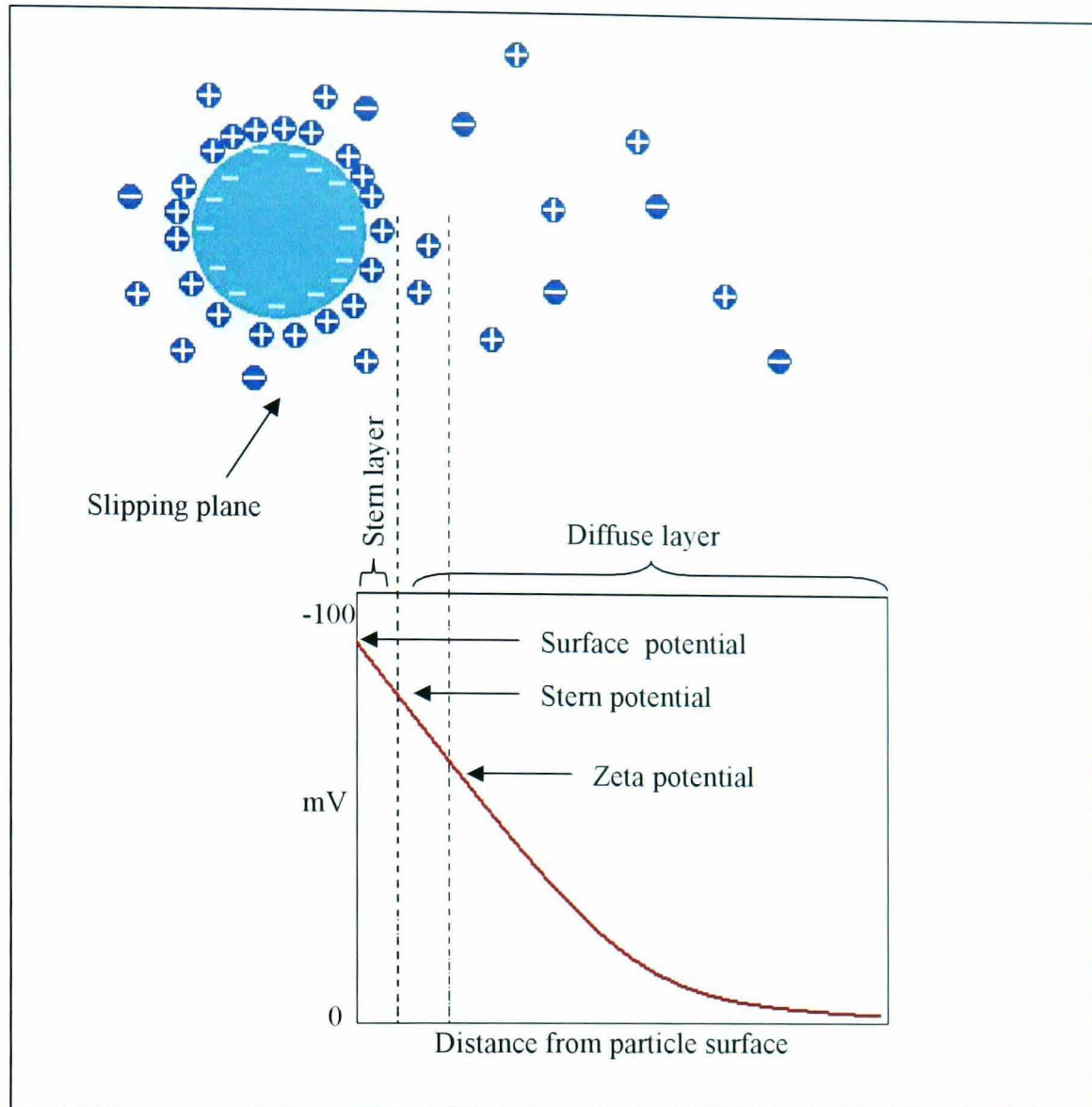


**Figure 2.2** Diagram showing the zeta potential of a charged particle.

Electrophoresis is the most commonly used method to determine the zeta potential. When an electric field is applied to an electrolyte, charged particles are attracted towards the electrode of opposite charge. The mobility of the particles is dependent on the strength of electric field, the dielectric constant of the medium, the viscosity of the medium and the zeta potential. Since the measurement of zeta potential is also dependent on the ionic strength of surrounding medium, as the ionic strength increases, the zeta potential decreases. In order to obtain zeta potential that are representative of the surface charge, it is best to perform measurements in low ionic strength buffers.



### 2.3.4 Photon correlation spectroscopy

Photon correlation spectroscopy (PCS) is a useful tool for particle size analysis for particles ranging from 10 nm up to a few micrometres in diameter. Its operation is based on the light scattering phenomenon. When small particles are illuminated by a beam of light, they will scatter it in all directions. The scattering intensity depends on the size of the particles and their optical properties. By measuring the intensity of light scattered, the particles size can be found by appropriate calculations (see below).

Particles in dispersions move due to a phenomenon known as ‘Brownian motions’. This motion occurs as the particles are bombarded by surrounding molecules. When a focused laser beam illuminates a small volume of the suspension of particles, due to the Brownian motion of particles, there are fluctuations in the scattering of light. Small particles move rapidly and so the fluctuations in the scattered light are rapid. In contrast, large particles move slowly and the scattered light fluctuations occur over a longer timescale. The movement of particles in suspension can be expressed in terms of ‘diffusion coefficient’. By knowing the change of scattering intensity over time, the diffusion coefficient could be obtained (Washington, 1992). According to the Stokes-Einstein equation (3), the diffusion coefficient is related to the particle diameter:

$$D = kt / 3\pi\eta d \quad (3)$$

*D = diffusion coefficient*

*k = Boltzmann's constant*

*t = absolute temperature*

*η = solvent viscosity*

*d = diameter of spherical particle*

Using the above equation, the diameter of particles can be found, with the assumptions that the particles are spherical in shape.

### 2.3.5 Transmission electron microscopy

Transmission electron microscopy (TEM) has been long established as a powerful tool to visualise the morphology of DNA condensates. It was first used to investigate how DNA is packaged in cell nuclei and viral particles (Haynes *et al.*, 1970, Gosule and Schellman, 1976). Later, this technique was adopted to study the DNA condensation by non-viral gene delivery system (Bloomfield 1996). TEM operates by flooding the sample with an electron beam and generating an image on a photographic plate beyond the sample. In order to visualise a sample in the TEM, one must have contrasting regions of electron transparency and electron opacity. This can be achieved by the use of a heavy metal stain, which possesses the ability to stop or strongly deflect the electrons so that they do not contribute to the final image

### 2.3.6 Atomic force microscopy

Since the invention of AFM in 1986 (Bennig *et al.*, 1986), it has developed rapidly and become popular for biological research (Hansma *et al.*, 1997). AFM uses the attractive or repulsive forces between tip and sample which cause the cantilever to deflect (Bennig *et al.*, 1986). A photo detector measures the cantilever deflection and from this information a map of the sample topography can be created. There are three main modes of AFM operation: contact, non-contact and tapping. The tapping mode was used in this study. It operates in the repulsive force region, but touches the surface only for short periods of time, in order to reduce damage to potentially fragile samples, such as biological molecules.

There are several advantages of AFM over TEM. First of all, it is possible to perform AFM imaging in aqueous environment, so that drying of the sample is not required. This allows the DNA complexes to be visualised in conditions much closer to the physiological environment. Also, staining is not necessary for AFM imaging. Thus, less sample manipulation is required

for AFM compared to TEM. Furthermore, three dimensional AFM images yield far more complete information than the two dimensional profiles provided by TEM images. However, there are still limitations with the use of AFM. The samples are needed to be adsorbed to a substrate; therefore the complexes that do not adhere cannot be imaged.

### **2.3.7 Flow cytometry**

A flow cytometer is generally referred to an instrument for detecting and measuring the amount of fluorescent dye on particles (figure 2.3). When a suspension of particles is loaded into the flow cytometer, they flow rapidly in a liquid stream which is regulated by the sheath fluid. The sheath fluid provides the supporting vehicle for directing particles through the flow system, so that the particles will be uniformly illuminated as they pass through the focused laser light beam. One unique feature of flow cytometry is that it measures fluorescence per single particle. This contrasts with the spectrophotometer in which the percent absorption and transmission of specific wavelengths of light is measured for a bulk volume of sample. When the fluorescent particles intercept the laser beam, the scattered and emitted light from the particles are converted to electrical pulses by optical detectors. The signals are then processed and analysed by a computer system (Givan 1992).

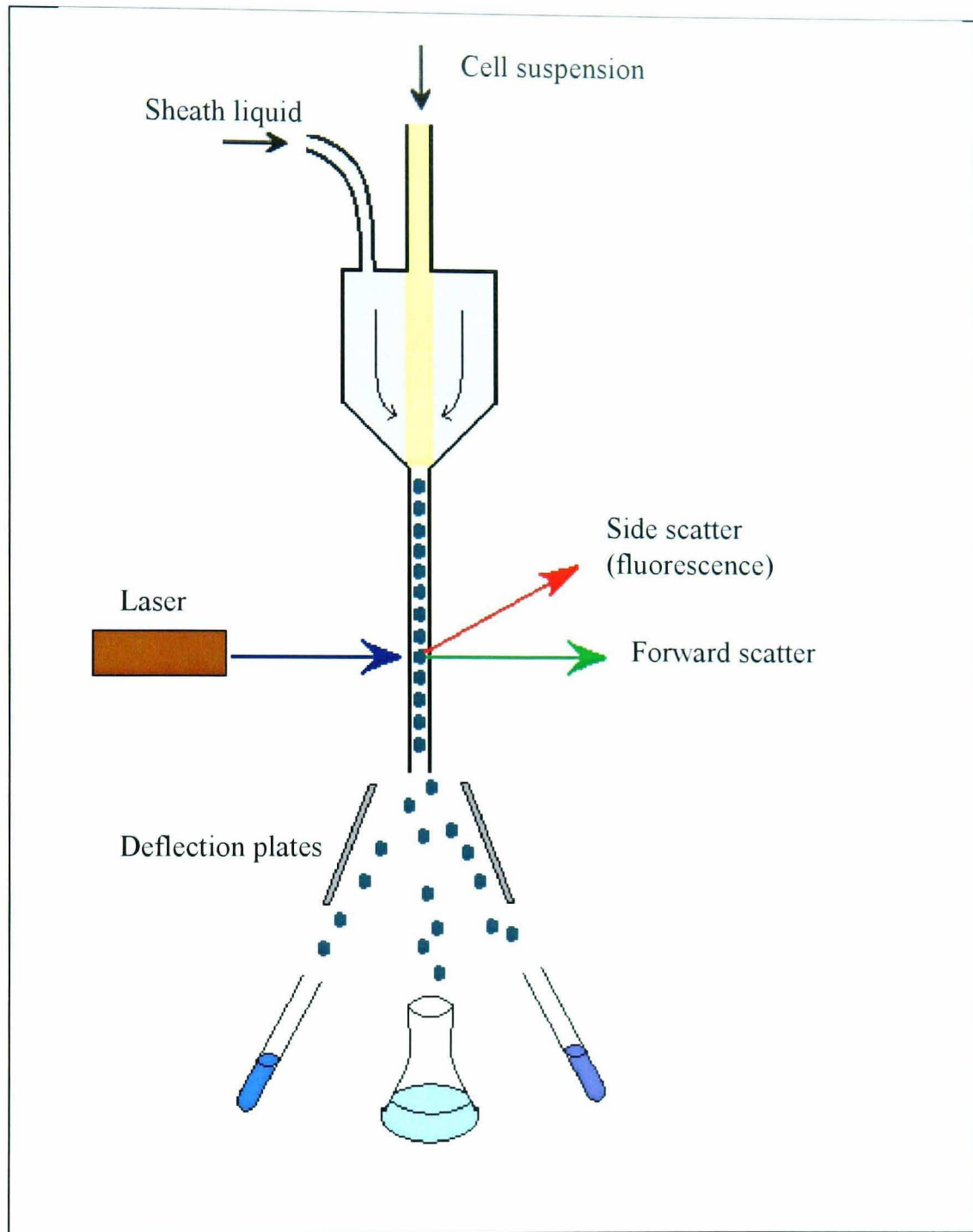


**Figure 2.3** Diagram showing the basic setup of a flow cytometry. One unique feature of flow cytometry is that it measures fluorescence per cell or particle. A focused beam of laser hits the moving cell and the light is scattered in all directions. Detectors receive the pulses of scattered light and they are converted into a form suitable for computer analysis and interpretation. Some flow cytometers are also "cell sorters" instruments which have the ability to selectively deposit cells from particular populations.

### 2.3.8 Laser scanning confocal microscopy

Confocal microscope has been frequently used in biological research (Amos and White, 2003), mainly because the technique enables visualisation deep within both living and fixed cells and tissues, and affords the ability to collect sharply defined optical sections without physically sectioning the cells or tissues. In addition, three-dimensional (3D) images of the specimens can be constructed. A schematic diagram of a typical confocal microscopy setup is shown in figure 2.4. When fluorescent specimens are imaged using a conventional widefield optical microscope, secondary fluorescence emitted by the specimen that is away from the region of interest often interferes with the resolution of those features that are in focus. This situation is especially problematic for thick specimens which have a thickness greater than 2 micrometers. The basic key to the confocal approach is the use of spatial filtering techniques to eliminate out of focus light or glare in specimens whose thickness exceeds the immediate plane of focus. This leads to a slight but significant improvement in both axial and lateral resolution.

Confocal microscopy offers several advantages over conventional optical microscopy, including the ability to control depth of field, elimination or reduction of background information away from the focal plane, and the ability to collect serial optical sections from thick specimens. With the confocal microscope, the  $z$  resolution, or optical sectioning thickness, depends on a number of factors: the wavelength of the excitation/emission light, pinhole size, numerical aperture of the objective lens, refractive index of components in the light path and the alignment of the instrument. The resolution of the confocal microscope is higher than in that found conventional optical microscope, but is still considerably less than that of the electron microscope. However, the electron microscope suffers from a lack of 3D information due to poor penetrating power of electrons. Therefore, confocal microscopy has become an important tool to bridge the gap between other microscopic techniques.

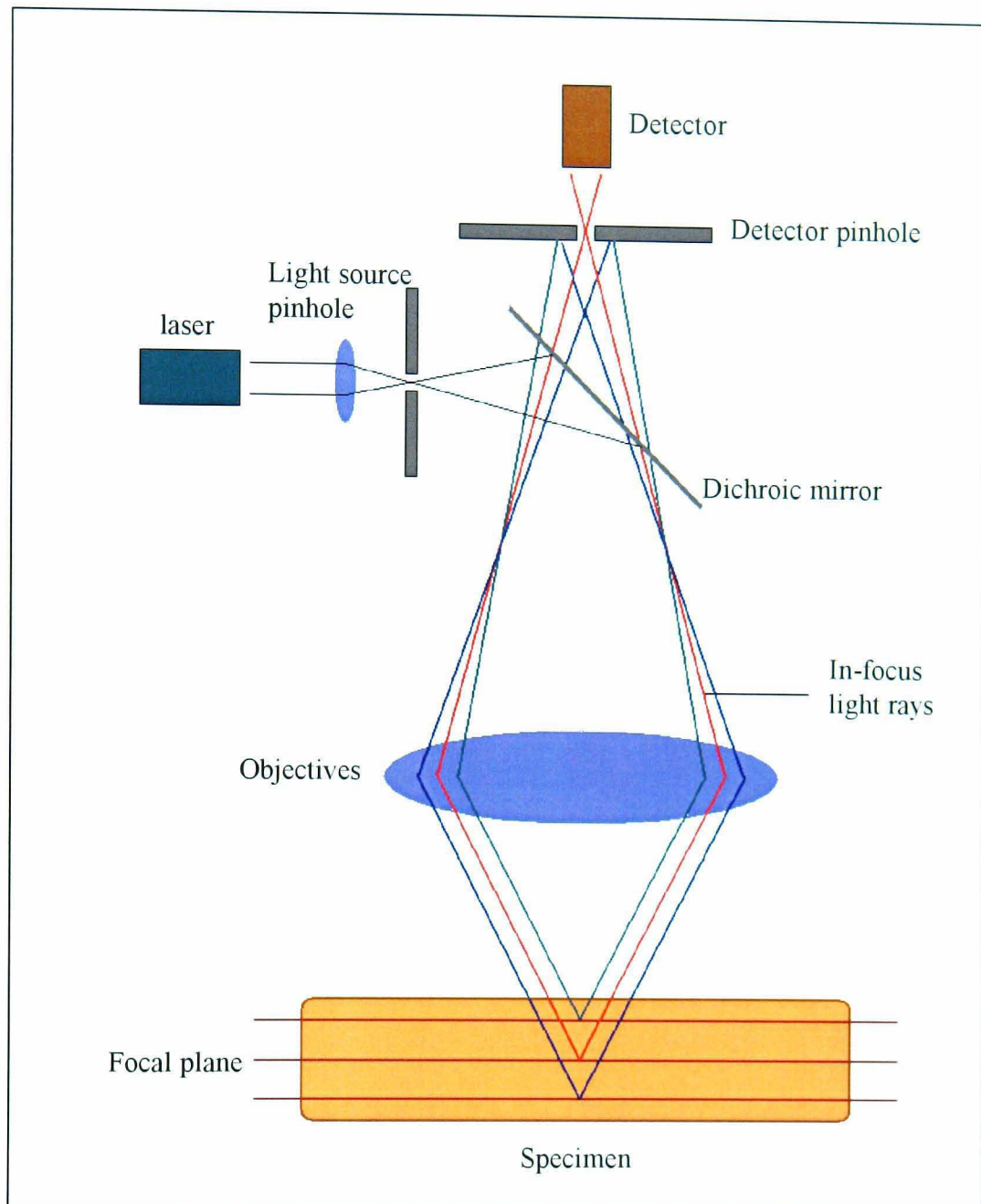


**Figure 2.4** Diagram showing the basic setup of a confocal microscope. The key feature of a confocal microscope is the ability to eliminate the out-of-focus information and collect serial optical sections from thick specimens. By having confocal pinholes, the microscope can efficiently reject the out of focus light. Only the light within the focal plane can be detected.

## CHAPTER 3

# PHYSICOCHEMICAL ANALYSIS OF DMA-MPC DIBLOCK COPOLYMER – DNA COMPLEXES

### 3.1 INTRODUCTION

For the development of non-viral gene delivery systems, it is essential to carry out the physicochemical characterisation in order to optimise the design of such a system for biological investigations. It also assists the understanding of the underlying mechanisms of the vector – DNA interaction.

The first criterion to be a potential non-viral gene delivery system is the ability to bind and form complexes with DNA effectively. The physicochemical properties of the resulting DNA complexes, such as surface charge and particle size can have a major influence on the efficiency of the system to deliver gene into the cells. In addition, the long term stability of the complexes, and the potential development of dried products, are equally important when the non-viral delivery system is to be developed into a commercial therapeutic product.

#### 3.1.1 Surface charge

The surface charge of a gene delivery system is a significant parameter affecting its ability to interact with cell surfaces. Since cell membranes are generally negatively charged, the overall positive charge of a delivery system can facilitate its association with cell membranes, and thus potentially enhance cellular uptake and transfection efficiency. In addition, charges on particles contribute to their colloidal stability, i.e., preventing aggregation of

DNA complexes. There is evidence suggesting that high positive zeta potential can facilitate the cellular uptake of DNA complexes and enhance their transfection efficiency *in vitro* (Godbey *et al.*, 1999, Gebhart and Kabanov, 2001, Choosakoonkriang *et al.*, 2003).

However, strongly charged particles are prone to opsonisation, which is one of the major barriers to successful gene delivery *in vivo*. Therefore, successful gene delivery systems could benefit from having a surface charge which is close to neutral. This can be possibly achieved by shielding of the surface charge of the complexes by a hydrophilic polymer. However, it is noted that other surface characteristics such as hydrophilicity also have important roles in preventing opsonins activation.

### **3.1.2 Particle size**

The particle size of DNA complexes plays an important role in cellular uptake. It is widely accepted that a small particle size is beneficial for efficient delivery of DNA into cells. Not only is endocytosis more efficient with particles size smaller than 150-200 nm, but the rate of movement in the cytoplasm was also found to be particle size dependent (Mahato *et al.*, 2000). In addition, particle size also plays a crucial role for biocompatibility, as small particles (around 100 nm) are more likely to evade from the RES (Harada-Shiba *et al.*, 2002, Adams *et al.*, 2003). Polyplexes have a tendency to aggregate in biological media even if they have an overall positive surface charge. Aggregation is also dependent on other parameters such as surface characteristics (hydrophilicity / hydrophobicity) of the polyplexes. Surface modification of DNA complexes by incorporation of a steric barrier can inhibit self – aggregation, reducing interactions between DNA complexes and blood components in the systemic circulation, and consequently preventing rapid elimination by the RES (Woodle and Lasic, 1992, Dash *et al.*, 1999, Ward *et al.*, 2002, Otsuka *et al.*, 2003).



### 3.1.3 Long-term stability

The high instability of non-viral gene delivery systems in liquid formulations has led to studies on freeze-dried (lyophilization) formulations in order to improve their long term stability (Anchordoquy *et al.*, 2001). The main concern with the freeze-dried complexes is whether they can retain the same properties as the freshly prepared complexes. Previous studies have shown that freeze-drying promotes aggregation, hence resulting in reduced transfection efficiency (Anchordoquy *et al.*, 1997, Talsma *et al.*, 1997). The use of sugar as a lyoprotectant has been reported to be effective in maintaining complex size as well as transfection efficiency (Cherng *et al.*, 1997, Brus *et al.*, 2004). Retention of particle size is important because it is known to be a major determinant of transfection efficiency in freeze-dried formulations. (Anchordoquy *et al.*, 1997, 1998).

### 3.1.4 Aims

The cationic DMA polymer has been previously demonstrated to bind and condense DNA effectively (van de Wetering *et al.*, 1998, Rungsardthong *et al.*, 2001). However, aggregation of the formed DNA complexes is the major problem associated with this system. A novel DMA-MPC diblock copolymer has been recently synthesized (Licciardi *et al.*, 2005). The zwitterionic MPC polymer is extremely biocompatible and hydrophilic (Ishihara *et al.*, 1998, Lewis, 2000). It is proposed in this study that MPC can be used as a potential steric stabilizer to the DNA complexes, thereby reducing complexes self -aggregation and producing small colloidal DNA complexes with particle size that is suitable for efficient cellular uptake.

Two series of DMA-MPC diblock copolymers were used in this study: (i) DMA<sub>x</sub>MPC<sub>30</sub> series in which the MPC block is constant with 30 monomeric units while the length of DMA block varies from 10 to 100 monomeric units, and (ii) DMA<sub>40</sub>MPC<sub>y</sub> series in which the DMA block is constant with 40

monomer units while the length of MPC block varies from 10 to 50 monomeric units. The aims of the work presented in this section were to investigate the effect of the compositions of the DMA-MPC diblock copolymers on the interaction with DNA, and the colloidal stability of the resulting complexes. DNA binding ability of the copolymer at different monomeric unit: nucleotide ratio was judged by ethidium bromide displacement assay and gel retardation assay. The physicochemical properties of the DNA complexes including particle size, zeta potential and colloidal stability of the DNA – complexes were also examined. Furthermore, the prospect of long term stability of the system was assessed by particle size measurement following freeze-drying of the complexes with the use of different lyoprotectants.

## 3.2 MATERIALS AND METHODS

### 3.2.1 Materials

Materials used were as described in Chapter 2, Section 2.1 unless otherwise specified below.

Tris acetate EDTA (TAE) buffer consisted of 40 mM Tris acetate, 20 mM glacial acetate acid and 1mM EDTA in ELGA water, with pH adjusted to 7.4 using glacial acetic acid. DNA loading buffer contained 0.25% w/v bromophenol blue in 40% w/v sucrose solution. The staining solution used in the gel retardation assay contained 0.1% w/v coomassie blue in 10% v/v glacial acetic acid and 50% v/v methanol, and the destaining solution contained 10% v/v methanol and 10% v/v glacial acetic acid.

### 3.2.2 Ethidium bromide displacement assay

Ethidium bromide (EtBr) (2  $\mu$ g) was added to 10% PBS (1 ml) in a fluorimetry cuvette and mixed by gentle agitation. The fluorescence of the solution was measured at an excitation wavelength of 560 nm and emission wavelength of 605 nm using Hitachi F-4500 fluorescence spectrophotometer (Hitachi Scientific Instruments, Finchampstead, UK). DNA (10  $\mu$ g) was added, the solution was mixed by gentle agitation and the fluorescence was measured again. Aliquots of the copolymer solution were then added in a stepwise manner, mixed gently and the fluorescence measured after each addition. The fluorescence readings for every sample were conducted in triplicate. The relative fluorescence was calculated as below (4):

$$\% \text{ Relative Fluorescence} = \frac{\text{Fluorescence (obs)} - \text{Fluorescence (EtBr)}}{\text{Fluorescence (DNA + EtBr)} - \text{Fluorescence (EtBr)}} \times 100 \quad (4)$$

Fluorescence (obs) = Fluorescence of DNA + EtBr + polymer

Fluorescence (EtBr) = Fluorescence of EtBr alone

Fluorescence (DNA + EtBr) = Fluorescence of DNA + EtBr

### 3.2.3 Gel retardation assay

Aliquots of the copolymer solutions of different volumes were added to the DNA solution (1 µg). TAE buffer was added to give the final volume (8 µl). Complexes were prepared over the following range of monomeric unit: nucleotide ratios: 0.25:1, 0.5:1, 0.75:1, 1.0:1, 1.25:1, 1.5:1, 1.75:1, 2.0:1, 5.0:1 and 10.0:1, while free polymer and free DNA served as controls. The samples were briefly mixed by vortexing and pulse-spun in a bench top microcentrifuge for 15 s. They were then incubated at room temperature for 30 min. DNA loading buffer (2 µl) was added to the samples, which were mixed and respun again. Samples were then loaded into 0.8% agarose gel (w/v) containing ethidium bromide (1 µg/ml). Electrophoresis was carried out at 70V in TAE buffer (pH 7.4) for 1 h. The DNA band was visualized under UV transillumination. Copolymers were stained by immersing the gel in staining solution for 1 h followed by washing with destaining solution overnight.

### 3.2.4 Zeta potential measurement

A solution of DNA (10µg) was added to 2% PBS solution (1 ml). An aliquot of DMA-MPC diblock copolymer solution was added and the samples were mixed by vortexing briefly to form complexes at 1:1, 2:1, 5:1 and 10:1 monomeric unit: nucleotide ratio (pH 7.4). Average zeta potential of the

sample was measured using Malvern Zetasizer 2000 (Malvern Instrument, Malvern, UK). Six measurements were made for each sample.

### 3.2.5 Particle size analysis

Solutions containing DNA (10 µg) were added to 10% PBS solution (500 µl, 0.2 µm filtered). An aliquot of DMA-MPC copolymer was added and the samples were mixed by vortexing briefly to form complexes at 0.2:1, 0.3:1, 0.5:1, 0.6:1, 0.7:1, 0.8:1, 0.9:1, 1.0:1, 2.0:1 and 5.0:1 monomeric unit: nucleotide ratios (pH 7.4). The average particle size, scattering intensity and polydispersity of the complexes were measured using a Malvern 4700 PCS system (Malvern Instrument, Malvern, UK). The measurements were performed at 25 °C, using a 40.6 mW argon-ion laser at a scattering angle of 90°. The data were obtained by using CONTIN analysis. Triplicate measurements were made for each sample.

### 3.2.6 Long term stability of polymer – DNA complexes

#### 3.2.6.1 Preparation of lyoprotectant containing complexes

Two approaches were adopted to prepare the lyoprotectant – containing DNA complexes solution. In the first approach, the lyoprotectant (sucrose or glucose) was added into the buffer before the formation of complexes. The solution of 40% w/v lyoprotectant was added to 10% PBS (pH 7.4) to give a final lyoprotectant concentration of 1%, 2% 5%, 10%, 15%, 20% and 25% w/v. The samples were mixed by brief vortexing for 1 min. DNA solution (20 µg) was then added, followed by the addition of the polymer solution. The samples were mixed again by brief vortexing for 1 min. In the second approach, the lyoprotectant was added after the formation of complexes. DNA solution (20 µg) was added to 10% PBS, followed by the addition of polymer solution. The samples were mixed by brief vortexing for 1 min.

40% w/v lyoprotectant was then added to give a final concentrations same as above. In this set of experiments, DMA<sub>60</sub>MPC<sub>30</sub> copolymer was used. All polymer – DNA complexes were prepared at 2:1 monomeric unit: nucleotide ratio and the final volume of each sample was 1000 µl. All the samples were allowed to stand at room temperature for 30 min before being subjected to analysis.

### 3.2.6.2 Freeze-drying of complexes and particle size measurements

The particle size of the polymer – DNA complexes prepared by both methods, as described in section 3.2.6.1 were measured using PCS as described earlier in section 3.2.5. Measurements were made both before and after freeze-drying of the complexes. To freeze-dry the polymer – DNA complexes, the samples were cooled rapidly by plunging into liquid nitrogen for 2 min. The samples were then transferred into a freeze drier (Modulyo, Edwards, UK) where they were placed under vacuum at temperature -40°C. The samples were allowed to dry in the freeze drier for 48 h. Following freeze drying, the samples were re-hydrated by adding 10% PBS (1000 µl, 0.2 µm filtered). The samples were then mixed by brief vortexing and the particle size was determined using PCS.

### 3.3 RESULTS

#### 3.3.1 Ethidium bromide displacement assay

As shown in figure 3.1 and 3.2, DMA homopolymer and all of the DMA-MPC diblock copolymers were able to induce a reduction in EtBr fluorescence, indicating the ability of these copolymers to bind with DNA. For all systems, the fluorescence level was 100% before the addition of the polymer. Typically, there was a steep fall in fluorescence for monomeric unit: nucleotide ratios from 0 to 1:1, except for the DMA<sub>10</sub>MPC<sub>30</sub> diblock copolymer. As the ratios were further increased, the fluorescence continued to decrease gradually and eventually reached a plateau. For DMA<sub>10</sub>MPC<sub>30</sub>, the reduction of fluorescence was only observed at ratio above 0.6:1, suggesting its decreased DNA binding ability relative to the other copolymers. Interestingly, MPC homopolymer was also found to displace EtBr, albeit to a minor extent. A shallow decrease in fluorescence was observed starting from an approximate 1:1 monomeric unit: nucleotide ratio, indicating that excess MPC homopolymer was required to promote interaction with DNA.

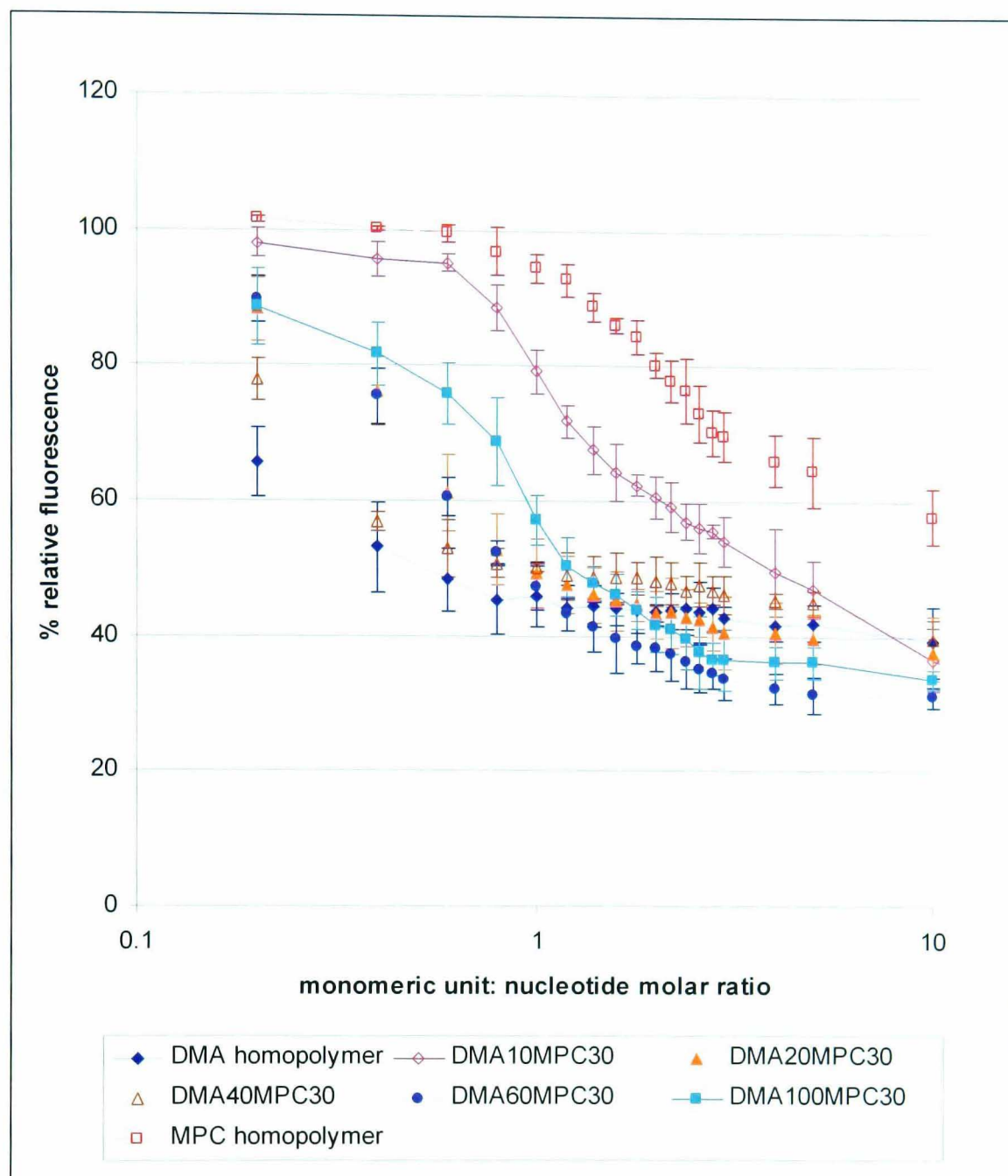


**Figure 3.1 EtBr displacement assay of  $\text{DMA}_x\text{MPC}_{30}$  copolymer series.** DMA homopolymer, MPC homopolymer or a series of  $\text{DMA}_x\text{-MPC}_{30}$  diblock copolymer was added to EtBr–DNA complexes at monomeric unit: nucleotide ratios of 0.2, 0.4, 0.6, 0.8, 1.0, 1.2, 1.4, 1.6, 1.8, 2.0, 2.2, 2.4, 2.6, 2.8, 3.0, 4.0, 5.0 and 10:1, and the fluorescence level was expressed in %. Initial relative fluorescence is equal to 100% ( $n=3$ ).



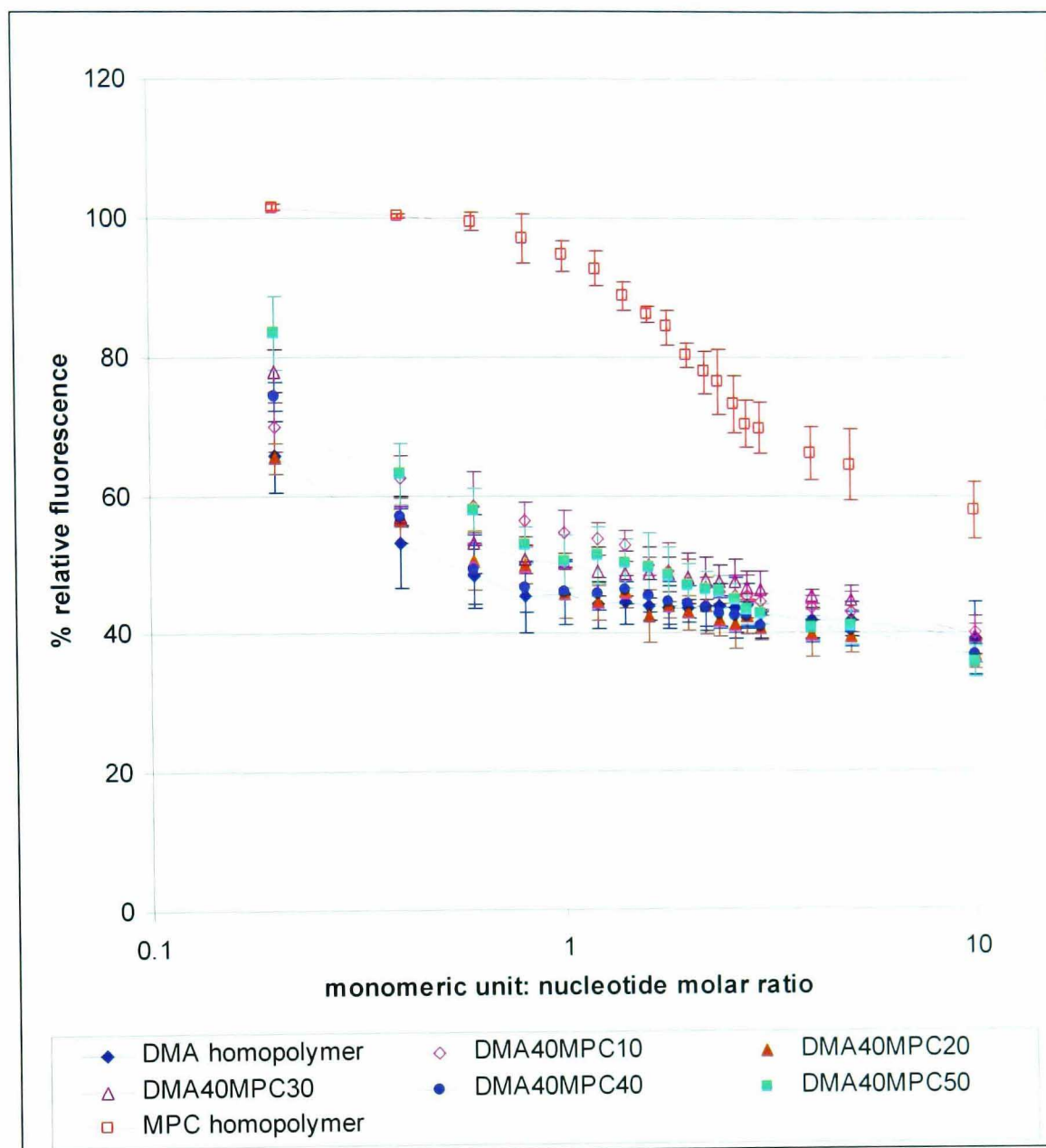


**Figure 3.2 EtBr displacement assay of DMA<sub>40</sub>MPC<sub>y</sub> copolymer series.** DMA homopolymer, MPC homopolymer or a series of DMA<sub>40</sub>-MPC<sub>y</sub> diblock copolymer was added to EtBr -DNA complexes at monomeric unit: nucleotide ratios of 0.2, 0.4, 0.6, 0.8, 1.0, 1.2, 1.4, 1.6, 1.8, 2.0, 2.2, 2.4, 2.6, 2.8, 3.0, 4.0, 5.0 and 10:1, and the fluorescence level was expressed in %. Initial relative fluorescence is equal to 100% (n=3).

### 3.3.2 Gel retardation assay

Figure 3.3 and 3.4 show the results obtained for the two series of DMA-MPC diblock copolymers, DMA and MPC homopolymer. The upper image shows the migration of free plasmid and the lower image shows the migration of free polymers. With the exception of the MPC homopolymer, the results follow the same general pattern: DNA bands were observed at low monomeric unit: nucleotide ratios, indicating the presence of free plasmid. As the amount of copolymer increased, the free plasmid bands gradually became dimmer, indicating that more plasmid became complexed with the copolymer, until the plasmid bands eventually disappeared. From this point onwards, although no free DNA migrated from the loading well, fluorescence could still be observed within the well. This indicates the presence of partially complexed DNA in the system, with some binding sites remaining available for EtBr complexation, but the high molecular weight and/or the overall neutrality of these complexes prevented their migration out of the well. In some systems, no fluorescence was detected within the loading well at high monomeric unit: nucleotide ratios, suggesting that the plasmid binding sites were almost completely occupied by the copolymer so that the EtBr – DNA interaction is prevented. Considering the copolymers behaviour in the system, free copolymer bands were absent at low ratios, indicating that the free copolymer is occupied in complexing with the DNA. However, free non-complexed copolymer could be detected at higher ratios, particularly for copolymers containing relatively high MPC portion, such as DMA<sub>40</sub>MPC<sub>40</sub> and DMA<sub>40</sub>MPC<sub>50</sub>.

The effect of the copolymer composition on DNA binding is evident. For DMA homopolymer (figure 3.3), DNA bands disappeared at ratio of 0.5:1 and excess polymer appeared at ratio 2:1. ‘Full complexation’ (no fluorescence in the well could be detected) occurred at a 5:1 ratio. In the DMA<sub>40</sub>MPC<sub>x</sub> copolymer series, the free DNA band disappeared at a relatively low molar ratio of 0.5:1 for DMA<sub>40</sub>MPC<sub>10</sub> (which has the shortest MPC chain) and ‘full complexation’ was achieved at a 5:1 molar ratio, since

no fluorescence was detected in the well under these conditions. At ratios between 0.5:1 and 2:1 the complexes remained in the well, as the overall charge of the complexes may be neutral and/or they were too large to move through the gel. Excess free copolymer appeared at a 5:1 molar ratio, indicating the association of 'excess' polymer (not engaged in binding DNA) with the complex. In general, the performance of DMA<sub>40</sub>MPC<sub>10</sub> is very similar to that observed for DMA homopolymer. However, as the MPC length was gradually increased, the complexing ability of the copolymers appeared to be impeded. Thus free DNA bands were observed for DMA<sub>40</sub>MPC<sub>20</sub>, DMA<sub>40</sub>MPC<sub>30</sub> and DMA<sub>40</sub>MPC<sub>40</sub> at ratios higher than for DMA homopolymer and 'full complexation' was not reached even at high ratios (fluorescence detected in the wells), suggesting that copolymers with higher MPC content were unable to complex DNA sufficiently to prevent EtBr intercalation. In addition, non-complexed copolymer appeared at lower molar ratios as the MPC block length was increased, indicating that the affinity of the copolymer molecules to associate with the complexes decreased.

MPC homopolymer did not complex considerably with DNA, since free DNA bands were observed at all molar ratios (figure 3.4). In the copolymer series with a constant MPC size (DMA<sub>y</sub>MPC<sub>30</sub>), intermediate DNA bands were observed for DMA<sub>10</sub>MPC<sub>30</sub> at monomeric: nucleotide ratios up to 1.25:1, whereupon the DNA bands disappeared and the complexes remained in the loading well. 'Full complexation' was not achieved, as fluorescence could be still detected in the well at a high ratio of 10:1. Similar behaviour is observed for the DMA<sub>20</sub>MPC<sub>30</sub> diblock copolymer as fluorescence was observed in the well at all ratios, indicating that the DNA was not 'fully' condensed even when using a significant excess of copolymer. For DMA<sub>60</sub>MPC<sub>30</sub> and DMA<sub>100</sub>MPC<sub>30</sub> copolymers, which consisted of longer DMA chain, free DNA bands disappeared at lower ratios and copolymer bands appeared at higher ratios, indicating higher complexing affinity.

Furthermore, an interesting phenomenon was observed in the gels for DMA<sub>10</sub>MPC<sub>30</sub> and DMA<sub>20</sub>MPC<sub>30</sub> copolymers: fluorescence smears were seen towards the cathodic side of the gel ratios ranging from 1.25:1 to 10:1 and 1:1 to 10:1, respectively. This indicates formation of overall positively charged complexes of partially complexed DNA with the molecular size of the complexes being small enough to migrate out from the well.

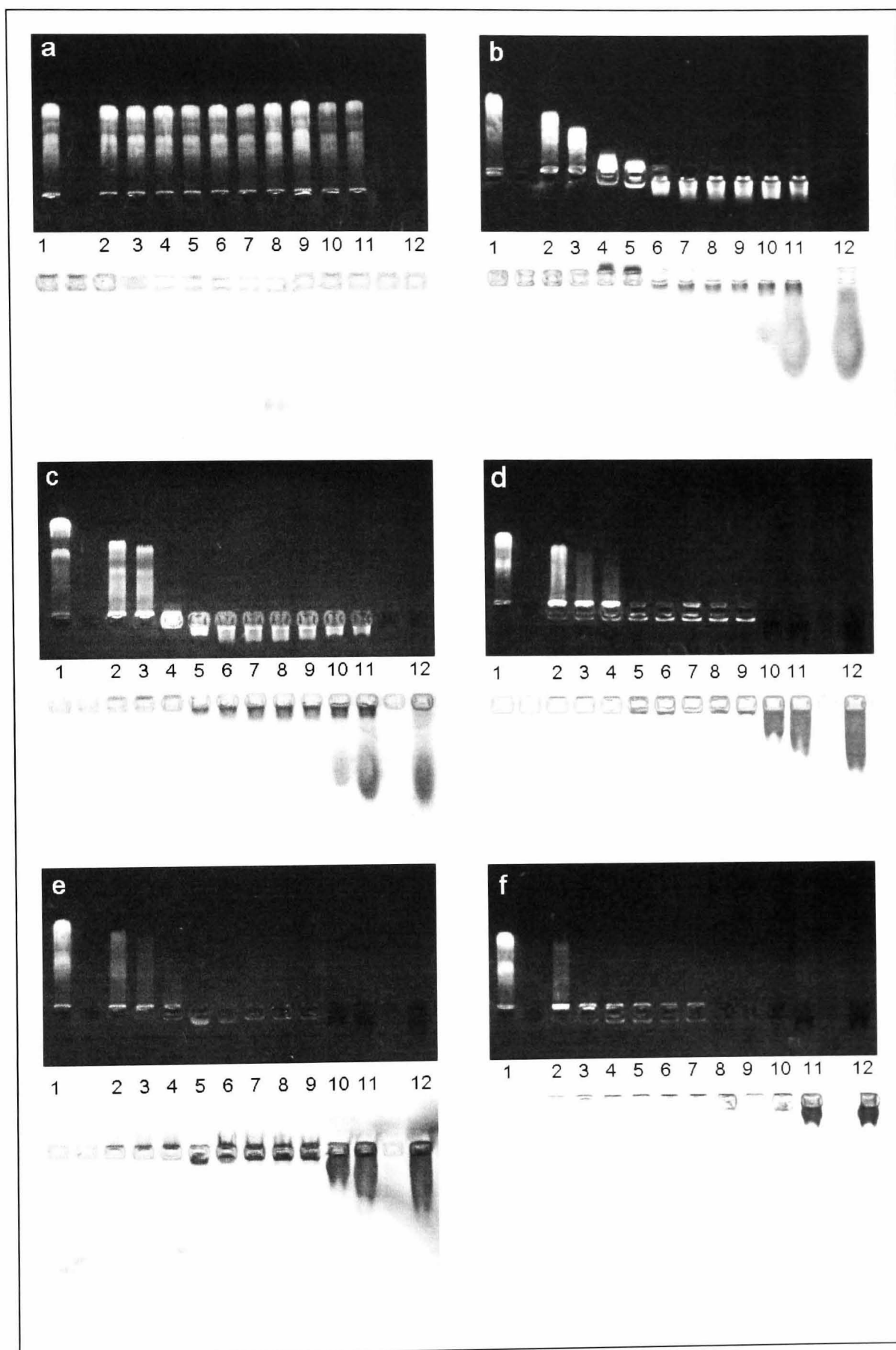


**Figure 3.3** Agarose gel retardation assay for  $\text{DMA}_x\text{MPC}_{30}$  copolymer series. Lane 1 is the DNA control. Lanes 2-11 correspond to 0.25:1, 0.5:1, 0.75:1, 1:1, 1.25:1, 1.5:1, 1.75:1, 2:1, 5:1 and 10:1 monomeric unit: nucleotide ratio. Lane 12 is the polymer control. (a) MPC homopolymer, (b)  $\text{DMA}_{10}\text{MPC}_{30}$ , (c)  $\text{DMA}_{20}\text{MPC}_{30}$ , (d)  $\text{DMA}_{40}\text{MPC}_{30}$ , (e)  $\text{DMA}_{60}\text{MPC}_{30}$  and (f)  $\text{DMA}_{100}\text{MPC}_{30}$ .

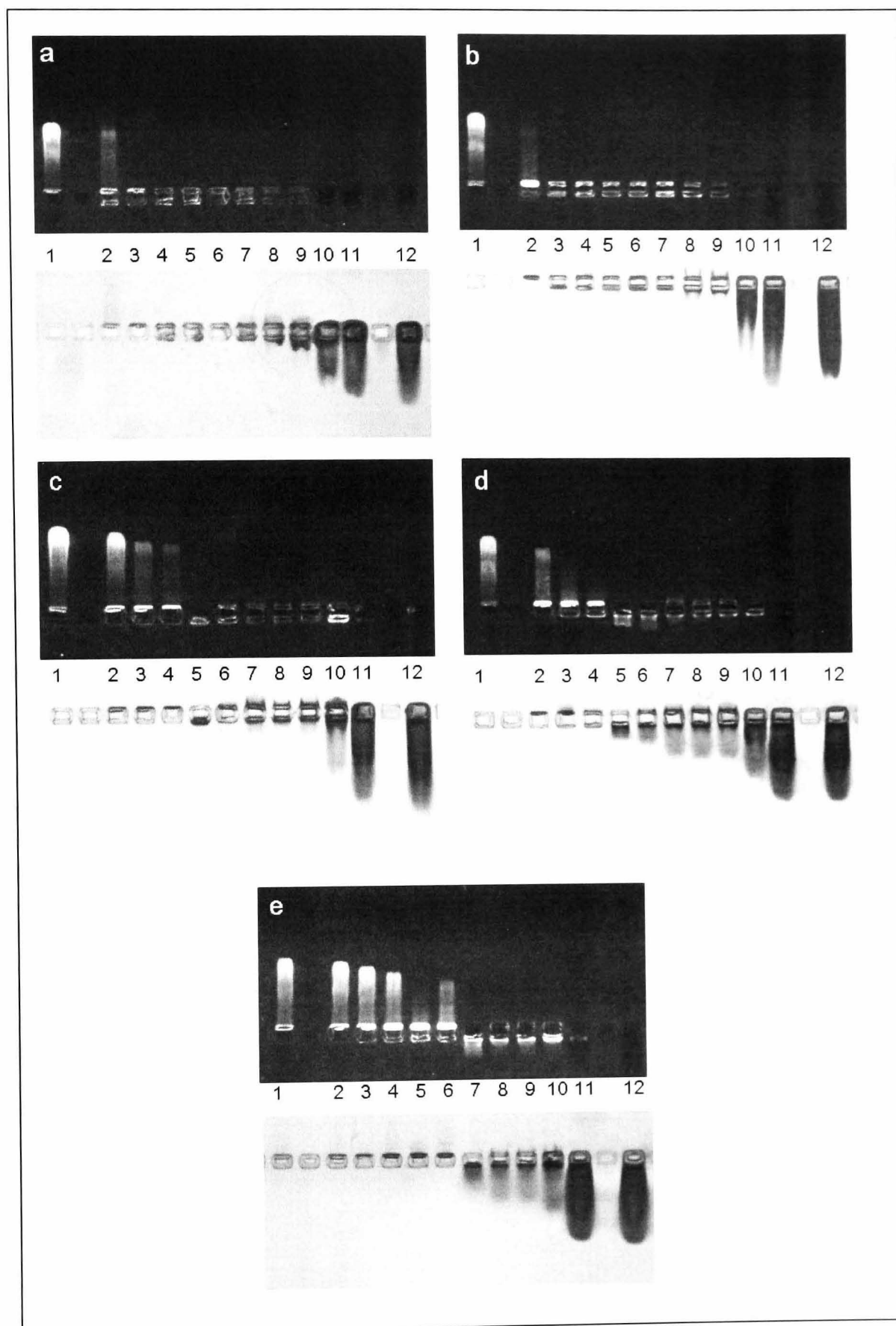


**Figure 3.4** Agarose gel retardation assay for  $\text{DMA}_{40}\text{MPC}_y$  copolymer series. Lane 1 is the DNA control. Lanes 2-11 correspond to 0.25:1, 0.5:1, 0.75:1, 1:1, 1.25:1, 1.5:1, 1.75:1, 2:1, 5:1 and 10:1 monomeric unit: nucleotide ratio. Lane 12 is the polymer control. (a) DMA homopolymer, (b)  $\text{DMA}_{40}\text{MPC}_{10}$ , (c)  $\text{DMA}_{40}\text{MPC}_{20}$ , (d)  $\text{DMA}_{40}\text{MPC}_{40}$  and (e)  $\text{DMA}_{40}\text{MPC}_{50}$ .

### 3.3.3 Zeta potential measurement

Figure 3.5 and 3.6 show the zeta potential measurements obtained for  $\text{DMA}_x\text{MPC}_{30}$  and  $\text{DMA}_{40}\text{MPC}_y$  complexed with plasmid DNA respectively. It is noted that the zeta potential measurement of DMA homopolymer – DNA complexes was not possible due to the formation of highly aggregating complexes. Both sets of results show a general trend that as monomeric units: nucleotide ratios increased, average zeta potentials increased. For all copolymer systems, apart from  $\text{DMA}_{40}\text{MPC}_{50}$ , the zeta potentials were around zero at 1:1 monomeric unit: nucleotide. At ratio 2:1 and onwards, the zeta potentials were around +10 mV, and the values were either increased slightly as ratios increased or remained relatively constant. For  $\text{DMA}_{40}\text{MPC}_{50}$ , the zeta potential was around -5mV at ratio 1:1. At ratio 2:1, the zeta potential was around zero and increased gradually as the ratio increased. For the  $\text{DMA}_x\text{MPC}_{30}$  copolymer series, zeta potentials of the complexes were not significantly different between the three different copolymers ( $p>0.05$ ), indicating that the length of DMA did not have significant effect on the zeta potentials of the complexes. For the  $\text{DMA}_{40}\text{MPC}_y$  copolymer series, there appears to be a trend whereby systems with longer chain of MPC have lower zeta potential compared with those with shorter MPC. This suggests that the hydrophilic stabilising layer formed by the MPC may contribute to the shielding effect of the of the DNA complexes.

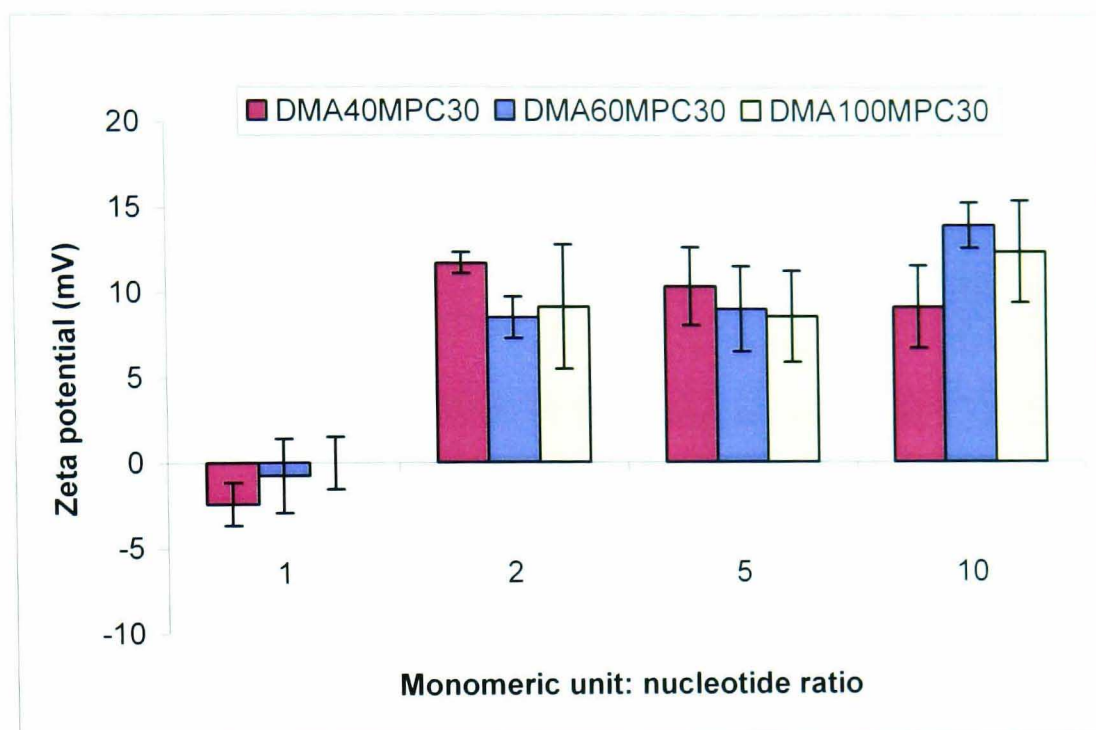


**Figure 3.5 Zeta potential measurements of  $\text{DMA}_x\text{MPC}_{30}$  – DNA complexes.** The complexes were formed between  $\text{DMA}_{40}\text{MPC}_{30}$ ,  $\text{DMA}_{60}\text{MPC}_{30}$  or  $\text{DMA}_{100}\text{MPC}_{30}$  and luciferase plasmid at 1:1, 2:1, 5:1 and 10:1 monomeric unit: nucleotide ratios. Complexes were prepared and measured in 2% (v/v) PBS (n=6).

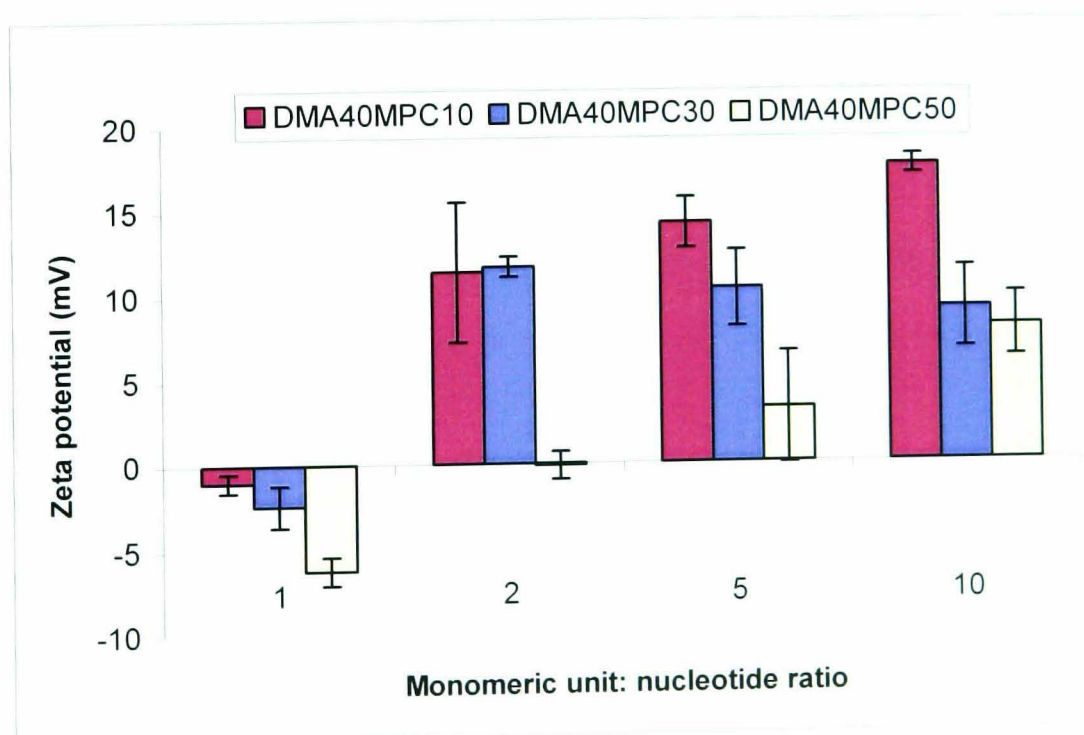


**Figure 3.6 Zeta potential measurements of  $\text{DMA}_{40}\text{MPC}_y$  – DNA complexes.** The complexes were formed between  $\text{DMA}_{40}\text{MPC}_{10}$ ,  $\text{DMA}_{40}\text{MPC}_{30}$  or  $\text{DMA}_{40}\text{MPC}_{50}$  and luciferase plasmid at 1:1, 2:1, 5:1 and 10:1 monomeric unit: nucleotide ratios. Complexes were prepared and measured in 2% (v/v) PBS (n=6).



### 3.3.4 Particle size analysis

In this study, the particle size of polymer – DNA complexes was measured using photon correlation spectroscopy (PCS). The mean diameter, scattering intensity and polydispersity data for complexes prepared at various monomeric unit: nucleotide ratios are shown in tables 3.1 and 3.2. The DNA complexes formed by the DMA homopolymer had particle diameters of around 150 to 200 nm at low monomeric unit: nucleotide ratios. However, once the ratio reached 0.9:1, the mean particle size increased dramatically to above 1  $\mu\text{m}$ . The scattering intensity was also increased. These data suggest that colloidal aggregation occurred once the complexes are close to neutrality and charge stabilization of the complexes was insufficient.

For DMA-MPC copolymers, the complex particle size depended critically on the copolymer composition. The behaviour of the DMA<sub>40</sub>MPC<sub>10</sub> copolymer was very similar to that of the DMA homopolymer. The mean particle diameter was around 150 nm and was well controlled up to a molar ratio of 0.7:1. At higher ratios, the particle size increased to over 300 nm. With the exception of the DMA<sub>10</sub>MPC<sub>30</sub> and DMA<sub>40</sub>MPC<sub>50</sub>, all other DMA-MPC copolymers typically produced complexes of around 140-160 nm diameters, with the size being well controlled at higher monomeric unit: nucleotide ratios. The polydispersities generally ranged from 0.2 to 0.4, and were significantly lower than that observed with DMA homopolymer. This indicates that discrete colloidal complexes were formed with relatively narrow size distributions.

Table 3.1 Particle size, scattering intensity and polydispersity of DNA complexes with DMA homopolymer and DMA<sub>x</sub>MPC<sub>30</sub> measured by PCS

Monomer: Nucleotide molar ratio	Particle size ± SD (nm) (Polydispersity ± SD)				
	Scattering intensity (KCps) ± SD				
	DMA10MPC30	DMA20MPC30	DMA40MPC30	DMA60MPC30	DMA100MPC30
0.2 : 1	566 ± 5 (1.0±0)	175 ± 8.7 (0.50±0.02)	145 ± 1 (0.26±0.02)	162 ± 12 (0.62±0.09)	131 ± 12 (0.34±0.16)
	38 ± 3	70 ± 12	1801 ± 31	149 ± 12	556 ± 261
0.3 : 1	130 ± 7 (0.36±0.02)	245 ± 17 (0.59±0.05)	145 ± 17 (0.35±0.12)	137 ± 1 (0.37±0.01)	119 ± 2 (0.24±0.01)
	88 ± 6	92 ± 7	256 ± 3	520 ± 6	456 ± 10
0.5 : 1	151 ± 23 (0.65±0.11)	250 ± 19 (0.68±0.05)	180 ± 3 (0.35±0.02)	144 ± 11 (0.46±0.10)	149 ± 13 (0.24±0.04)
	68 ± 4	130 ± 6	270 ± 7	770 ± 21	1215 ± 186
0.6 : 1	119 ± 10 (0.41±0.06)	138 ± 3 (0.35±0.02)	260 ± 3 (0.44±0.01)	128 ± 5 (0.25±0.03)	131 ± 1 (0.15±0.0)
	78 ± 7	108 ± 6	574 ± 9	993 ± 23	146 ± 26
0.7 : 1	102 ± 17 (0.75 ± 0.44)	162 ± 5 (0.42±0.03)	192 ± 6 (0.41±0.04)	151 ± 4 (0.36±0.05)	148 ± 5 (0.17±0.08)
	186 ± 9	155 ± 9	651 ± 15	1336 ± 7	1654 ± 169
0.8 : 1	157 ± 9 (0.51 ± 0.03)	149 ± 2 (0.34±0.01)	152 ± 2 (0.28±0.01)	150 ± 9 (0.30±0.09)	181 ± 19 (0.26±0.03)
	349 ± 17	153 ± 14	632 ± 4	1666 ± 60	1527 ± 59
0.9 : 1	149 ± 7 (0.52 ± 0.03)	155 ± 2 (0.37±0.01)	158 ± 2 (0.33±0.01)	152 ± 3 (0.25±0.04)	120 ± 0 (0.12±0.03)
	371 ± 15	173 ± 3	338 ± 5	1555 ± 6	1122 ± 195
1.0 : 1	294 ± 88 (0.88 ± 0.19)	141 ± 2 (0.22±0.01)	130 ± 1 (0.22±0.01)	154 ± 2 (0.21±0.02)	130 ± 10 (0.17±0.03)
	509 ± 72	288 ± 5	416 ± 6	1341 ± 4	1599 ± 659
2.0 : 1	202 ± 60 (0.70 ± 0.25)	127 ± 1 (0.30 ± 0.01)	136 ± 1 (0.32±0.01)	113 ± 3 (0.35±0.03)	141 ± 4 (0.21±0.03)
	418 ± 54	416 ± 3	587 ± 10	927 ± 27	1468 ± 62
5.0 : 1	395 ± 159 (0.69±0.24)	123 ± 0 (0.31±0.01)	151 ± 1 (0.37 ± 0.01)	137 ± 13 (0.49±0.1)	125 ± 9 (0.21±0.01)
	386 ± 46	359 ± 4	591 ± 20	987 ± 58	1052 ± 104

Table 3.2 Particle size, scattering intensity and polydispersity of DNA complexes with DMA homopolymer and DMA<sub>40</sub>MPC<sub>Y</sub> measured by PCS

Monomer:nucleotide molar ratio	Particle size $\pm$ SD (nm) (Polydispersity $\pm$ SD)		Scattering intensity (KCps) $\pm$ SD		
	DMA homopolymer	DMA <sub>40</sub> MPC <sub>10</sub>	DMA <sub>40</sub> MPC <sub>20</sub>	DMA <sub>40</sub> MPC <sub>40</sub>	DMA <sub>40</sub> MPC <sub>50</sub>
	<b>0.2:1</b>	226 $\pm$ 2 (0.40 $\pm$ 0.01) 292 $\pm$ 2	152 $\pm$ 2 (0.22 $\pm$ 0.02) 342 $\pm$ 13	251 $\pm$ 42 (0.78 $\pm$ 0.08) 346 $\pm$ 10	143 $\pm$ 9 (0.33 $\pm$ 0.11) 203 $\pm$ 3
<b>0.3:1</b>	178 $\pm$ 8 (0.39 $\pm$ 0.06) 453 $\pm$ 11	146 $\pm$ 1 (0.21 $\pm$ 0.02) 479 $\pm$ 6	202 $\pm$ 14 (0.55 $\pm$ 0.05) 655 $\pm$ 19	118 $\pm$ 4 (0.33 $\pm$ 0.10) 244 $\pm$ 9	147 $\pm$ 3 (0.3 $\pm$ 0.05) 528 $\pm$ 167
<b>0.5:1</b>	168 $\pm$ 3 (0.38 $\pm$ 0.04) 527 $\pm$ 7	144 $\pm$ 2 (0.21 $\pm$ 0.01) 635 $\pm$ 8	206 $\pm$ 27 (0.49 $\pm$ 0.07) 1038 $\pm$ 75	138 $\pm$ 10 (0.31 $\pm$ 0.01) 361 $\pm$ 8	157 $\pm$ 2 (0.26 $\pm$ 0.04) 603 $\pm$ 5
<b>0.6:1</b>	154 $\pm$ 2 (0.32 $\pm$ 0.02) 739 $\pm$ 11	186 $\pm$ 2 (0.20 $\pm$ 0.01) 1194 $\pm$ 18	192 $\pm$ 11 (0.53 $\pm$ 0.06) 1434 $\pm$ 71	160 $\pm$ 27 (0.26 $\pm$ 0.09) 463 $\pm$ 17	173 $\pm$ 16 (0.26 $\pm$ 0.04) 612 $\pm$ 20
<b>0.7:1</b>	196 $\pm$ 5 (0.30 $\pm$ 0.01) 1911 $\pm$ 23	198 $\pm$ 8 (0.23 $\pm$ 0.09) 1045 $\pm$ 17	219 $\pm$ 8 (0.59 $\pm$ 0.03) 1339 $\pm$ 38	154 $\pm$ 20 (0.43 $\pm$ 0.20) 565 $\pm$ 36	187 $\pm$ 32 (0.48 $\pm$ 0.05) 589 $\pm$ 20
<b>0.8:1</b>	540 $\pm$ 140 (0.46 $\pm$ 0.07) 2659 $\pm$ 25	201 $\pm$ 12 (0.24 $\pm$ 0.10) 853 $\pm$ 38	242 $\pm$ 21 (0.63 $\pm$ 0.05) 1320 $\pm$ 80	139 $\pm$ 1 (0.24 $\pm$ 0.03) 694 $\pm$ 9	182 $\pm$ 32 (0.48 $\pm$ 0.05) 564 $\pm$ 25
<b>0.9:1</b>	1704 $\pm$ 99 (0.69 $\pm$ 0.10) 2226 $\pm$ 69	309 $\pm$ 62 (0.53 $\pm$ 0.41) 925 $\pm$ 39	214 $\pm$ 12 (0.49 $\pm$ 0.06) 1671 $\pm$ 52	145 $\pm$ 4 (0.29 $\pm$ 0.05) 786 $\pm$ 33	286 $\pm$ 31 (0.48 $\pm$ 0.05) 564 $\pm$ 39
<b>1.0:1</b>	1412 $\pm$ 172 (0.5 $\pm$ 0.04) 2687 $\pm$ 69	356 $\pm$ 10 (0.36 $\pm$ 0.04) 1656 $\pm$ 27	208 $\pm$ 6 (0.45 $\pm$ 0.04) 1964 $\pm$ 33	143 $\pm$ 2 (0.21 $\pm$ 0.01) 733 $\pm$ 12	242 $\pm$ 34 (0.41 $\pm$ 0.19) 514 $\pm$ 39
<b>2.0:1</b>	1105 $\pm$ 138 (0.54 $\pm$ 0.06) 2714 $\pm$ 53	375 $\pm$ 7 (0.43 $\pm$ 0.04) 1563 $\pm$ 22	186 $\pm$ 5 (0.33 $\pm$ 0.03) 1792 $\pm$ 34	146 $\pm$ 2 (0.3 $\pm$ 0.02) 545 $\pm$ 10	357 $\pm$ 35 (0.49 $\pm$ 0.25) 476 $\pm$ 20
<b>5.0:1</b>	1437 $\pm$ 179 (0.57 $\pm$ 0.05) 2687 $\pm$ 40	377 $\pm$ 9 (0.43 $\pm$ 0.06) 1600 $\pm$ 36	204 $\pm$ 9.7 (0.42 $\pm$ 0.06) 1510 $\pm$ 74	165 $\pm$ 15 (0.31 $\pm$ 0.01) 518 $\pm$ 27	380 $\pm$ 41 (0.49 $\pm$ 0.25) 456 $\pm$ 50

In comparison to other copolymers, the DNA complexes with the DMA<sub>10</sub>MPC<sub>30</sub> copolymer were initially (at ratio 0.2:1) large (~ 500 nm), polydisperse (1.0) and producing weak scattering intensity. As the ratio increased, the particle size decreased to approximately 120 to 150 nm, whereas the scattering intensity increased gradually. When the ratio reached above 1.0:1, the particle size increased to around 300 nm with the scattering intensity continuing to increase. A similar trend was observed for the DNA complexes formed by the DMA<sub>40</sub>MPC<sub>50</sub> copolymer, another copolymer with high proportion of MPC content.

### 3.3.5 Long term stability of polymer – DNA complexes

The DMA<sub>60</sub>MPC<sub>30</sub> copolymer was chosen for the long term stability study of DNA complexes due to its promising DNA condensation and steric stabilising properties as shown in the previous studies. The DNA complexes (at 2:1 monomeric unit: nucleotide ratio) were prepared with a varying concentration of sucrose or glucose (lyoprotectant) and the size of complexes were measured before and after freeze-drying. DNA complexes in the absence of sugar were prepared as control. The results are shown in tables 3.3 – 3.6.

The presence of sugar affects the particle size in the freshly prepared samples (before freeze-drying). When sugar was first added into the buffer before the formation of DNA complexes, particle size increased gradually with sugar concentration. The particle size of complexes was around 120 nm without sugar, and complexes size increased gradually with sugar concentration. With 25% w/v sugar (glucose or sucrose), the particle size increased to above 200 nm, which was significantly larger compared to the sample without sugar. A similar effect was observed when sugar was added after the formation of complexes, but to a lesser extent.

After freeze-drying and subsequent rehydration, DNA complexes in the absence of sugar formed large aggregates (~2 µm) with high polydispersity, indicating that freeze-drying promoted aggregation of complexes. In the presence of sugar, there was a marked decrease in particle size of freeze-dried complexes following rehydration, confirming the importance of sugar in preserving particle size. The particle size was comparable to the corresponding unfrozen control at around 2% -10% w/v sugar. There was no substantial change in particle size and polydispersity as the sugar concentration further increased.

In comparing the two method of lyoprotectant containing complexes preparation, when sugar was added first into the buffer (before formation of

DNA complexes), a higher sugar concentration was necessary to preserve particle size compared to those with sugar added after the formation of DNA complexes. When sucrose or glucose was first added, a sugar concentration of 5% or 10% w/v respectively was required to preserve particle size during freeze drying. However, when the sugar was added after formation of complexes, 2% w/v sugar concentration (for both sucrose and glucose) was sufficient to preserve particle size.

**Table 3.3 The effect of sucrose as lyoprotectant on particle size, with sucrose added before complexes formation.** The particle size, scattering intensity and polydispersity of DMA<sub>60</sub>MPC<sub>30</sub>-DNA complexes were measured by PCS before and after freeze-drying.

Sucrose % w/v	Particle size (nm)		Scattering Intensity (KCps)		Polydispersity	
	Before	After	Before	After	Before	After
0	123 ± 7	1922 ± 647	312 ± 15	29 ± 1	0.37 ± 0.1	0.84 ± 0.2
1	121 ± 5	1699 ± 640	311 ± 7	87 ± 7	0.33 ± 0.1	0.96 ± 0.1
2	125 ± 2	729 ± 161	375 ± 8	59 ± 2	0.24 ± 0.0	0.95 ± 0.2
5	183 ± 2	211 ± 10	282 ± 4	304 ± 7	0.37 ± 0.0	0.44 ± 0.1
10	181 ± 3	220 ± 9	325 ± 10	351 ± 8	0.21 ± 0.1	0.37 ± 0.1
15	188 ± 2	231 ± 17	256 ± 5	271 ± 15	0.20 ± 0.0	0.45 ± 0.1
20	176 ± 16	362 ± 26	224 ± 4	217 ± 7	0.4 ± 0.1	0.32 ± 0.1
25	241 ± 13	289 ± 32	263 ± 7	315 ± 14	0.29 ± 0.1	0.37 ± 0.1

**Table 3.4 The effect of sucrose as lyoprotectant on particle size, with sucrose added after complexes formation.** The particle size, scattering intensity and polydispersity of DMA<sub>60</sub>MPC<sub>30</sub>-DNA complexes were measured by PCS before and after freeze-drying.

Sucrose % w/v	Particle size (nm)		Scattering Intensity (KCps)		Polydispersity	
	Before	After	Before	After	Before	After
0	123 ± 7	1922 ± 647	313 ± 15	29 ± 1	0.37 ± 0.1	0.84 ± 0.2
1	109 ± 0	473 ± 30	278 ± 23	56 ± 2	0.22 ± 0.1	0.61 ± 0.1
2	97 ± 1	254 ± 7	320 ± 5	735 ± 20	0.22 ± 0.1	0.47 ± 0.0
5	155 ± 15	214 ± 26	242 ± 28	379 ± 24	0.49 ± 0.1	0.53 ± 0.1
10	205 ± 2	248 ± 5	592 ± 5	777 ± 26	0.18 ± 0.0	0.31 ± 0.0
15	181 ± 13	220 ± 23	381 ± 15	494 ± 34	0.31 ± 0.1	0.38 ± 0.1
20	190 ± 13	192 ± 6	305 ± 23	451 ± 5	0.33 ± 0.1	0.33 ± 0.0
25	256 ± 5	297 ± 8	241 ± 7	418 ± 25	0.27 ± 0.0	0.44 ± 0.1

**Table 3.5 The effect of glucose as lyoprotectant, with glucose added before complexes formation.** The particle size, scattering intensity and polydispersity of DMA<sub>60</sub>MPC<sub>30</sub>-DNA complexes were measured by PCS before and after freeze-drying.

Glucose % w/v	Particle size (nm)		Scattering Intensity (KCps)		Polydispersity	
	Before	After	Before	After	Before	After
0	123 ± 7	1922 ± 647	312 ± 15	29 ± 1	0.37 ± 0.1	0.84 ± 0.2
1	193 ± 15	1514 ± 619	262 ± 6	62 ± 12	0.46 ± 0.1	1.0 ± 0.0
2	187 ± 9	445 ± 36	286 ± 8	73 ± 6	0.40 ± 0.1	0.79 ± 0.1
5	197 ± 11	368 ± 25	265 ± 20	516 ± 13	0.58 ± 0.1	0.57 ± 0.0
10	194 ± 6	211 ± 7	300 ± 10	617 ± 39	0.28 ± 0.1	0.27 ± 0.0
15	191 ± 15	285 ± 27	137 ± 6	218 ± 8	0.44 ± 0.1	0.48 ± 0.1
20	238 ± 11	237 ± 4	144 ± 0	217 ± 7	0.10 ± 0.0	0.36 ± 0.0
25	221 ± 15	312 ± 20	155 ± 7	533 ± 18	0.36 ± 0.1	0.52 ± 0.1

**Table 3.6 The effect of glucose as lyoprotectant, with glucose added after complexes formation.** The particle size, scattering intensity and polydispersity of DMA<sub>60</sub>MPC<sub>30</sub>-DNA complexes were measured by PCS before and after freeze-drying.

Glucose % w/v	Particle size (nm)		Scattering Intensity (KCps)		Polydispersity	
	Before	After	Before	After	Before	After
0	123 ± 7	1922 ± 647	312 ± 15	29 ± 1	0.37 ± 0.1	0.84 ± 0.2
1	98 ± 1	616 ± 75	182 ± 17	93 ± 2	0.35 ± 0.0	0.86 ± 0.1
2	131 ± 17	251 ± 59	182 ± 9	94 ± 6	0.40 ± 0.1	0.77 ± 0.2
5	101 ± 3	150 ± 2	205 ± 4	337 ± 4	0.20 ± 0.0	0.35 ± 0.0
10	134 ± 1.0	150 ± 4	229 ± 5	267 ± 3	0.29 ± 0.0	0.33 ± 0.0
15	160 ± 13	174 ± 5	264 ± 10	273 ± 6	0.37 ± 0.1	0.33 ± 0.1
20	180 ± 7	196 ± 4	312 ± 2	340 ± 10	0.30 ± 0.0	0.3 ± 0.0
25	191 ± 2	242 ± 17	247 ± 2	272 ± 1	0.29 ± 0.0	0.21 ± 0.1



### 3.4 DISCUSSION

#### 3.4.1 Characterisation of polymer – DNA complexes

DMA based copolymers have been extensively studied for gene delivery in recent years. The DMA – PEG diblock copolymers with various architectures have also been investigated in order to address the poor colloidal stabilities of DNA complexes produced by DMA homopolymers and improve their biological properties (van de Wetering *et al.*, 1998, Rungsardthong *et al.*, 2001). The DMA-MPC diblock copolymers described herein offer a potential alternative chemical structure for conferring the necessary steric stabilization.

The DMA<sub>x</sub>MPC<sub>30</sub> copolymer series was used to explore the effect of systematically varying the DMA block size on the DNA binding and condensation efficiency. DMA<sub>10</sub>MPC<sub>30</sub> interacted with DNA, but with reduced affinity compared to other copolymers and DMA homopolymer, as shown in both EtBr displacement assay and gel retardation assay. In a previous study, it was reported that a DMA homopolymer with a mean degree of polymerisation of 32 was able to condense DNA at the experimental pH of 8.0, at which the polymer was approximately 24 % protonated. This corresponded to only eight cationic residues per DMA chain (Rungsardthong *et al.*, 2003). Thus it appears that the presence of the MPC block, rather than the relatively short DMA block, is the reason for the relatively weak DNA binding affinity shown by DMA<sub>10</sub>MPC<sub>30</sub>. However, the charge distribution along the chain should also be considered. At pH 8, DMA with a degree of polymerisation of 32 (24% protonation) has charge distributed widely along the chain of DMA polymer (figure 3.7), which is different from DMA<sub>10</sub>MPC<sub>30</sub> at pH 7.4 (>55 % protonation) (figure 3.8). Thus, a minimum length of DMA may still be required to condense DNA. Therefore, it is still possible that the length of DMA in DMA<sub>10</sub>MPC<sub>30</sub> is simply not long enough to achieve efficient DNA condensation.

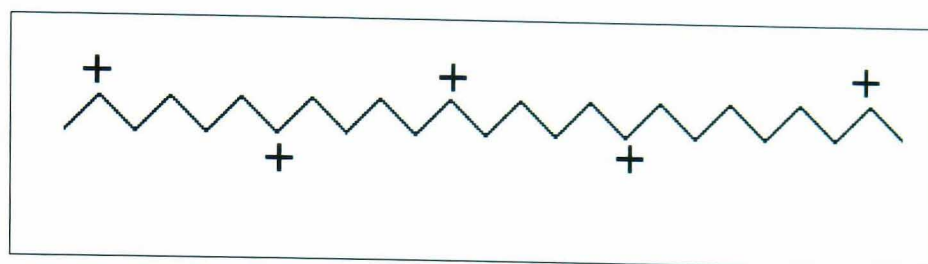


**Figure 3.7** Schematic diagram to show the charge distribution along the chain of DMA<sub>32</sub> at pH 8.

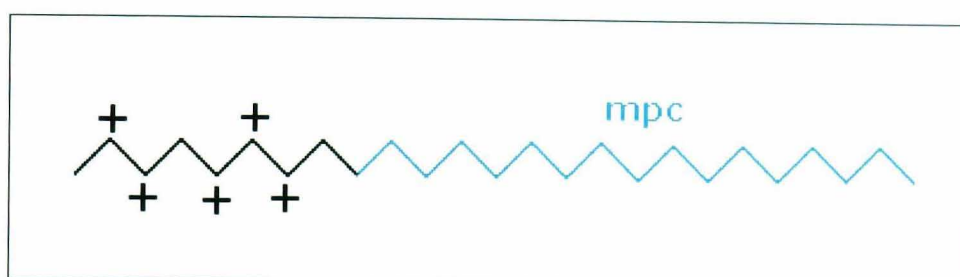


**Figure 3.8** Schematic diagram to show the charge distribution along the chain of DMA<sub>10</sub>MPC<sub>30</sub> at pH 7.4.

Increasing the size of DMA moiety resulted in higher condensation ability, as indicated by gel retardation assays. In addition, copolymers with relatively high DMA content associated with the complexes at ratios above 1:1 and, consequently, the complexes would be expected to possess positive surface charge, as confirmed by the zeta potential measurements, even though the charge was partially screened by the MPC layer. With the exception of DMA<sub>10</sub>MPC<sub>30</sub>, all the copolymers investigated in the DMA<sub>x</sub>MPC<sub>30</sub> series formed DNA complexes in sub-200 nm particle size range. However, light scattering data indicated that longer DMA block lengths lead to the formation of less ‘soluble’ complexes. DNA complexes formed with DMA<sub>60</sub>MPC<sub>30</sub>

and DMA<sub>100</sub>MPC<sub>30</sub> have relatively high scattering intensities, which suggests formation of fairly compact DNA condensates.

In the DMA<sub>40</sub>MPC<sub>y</sub> copolymer series, the cationic moiety possessed a corresponding size comparable to DMA-PEG diblock copolymers which have previously demonstrated to condense DNA (van de Wetering *et al.*, 1998). The effects that varying the MPC size may have on the copolymers' binding and condensing ability, and the effectiveness of MPC to provide steric stabilization were studied. The data demonstrate that as the size of MPC moiety increased, the DNA binding ability of the copolymers was reduced. The EtBr displacement and gel retardation assays clearly showed that copolymers with shorter MPC blocks (DMA<sub>40</sub>MPC<sub>10</sub> and DMA<sub>40</sub>MPC<sub>20</sub>) had higher DNA binding affinities, comparable to the DMA homopolymer. Full complexation was achieved (as indicated by the disappearance of fluorescence within the well) and 'excess' of polymer associated with the complexes at ratios above 1:1.

Copolymers with longer MPC blocks (DMA<sub>40</sub>MPC<sub>30</sub>, DMA<sub>40</sub>MPC<sub>40</sub> and DMA<sub>40</sub>MPC<sub>50</sub>) exhibited decreased affinity for DNA complexation, suggesting that the size of zwitterionic MPC residues was deleterious to complexation. Also, 'excess' of polymer immediately above 1:1 ratio is seen as free in the retardation gels, contrary to the homopolymer and copolymers with low MPC content. Similar behaviour was observed with DMA-PEG diblock copolymers in a separate study (Rungsardthong *et al.*, 2001). Both phenomena suggest that the presence of a steric stabilising moiety in the copolymer reduces the association of 'excess' polymer with the complexes. MPC molecule is strongly hydrated, with approximately 12 water molecules per MPC residue (Ishihara *et al.*, 1998, Konno *et al.*, 2001). Thus the space that MPC occupies, together with associated water surrounding MPC chains, may produce steric hindrance during DNA complexation. Furthermore, complexes with longer MPC chains had lower (less positive) zeta potential, suggesting the charge shielding effect offered by the MPC molecules.

Although the MPC moiety appeared to hinder DNA complexation and condensation, it nevertheless prevents aggregation by imparting steric stabilization of the complexes. DNA complexes with the DMA<sub>40</sub>MPC<sub>10</sub> copolymer formed aggregates, as indicated by particle size data. However, the DMA<sub>40</sub>MPC<sub>20</sub> complexes were somewhat less aggregated compare to DMA<sub>40</sub>MPC<sub>10</sub> complexes. Both DMA<sub>40</sub>MPC<sub>30</sub> and DMA<sub>40</sub>MPC<sub>40</sub> formed complexes with hydrodynamic diameters of approximately 150 nm diameter and aggregation was no longer observed. Although the zeta potential of DMA<sub>40</sub>MPC<sub>10</sub> – DNA complexes was more positive than that of DMA<sub>40</sub>MPC<sub>30</sub>, the hydrophobic interactions between the former complexes were sufficiently strong that they overcome the electrostatic repulsion, resulting in self-aggregation. On the other hand, DMA<sub>40</sub>MPC<sub>30</sub> – DNA complexes with lower zeta potentials were able to remain discrete due to the presence of steric stabilizer formed by the hydrophilic MPC. It appeared that 30 to 40 monomeric units of MPC are sufficient to prevent complex aggregation and provide effective steric stabilization. Further increase in the size of the MPC block in DMA<sub>40</sub>MPC<sub>50</sub> copolymer resulted in larger complexes with a higher polydispersity. Together with the results from the gel retardation assay and EtBr displacement assay, it is suggested that the complexes formed with DMA<sub>40</sub>MPC<sub>50</sub> were less well condensed than the other complexes in the same series. This is probably due to the presence of large the MPC block which hinders the interaction between cationic DMA block and the negatively charged DNA.

Interestingly, the addition of MPC homopolymer at high molar ratios led to reduced fluorescence from DNA-EtBr complexes, suggesting some, albeit relatively weak, ability to interact with DNA when present in significant excess. The MPC repeat unit comprises a zwitterionic PC group, so it is tempting to suggest that the cationic quaternary amine group might be responsible for the DNA interaction. However, the formation of MPC-DNA complexes is not supported by the gel retardation assay data. It may be possible that if these relatively weak MPC-DNA ‘complexes’ were formed.

they could dissociate relatively easily due to the electric current applied during electrophoresis.

The above observations demonstrate that the balance in the block composition plays a primary role in influencing DNA condensation by the DMA-MPC copolymers. Comparing copolymers with the same DMA:MPC block ratio but different overall size is instructive. A higher degree of DNA condensation (the respective gel retardation assays) and effective steric stabilization was observed for DMA<sub>60</sub>MPC<sub>30</sub>, relative to DMA<sub>40</sub>MPC<sub>20</sub>. Similarly, the DMA<sub>20</sub>MPC<sub>30</sub> and DMA<sub>40</sub>MPC<sub>50</sub> copolymers have comparable (though not precisely the same) DMA:MPC block ratios. Although the latter copolymer has a significantly longer condensing cationic block, its DNA complexing ability is comparable to that of DMA<sub>20</sub>MPC<sub>30</sub>. These comparisons illustrate that both the overall size of the copolymer molecule and the DMA to MPC block ratio are affecting the DNA binding and condensing performance of these copolymers.

### **3.4.2 Freeze-dried formulations to enhance long term stability of DNA complexes**

In order to investigate the prospect of long term stability of the DNA delivery system, DNA complexes were subjected to freeze-drying with the use of lyoprotectants and the particle sizes of the complexes were assessed using PCS. It was noticed that the presence of sugar affected the particle size of the DNA complexes before freeze-drying. One of the possible explanations is that the presence of sugar and the consequently increased viscosity might hinder the formation of complexes between the polymer and DNA (Tajmir-Riahi *et al.*, 1994). It was reported that the interaction between DNA and sugar results in a conformational change of DNA (Washington 1992), which may also affect the affinity of DNA to interact with the polymer. In addition, during PCS measurements, the value of the viscosity of the medium was not

adjusted, which would result in the viscosity value used in the size data calculation being inadequate.

After freeze-drying and rehydration, DNA complexes without sugar as lyoprotectant resulted in the formation of large aggregates. It is believed that aggregation occurred as particles were concentrated in the unfrozen fraction during freeze-drying. The rate of freezing has been reported to have a significant impact on the size of freeze-dried complexes (Anchordoquy *et al.*, 1998, Li *et al.*, 2000). During slow freezing, the formation of large ice crystals allows complexes to concentrate in the unfrozen solution for a longer time, and thus aggregation is facilitated. In contrast, when freezing is rapid, smaller ice crystals are formed and less aggregation is observed. In our study, all the samples were frozen rapidly in liquid nitrogen first before being transferred into a freeze-drier. Aggregation during the freezing stage was minimized. Formation of large aggregates might have also occurred during dehydration and rehydration.

From the results, sugars were found to be effective in preserving the size of DNA complexes. The exact mechanism is not certain. The most accepted hypothesis is the particle isolation hypothesis, which suggested that sugars inhibit aggregation by isolating individual particles in the unfrozen fraction (Allison *et al.*, 2000). Here, it was found that the concentration of sugar also affected the size of particles. At low sugar concentration of 1% w/v, there was a slight reduction in particle size but the amount of sugar was insufficient to fully prevent aggregation. As the sugar concentration increased, the particle size, as well as the polydispersity, decreased gradually. The volume of unfrozen fraction was larger in samples with a greater amount of sugar. This effect may contribute to the progressively smaller particle size observed at higher sugar concentrations as the particles were less likely to concentrate (Allison *et al.*, 2000). Since it has been reported that a high concentration of sugar might affect *in vitro* transfection (Cherng *et al.*, 1997), it is important to keep the effective sugar concentration as low as possible.

This study clearly demonstrated the ability of both glucose and sucrose to preserve particle size on freeze-drying. There are no significant differences between the two types of sugar in preserving particle size. The results are consistent with other groups (Alison *et al.*, 2000, Kwok *et al.*, 2000) who showed that both sucrose and glucose could effectively prevent aggregation of lipid – DNA complexes during freeze-drying. Indeed, it is the method of preparing the lyoprotectant containing DNA complexes that appeared to be a crucial factor in determining the particle size. From the results, it was found that a lower sugar concentration was needed to preserve particle size when sugar was added after the formation of DNA complexes. This could possibly explain by the observation that a smaller initial particle size was achieved when sugar was added after the formation of DNA complexes prior to freeze-drying.

As mentioned above, particles are concentrated in the unfrozen fraction during freeze-drying. The volume of unfrozen fraction however was determined by the initial solute concentration. In other studies, it was found that a lower sugar concentration was required for protection of particles in a more diluted suspensions, suggests that ‘crowding’ of particles facilitates aggregation (Anchordoquy *et al.*, 2001). Therefore, the amount of sugar was also described in terms of sugar: DNA (w/w) ratio. In our study, 2% sugar concentration, which is equivalent to 1000:1 sugar: DNA (w/w) ratio, was sufficient to preserve polymer – DNA complexes. Similarly, a ratio of 1250:1 was required to protect lipid – DNA complexes (Molina *et al.*, 2001).

### 3.5 CONCLUSIONS

This chapter examined different compositions of DMA-MPC diblock copolymers as potential non-viral vector for gene delivery, and the prospects of long term stability of this system. From the view of physicochemical characterisation, a desirable non-viral gene delivery system should be able to condense DNA efficiently to form sterically stabilized complexes. It is demonstrated in this study that the MPC block is effective in providing steric stabilization for the DNA complexes. However, a long MPC block also hinders the interaction between the cationic DMA and DNA. Therefore, the balance in the block composition of DMA-MPC copolymers plays an important role in designing an optimal gene delivery system.

The DMA<sub>60</sub>MPC<sub>30</sub> system appears to be a suitable candidate with desirable characteristics as mentioned above. Thus, it was chosen for the long term stability study of polymer – DNA complexes. The data shows that both glucose and sucrose demonstrate the ability to preserve particle size of polymer – DNA complexes during freeze-drying. The amount of sugar and the sequence at which sugar was added are important factors affecting the particle size. The DNA complexes were better preserved during freeze-drying when sugar was added after formation of complexes, and the size of complexes that were comparable to the unfrozen control could be achieved at 1000:1 sugar: DNA (w/w) ratio.



## CHAPTER 4

### MORPHOLOGICAL STUDY OF DMA-MPC DIBLOCK COPOLYMER – DNA COMPLEXES

#### 4.1 INTRODUCTION

One of the essential characteristics of non-viral gene delivery systems is the ability to condense DNA into small compact structures. DNA are large polar macromolecules that are not readily taken up by cells. A wormlike chain (WLC) model is often used to describe the conformation of DNA molecules in solution (Lu *et al.*, 2002). In the uncondensed state, DNA are easily degraded by enzymes. The condensed conformations of DNA can provide protection from nucleases (Kwoh *et al.*, 1999, Richardson *et al.*, 1999). In addition, the reduced dimension of the DNA in condensed conformation facilitates its transport in the extracellular matrix and enhance cellular uptake.

Cationic polymers have been widely used for DNA condensation through electrostatic interaction. Their effectiveness at condensing DNA depends on the chemical structure, polymer architecture, charge density and molecular weight. To assist the design of an efficient non-viral gene delivery system, it is necessary to understand the condensation of DNA by examining the morphology of the polymer – DNA complexes.

##### 4.1.1 Theoretical aspects of DNA condensation

DNA condensation is defined as the collapse of extended DNA chains into compact orderly particles containing only one or a few molecules of DNA (Bloomfield 1997). DNA is a very long negatively charged macromolecule

which is orders of magnitude longer than any dimensions of a cell can fit in. The dimensions and morphology of DNA condensates are largely independent of the size of the DNA when the length of DNA is above 400 base pairs (Bloomfield, 1991). This striking phenomenon has attracted much attention and has been investigated by many researchers in different areas of science.

DNA condensation arises from very complex intermolecular and intramolecular interactions (Marquet and Houssier, 1991, Bloomfield, 1996). For condensation to occur, the DNA needs to overcome a number of energetic barriers, including Coulombic barriers due to the repulsion of negatively charged phosphate groups of DNA, entropy loss when organising the extended DNA molecule into well-defined structures, and bending of the stiff double helix. Polycations are among the most well-studied *in vitro* condensing agents. They act by decreasing repulsions between DNA segments. Thermodynamic studies show that condensation of DNA occurs spontaneously when approximately 90% of the phosphate backbone is neutralized by polycations (Wilson and Bloomfield, 1979, Bloomfield, 1998).

A number of simulation models have been developed in attempt to explain the electrostatic interactions occurring during the DNA condensation process. Traditional approximations such as Poisson-Boltzmann and Debye-Hückel theories are only valid for weakly charged objects and low-valent counterions and cannot fully explain the complicated DNA condensation process (Neu, 1999, Sader and Chan, 1999). Monte Carlo simulation is a widely accepted model used to investigate the transition from coil and globule state in alternate ionic strengths (Crothers *et al.*, 1990, Lyubartsev and Nordenskiöld, 1995, Ivanov *et al.*, 2000). There are many other simulation models described in the literature (Klenin *et al.*, 1998, Sottas *et al.*, 1999, Stevens, 2001, Sarraguça and Pais, 2004). However, the debates of the relative significance of all these models in the process of DNA condensation are beyond the scope of this thesis.

Experimental methods to investigate DNA condensation include visualisation of DNA condensates using technique such as electron microscopy and atomic force microscopy. A range of different structures of DNA condensates have been observed. Toroids and rods are the most commonly reported morphology for DNA condensates (Bloomfield, 1998). A toroid typically has an outer diameter of 50 nm and an inner diameter of 15 nm. It is believed that a toroid is formed from circumferentially wound DNA, with local hexagonal packing of the parallel double strands (Marx and Ruben, 1983). The rod structure is less commonly reported than the toroidal structure. The relationship between toroids and rods is not clearly understood. It has been suggested that a rod is formed when the solvent is non-polar, as the non-polar environment may lower the free energy of exposed heterocyclic bases, favouring sharp local kinking over gradual bending (Bloomfield 1998). More recently, it is suggested that rod formation is related to the stiffness of the molecules (Maurstad *et al.*, 2003).

### 4.1.2 Aims

Transmission electron microscopy (TEM) is a traditional tool used to visualise DNA condensates (Bloomfield, 1996), whereas atomic force microscopy (AFM) has become popular in recent years for such investigations (Hansma *et al.*, 1998, Pope *et al.*, 1999, Liu *et al.*, 2001, Danielsen *et al.*, 2004). The aim of this study was to examine the morphology of DNA complexes produced with DMA homopolymer and a series of DMA-MPC diblock copolymer, using TEM and AFM. The basic principles of these two techniques are described in section 2.3.5 and 2.3.6 respectively. The images of DNA complexes obtained from both techniques are compared. The morphology of the complexes in relation to the process of DNA condensation and the development of gene delivery system are also discussed.

## 4.2 MATERIALS AND METHODS

### 4.2.1 Materials

Materials used were as described in chapter 2, section 2.1 unless stated otherwise in the following sections.

### 4.2.2 Morphology study using TEM

DNA solution (2.5  $\mu\text{g}$ ) was added to 10% PBS solution, followed by addition of polymer solution. All the complexes were prepared in a 2:1 monomeric unit: nucleotide ratio and the total volume of each solution was 250  $\mu\text{l}$ . The samples were incubated at room temperature for 30 min. Drops (20  $\mu\text{l}$ ) of sample were placed onto a copper grid coated with pioloform resin (TAAB Laboratory Equipment, Reading, UK) for 30 s. Excess buffer was removed using filter paper. The sample was stained with uranyl acetate (4% w/v solution of uranyl acetate in 50% ethanol) for 2 min. The grid was then washed in 50% ethanol once and distilled water twice prior to air-drying. The samples were analyzed under the TEM (Jeol JEM-1010 TEM, Jeol Ltd., Welwyn Garden City, UK) at a voltage of 80 kV. Micrographs were taken at 25K to 100K magnification using Kodak Megaplug digital camera 1.6i. Control grids containing DNA only, polymer only and buffer medium were prepared and stained in the same way. Image analysis was carried out using analySIS Pro 3.1, Soft Imaging System.

### 4.2.3 Morphology study using AFM

All the AFM experiments described in this chapter were performed by Anne Chim of the Laboratory of Biophysics and Surface Analysis, University of

Nottingham, in collaboration with the author and the Advanced Drug Delivery Group.

The samples of DNA controls contained 1  $\mu\text{g/ml}$  plasmid DNA 10% PBS solution and 2 mM  $\text{NiCl}_2$ . After 30 min incubation at room temperature, 15  $\mu\text{l}$  of the sample was deposited onto freshly cleaved muscovite mica (Agar Scientific, Essex, UK) of approximately 1  $\text{cm}^2$  and allowed to stand one minute before washing twice with 50  $\mu\text{l}$  of distilled water, drying under nitrogen gas and imaging in air. DMA-MPC copolymer – DNA complexes at a 2:1 monomeric unit: nucleotide ratio in 30  $\mu\text{l}$  of 10% PBS solution were incubated at room temperature for 30 min prior to immobilization onto freshly cleaved muscovite mica and imaged directly in liquid.

All AFM imaging was carried out using a Tapping Mode (TM) Atomic Force Microscopy on a Veeco™ Nanoscope (IIIa) MultiMode system (Veeco Instruments, Santa Barbara, CA, USA). Topographical images were taken at 512 x 512 pixel resolution, plane-flattened and analyzed either by the computer program accompanying the Nanoscope IIIa Multimode AFM or by an offline-processing package, SPIP (version 2.2.2) (Image Metrology, Lyngby, Denmark). For imaging in air, NP tips on 160  $\mu\text{m}$  silicon cantilevers (Olympus OMCL-AC160Ts-W2) with a resonant frequency between 300-400 kHz were used. For imaging in liquid, an AFM liquid cell and oxidation-sharpened NP-S tips on a V-shaped, silicon nitride cantilever, with a spring constant of around 0.1 N/m (Nanoprobe, Veeco Instruments) and resonant frequency between 8-10 kHz were used.

## 4.3 RESULTS

### 4.3.1 Morphology of DNA complexes under TEM

Representative images of DNA complexes produced with DMA homopolymer at monomeric unit: nucleotide ratios 2:1 are displayed in figures 4.1.

TEM images show that DNA complexes formed with DMA homopolymer were highly condensed and aggregated. The complexes, stained with uranyl acetate, are visualized as clumps of electron-dense aggregates. This observation is consistent with PCS results (chapter 3), which also suggest that the DMA homopolymer – DNA complexes are highly aggregating. In order to increase colloidal stability of the complexes, hydrophilic MPC moiety was introduced into the system. The morphology of DNA complexes formed with DMA-MPC diblock copolymers are shown in figures 4.2 – 4.11.

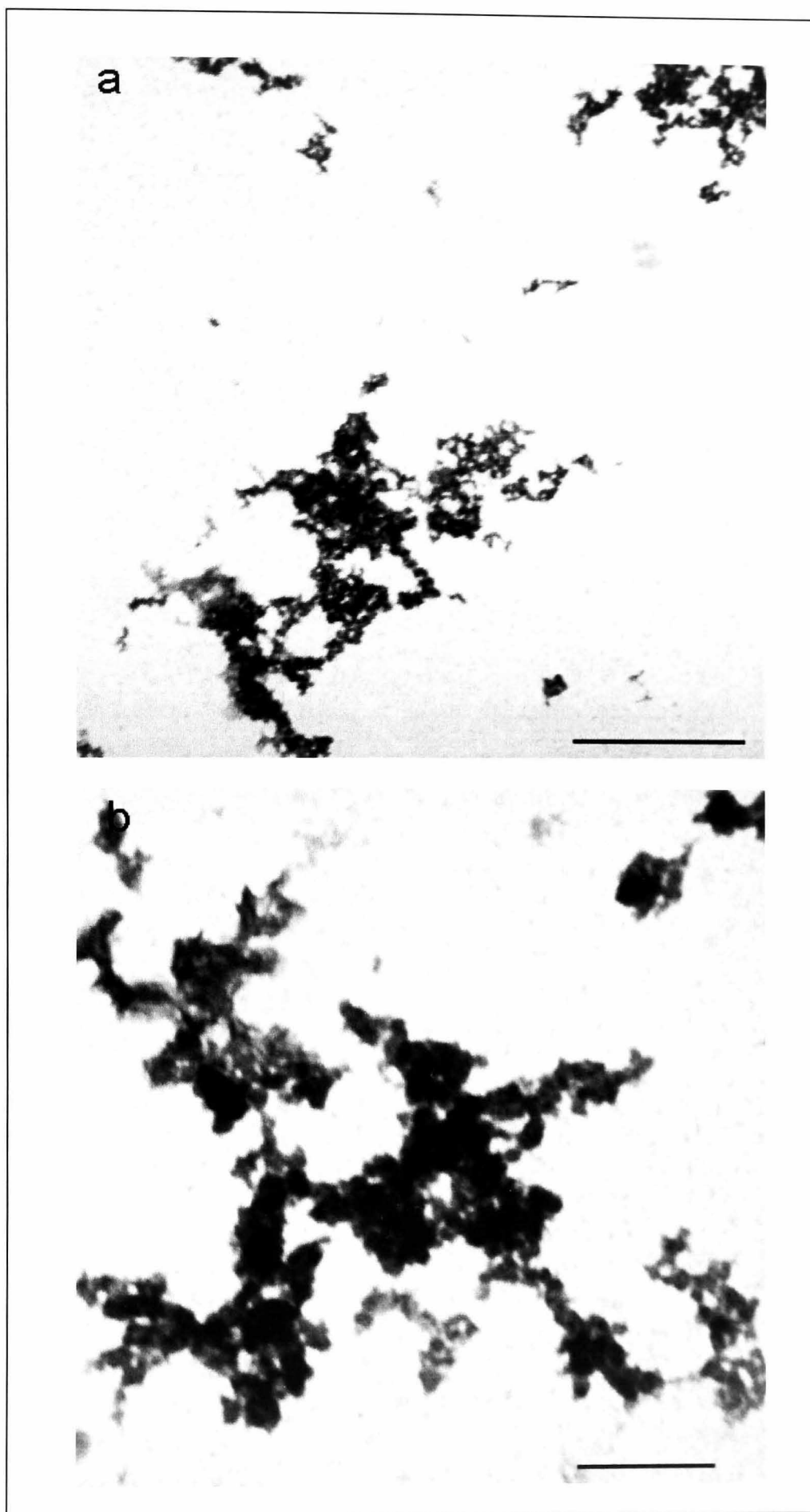


**Figure 4.1** TEM images of DMA homopolymer – DNA complexes at 2:1 monomeric unit: nucleotide ratio. Complexes were prepared in 10% (v/v) PBS and stained with uranyl acetate. The bars represent (a) 1000 nm and (b) 200 nm.

For the DMA<sub>40</sub>MPC<sub>y</sub> series, it is clearly shown that as the length of MPC increased, the level of aggregation decreased. For DMA<sub>40</sub>MPC<sub>10</sub>, which has a relatively short MPC chain, the DNA complexes were aggregating (figure 4.2) and the TEM images are similar to that observed with DMA homopolymer. For DMA<sub>40</sub>MPC<sub>20</sub>, the complexes were only partially aggregating (figure 4.3). The majority of the non-aggregating complexes appeared as rod-like structures, with a small proportion of complexes appeared as toroidal structures. For DMA<sub>40</sub>MPC<sub>30</sub> and DMA<sub>40</sub>MPC<sub>40</sub> (figure 4.4 and 4.5 respectively), aggregation of complexes was no longer observed. Complexes formed by these two copolymers comprised a mixture of well condensed toroidal and rod-like structures, or ‘intermediate’ structures. The measurement of the toroids and rod structures are shown in table 4.1. The average outer diameter of the toroids are  $52 \pm 12$  nm and  $51 \pm 7$  nm for DMA<sub>40</sub>MPC<sub>30</sub> and DMA<sub>40</sub>MPC<sub>40</sub> respectively. These dimensions are consistent with typical toroidal structures reported by other groups using different cationic polymers (Tang and Szoka *et al.*, 1997). When the length of MPC is further increased, the complexes appeared to be less well condensed. For DNA complexes formed with DMA<sub>40</sub>MPC<sub>50</sub>, plectonemic-like and loose rings structures are observed instead of well-defined rods and toroids (figure 4.6).



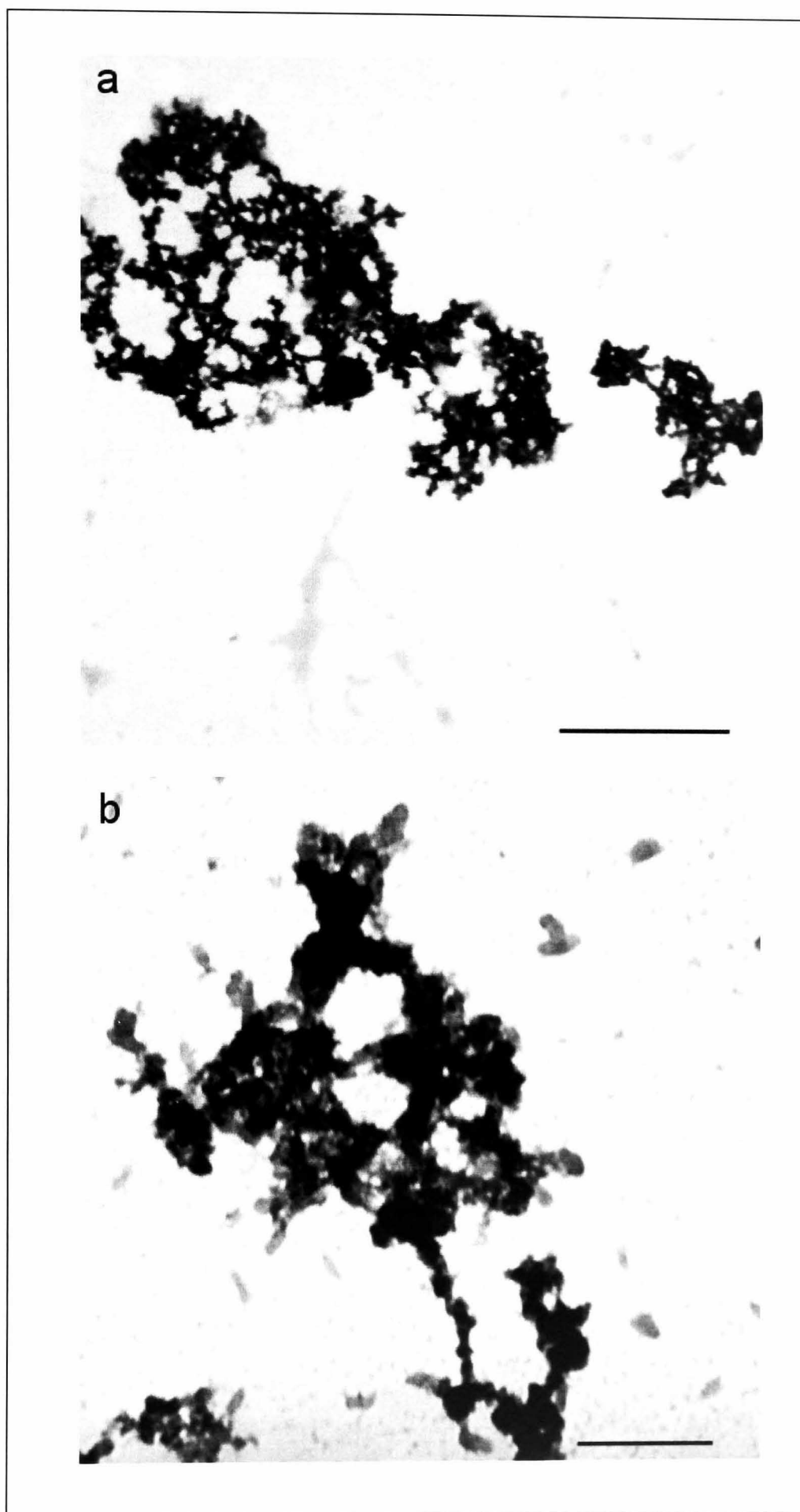


**Figure 4.2** TEM images of DMA<sub>40</sub>MPC<sub>10</sub> – DNA complexes at 2:1 monomeric unit: nucleotide ratio. Complexes were prepared in 10% (v/v) PBS and stained with uranyl acetate. The bars represent (a) 1000 nm and (b) 200 nm.

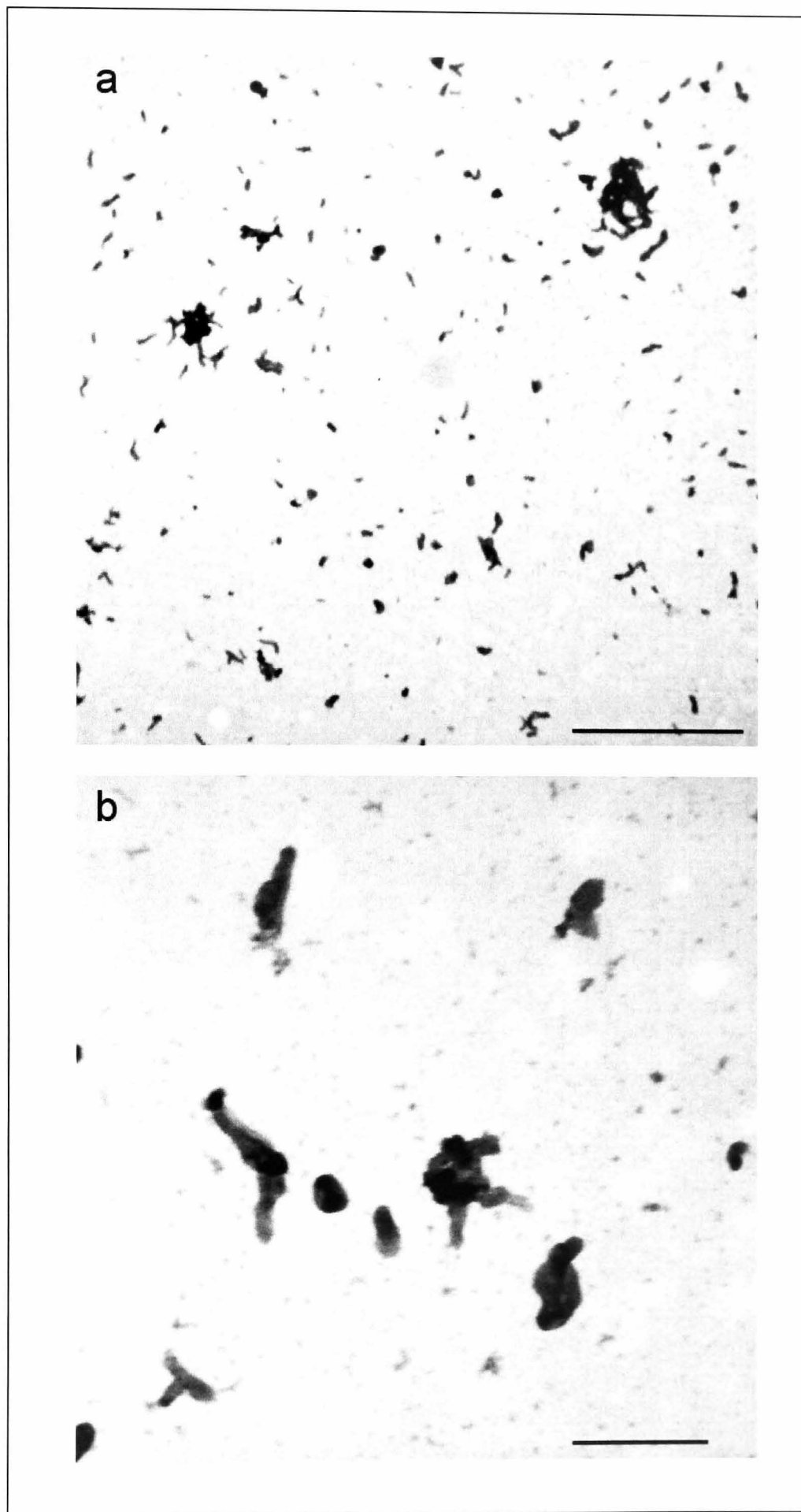


**Figure 4.3** TEM images of DMA<sub>40</sub>MPC<sub>20</sub> – DNA complexes at 2:1 monomeric unit: nucleotide ratio. Complexes were prepared in 10% (v/v) PBS and stained with uranyl acetate. The bars represent (a) 1000 nm and (b) 200 nm.

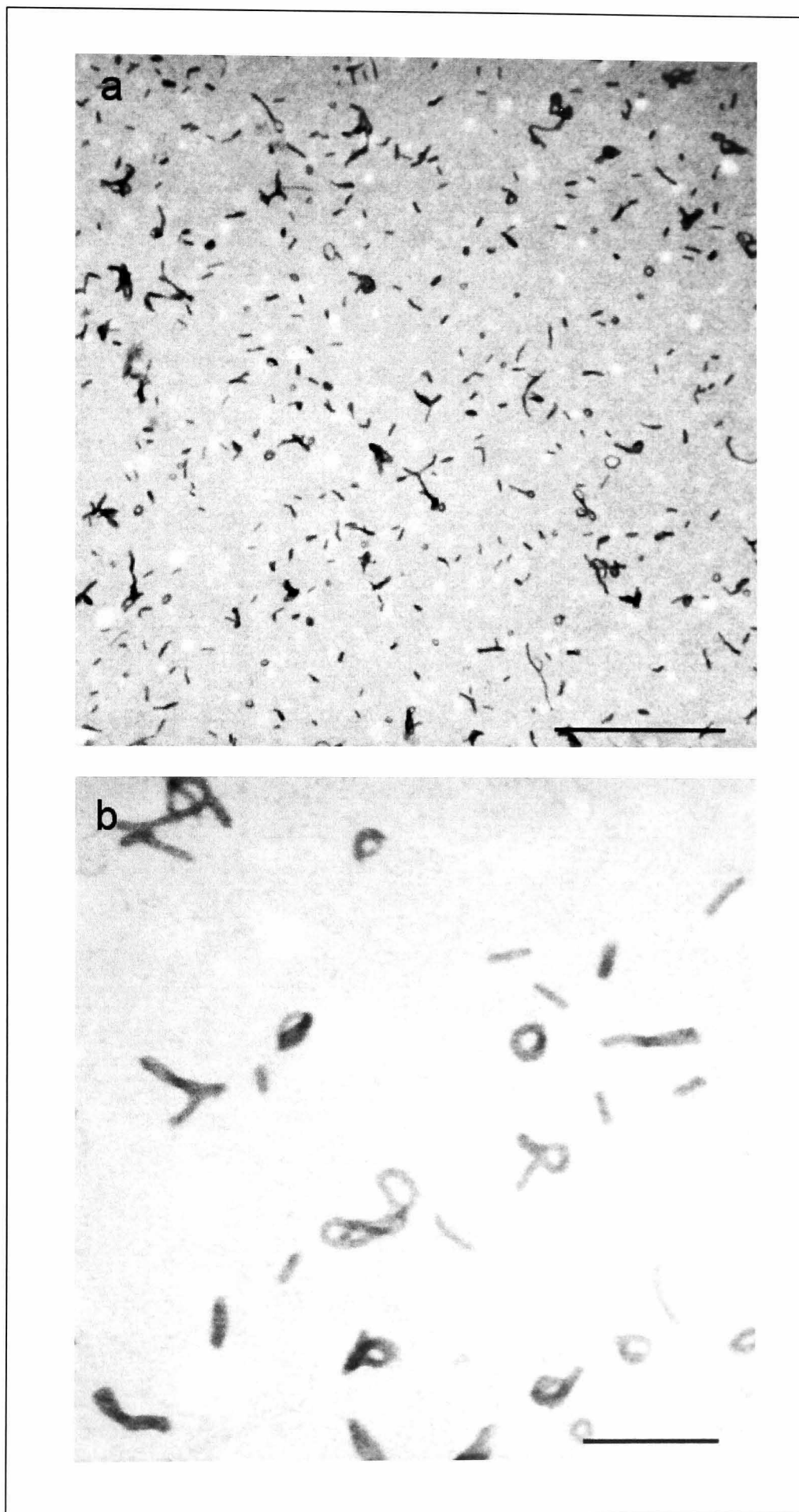


**Figure 4.4** TEM images of DMA<sub>40</sub>MPC<sub>30</sub> – DNA complexes at 2:1 monomeric unit: nucleotide ratio. Complexes were prepared in 10% (v/v) PBS and stained with uranyl acetate. The bars represent (a) 1000 nm and (b) 200 nm.

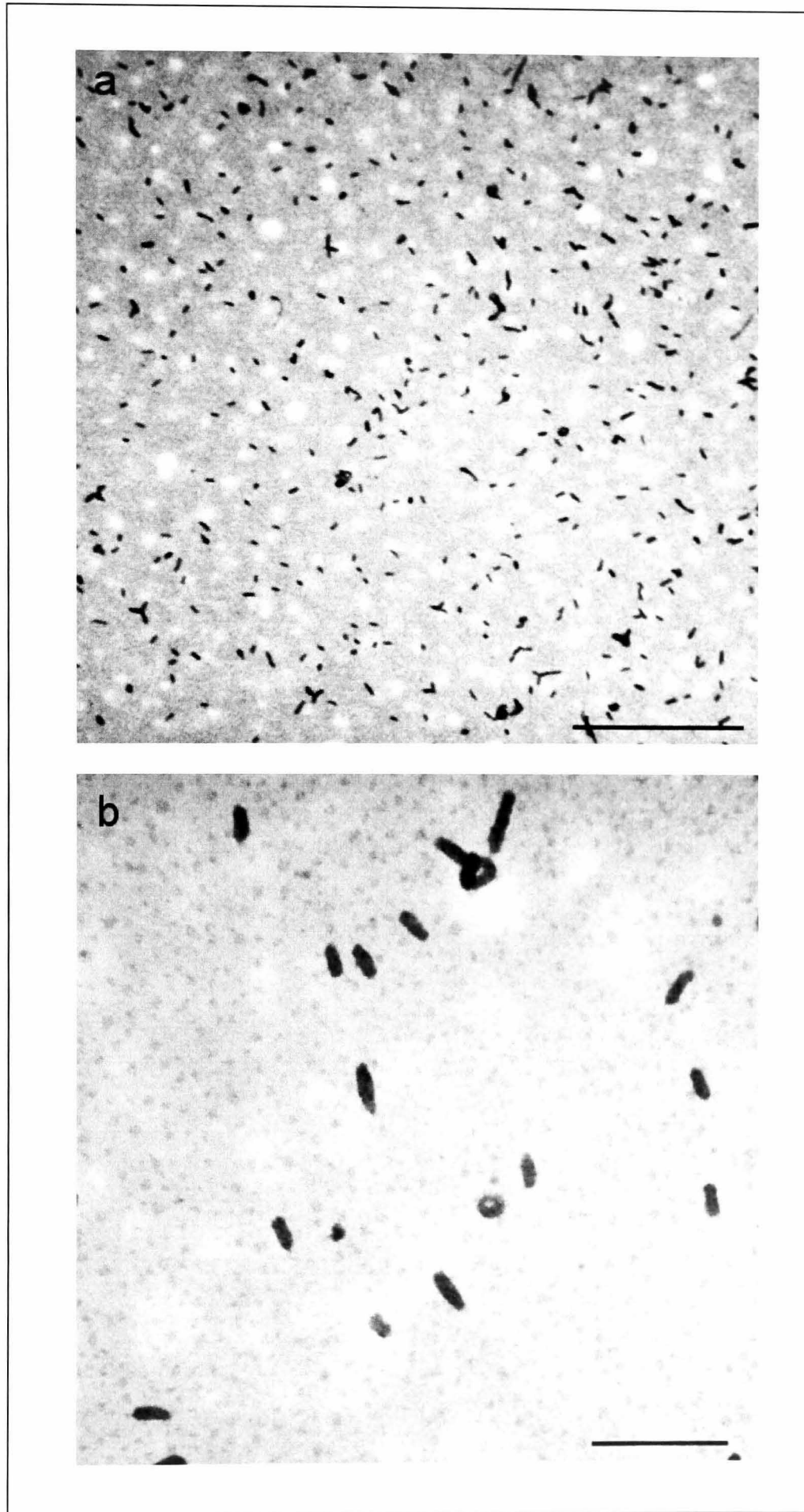


**Figure 4.5** TEM images of DMA<sub>40</sub>MPC<sub>40</sub> – DNA complexes at 2:1 monomeric unit: nucleotide ratio. Complexes were prepared in 10% (v/v) PBS and stained with uranyl acetate. The bars represent (a) 1000 nm and (b) 200 nm.

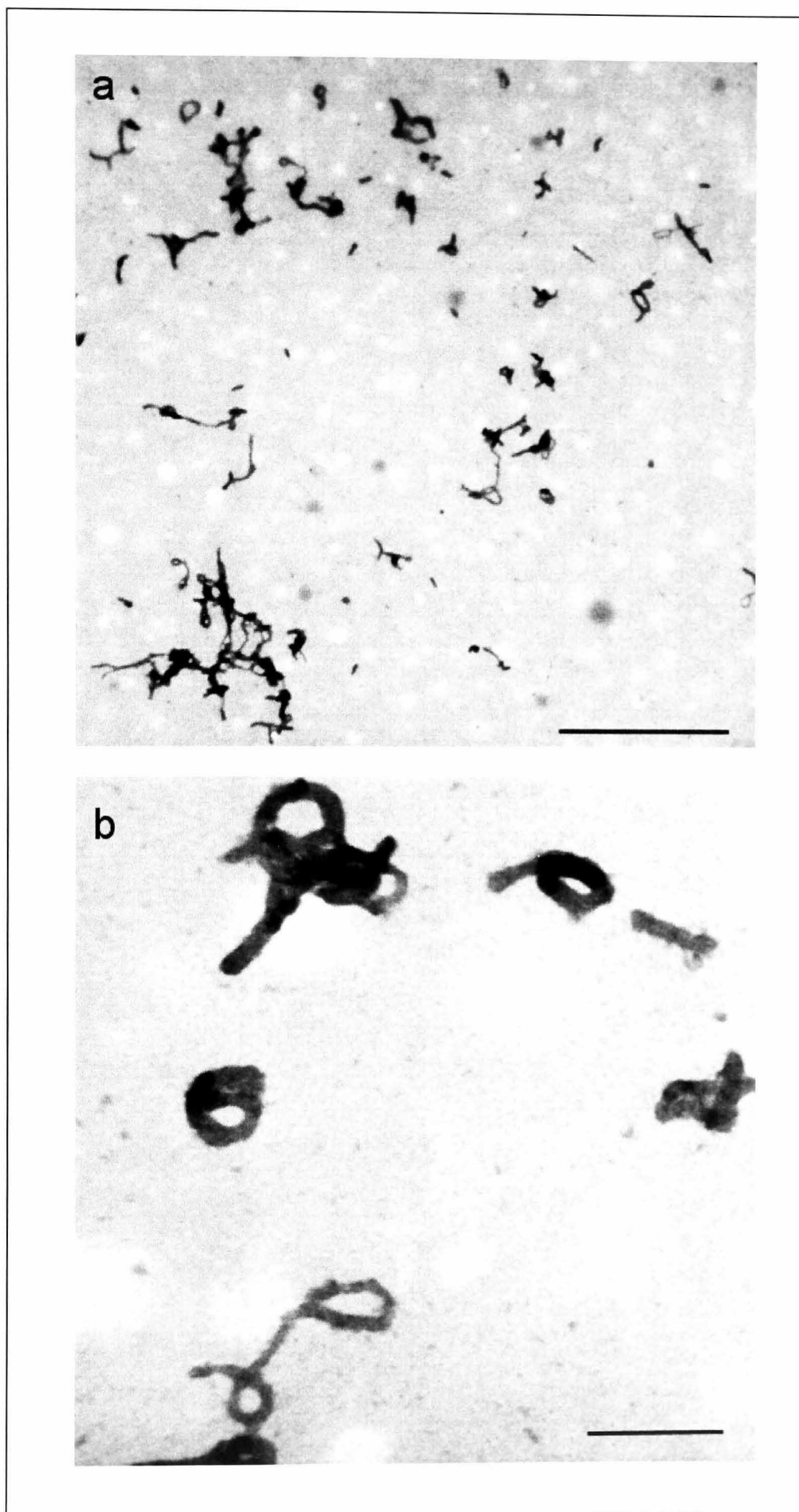


**Figure 4.6** TEM images of DMA<sub>40</sub>MPC<sub>50</sub> – DNA complexes at 2:1 monomeric unit: nucleotide ratio. Complexes were prepared in 10% (v/v) PBS and stained with uranyl acetate. The bars represent (a) 1000 nm and (b) 200 nm.

**Table 4.1 Measurements of rods and toroids structures formed with DMA<sub>40</sub>MPC<sub>30</sub> and DMA<sub>40</sub>MPC<sub>40</sub> under TEM.** The outer diameter of toroids, length of rods, and the thickness of DNA condensates were measured ( $n = 20$ ).

<b>Copolymer system</b>	<b>Outer diameter of toroid (nm) <math>\pm</math> sd</b>	<b>Length of rods (nm) <math>\pm</math> sd</b>	<b>Thickness (nm) <math>\pm</math> sd</b>
DMA <sub>40</sub> MPC <sub>30</sub>	52 $\pm$ 12	71 $\pm$ 19	17 $\pm$ 3
DMA <sub>40</sub> MPC <sub>40</sub>	51 $\pm$ 7	62 $\pm$ 17	15 $\pm$ 3

A range of morphologies is obtained for the DNA complexes prepared using the DMA<sub>x</sub>MPC<sub>30</sub> copolymers. TEM images show that as the length of DMA increased, the level of condensation increased accordingly. For the DMA<sub>10</sub>MPC<sub>30</sub> copolymer, loosely condensed, ‘spaghetti-like’ structures were observed (figure 4.7). For the DMA<sub>20</sub>MPC<sub>30</sub> copolymer, the complexes appeared as loose ring and long linear structures, with a significant fraction of well-defined toroids and rods (figure 4.8). Both ring-like and linear structures had similar widths. For DMA<sub>40</sub>MPC<sub>30</sub> copolymer, the complexes appeared as shorter rods, tight toroids, or intermediate between the two, with rods as the dominant species (figure 4.4). As the length of DMA further increased, toroids were no longer observed. DNA complexes formed by DMA<sub>60</sub>MPC<sub>30</sub> and DMA<sub>100</sub>MPC<sub>30</sub> copolymers appeared as highly condensed compact globular particles (figure 4.9 and 4.10 respectively). These particles appeared as either short, thick rods or oval-shaped structure. Measurements including the thickness, contour lengths and diameter of the condensates are shown in table 4.2 and 4.3.

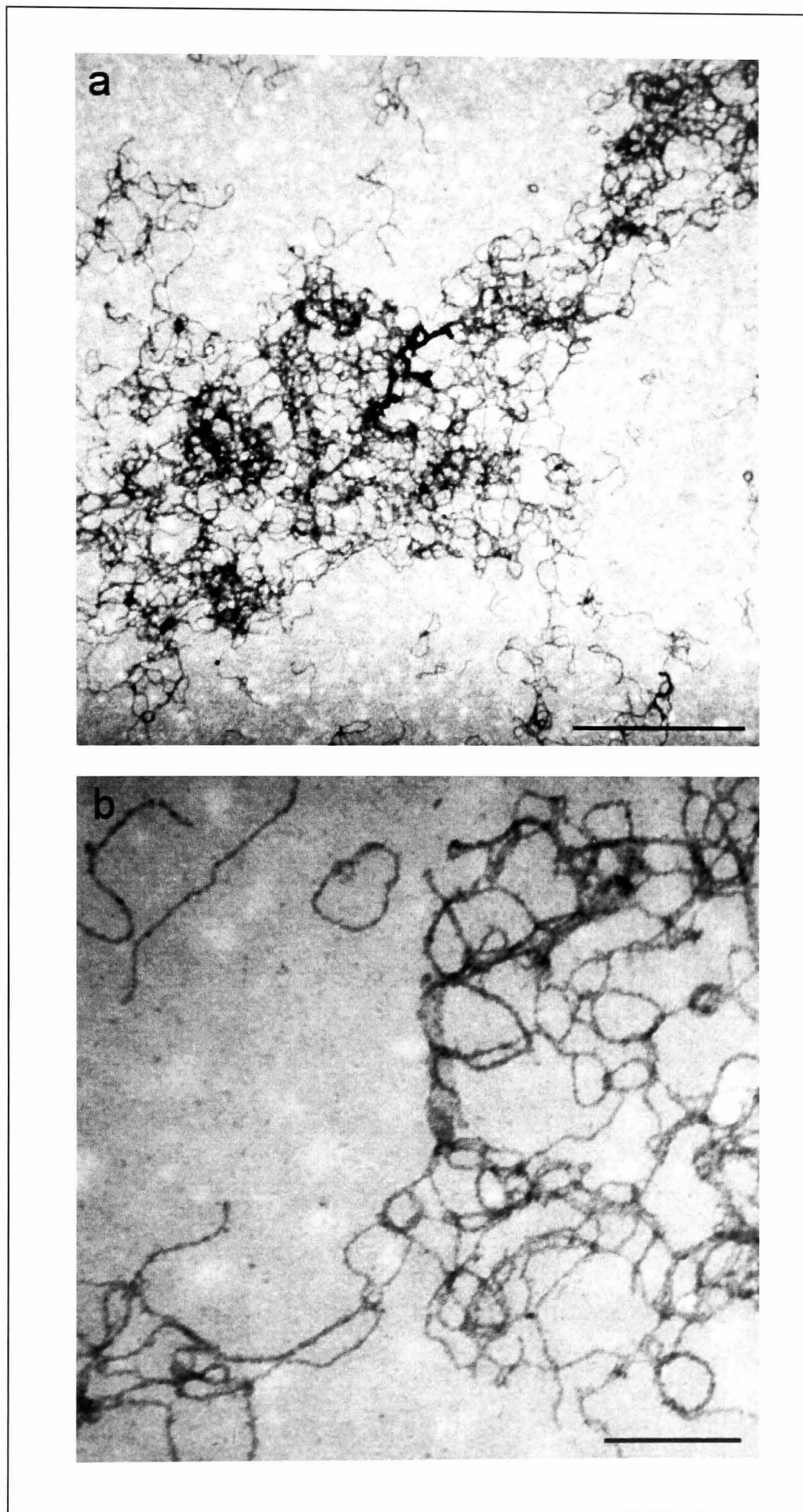


**Figure 4.7** TEM images of DMA<sub>10</sub>MPC<sub>30</sub> – DNA complexes at 2:1 monomeric unit: nucleotide ratio. Complexes were prepared in 10% (v/v) PBS and stained with uranyl acetate. The bars represent (a) 1000 nm and (b) 200 nm

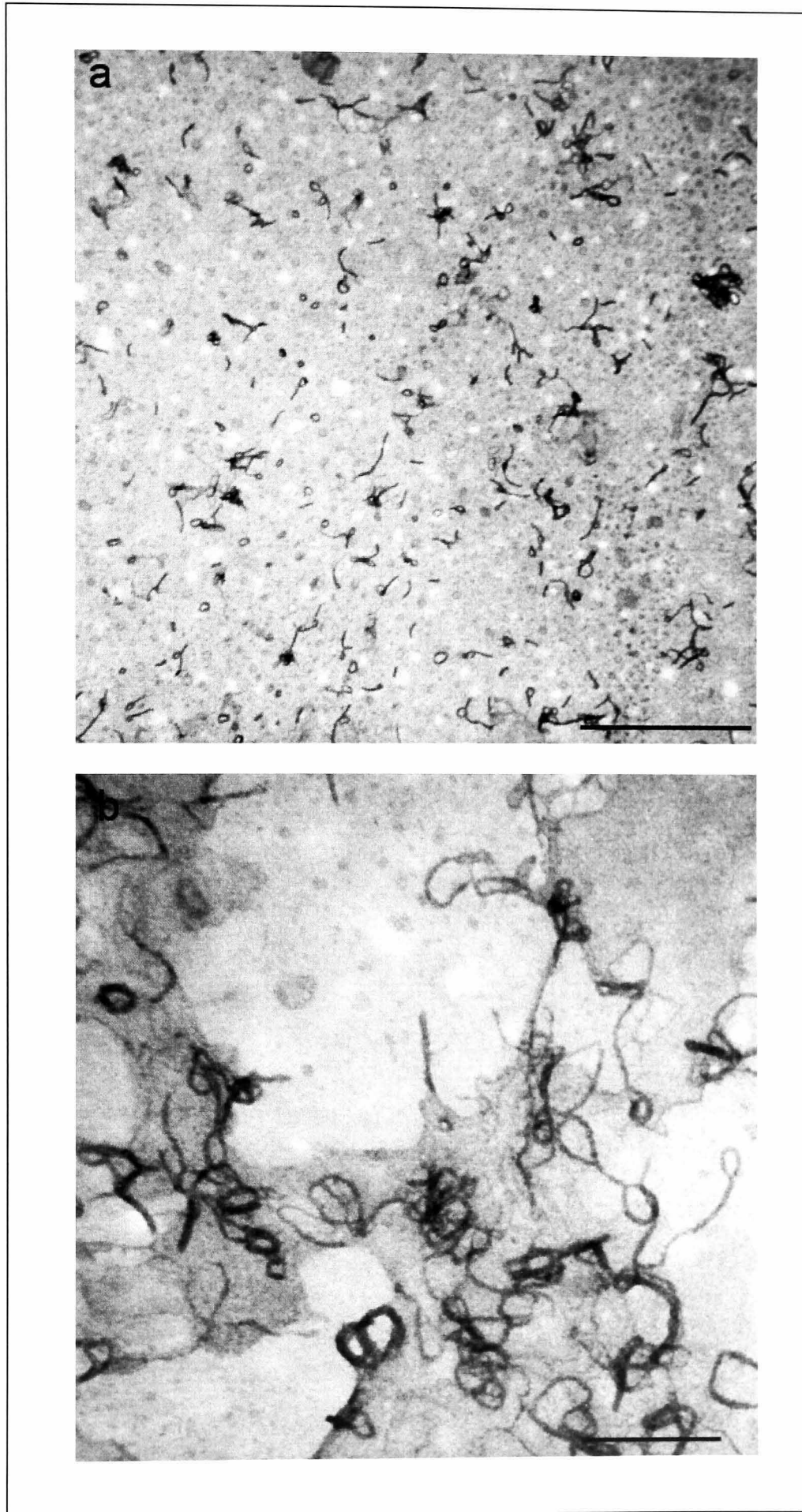


**Figure 4.8** TEM images of DMA<sub>20</sub>MPC<sub>30</sub> – DNA complexes at 2:1 monomeric unit: nucleotide ratio. Complexes were prepared in 10% (v/v) PBS and stained with uranyl acetate. The bars represent (a) 1000 nm and (b) 200 nm



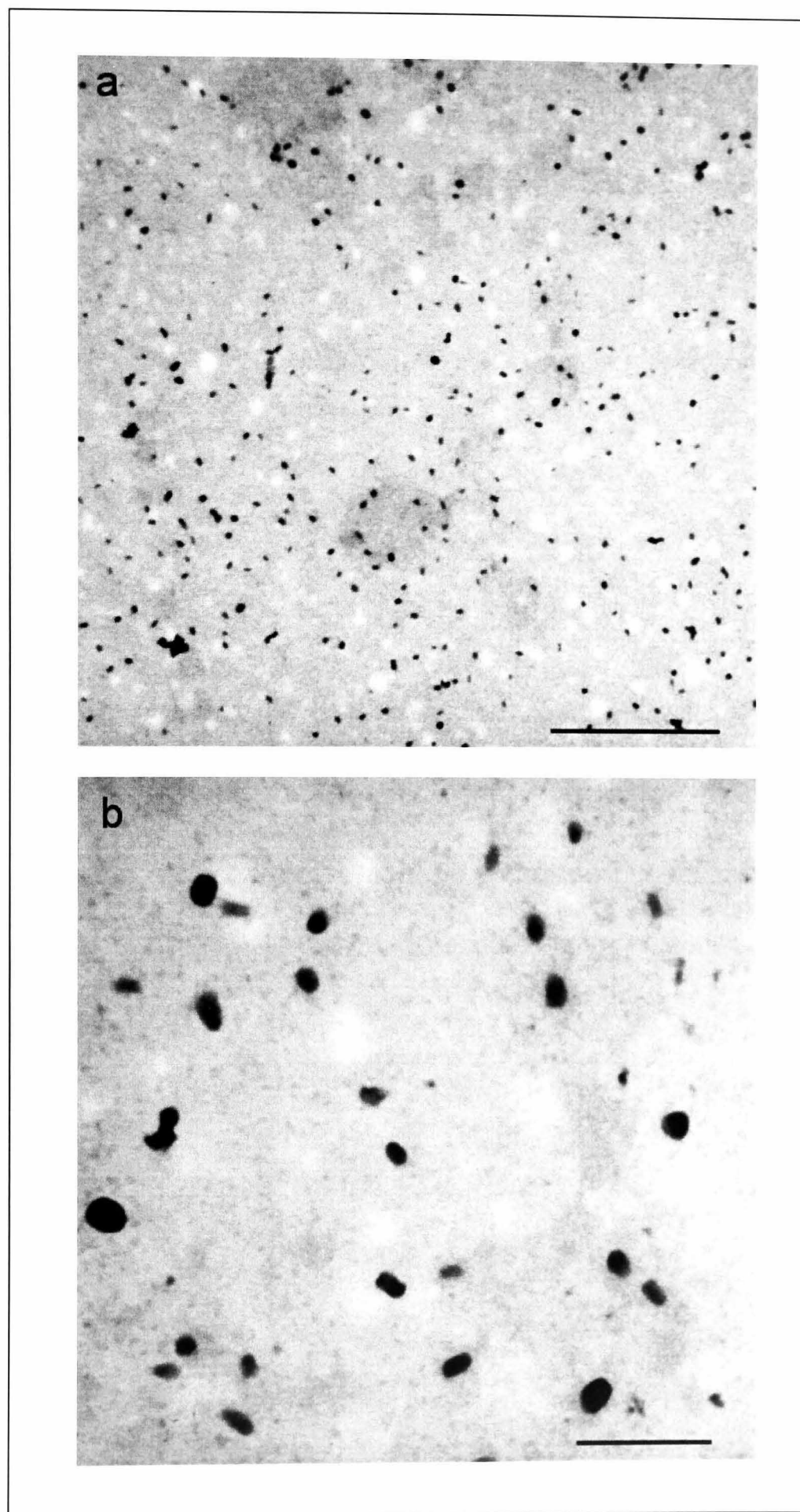


**Figure 4.9** TEM images of DMA<sub>60</sub>MPC<sub>30</sub> – DNA complexes at 2:1 monomeric unit: nucleotide ratio. Complexes were prepared in 10% (v/v) PBS and stained with uranyl acetate. The bars represent (a) 1000 nm and (b) 200 nm

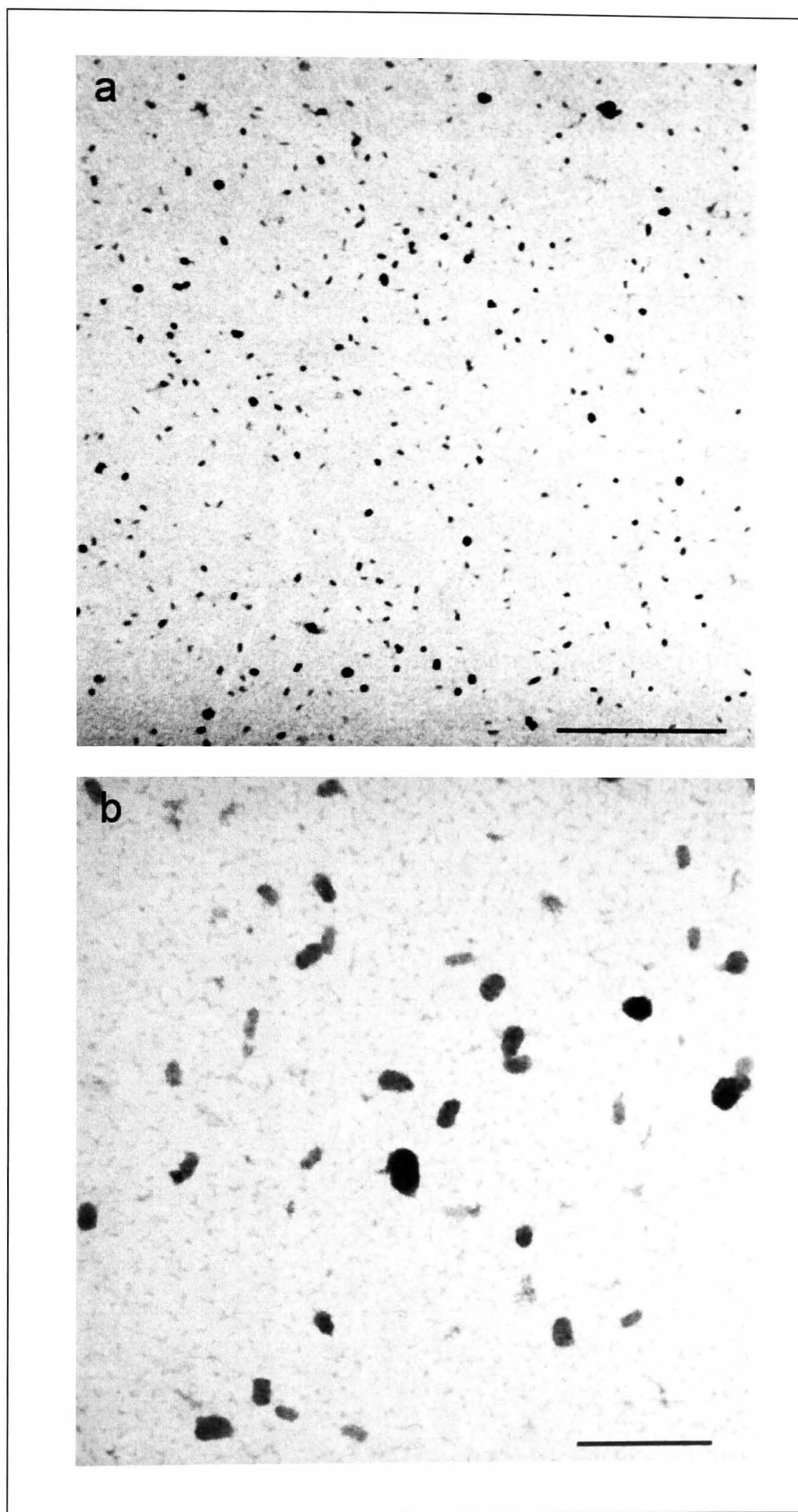


**Figure 4.10** TEM images of DMA<sub>100</sub>MPC<sub>30</sub> - DNA complexes at 2:1 monomeric unit: nucleotide ratio. Complexes were prepared in 10% (v/v) PBS and stained with uranyl acetate. The bars represent (a) 1000 nm and (b) 200 nm

**Table 4.2 Measurements of rods/linear and toroids structures formed with DMA<sub>10</sub>MPC<sub>30</sub>, DMA<sub>20</sub>MPC<sub>30</sub>, and DMA<sub>40</sub>MPC<sub>30</sub> under TEM.** The thickness and contour lengths of rods and toroids of DNA condensates were measured ( $n = 20$ ).

Copolymer System	Thickness (nm) $\pm$ sd	Contour length of linear structure (nm) $\pm$ sd	Contour length of toroid (nm) $\pm$ sd
DMA <sub>10</sub> MPC <sub>30</sub>	7 $\pm$ 1	537 $\pm$ 342	n/a
DMA <sub>20</sub> MPC <sub>30</sub>	11 $\pm$ 2	142 $\pm$ 117	155 $\pm$ 37
DMA <sub>40</sub> MPC <sub>30</sub>	17 $\pm$ 3	71 $\pm$ 19	137 $\pm$ 30

**Table 4.3 Measurements of toroids or globular structures formed with DMA<sub>20</sub>MPC<sub>30</sub>, DMA<sub>40</sub>MPC<sub>30</sub>, DMA<sub>60</sub>MPC<sub>30</sub> and DMA<sub>100</sub>MPC<sub>30</sub> under TEM.** The diameter of toroids for DMA<sub>20</sub>MPC<sub>30</sub> and DMA<sub>40</sub>MPC<sub>30</sub> ( $n = 20$ ) and the average size of globular particles for DMA<sub>60</sub>MPC<sub>30</sub> and DMA<sub>100</sub>MPC<sub>30</sub> ( $n = 100$ ) were measured.

Copolymer system	Outer diameter of toroids / Size of globular particles (nm) $\pm$ sd
DMA <sub>20</sub> MPC <sub>30</sub>	54 $\pm$ 13 (toroids)
DMA <sub>40</sub> MPC <sub>30</sub>	52 $\pm$ 12 (toroids)
DMA <sub>60</sub> MPC <sub>30</sub>	48 $\pm$ 9 (particles)
DMA <sub>100</sub> MPC <sub>30</sub>	42 $\pm$ 9 (particles)

### 4.3.2 Morphology of DNA complexes under AFM

According to the TEM images, it is found that the extent of DNA condensation is largely dependent on the length of DMA within the copolymer. Therefore, it is interesting to further investigate the behaviour of DNA complexes of this copolymer series (DMA<sub>x</sub>MPC<sub>30</sub>) in a liquid environment using AFM.

Figure 4.11 shows an AFM image of luciferase plasmid (a) in a liquid environment and (b) dried in air. Both images show a typical relaxed circular plasmid with structure consistent with other published images of

uncondensed DNA (Hansma *et al.*, 1998, Golan *et al.*, 1999, Maurstad *et al.*, 2003). The average contour length of the plasmid in liquid measured under the AFM was  $1802 \text{ nm} \pm 102 \text{ nm}$  ( $n = 3$ ).

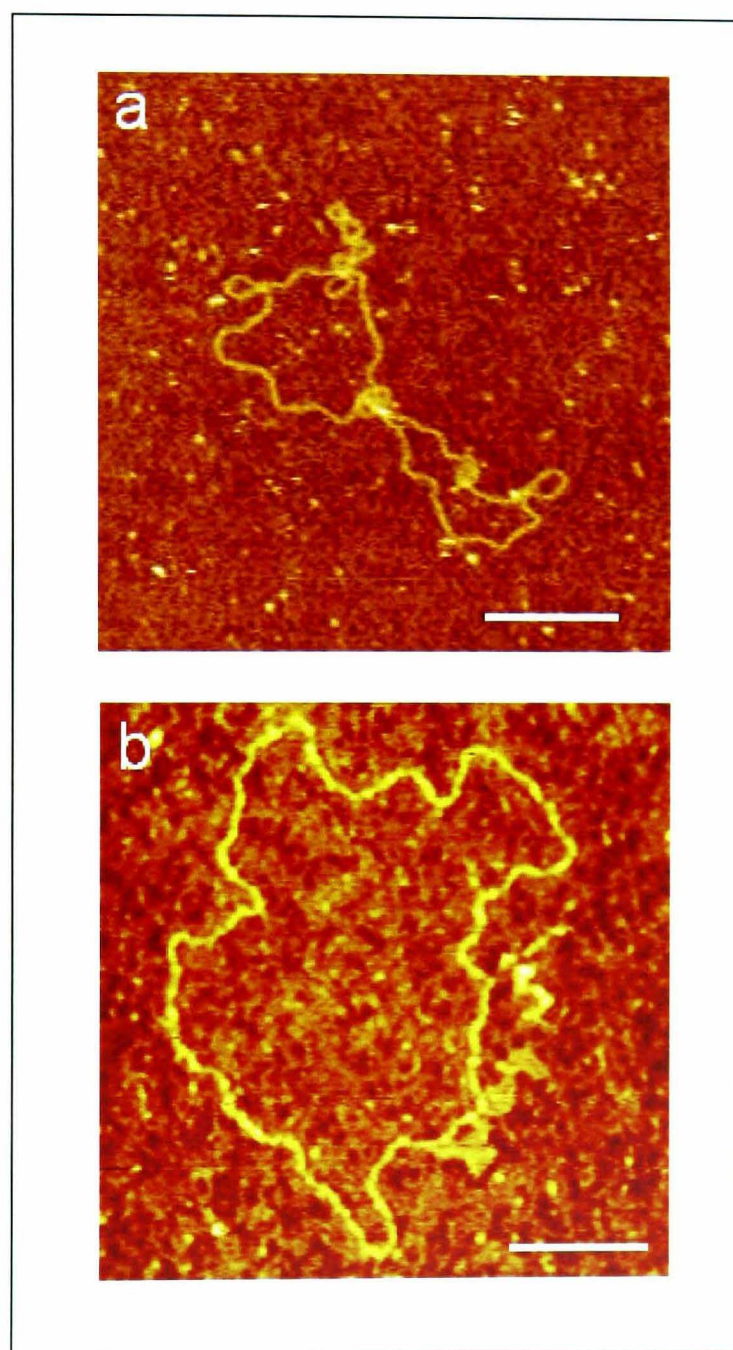


**Figure 4.11** AFM images of uncondensed luciferase plasmid (a) in liquid environment, with a  $z$  range of 10 nm, (b) dried in air, with a  $z$  range of 5 nm. The bars represent 200 nm.

The morphology of DNA complexes (in liquid) formed with DMA<sub>10</sub>MPC<sub>30</sub>, DMA<sub>20</sub>MPC<sub>30</sub>, DMA<sub>40</sub>MPC<sub>30</sub> and DMA<sub>60</sub>MPC<sub>30</sub> are shown in figures 4.12 – 4.15.

From the AFM images, it is clearly seen that DNA was only barely condensed with DMA<sub>10</sub>MPC<sub>30</sub> copolymer. Some of the condensates were simple flower-like structures composed of a central focus and loops of DNA that form ‘petals’ (figure 4.12b). Others simply consisted of plectonomic loops without a focus point. There were also structures that appeared as open loops which was similar to the uncondensed DNA (figure 4.12c). For DMA<sub>20</sub>MPC<sub>30</sub> copolymer, the majority of the complexes formed were flower-like structures. Compared to DMA<sub>10</sub>MPC<sub>30</sub>, these structures were highly looped and the central focus appeared to be larger and more intense (figure 4.13b). Oblong looped structures with multiple focal points can also be seen (figure 4.13c). These structures have been previously reported by other groups using spermidine and silanes as DNA condensing agents (Fang and Hoh, 1999). For DMA<sub>40</sub>MPC<sub>30</sub>, the complexes appeared as blobs of condensates with folded loops of DNA surrounding the central cores (figure 4.14). These structures were similar to those reported for PEI-DNA condensates (Dunlap *et al.*, 1997). For DMA<sub>60</sub>MPC<sub>30</sub>, the complexes were very similar to those observed with DMA<sub>40</sub>MPC<sub>30</sub>, although the centre core appeared larger and the complexes were more tightly packed (figure 4.15).

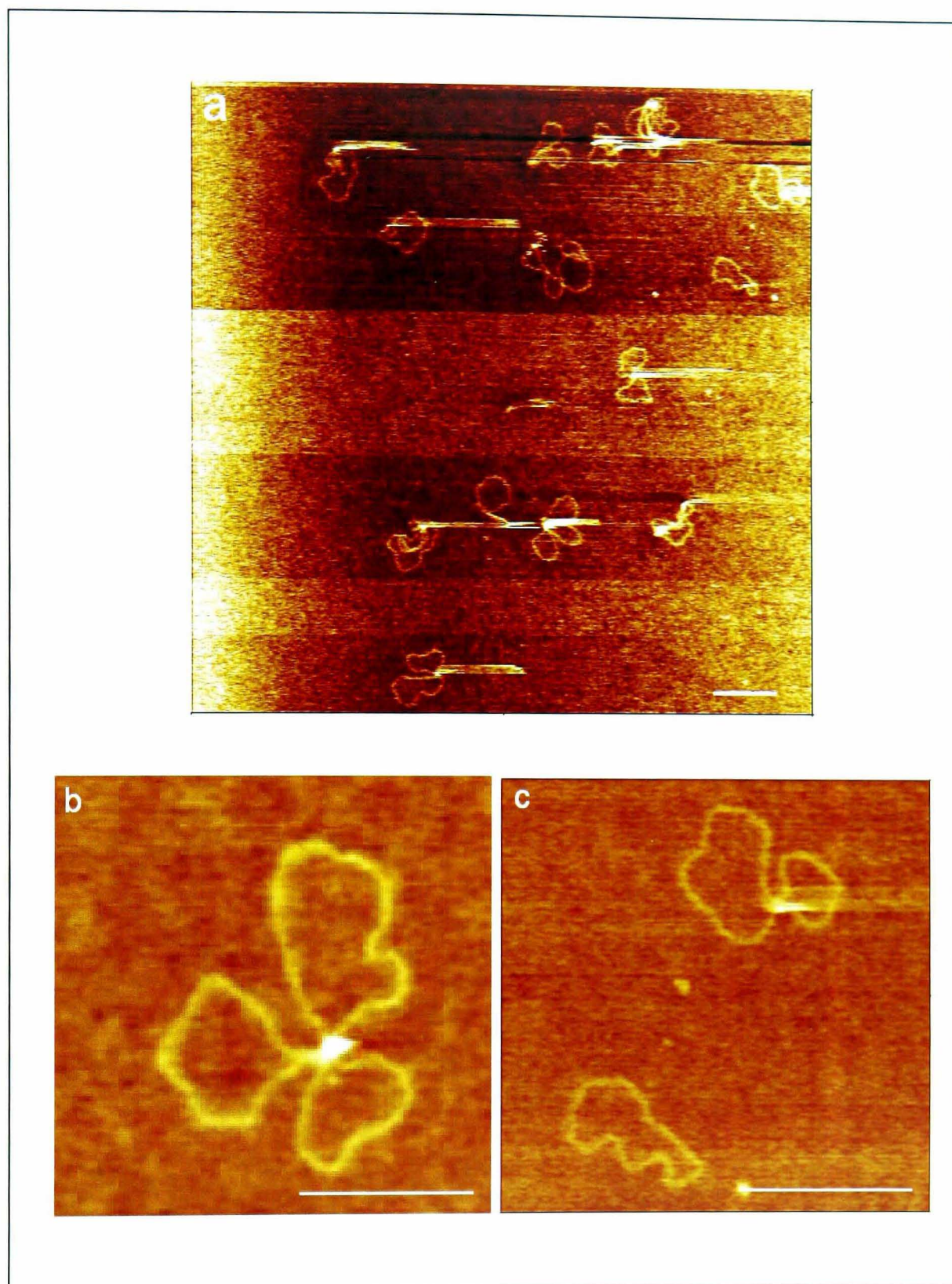


**Figure 4.12** AFM images of DMA<sub>10</sub>MPC<sub>30</sub> – DNA complexes at 2:1 monomeric unit: nucleotide ratio. Complexes were prepared in 10% (v/v) PBS. The bars represent 200 nm. (a) scan size 2  $\mu\text{m}^2$  with a  $z$  range of 5 nm, (b and c) scan size 0.5  $\mu\text{m}^2$  with a  $z$  range of 10 nm.

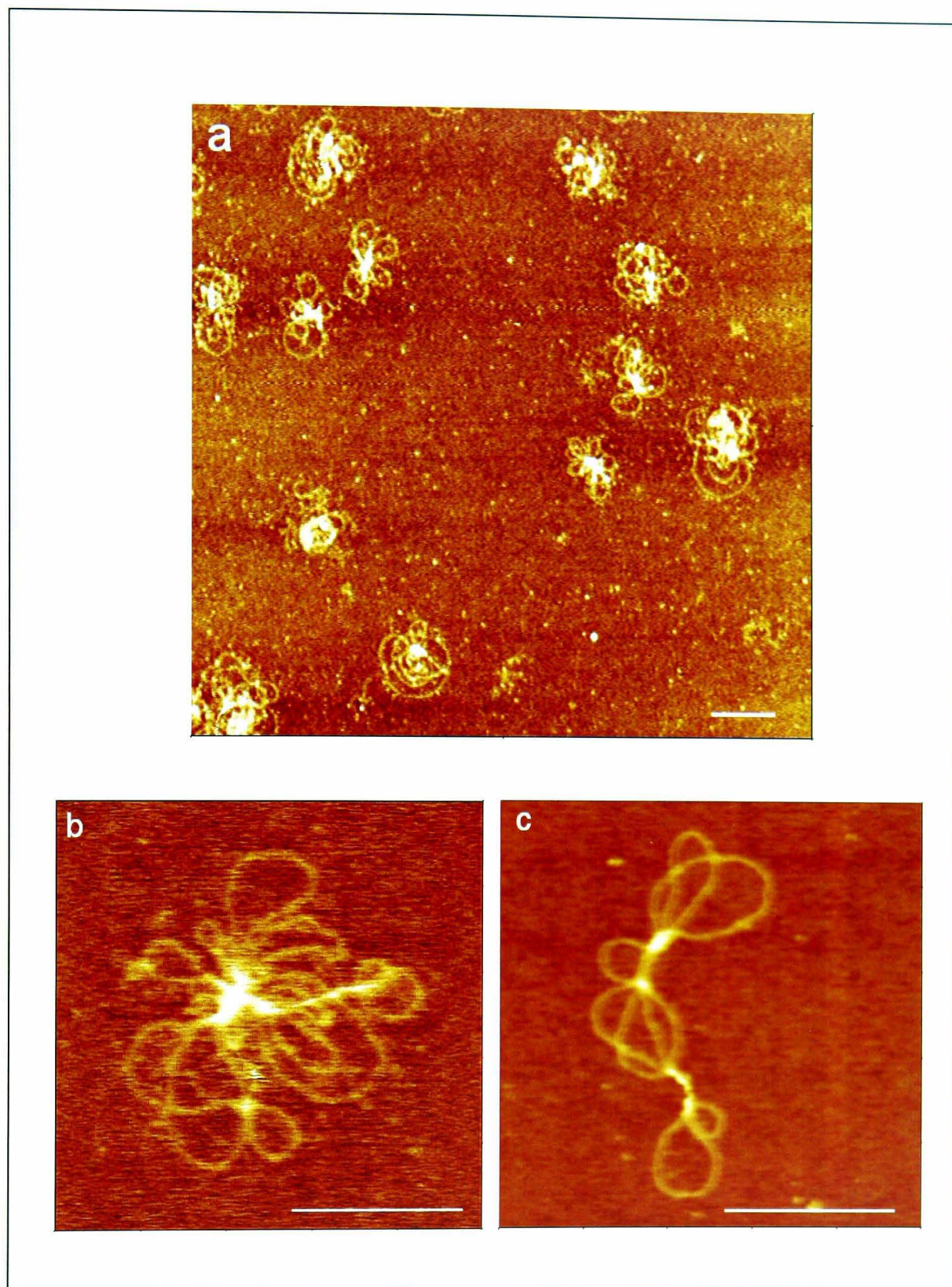


**Figure 4.13** AFM images of DMA<sub>20</sub>MPC<sub>30</sub> – DNA complexes at 2:1 monomeric unit: nucleotide ratio. Complexes were prepared in 10% (v/v) PBS. The bars represent 200 nm. (a) scan size 2  $\mu\text{m}^2$  with a  $z$  range of 5 nm, (b and c) scan size 0.5  $\mu\text{m}^2$  with a  $z$  range of 10 nm.

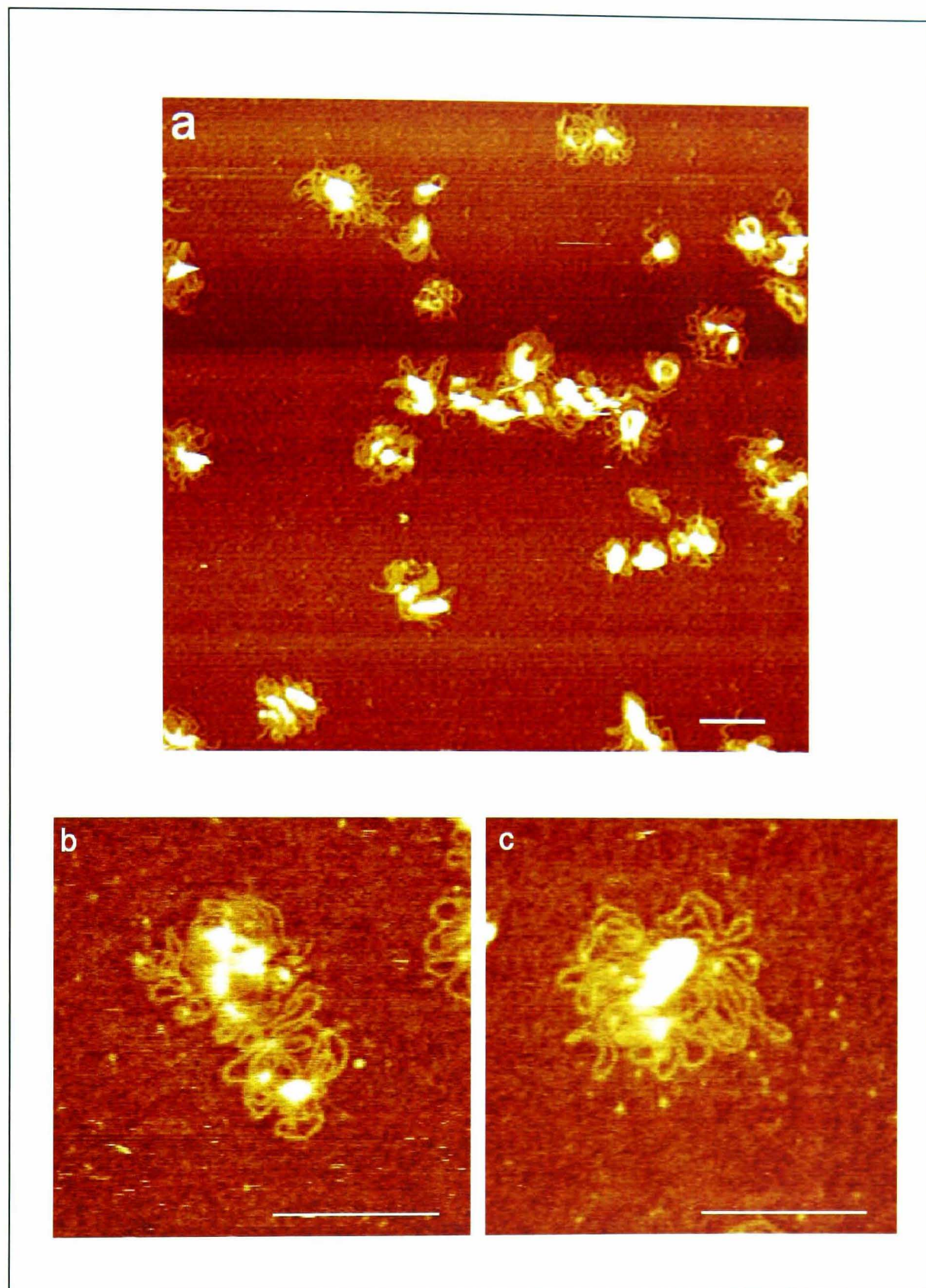


**Figure 4.14** AFM images of DMA<sub>40</sub>MPC<sub>30</sub> – DNA complexes at 2:1 monomeric unit: nucleotide ratio. Complexes were prepared in 10% (v/v) PBS. The bars represent 200nm. (a) scan size 2  $\mu\text{m}^2$  with a  $z$  range of 18 nm, (b and c) scan size 0.5  $\mu\text{m}^2$  with a  $z$  range of 10 nm.



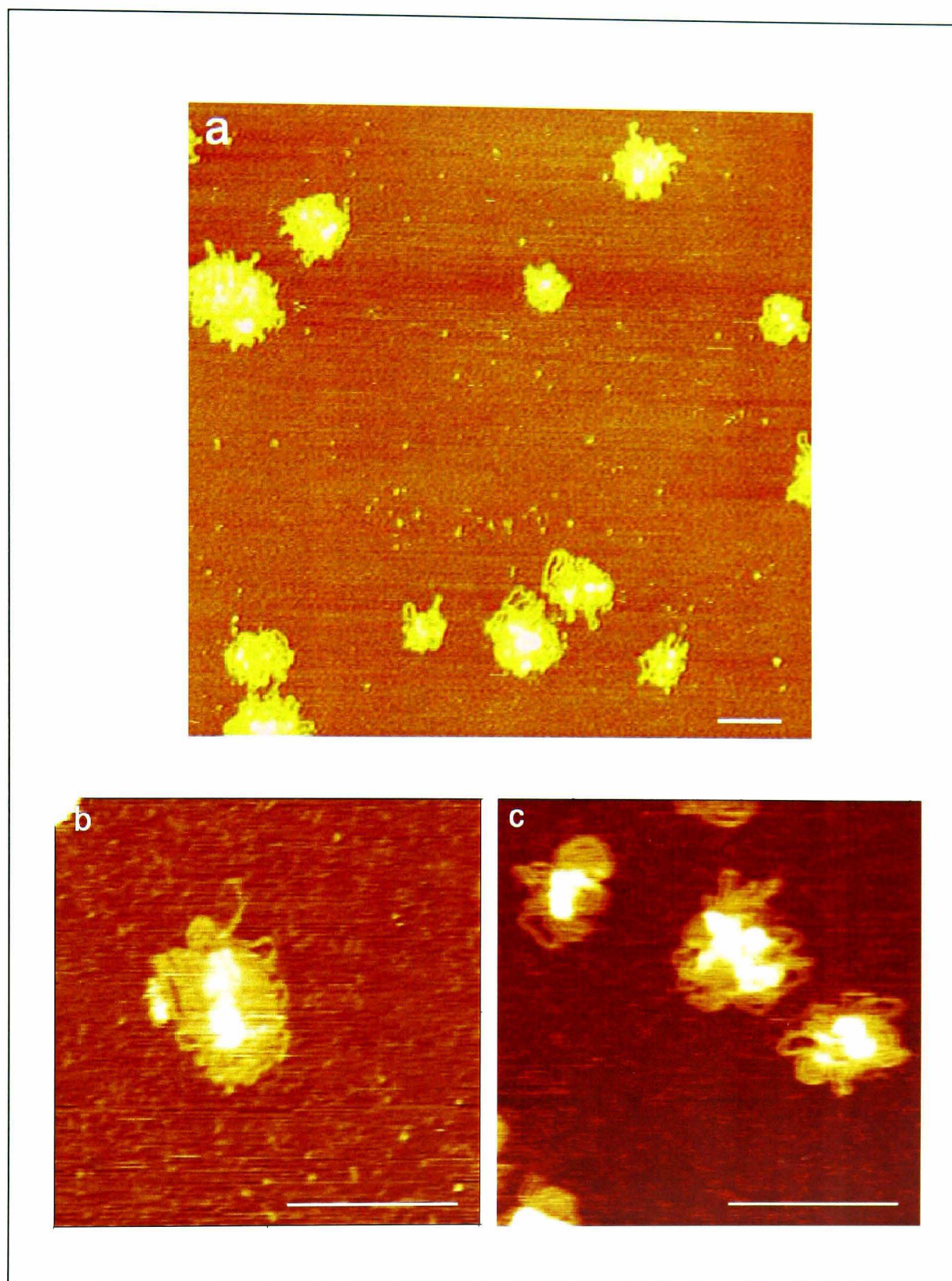


**Figure 4.15** AFM images of DMA<sub>60</sub>MPC<sub>30</sub> – DNA complexes at 2:1 monomeric unit: nucleotide ratio. Complexes were prepared in 10% (v/v) PBS. The bars represent 200 nm. (a) scan size 2  $\mu\text{m}^2$  with a  $z$  range of 8 nm, (b and c) scan size 0.5  $\mu\text{m}^2$  with a  $z$  range of 10 nm.

Table 4.4 shows the contour length measurement of flower-like structures of DMA<sub>10</sub>MPC<sub>30</sub> and DMA<sub>20</sub>MPC<sub>30</sub>, and the dimensions of flower-like or blob structures of DMA<sub>20</sub>MPC<sub>30</sub>, DMA<sub>40</sub>MPC<sub>30</sub> and DMA<sub>60</sub>MPC under the AFM. Since the central cores of the complexes of DMA<sub>40</sub>MPC<sub>30</sub> and DMA<sub>60</sub>MPC<sub>30</sub> are tightly packed with dense material, it is not possible to measure the contour length of these condensates.

**Table 4.4 Measurements of contour length and dimensions of DNA condensates formed with DMA<sub>x</sub>MPC<sub>30</sub> under AFM.** DMA<sub>10</sub>MPC<sub>30</sub> ( $n = 10$ ), DMA<sub>20</sub>MPC<sub>30</sub> ( $n = 20$ ), DMA<sub>40</sub>MPC<sub>30</sub> ( $n = 20$ ), and DMA<sub>60</sub>MPC<sub>30</sub> ( $n = 20$ ).

Copolymer System	Contour length of condensate (nm) $\pm$ sd	Dimensions of flower-like / blob structures (nm) $\pm$ sd
DMA <sub>10</sub> MPC <sub>30</sub>	1014 $\pm$ 454	n/a
DMA <sub>20</sub> MPC <sub>30</sub>	1795 $\pm$ 278	156 $\pm$ 56
DMA <sub>40</sub> MPC <sub>30</sub>	n/a	151 $\pm$ 59
DMA <sub>60</sub> MPC <sub>30</sub>	n/a	146 $\pm$ 56

## 4.4 DISCUSSION

### 4.4.1 Comparison of TEM and AFM data

In general, both imaging techniques indicate that more efficient DNA condensation occurs as the DMA block length increases. TEM studies revealed striking morphological differences for DNA complexes prepared with different compositions of the copolymers. On the other hand, the morphological differences of the complexes under the AFM were somewhat less dramatic. When comparing the dehydrated (TEM) and hydrated (AFM) complexes images, only structures of DMA<sub>10</sub>MPC<sub>30</sub> – DNA complexes were fairly similar. With this system, the DNA is barely condensed. Therefore the structures were perhaps less affected by the differing sample preparation protocols and environments applied by these two imaging techniques. However, there are certainly significant structural differences between TEM and AFM data for other DMA-MPC copolymers – DNA complexes. Under the TEM, DNA complexes formed with DMA<sub>20</sub>MPC<sub>30</sub> appeared as either linear or ring-like structure, whereas under AFM, the majority of the complexes appeared as flower-like structures. For DMA<sub>40</sub>MPC<sub>30</sub> and DMA<sub>60</sub>MPC<sub>30</sub>, the DNA complexes under TEM appeared as a mixture of rod and toroids structures, and highly dense oval-shaped particles respectively, whereas under the AFM, the complexes appeared as block-like structures with loops of DNA protruding out in both system. Generally, the structures observed under the TEM appeared to be better condensed compared to AFM.

The discrepancy between the techniques may be simply because dried samples were studied under TEM and hydrated / liquid samples under AFM. The MPC chains are extremely hydrophilic. Each MPC unit binds approximately 10-12 water molecules (Ishihara *et al.*, 1998; Konno *et al.*, 2001). Hence dehydration of the DNA complexes would be expected to have a dramatic impact on the morphology of MPC chain and consequently the DNA complexes morphology.

Furthermore, heavy metal staining is necessary to enable visualization of the complexes under the TEM. In this study, a 50% ethanolic solution of uranyl acetate was used as a stain for the DNA and the image produced was actually the shadow of the stain. It has been shown that the presence of ethanol can affect the extent of DNA condensation. Thus the TEM images need to be interpreted with caution. In addition, an extraordinary behaviour of MPC polymers in water : ethanol mixtures has been previously reported (Lewis *et al.*, 2000). It has been found that in 50 : 50 water : ethanol (v/v) solution, the MPC polymer chains collapse and interact with each another, leading to the formation of precipitate. The reason of this observation is not fully understood. However, the compact structures observed under TEM after staining could be a consequence of this behaviour.

In contrast, neither drying nor staining is necessary for AFM studies, so one can assume that this less invasive sample preparation significantly decreases the probability of artefacts. However, the complexes still require adsorption onto a substrate for AFM imaging. For this reason, DNA complexes that do not adhere onto the substrate cannot be imaged. Thus, repeated AFM experiments under the same conditions may reveal different structures adsorbed onto the mica surface. This was particularly true for condensates formed in the presence of the DMA<sub>20</sub>MPC<sub>30</sub> and DMA<sub>40</sub>MPC<sub>30</sub> copolymers, for which a range of variably condensed DNA complexes apparently co-exist in solution. It is not yet clear whether the complexes observed by AFM are truly representative of the entire population present in the bulk solution.

### 4.4.2 DNA condensation

A range of different structures of DNA condensates have been reported by many researchers. A few questions have been raised regarding the condensation of DNA:

1. How are these different structures formed?
2. Which is the most stable form of condensates?
3. How are these structures related to the development of gene delivery systems?

One of the aims of the present study is to gain the insight of how the DNA is condensed by examining the morphology of the condensates with different compositions of copolymer. Due to the different environmental condition of the sample and the remarkable difference of morphology between TEM and AFM images, it is hard to propose a pathway of DNA condensation by putting the two sets of images together.

On studying the TEM images alone, it was found that the morphology of DMA-MPC copolymer – DNA complexes varies markedly with different compositions of the copolymer. By increasing the length of MPC, the morphology of the complexes changed from highly aggregating condensates to discrete rod and toroid structures. This suggests that the hydrophilic MPC is able to provide efficient steric stabilization to the complexes. However, as the MPC further increased, the complexes became less condensed, indicating that high levels of MPC would indeed affect the condensation of DNA. On the other hand, by increasing the length of DMA, DNA progressively became more effectively condensed, as the morphology of the complexes changed from loosely condensed ‘spaghetti-like’ structures, to well condensed rods and toroids. The average contour length of the condensates decreased and the thickness increased, probably due to the successive folding and coiling of DNA molecules.

The relationship between toroids and rods is not fully understood. These two types of structures were frequently found to co-exist (Martin *et al.*, 2000, Liu *et al.*, Maurstad *et al.*, 2003), though toroids were reported to be the dominant species in most cases. It has been suggested that toroids and rods are formed by different condensation pathways (Bloomfield 1997), yet there is also evidence suggesting that rods and toroids are actually interchangeable

*via* real time observation (Martin *et al.*, 2000). Martin *et al.* were able to capture a series of AFM images which showed that toroids and rods existed dynamically, having the ability to reversibly equilibrate between each other. It has been postulated that DNA rods may bend around (Dunlap *et al.*, 1997) or open up to form toroids (Golan *et al.*, 1999), or that toroids collapse to give rods (Erbacher *et al.*, 1998).

Although it is not possible to confirm in our systems whether rods and toroids are indeed interchangeable using TEM, a series of ‘snapshots’ of DNA condensates formed with DMA<sub>20</sub>MPC<sub>30</sub> and DMA<sub>40</sub>MPC<sub>30</sub> copolymers has suggested that linear and ring structures are very likely to be in the process of interchanging. Figure 4.16 and 4.17 show a number of ‘intermediate’ DNA condensates. It appeared that some rods may open up or bend around to form toroids, or toroids collapse to give rods. Based on these ‘snapshots’, it is impossible to judge which are the precursors of the others. Nevertheless, these structures may provide clues to the way in which DNA may condense into toroids and rods.

It is not clear which morphology, rod or toroid, is the more stable form of condensates. Although toroids have been reported to be the most common morphology for DNA condensates (Bloomfield 1996), rods clearly predominate for complexes formed with DMA<sub>20</sub>MPC<sub>30</sub>, DMA<sub>40</sub>MPC<sub>30</sub> and DMA<sub>40</sub>MPC<sub>40</sub> copolymers. Table 4.5 shows the estimated relative proportions of toroids and rods for the three systems under TEM. Other polymeric vectors such as chitosan also produced a high proportion of rods (Danielsen *et al.*, 2004). The preference between rod or toroid structure seems to be dependent on the properties of the condensing agent. Theoretical studies indicate that the chain stiffness of macromolecules plays an important role in coil-globule transitions. This can be applied to the structural behaviour of DNA condensates (Noguchi and Yoshikawa, 1998, Stevens 2001, Maurstad and Stokke, 2005). A toroidal morphology is more likely for a stiff chain, whereas a rod is favoured when the polymer chain is flexible (Ivanov *et al.*, 2000). Our results therefore suggest that the chains of DNA

condensates are relatively flexible due to DNA complexation with the DMA-MPC copolymers, allowing coexistence of toroids and rods to occur.

As the DNA was further condensed, toroids are no longer observed. Short thicker rods or highly dense compact particles are seen for DMA<sub>60</sub>MPC<sub>30</sub> and DMA<sub>100</sub>MPC<sub>30</sub> copolymer. In contrast to toroidal structures, these condensates were stained in the centre. These condensates may be formed by further coiling and folding of rod structures, or indeed forms of densely packed toroidal condensates.

**Table 4.5 Comparison of the relative populations (%) of toroids and rods under TEM.** DNA condensates were formed with DMA<sub>20</sub>MPC<sub>30</sub> DMA<sub>40</sub>MPC<sub>30</sub> and DMA<sub>40</sub>MPC<sub>40</sub> at monomeric unit: nucleotide ratio 2:1 (n=300).

Copolymer system	% of toroids	% of rods	% of 'intermediate'
DMA <sub>20</sub> MPC <sub>30</sub>	22.7	49.3	28
DMA <sub>40</sub> MPC <sub>30</sub>	16.7	74	9.3
DMA <sub>40</sub> MPC <sub>40</sub>	4.3	89.5	6.2

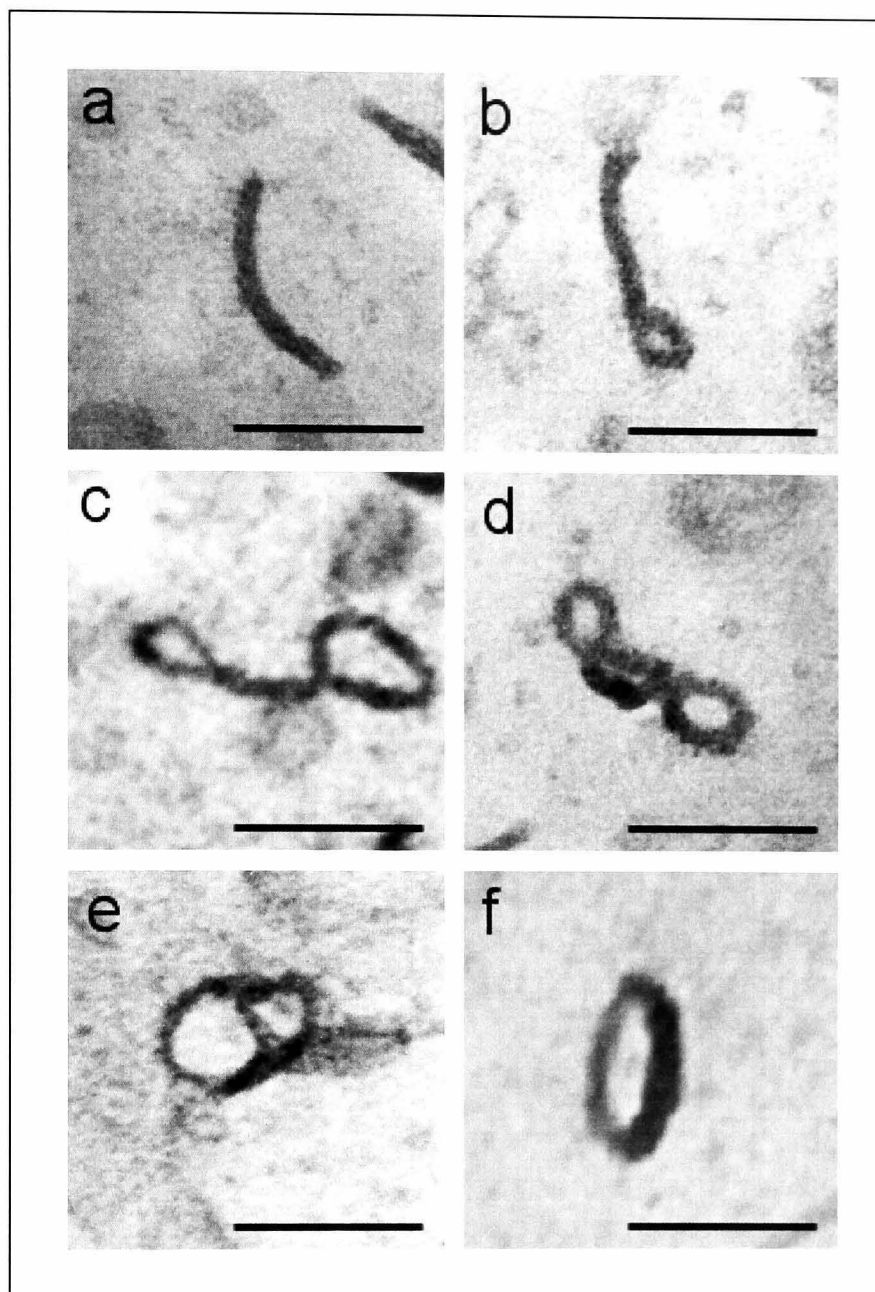


**Figure 4.16** TEM images of intermediate DNA structures (between rods and toroids) formed with DMA<sub>20</sub>MPC<sub>30</sub> copolymer. The DNA complexes were prepared at monomeric unit: nucleotide ratio 2:1 in 10% (v/v) PBS and stained with uranyl acetate. The bar represents 100 nm.



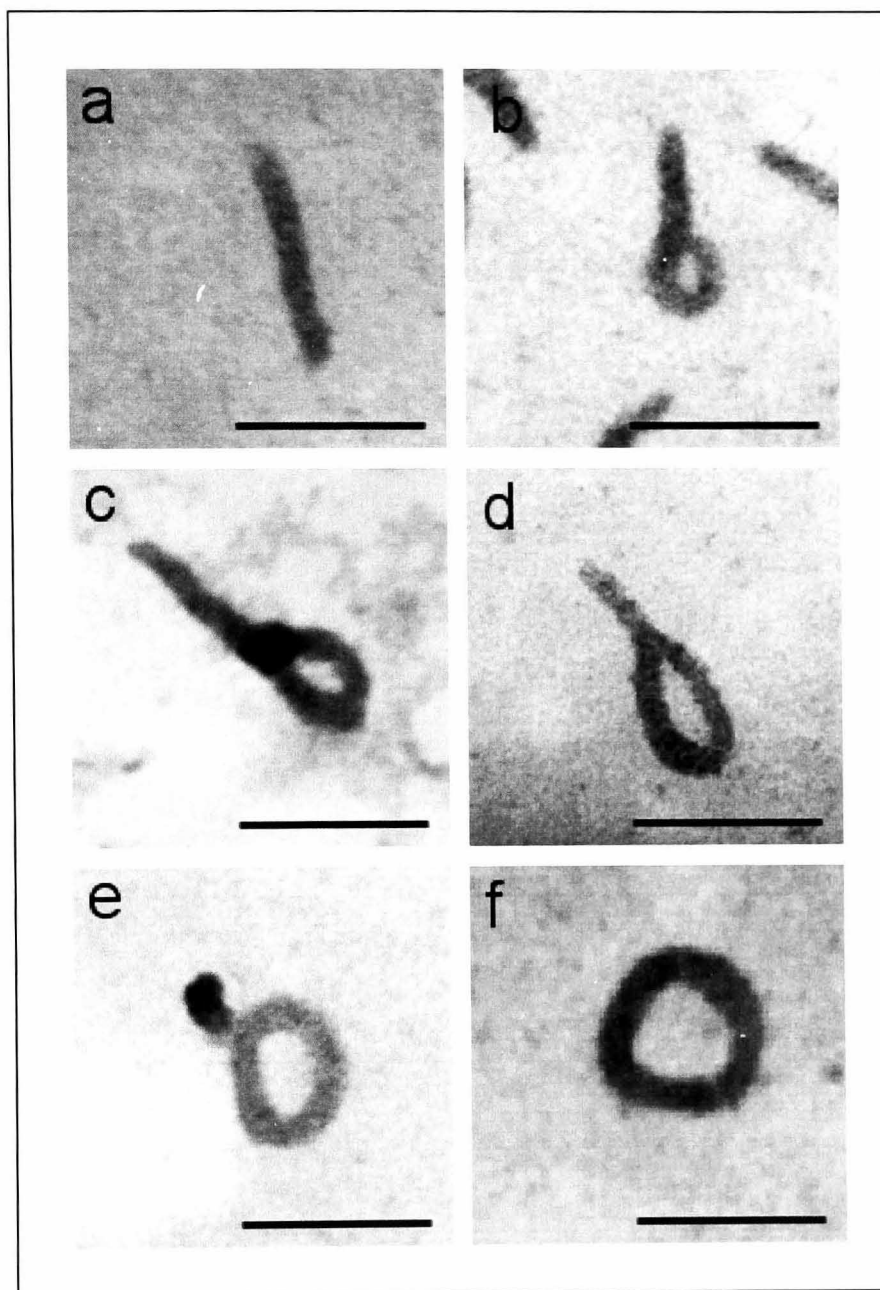


**Figure 4.17** TEM images of intermediate DNA structures (between rods and toroids) formed with DMA<sub>40</sub>MPC<sub>30</sub> copolymer. The DNA complexes were prepared at monomeric unit: nucleotide ratio 2:1 in 10% (v/v) PBS and stained with uranyl acetate. The bar represents 100 nm.

From the AFM images, it is also suggested that the level of DNA condensation increases with increased the length of DMA within the copolymer. It is clear that the DNA is only barely condensed with DMA<sub>10</sub>MPC<sub>30</sub>. Initially, the partially condensed DNA consists of a single focal point where the condensation of DNA is believed to initiate. This is the site where strands of DNA meet. Loops of uncondensed DNA can be observed surrounding the focal point. As the length of DMA increases, the size of the focal point becomes larger as strands of DNA are packed together and condensed. The number of focal points also increased in some of the condensates. Interestingly, it was found that the contour length of the uncondensed plasmid (1.8  $\mu\text{m}$ ) was longer than that of DMA<sub>10</sub>MPC<sub>30</sub> condensates, but similar to that of DMA<sub>20</sub>MPC<sub>30</sub> condensates (table 4.4). At 2:1 monomeric: nucleotide ratio, DMA<sub>10</sub>MPC<sub>30</sub> was able to condense DNA to a slight extent, as suggested in the gel retardation assay (chapter 3). The copolymer may cause coiling of DNA around its circumference, which leads to a shorter contour length of the DNA. The contour length of DMA<sub>20</sub>MPC<sub>30</sub> complexes is longer than that of DMA<sub>10</sub>MPC<sub>30</sub>, suggesting that more than one plasmid may be present in each DMA<sub>20</sub>MPC<sub>30</sub> condensate. Eventually, compact condensates were formed, as seen with DMA<sub>40</sub>MPC<sub>30</sub> and DMA<sub>60</sub>MPC<sub>30</sub> complexes.

It is obvious that the DNA complexes formed with copolymer with longer DMA are more condensed and compacted. However, the condensation appears to be incomplete even with DMA<sub>60</sub>MPC<sub>30</sub>, as loops of folded DNA can easily be seen around the centre core of the condensates. Since the centre core of the complex is tightly packed with dense material, it is not possible to measure the contour length of each condensate. However, it is speculated that each of these condensates may consist of more than one plasmid.

So how do the DNA structures relate to the development of a gene delivery system? It is believed that the condensed state of the DNA protects it from nucleases activity and allows it to pass more easily through small openings in the biological barriers. It is known that certain compositions of DMA-

MPC copolymer are able to condense DNA efficiently to form complexes with a small particle size. Based on the AFM images, loops of DNA are seen to be exposed to the environment for all complexes studied, suggesting that the complexes may be susceptible to enzymatic activity. However, further experiments are needed before conclusions can be made. The ability of these copolymers to protect DNA from enzymatic degradation was investigated and described in Chapter 5.

## 4.5 CONCLUSIONS

This study demonstrates that the structure and morphology of DNA complexes formed by the DMA-MPC diblock copolymer is highly dependent on the composition of the copolymer. In general, copolymers with longer DMA blocks produced more condensed structures. The hydrophilic MPC is able to provide steric stabilization to the DNA complexes. However, long MPC chains appeared to hinder electrostatic interaction between the DNA and the copolymer, resulting in the formation of partial or loosely condensed structure.

The morphology of the dehydrated DNA complexes observed by TEM was significantly different to the *in situ* AFM images obtained in the liquid environment. These differences are most likely attributed to the highly hydrophilic nature of the MPC block. Dehydration of the steric stabilizing component may have a significant impact on the resulting morphology, thus explaining the discrepancy between liquid AFM and dried TEM images. The different sample preparation procedures and environments may also affect the resulting morphology observed in TEM and AFM. The TEM images show that as the condensation of DNA progress, the morphology of DNA complexes changed from loosely condensed 'spaghetti-like' structures to rods, toroids, or 'intermediate' structures of the two, and finally into well condensed compact oval-shape particles. On the other hand, the AFM images show that the condensation of DNA is likely to be initiated from a single focal point, which subsequently increased in number and size to give structures with a compact, dense core, with loops of uncondensed / partially condensed DNA protruding from the centre of the condensates. Nevertheless, both imaging techniques have provided useful insights into the process of DNA condensation.

## CHAPTER 5

### BIOLOGICAL STUDY OF DMA-MPC DIBLOCK COPOLYMER – DNA COMPLEXES

#### 5.1 INTRODUCTION

An important part of the development of non-viral gene delivery systems is the evaluation of their biological properties. The major disadvantage of non-viral delivery systems is their low efficiency compared to viral vectors. Biological characteristics such as transfection efficiency have become the prime interest in determining the potential of a non-viral delivery system. In the previous chapters, the physicochemical properties of DMA-MPC diblock copolymer were assessed and the initial results suggest that certain compositions of this copolymer system appear to be promising candidates for further investigation. Before moving on to an *in vivo* study, relatively straight forward and low cost *in vitro* screening of a system is often carried out. Although the *in vitro* study may not always truly reflect the performance of a system *in vivo*, it is still valuable in indicating candidate systems that are eligible for further development.

##### 5.1.1 Aims

The aims of this chapter were to examine the biological properties of DMA-MPC diblock copolymers for gene delivery, including its capability to protect DNA from enzymatic degradation and membrane interaction of polymer – DNA complexes using liposomes as model membranes. In addition, the cellular association of the copolymer – DNA complexes using flow cytometry, and transfection efficiency of the DNA complexes *in vitro* were

also investigated. How the different composition of the copolymers and their physicochemical properties relate to the biological performance were discussed.

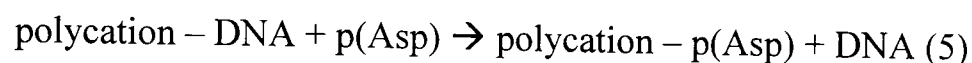
### 5.1.2 Principle of enzymatic degradation study

Once the polymer – DNA complexes are present inside the blood circulation, they are intermediately exposed to enzymatic activities (Wickstrom 1986, Eder *et al.*, 1991). This leads to the rapid degradation of any unprotected DNA before transfection takes place. In order to achieve successful transfection, the DNA must survive the journey from the site of administration to the nucleus of the target cells. In other words, the therapeutic DNA must be efficiently protected from enzymatic degradation.

In the enzymatic degradation study, the ability of different structures of DMA-MPC copolymers to resist DNase I enzyme degradation of DNA was determined by a fluorescence study (Dash *et al.*, 1997) and gel electrophoresis (Arigita *et al.*, 1999, Hill *et al.*, 2001, Tiyaboonchai *et al.*, 2003). DNase I is a pancreatic endonuclease which catalyses the hydrolysis of double-stranded DNA (Pan *et al.*, 1998). In the presence of  $Mg^{2+}$ , DNase I hydrolyses each strand of a duplex independently leading to random single strand breaks. The purine-pyrimidine bonds are subsequently preferentially cleaved resulting in double strand breaks, leading to a final product of di- and higher oligonucleotides (Fojta *et al.*, 1999).

In order to examine if there is any protection of DNA in the polymer – DNA complexes, DNA must be released from the complexes after they were subjected to enzymatic activity. One of the approaches to release the DNA is through the ‘polyelectrolyte displacement’ of the complexes with a polyanion, such as poly(aspartic acid) (pAsp) (Kayatose and Kataoka 1997) (equation 5). Other approaches include the use of sodium dodecyl sulphate (SDS)

(Bielinska *et al.*, 1997, Murphy *et al.*, 1998) or heparin (Ruponen *et al.*, 1999, Moret *et al.*, 2001) as displacement agents.



A fluorescent probe intercalation study is a simple technique to estimate the amount of DNA in a sample. The polymer – DNA complexes were first incubated with the enzymes, followed by the dissociation of the complexes. Any free DNA released from the complexes would interact with a fluorescent probe such as EtBr to induce fluorescence. By measuring the fluorescence intensity, the amount of DNA preserved can be estimated. Gel electrophoresis studies follow a similar principle. Any protected DNA released from the complexes after the displacement reaction would intercalate with EtBr to give fluorescence, which could be visualized on the agarose gel under UV transillumination. In addition, DNA with different size or molecular weight is separated during electrophoresis so that any alteration of DNA molecular weight caused by enzymes activities could be detected.

### **5.1.3 Principle of model membrane interaction study**

In the delivery of DNA into cells, DNA complexes have to initially come in contact with cellular membranes. In order to contribute to the rational design of an efficient gene delivery system, it is important to understand the interaction between the membrane and the DNA complexes. It is known that the composition of biological membranes is highly dependent on the cell type and function. Nevertheless, they all share the same basic phospholipid bilayer structure. The study of interactions between DNA complexes and phospholipid bilayers is useful in predicting any non-specific cellular interaction.

The purpose of model membrane interaction study is to investigate the interaction between DNA complexes with different copolymers composition (length of DMA block) and the phospholipids bilayers using liposomes as model membranes. 1,6-diphenyl-1,3,5-hexatriene (DPH) was employed as membrane fluorescence probe to study of the effects of DNA complexes on the hydrophobic core of bilayers. The non-ionic DPH is essentially non-fluorescent in water, only inducing fluorescence when bound to lipid bilayers (Lentz, 1989). DPH is situated towards the centre of the lipid bilayers as shown in figure 5.1. The fluorescence intensity will alter only when the complexes have interacted with the hydrophobic core of the bilayers.

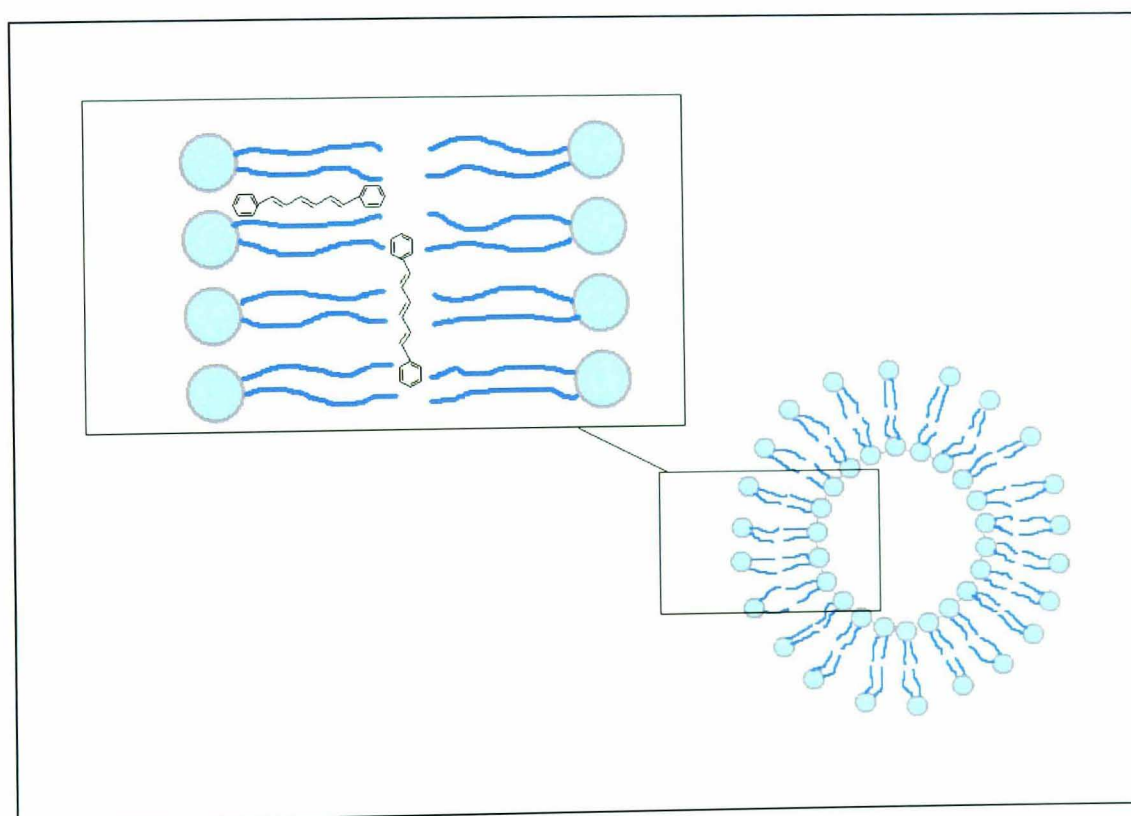


**Figure 5.1 Location and orientation of DPH in a phospholipid bilayer.** DPH is generally assumed to be orientated parallel to the lipid acyl chain axis, but can also reside in the centre of the lipid bilayer parallel to the surface (Mulders *et al.*, 1986, Wang *et al.*, 1991).



## 5.2 MATERIALS AND METHODS

### 5.2.1 Materials

Materials used were as described in Chapter 2, Section 2.1 unless otherwise specified below.

Tris acetate EDTA (TAE) buffer consisted of 40 mM Tris acetate, 20 mM glacial acetate acid and 1mM EDTA in ELGA water, with pH adjusted to 7.4 using glacial acetic acid. DNA loading buffer contained 0.25% w/v bromophenol blue in 40% w/v sucrose solution.

OptiMEM-I was purchased from Gibco, UK. Lipofectamine <sup>TM</sup> was purchased from Invitrogen, USA. Luciferase assay system was purchased from Promega, USA. YOYO-1 iodide was purchased from Molecular Probes, UK.

### 5.2.2 Cell lines and routine subculture

A549 cells (human lung carcinoma) were used. They were cultured and maintained as described in Chapter 2, section 2.2.2.

### 5.2.3 Enzymatic degradation assay

#### 5.2.3.1 Fluorescence Study

Polymer – DNA complexes (10 µg/ml of DNA) were prepared at monomeric unit: nucleotide ratios 1:1, 5:1 and 10:1 in 10% PBS (pH 7.4). Free DNA was used as a control. MgCl<sub>2</sub> was added in order to activate the enzymes. After 30 min, the complexes were incubated with DNase I (1 U/µg DNA) for

10 min at 37°C. The activity of DNase was then stopped by the addition of EDTA. Complexes were dissociated by addition of poly-L-aspartic acid (pAsp). EtBr (2 µg) was then added to each sample. Any free DNA released from the complexes would intercalate with EtBr to give fluorescence, which is directly proportional to the amount of DNA in the sample. The fluorescence intensity of the solution was measured at an excitation wavelength of 560 nm and an emission wavelength of 605 nm using Hitachi F-4500 fluorescence spectrophotometer (Hitachi Scientific Instruments, Finchampstead, UK). The result was presented as the percentage of fluorescence compared to untreated free DNA control.

#### 5.2.3.2 Gel electrophoresis

First, the polymer – DNA complexes were tested for complex dissociation with the presence of pAsp. Polymer – DNA complexes (2 µg of DNA) were prepared at different monomeric unit: nucleotide ratios of 0.25:1, 0.5:1, 1:1, 1.5:1, 2:1, 5:1 and 10:1 in TAE x 1 buffer (pH 7.4) to give a final volume of 12 µl. The complexes were incubated at room temperature for 30 min. Dissociation of complexes was achieved by addition of excess of pAsp (12.5/1 w/w pAsp/DNA). The mixture was incubated for a further 10 min, followed by addition of 3 µl DNA loading buffer. pAsp treated complexes were analysed by gel electrophoresis (0.8% agarose gel containing 1 µg/ml EtBr) in TAE x 1 buffer (pH 7.4). The electrophoresis was run at 60V for 45 min, after which the DNA was visualized and photographed on a UV transilluminator.

In the second part of the experiment, the complexes were tested for their ability to resist DNase I degradation. Polymer – DNA complexes were prepared as previously described. After 30 min, MgCl<sub>2</sub> was added (to final concentration of 10 mM) in order to activate the enzymes, and the complexes were incubated with DNase I (1 U/µg DNA) for 10 min at 37°C. The activity of DNase was then stopped by addition of 5 µl EDTA (0.5M) which chelated

with  $Mg^{2+}$ . Complexes were dissociated by addition of pAsp as above, followed by addition of DNA loading buffer. The samples were then analyzed by gel electrophoresis as described above. Free DNA without any treatment, DNA incubated with DNase I and DNA marker lambda-Hind III were served as control.

## 5.2.4 Model membrane interaction study

### 5.2.4.1 Preparation of liposomes – model membranes

Egg-phosphatidylcholin (100 mg) was dissolved in chloroform (1 ml) to give a stock solution with concentration 100 mg/ml. Cholesterol (100 mg) was dissolved in chloroform (1 ml) to give a stock solution with concentration 100 mg/ml. Required amount of lipids suspensions (phosphatidylcholin to cholesterol 2:1 molar ratio) in chloroform were mixed by vortexing. To prepare 1,6-diphenyl-1,3,5-hexatrien (DPH) – labelled liposomes, the fluorescence probe was dissolved in the mixture at 1:200 DPH: phospholipid molar ratio and the mixture was kept in the dark for 1 h at room temperature. The lipid mixture was then evaporated under a stream of nitrogen to prepare the lipid film. The lipid film was hydrated with PBS at room temperature. The suspension was freeze-thawed for five cycles by immersing into liquid nitrogen in order to get the multilamellar vesicles. The resulting vesicles were extruded through polycarbonate filters (double filters) with a pore size of 200 nm using a miniextruder fitted with two syringes (1 ml and 0.25 ml) to obtain unilamellar vesicles. Both polycarbonate filters and the syringes were obtained from LiposoFast System, Avestin Inc., Canada. The samples were subjected to 21 passes through the extruder. An odd number of passages were performed to avoid contamination of the samples with multilamellar vesicles that might not pass through the filter. Unilamellar vesicles were collected and stored it at 4°C before use.

#### 5.2.4.2 Fluorescence study

To prepare polymer – DNA complexes, calf thymus DNA (50 µg) was added to 10% PBS (200 µl), following by the addition of polymer solutions to make complexes with 2:1 and 10:1 monomeric unit: nucleotide molar ratios. The complexes were incubated at room temperature for 30 min. DPH labelled liposomes suspensions were added into 10% PBS (1 ml) to give a final concentration of 0.09 mM phospholipids. The fluorescence intensity was measured using Hitachi F-4500 fluorescence spectrophotometer (Hitachi Scientific Instruments, Finchamstead, UK). The excitation and emission wavelengths of DPH are 365 to 425 nm respectively. Aliquots of the DNA solution (250 µg/ml) or polymer – DNA complexes solution were then added to the liposomes suspension in a stepwise manner and the sample was mixed gently. The fluorescence intensity was measured after each addition. The same volume of 50 mM sodium dodecyl sulphate (SDS) and 10% PBS were added to the model membranes as positive and negative controls respectively.

#### 5.2.5 Flow cytometry study

DNA was labelled with YOYO-1 iodide (1 molecule of the dye per 300 base pairs of the nucleotide) (Ogris *et al.*, 2000) according to the manufacturer's protocol. The excitation and emission wavelengths for YOYO-1 are 491 and 509 nm, respectively. Six well plates were seeded with  $2 \times 10^5$  cells per well and the cells were incubated at 37 °C and 5% CO<sub>2</sub> for 24 h. After 24 h, the medium was aspirated off from the wells and gently replaced with DNA-copolymer complexes. The complexes were prepared in OptiMEM-I (2 ml) by addition of copolymer solution to luciferase plasmid (8 µg), followed by incubation for 30 min at room temperature prior to addition to cells. All complexes were prepared using a 2:1 monomeric unit: nucleotide ratio. Lipofectamine™ was complexed with DNA according to the manufacturer's protocol at a lipofectamine: DNA ratio of 2:1 (w/w). The cells were then incubated at 37°C and 5% CO<sub>2</sub> for 3 h. After 3 h, the complexes were

aspirated off from the wells. The cells were trypsinized using trypsin – EDTA and centrifuged at 800 rpm for 5 min. They were then washed twice with ice-cold PBS. Finally, they were suspended in 1 ml of PBS. The cell samples collected were stored in ice until analysis was performed. The percentage of fluorescent cells in the population and the fluorescence level of the cells were measured by flow cytometry (Beckman Coulter Epics XL). The measurements were performed using an Argon-Krypton Ion laser with an emission wavelength of 488 nm. Data were analyzed using EXPO32 version 1.0, Applied Cytometry system.

### 5.2.6 Transfection study

Six well plates were seeded with  $1 \times 10^5$  cells per well and the cells were incubated at 37 °C and 5% CO<sub>2</sub> for 24 h. After 24 h, the medium was aspirated off from the wells and gently replaced with DNA-copolymer complexes. Complexes containing 4 µg of DNA were prepared as described above. The cells were incubated for 4 h at 37 °C and 5% CO<sub>2</sub>. Following incubation, the complexes were removed and replaced with RMPI-1640 medium and the cells were incubated for a further 24 h before analysis.

#### 5.2.6.1 Detection of luciferase

The medium was removed from the cells, which were then washed with PBS twice. Luciferase detection was performed with a luciferase detection kit. Cell lysis buffer (300 µl) was added to each well. A pipette tip was used to scrape all cells from the well substrate, after which the lysate was centrifuged at 13,500 rpm for 5 min and the supernatants were collected. The luciferase activity of each sample was measured by gently mixing reconstituted luciferin reagent (100 µl) with cell lysate (20 µl) in a scintillation vial insert, and inserting into a luminometer (TD 20/20, Progema).

5.2.6.2 Determination of cellular proteins

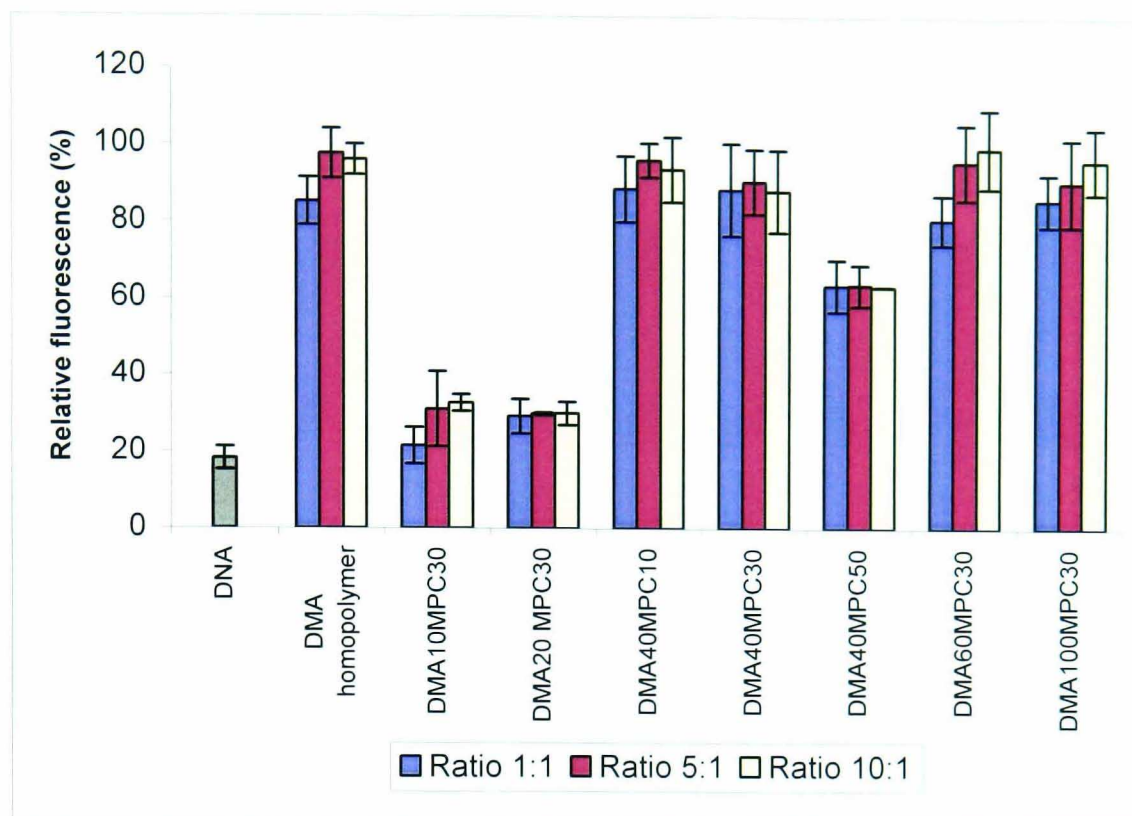
Recoverable cellular protein in each sample was determined *via* the Bradford assay (Bradford, 1976). A calibration curve was plotted using bovine serum albumin standard prepared over a concentration range of 1 – 1400  $\mu\text{g}/\mu\text{l}$ . Aliquots of each standard (100  $\mu\text{l}$ ) were added to polystyrene cuvettes, to which Bradford reagent (3 ml) was added. They were allowed to stand at room temperature for at least 5 min before  $A_{595}$  was measured using a UV-visible spectrophotometer. A linear standard curve was used to give an equation that related  $A_{595}$  to protein concentration, which could be used to determine the unknown protein concentration of cell lysates. Aliquots of lysate samples (20  $\mu\text{l}$ ) were first diluted with water (80  $\mu\text{l}$ ) before adding Bradford reagent and measuring  $A_{595}$  as described above. Results in terms of light units / ml obtained from luminescence measurements were divided by  $\mu\text{g}$  protein per ml to give a final value of light units /  $\mu\text{g}$  cellular protein.

## 5.3 RESULTS

### 5.3.1 Enzymatic degradation study

In the fluorescence enzymatic degradation study, the relative amount of DNA released from the complexes is shown in figure 5.2. The fluorescent intensity was expressed as percentage compared to untreated DNA control. After incubation with DNase I for 30 min, the fluorescence intensity of the control DNA decreased to only 20%, indicating that the majority of the DNA was degraded by nuclease. When DNA was complexed with DMA homopolymers, over 80% of the fluorescence was retained at 1:1 monomeric unit: nucleotide ratio. At ratio 5:1 and 10:1, the extent of protection was further increased as over 95% of fluorescence could be detected.

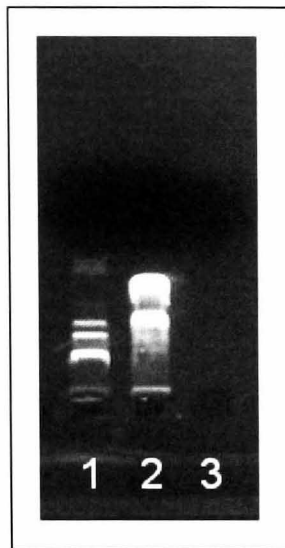
Different degrees of protection were observed with different compositions of the copolymers. Similar results were observed for DMA<sub>40</sub>MPC<sub>10</sub>, DMA<sub>40</sub>MPC<sub>30</sub>, DMA<sub>60</sub>MPC<sub>30</sub> and DMA<sub>100</sub>MPC<sub>30</sub> copolymer systems compared to DMA homopolymers. Over 80% of fluorescence was detected after the complexes were subjected to DNase I activity compared to untreated DNA controls. For DMA<sub>10</sub>MPC<sub>30</sub> and DMA<sub>20</sub>MPC<sub>30</sub> copolymers, there were significant reductions of fluorescence intensity compared to the control ( $p < 0.05$ ). Only about 30 % of fluorescence could be detected in these cases. For DMA<sub>40</sub>MPC<sub>50</sub> copolymers, a slightly higher amount of fluorescence, with approximately 60% of fluorescence remained.



**Figure 5.2 Enzymatic degradation study using fluorescent probe intercalation method.** The diagram shows the relative fluorescence following the addition of EtBr to polymer – DNA complexes, which were incubated with DNase I (37°C, 10 min) and displaced by pAsp. DNA complexes were prepared at monomeric unit: nucleotide ratios 1:1, 5:1 and 10:1 and the results were expressed in % of fluorescence intensity produced compared to the untreated DNA (n=3). Naked DNA was used as control.

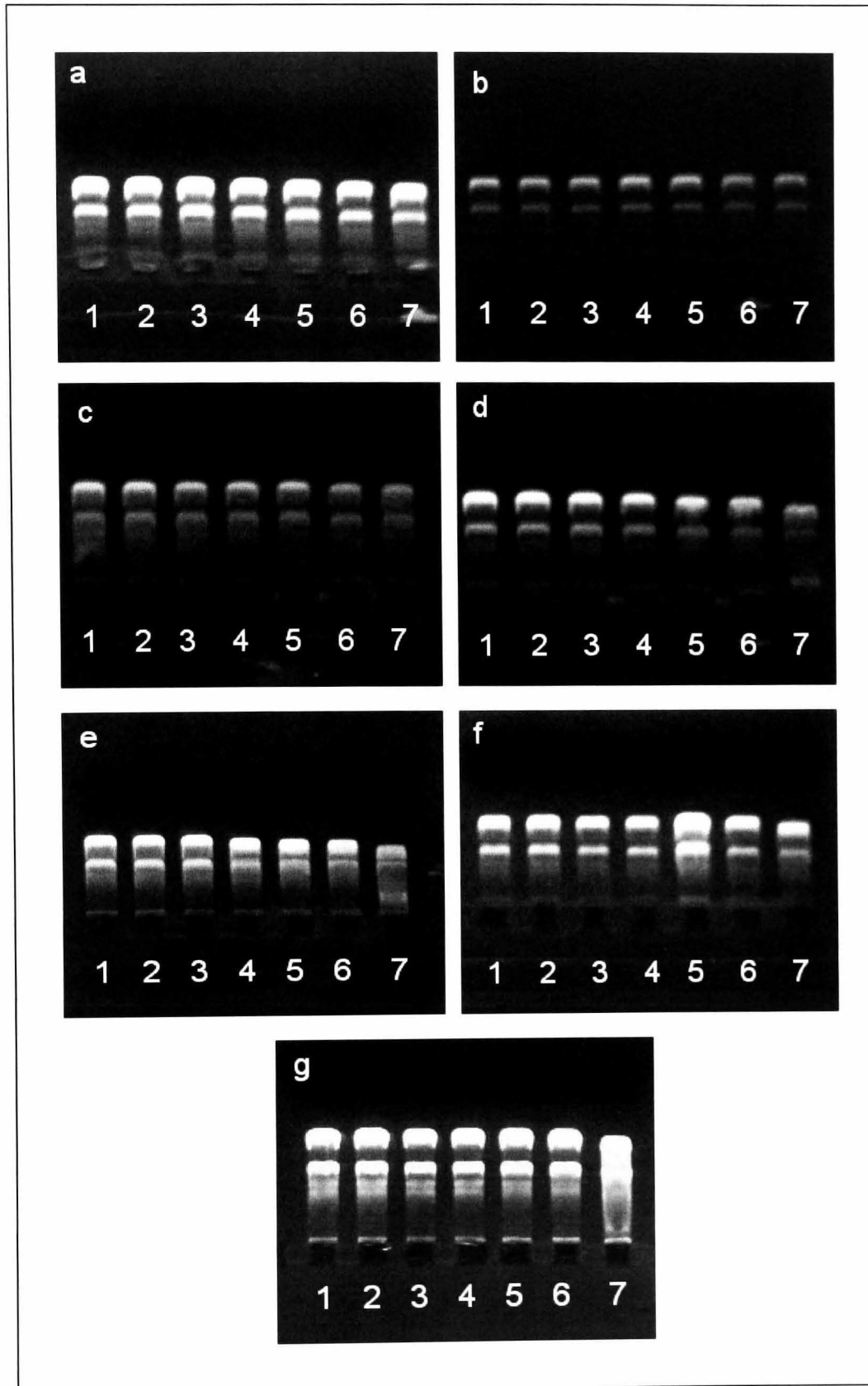
In the gel electrophoresis study, the ability of polymers to protect DNA from enzyme degradation was assessed by comparing the topology of released DNA from the complexes with the naked DNA control. Figure 5.3 shows the gel of naked DNA without treatment and after subjecting to DNase I degradation. No fluorescence could be detected after the naked DNA was incubated with DNase I (lane 3), indicating a high level of enzymatic degradation. Displacement of DNA from polymer – DNA complexes at different monomeric unit: nucleotide ratios was carried out using pAsp (figure 5.4). The results show that DMA homopolymers and DMA-MPC copolymers were able to dissociate to release free DNA as the released DNA had the same molecular weight as the untreated DNA control.





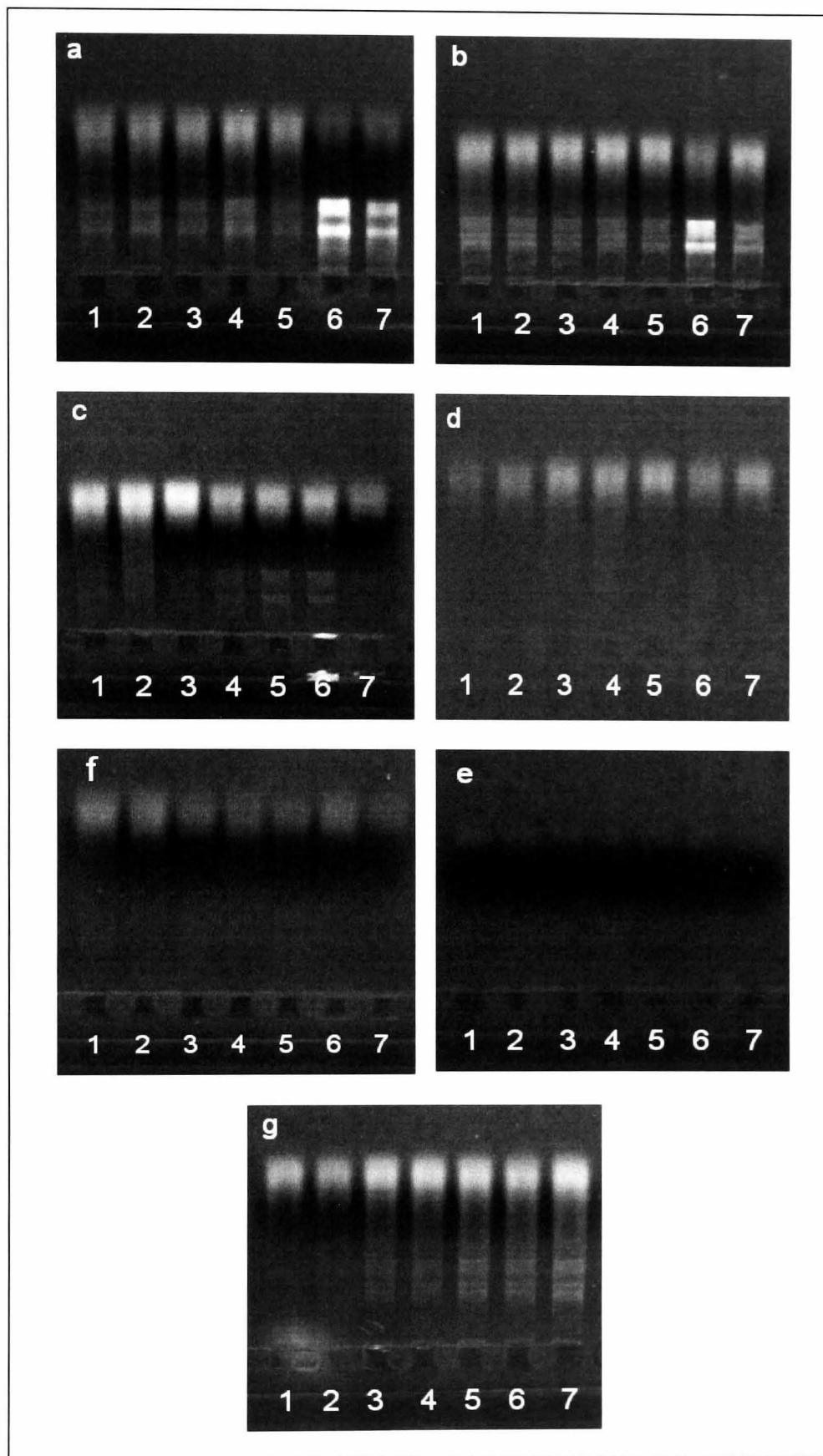
**Figure 5.3 Gel electrophoresis of naked DNA in enzymatic degradation study.** Lane 1 contained lambda Hind III DNA marker. Lane 2 contained untreated DNA control. Lane 3 contained naked DNA after DNase I incubation at 37°C for 10 min.

Figure 5.5 shows the results of polymer – DNA complexes after incubation with DNase I followed by displacement of DNA from the complexes using pAsp. Presence of DNA bands on the gel indicate the ability of polymer to protect DNA from enzymatic degradation. Both low and high molecular weight DMA homopolymers offered some degree of protection of DNA against DNase I degradation at ratios as low as 0.25:1. As the ratio increased, the degree of protection appeared to increase accordingly judged by the fluorescence intensity on the gel. For both homopolymers, a low molecular weight DNA fragment was also seen in the gel.



**Figure 5.4 Gel electrophoresis of polymer – DNA complexes dissociated with pAsp.** Lane 1-7 contained polymer – DNA complexes ratios at 0.25:1, 0.5:1, 1:1, 1.5:1, 2:1, 5:1 and 10:1 respectively after pAsp induced dissociation. (a) DMA homopolymer (low molecular weight), (b) DMA homopolymer (high molecular weight), (c) DMA<sub>40</sub>MPC<sub>10</sub>, (d) DMA<sub>40</sub>MPC<sub>30</sub>, (e) DMA<sub>40</sub>MPC<sub>50</sub>, (f) DMA<sub>60</sub>MPC<sub>30</sub> and (g) DMA<sub>100</sub>MPC<sub>30</sub>.

For the DMA-MPC diblock copolymers, only DMA<sub>40</sub>MPC<sub>10</sub> and DMA<sub>100</sub>MPC<sub>30</sub> were able to provide preservation of DNA structure from DNase I degradation, as similar molecular weight of released DNA compared to the control was seen at high ratios. However, the fluorescence intensity of the DNA bands appeared to be dimmer compared to DMA homopolymers, suggesting that less protection was offered by these copolymers. For other DMA-MPC copolymers studied, the original DNA topology could not be seen. Only low molecular weight DNA fragments were observed at the top of the gel.



**Figure 5.5 Gel electrophoresis of polymer – DNA complexes in an enzymatic degradation study.** DNA complexes were incubated with DNase I at 37°C for 10 min followed by dissociation with pAsp. Lane 1-7 contained polymer – DNA complexes ratios at 0.25:1, 0.5:1, 1:1, 1.5:1, 2:1, 5:1 and 10:1 (a) DMA homopolymer (low Mw), (b) DMA homopolymer (high Mw), (c) DMA<sub>40</sub>MPC<sub>10</sub>, (d) DMA<sub>40</sub>MPC<sub>30</sub>, (e) DMA<sub>40</sub>MPC<sub>50</sub>, (f) DMA<sub>60</sub>MPC<sub>30</sub> and (g) DMA<sub>100</sub>MPC<sub>30</sub>.

### 5.3.2 Model membranes interaction study

DPH labelled liposomes were used as model membranes to investigate the effect of polymer – DNA complexes on the hydrophobic core of lipid bilayers. Sodium dodecyl sulphate (SDS) is an anionic surfactant which is known to be able to permeate and solubilise biological membranes (Kragh-Hansen *et al.*, 1998). It has been frequently used as a model substance to study structural changes in cell membranes. In this study, SDS was employed as a positive control and the results are shown in figure 5.6. The solubilisation of phospholipid by SDS induced a significant reduction of fluorescence intensity of DPH-labelled liposomes as the DPH was displaced. The fluorescence intensity continued to decrease as the amount of SDS increased until a plateau was reached. However, a total displacement of DPH was not achieved. On the other hand, 10% PBS which does not interact lipid membranes was used as a negative control. The slight reduction in fluorescence intensity caused by 10% PBS was solely due to dilution effect. The DNA solution was added to the DPH labelled liposomes to examine whether DNA alone could interact with the membrane model. No significant change in fluorescence intensity was observed as compared to the control (10% PBS).

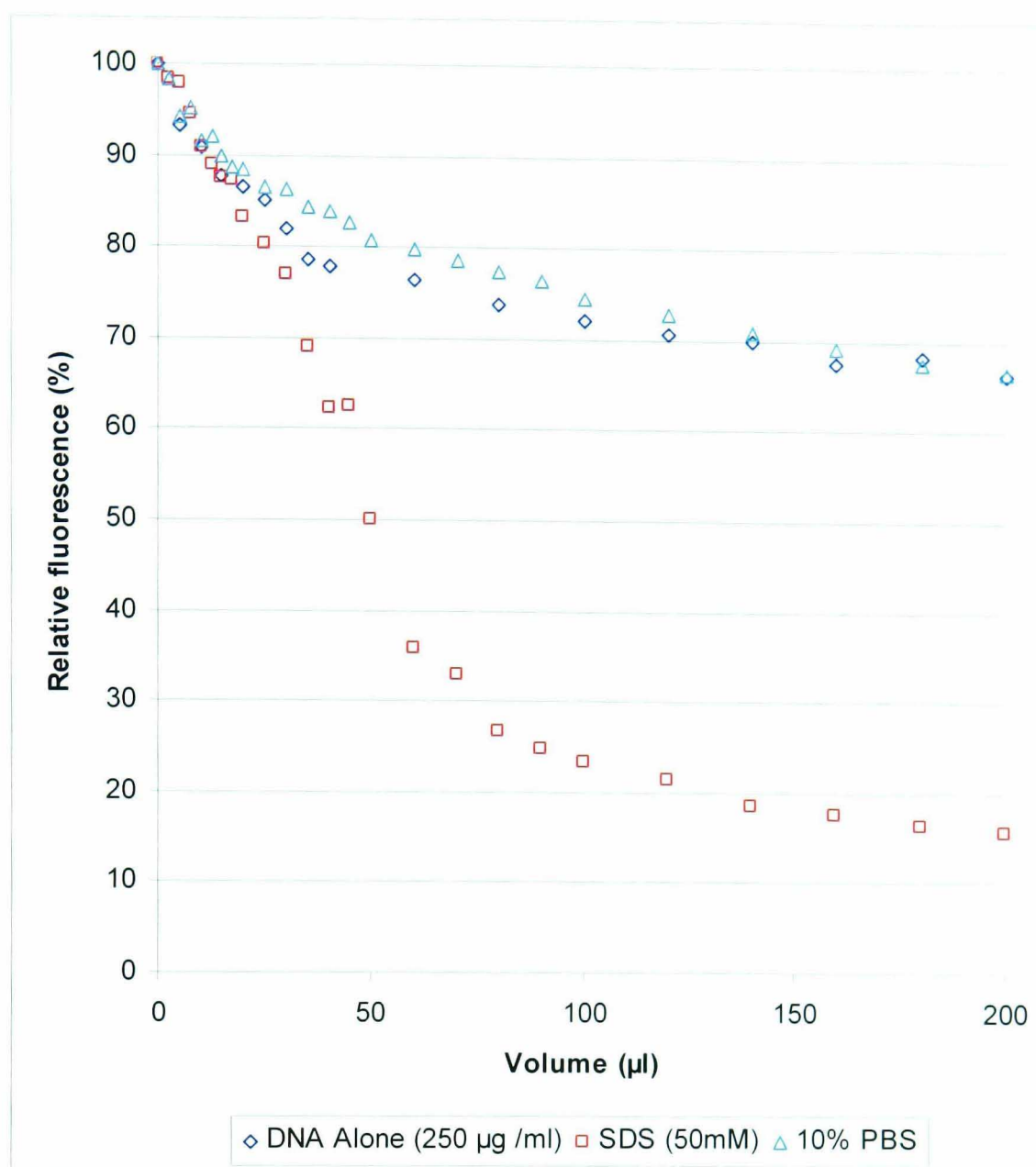


**Figure 5.6 The effect of DNA (250 µg/ml) on model membranes.** DPH labelled liposomes were used as model membranes. Fluorescence intensity was measured after the addition of DNA solution on liposomes and the results were expressed as relative fluorescence (%). Equivolume of SDS (50 mM) and 10% PBS were used as controls (n=3).

The effect of polymer – DNA complexes on phospholipid bilayers was studied by adding the complexes to the DPH labelled liposomes (figure 5.7 and 5.8). Since DPH is situated at the hydrophobic interior of the lipid bilayers (Mulders *et al.*, 1986, Wang *et al.*, 1991), it is assumed that the fluorescence intensity will only be affected when the interior of the bilayers is perturbed. Any interaction with the surface of the liposomes may not be

able to induce any noticeable change of fluorescence intensity as the DPH situated at the hydrophobic core of the liposomes is not disturbed. A similar trend was observed for all polymer – DNA complexes. A sharp decrease in relative fluorescence intensity was detected when small amount of DNA complex was added to the model membranes. As the amount of DNA complex increased, the relative fluorescence intensity decreased gradually. However, a plateau was not reached as the dilution effect caused the fluorescence level to decrease.

For DNA complexes prepared at 2:1 monomeric unit: nucleotide ratio (figure 5.7), all complexes induced a greater reduction of relative fluorescence intensity compared to the control (10% PBS) at the beginning. Among all the MPC containing copolymer – DNA complexes, DMA<sub>100</sub>MPC<sub>30</sub> – DNA complexes caused the largest reduction of fluorescence intensity. Interestingly, as the amount of DNA complex increased, the loss of fluorescence intensity appeared to be retarded. When a large amount of DNA complex was added (50µg DNA) to the liposomes, the relative fluorescence intensity of DMA<sub>20</sub>MPC<sub>30</sub> – DNA complex treated liposomes was similar to the control. For other copolymer – DNA complexes, the relative fluorescence intensity was only approximately 5% lower than the control. For DMA homopolymer – DNA complexes, the relative fluorescence intensity was about 10% lower than the control. At 10:1 monomeric unit: nucleotide ratio (figure 5.8), the copolymer – DNA complexes behaved similarly as those prepared at a 2:1 ratio. However, it was noticeable that the DMA homopolymer – DNA complexes at 10:1 monomeric unit: nucleotide ratio induced a greater reduction in fluorescence intensity than at the 2:1 ratio. When a large amount of DMA homopolymer – DNA complex was added (50µg DNA) to the liposomes, the relative fluorescence intensity was approximately 15% lower than the control.

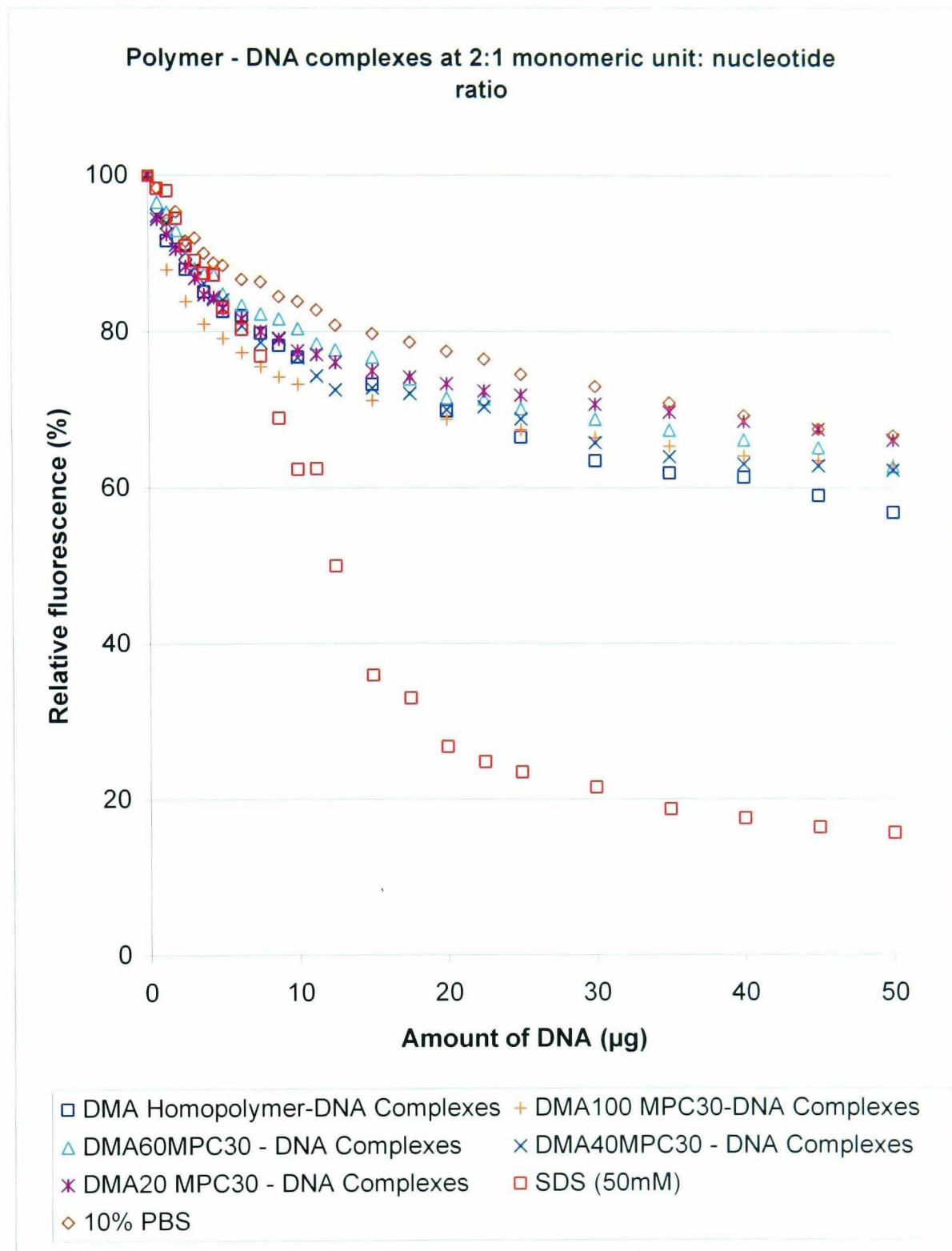


**Figure 5.7** The effect of polymer – DNA complexes prepared at 2:1 monomeric unit: nucleotide ratio on model membranes. DPH labelled liposomes were used as model membranes. Fluorescence intensity was measured after the addition of DNA complexes on the liposomes and the results were expressed as relative fluorescence (%). Equivolume 10% PBS and SDS (50 mM) were used as controls (n=3).



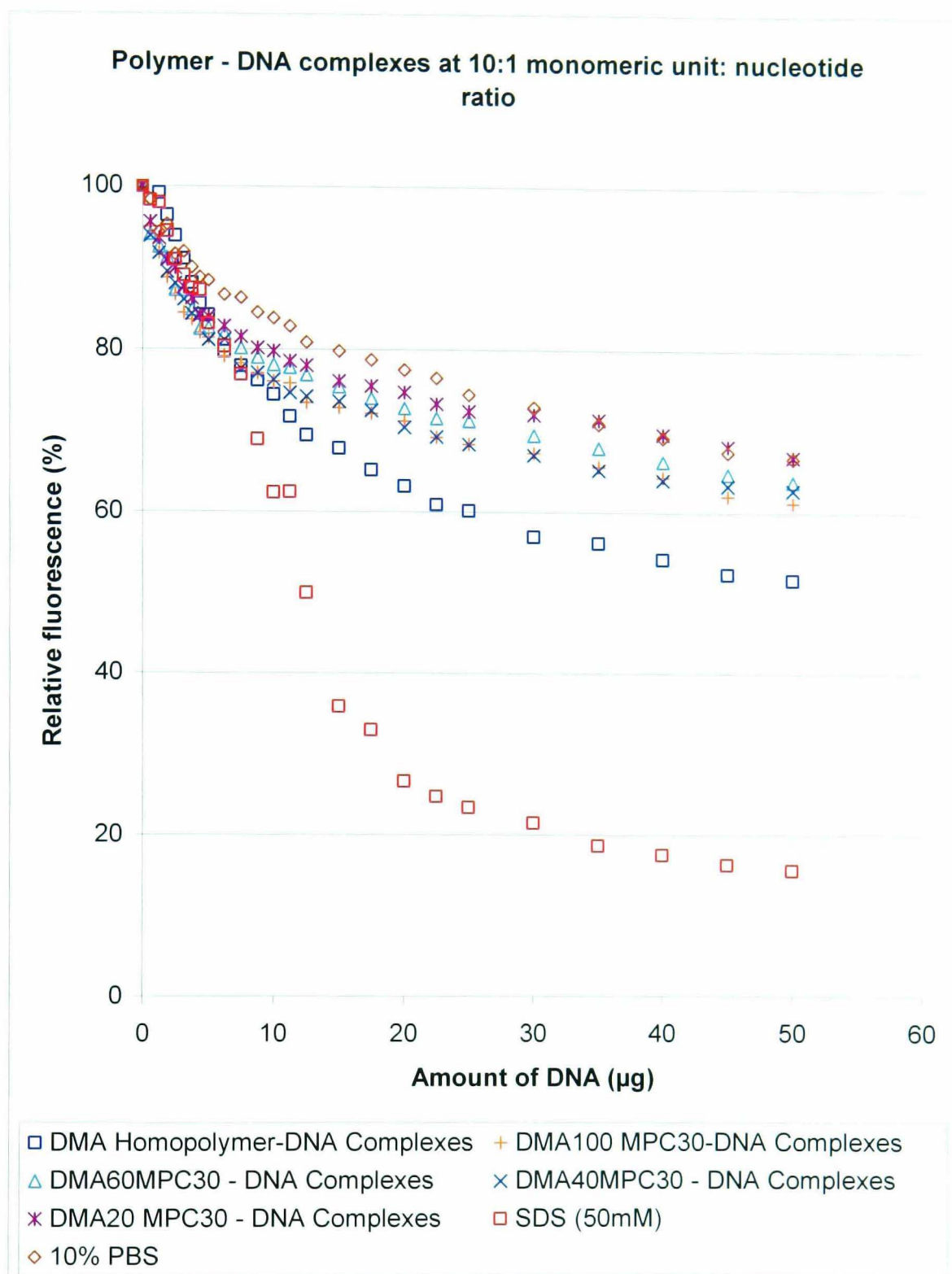


**Figure 5.8** The effect of polymer – DNA complexes prepared at 10:1 monomeric unit: nucleotide ratio on model membranes. DPH labelled liposomes were used as model membranes. Fluorescence intensity was measured after the addition of DNA complexes on the liposomes and the results were expressed as relative fluorescence (%). Equivolume 10% PBS and SDS (50 mM) were used as controls (n=3).

### 5.3.3 Flow cytometry study

In this study, flow cytometry was used to investigate the cellular association of the copolymer – DNA complexes. DNA was labelled with YOYO-1 fluorescent probe and the cellular association of the complexes was evaluated by measuring the fluorescence intensity associated with the cells. The results were expressed as the percentage of cells that showed a significant increase in fluorescence compared to the untreated control cells (figure 5.9), and the level of cell-associated fluorescence (figure 5.10).

From figure 5.9, it can be seen that when the cells were incubated with naked DNA, the percentage of fluorescing cells was low, approximately 10% of total cell populations. In contrast, when DNA was complexed with DMA homopolymer, the percentage of fluorescing cells markedly increased. Over 95% of cells showed associated fluorescence, which was comparable to that achieved with lipoplexes formed with lipofectamine™. For the copolymer complexes, as MPC content in the DMA<sub>40</sub>MPC<sub>y</sub> increased, the percentage of fluorescing cells decreased accordingly. When the cells were treated with DMA<sub>40</sub>MPC<sub>10</sub> – DNA complexes, approximately 60% of cells showed associated fluorescence. When the cells were treated with DMA<sub>40</sub>MPC<sub>50</sub> – DNA, the percentage of fluorescing cells was only about 10%, which was similar to those obtained with naked DNA. On the other hand, when the DMA content of the DMA<sub>x</sub>MPC<sub>30</sub> series increased, the percentage of fluorescing cells increased. Approximately 20% of cells showed associated fluorescence for DMA<sub>10</sub>MPC<sub>30</sub> and DMA<sub>20</sub>MPC<sub>30</sub> complexes. In contrast, more than 95% of cells showed associated fluorescence for the DMA<sub>100</sub>MPC<sub>30</sub> complexes, which was comparable to that achieved with the DMA homopolymer and lipofectamine™.

Although the percentage of fluorescing cells for DMA<sub>100</sub>MPC<sub>30</sub> complexes was similar to that of DMA homopolymer and lipofectamine™, the fluorescence intensity differed significantly. From figure 5.10, it is obvious that all the MPC- based copolymer complexes displayed much lower cellular

association as the fluorescence level were significantly lower than that of DMA homopolymer ( $p < 0.05$  in all cases). Only complexes formed with DMA homopolymer and lipofectamine™ displayed a significant increase in fluorescence level compared to naked DNA ( $p < 0.05$ ). The fluorescence intensity of the cells incubated with MPC copolymer complexes was comparable to that obtained with naked DNA. Complexes with higher DMA contents had somewhat higher cellular association, with the highest value obtained for the DMA<sub>100</sub>MPC<sub>30</sub> copolymer. However, the fluorescence intensity was still relatively low and was only about 25% of those obtained for DMA homopolymer, and 10% of lipofectamine™.

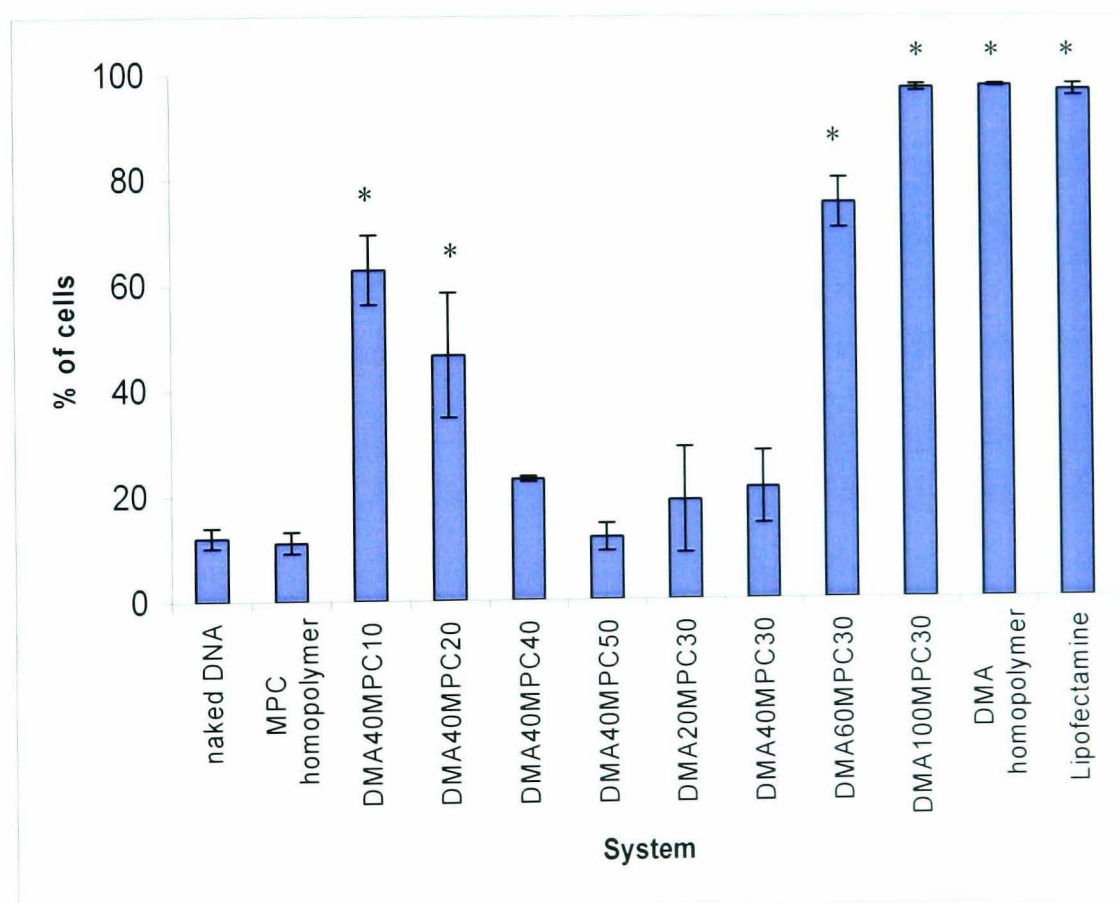


**Figure 5.9 Percentage of A549 cells exhibiting associated fluorescence at 180 min in flow cytometry study.** DNA was labelled with YOYO-1 fluorescent probe. All copolymer complexes were prepared at a 2:1 monomer unit: nucleotide ratio. Naked DNA and Lipofectamine™ were used as negative and positive control respectively ( $n=3$ ). \*  $P < 0.05$  when compared with naked DNA.

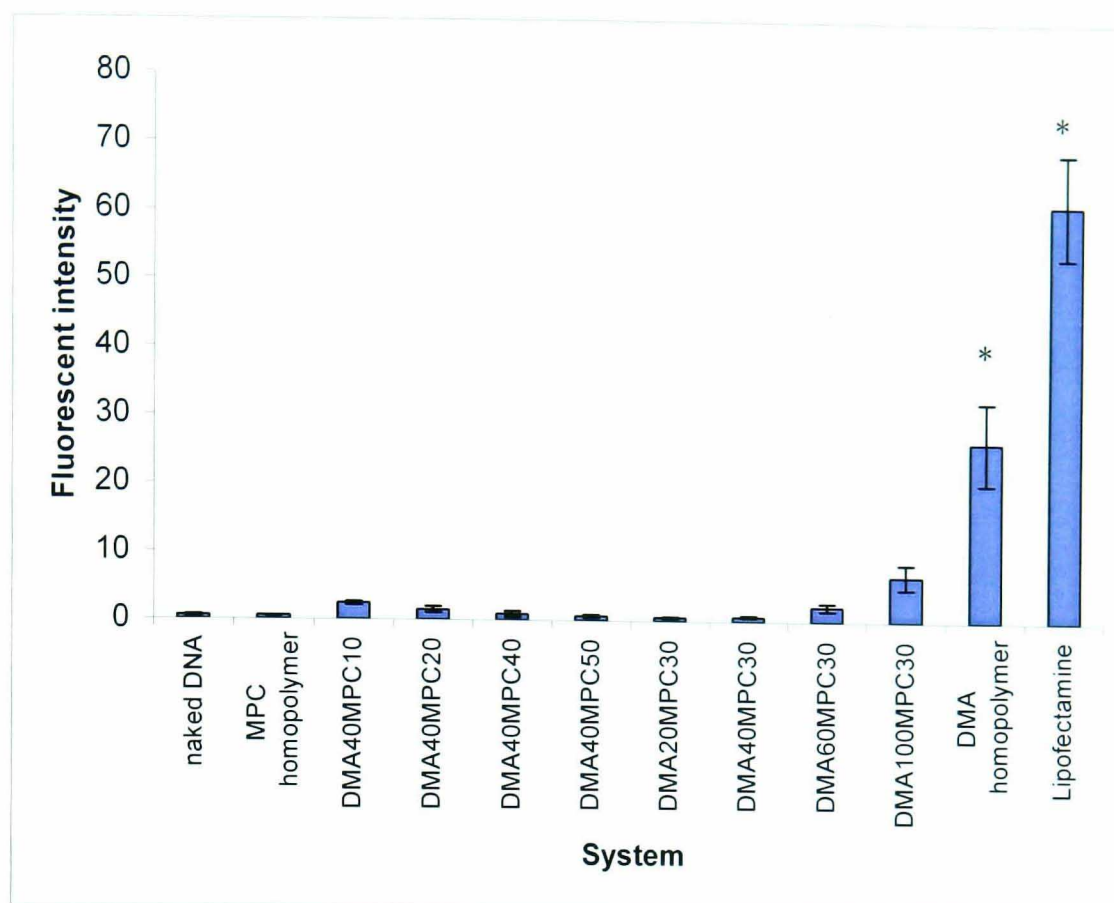


**Figure 5.10** The average fluorescence intensity associated with A549 cells at 180 min in flow cytometry study. DNA was labelled with YOYO-1 fluorescent probe. All complexes were prepared at a 2:1 monomeric unit: nucleotide ratio. Naked DNA and Lipofectamine™ were used as negative and positive control respectively (n=3). \*  $P < 0.05$  when compared with naked DNA.

#### 5.3.4 Transfection study

Transfection studies were carried out on A549 cells using the luciferase plasmid. This particular cell line was chosen for the study because earlier experiments in our group showed that DMA homopolymer – DNA complexes displayed reasonable transfection efficiency on this cell line (Rungsardthong *et al.*, 2001). The aim of the study was to compare the level of gene expression *in vitro* with different compositions of DMA-MPC copolymer. Naked DNA and Lipofectamine™ were used as controls.

The transfection results are displayed in figure 5.11. Each of the DMA-MPC copolymer – DNA complexes showed significantly lower transfection efficiencies than that of the DMA homopolymer. The transfection data in general displayed a similar trend to the flow cytometry study: the higher the cellular association, the higher the transfection efficiency. For the DMA<sub>40</sub>MPC<sub>y</sub> series, DMA<sub>40</sub>MPC<sub>10</sub> had the highest transfection efficiency. The transfection level decreased as the length of MPC increased, whereby DMA<sub>40</sub>MPC<sub>50</sub> had the lowest transfection level. On the other hand, for the DMA<sub>x</sub>MPC<sub>30</sub> series, the transfection efficiency increased as the DMA length increased. Complexes formed using the DMA<sub>100</sub>MPC<sub>30</sub> copolymer showed the highest level of transfection, but even this was 10 times lower than that of DMA homopolymer complexes. The transfection efficiencies of most of the copolymer – DNA complexes were not significantly different from naked DNA ( $p > 0.05$  for all copolymer – DNA complexes except DMA<sub>40</sub>MPC<sub>10</sub> and DMA<sub>100</sub>MPC<sub>30</sub>). Neither DMA homopolymer nor DMA<sub>100</sub>MPC<sub>30</sub> copolymer had transfection efficiency that was comparable to the commercial transfection agent lipofectamine™. The low transfection efficiencies of MPC containing copolymers correlate with cellular association, as suggested by flow cytometry study.

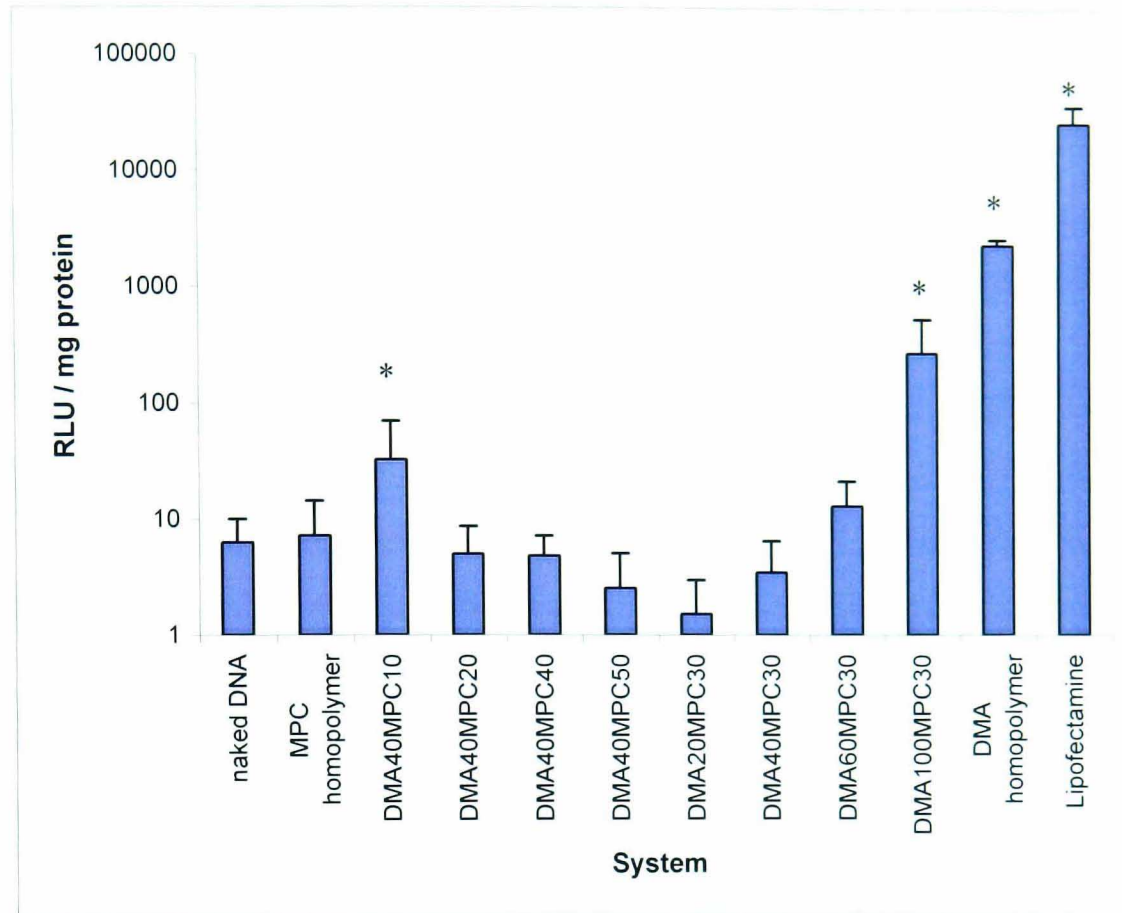


**Figure 5.11** Transfection efficiency of polymer – DNA complexes (2:1 monomeric unit: nucleotide ratio) on A549 cells. Data were presented in terms of relative light units (RLU) per mg protein. Naked DNA and Lipofectamine were used as controls (n=3). \*  $P < 0.05$  when compared with naked DNA.

## 5.4 DISCUSSION

A number of biological properties such as protection of DNA from enzymatic degradation, membrane interaction, cellular association and the transfection efficiency of DMA-MPC copolymer system were investigated in this chapter. In order to assess the polymers' ability to protect DNA from degradation, DNA was released from the complexes after subjection to enzymatic activity. Poly(L)aspartic acid (pAsp) was used to release DNA from the polymer – DNA complexes through a displacement reaction (Kayatose and Kataoka 1997). The gel electrophoresis study shows that the copolymer – DNA complexes were dissociated by pAsp and that the released DNA has a molecular weight the same as the DNA control. Although this is an artificial way to dissociate the DNA complexes, the use of polyanions may mimic the situation that the complexes encounter inside cells. The presence of negatively charged biopolymers, such as proteins, may act on the complexes to release the therapeutic DNA. Dissociation of the complexes and the release of DNA is a critical step in the transfection process (van de Wetering *et al.*, 1999) as only unbound and intact DNA can be transcribed into RNA. The results here show that dissociation of copolymer - DNA and the release of DNA can be achieved with the presence of anionic polymers.

pAsp was also used to dissociate the DNA – complexes following their exposure to enzymatic activity so that any protected DNA can be released and evaluated. Following DNase I incubation and dissociation of complexes, the released DNA was allowed to interact with EtBr to give fluorescence. The percentage of DNA remaining in the complexes was expressed as a percentage of the fluorescence intensity of EtBr induced by untreated DNA controls. The gel electrophoresis study was able to provide an even clearer picture as the released DNA was separated according to the molecular weight so that any alteration in the structure of DNA could be seen. The results from the fluorescence study showed that only 20% of the fluorescence could be detected after naked DNA was incubated with DNase I. As for the DMA

homopolymer – DNA complexes, over 80% of fluorescence could be detected. Similar results were observed for DMA<sub>40</sub>MPC<sub>10</sub>, DMA<sub>40</sub>MPC<sub>30</sub>, DMA<sub>60</sub>MPC<sub>30</sub> and DNA<sub>100</sub>MPC<sub>30</sub>. For the copolymers with relatively long MPC components, a reduced amount DNA was protected as the fluorescence level was considerably lower. This suggests that a long MPC chain had a negative effect on DNA protection efficiency. A previous study demonstrated that a high MPC content hindered the interaction between the cationic DMA and the negatively charged DNA as discussed in Chapter 3. As a result, loosely condensed structures were formed and the DNA could be more susceptible to enzymatic attack.

In the gel electrophoresis study, it was demonstrated that the DMA homopolymer was able to protect the DNA structure and that this protection could be achieved at a monomeric unit: nucleotide ratio of as low as 0.25:1. The level of protection appeared to increase with the ratio. However a small amount of low molecular weight DNA fragments still appeared on the gel, indicating that protection was not entirely complete. Amongst the DMA-MPC copolymers studied here, it appeared that only DMA<sub>40</sub>MPC<sub>10</sub> and DMA<sub>100</sub>MPC<sub>30</sub> could preserve the structure of DNA, though to a lesser extent compared to the homopolymers, judged by the intensity of fluorescent DNA bands. Other copolymers with a relatively high proportion of MPC failed to preserve DNA structure as only low molecular weight DNA fragments were observed. Although the fluorescence studies suggested that copolymers such as DMA<sub>40</sub>MPC<sub>30</sub> and DMA<sub>40</sub>MPC<sub>50</sub> could provide some degree of protection, none of them could successfully retain the original DNA structure. This is not desirable as the breakdown of DNA leads to the loss of therapeutic information of the gene, subsequently preventing gene expression (Adami *et al.*, 1998).

As mentioned before, the presence of MPC has an adverse effect on DNA condensation, resulting in the formation of loosely condensed structures in which the DNA was more susceptible to enzymatic attack. As shown in Chapter 4, the structures of DMA<sub>20</sub>MPC<sub>30</sub> and DMA<sub>40</sub>MPC<sub>30</sub> – DNA



complexes (in liquid under AFM) are ‘flower-like’ with loops of DNA around the perimeter in the form of petals. These uncondensed regions are probably the sites where enzymatic attack of DNA is initiated (Abdelhady *et al.*, 2003). The incomplete condensation of DNA by those copolymers may explain the unsuccessful DNA protection.

The results from the fluorescence study indicated that the measurement of fluorescence intensity after DNA interaction with EtBr is not an ideal approach for studying the state of released DNA after DNase I incubation, as EtBr yields fluorescence with intact plasmid as well as small molecular weight DNA fragments. Gel electrophoresis on the other hands revealed the molecular weight of the released DNA, hence it gave a better indication of the level of DNA degradation. Nevertheless, the fluorescence study gave a good indication of how the compositions of the copolymers might affect their ability to protect DNA from degradation.

In the model membranes interaction study, DNA alone was not able to induce any changes of fluorescence intensity of DPH labelled liposomes, indicating that there was no significant interaction between DNA and the phospholipid membranes. All the homopolymer polymer – DNA complexes investigated were able to induce a reduction in fluorescence level to various extents. Since the reduction of fluorescence intensity was greater than that caused by 10% PBS control, the loss of fluorescence was not only due to dilution effect, but also the perturbation of the hydrophobic core of the model membranes. However, it is difficult to determine the nature of the interaction between the DNA complexes and the phospholipid bilayers with this technique. The change in fluorescence intensity of DPH only provides an estimation of the relative extent of interaction between the phospholipid bilayers and the DNA complexes, but is not able to distinguish the exact mechanism of interaction. Both electrostatic and hydrophobic interactions could be involved. To gain an insight into any membrane structure alteration caused by the complexes, such as the fluidity and the stability of the model membranes, the orientation and polarization of DPH probes could be measured (Nagy *et al.*, 2003).

In general, all the DMA-MPC copolymer – DNA complexes investigated in this study appeared to be less membrane active compared to the DMA homopolymer – DNA complexes. This was particularly obvious when DNA complexes were prepared at high monomeric unit: nucleotide ratio (10:1). It is possible that the hydrophilic MPC formed a steric barrier that effectively reduced the interaction between phospholipid membranes and the DNA complexes.

In the flow cytometry and transfection study, all the copolymer systems investigated had a significantly lower cellular association and transfection efficiency compared to the homopolymer system. When DNA complexes with DMA homopolymer at 2:1 monomeric unit: nucleotide ratio, it is expected the complexes would have cationic character due the association of excess DMA homopolymer molecules with the complexes above the 1:1 (as shown in gel retardation assay in chapter 3). Hence, their cellular association is most likely a consequence of the charge interaction with the cell surface.

In contrast, all the DMA-MPC copolymer – DNA complexes showed poor cellular association with low transfection efficiency, which were comparable to that obtained with naked DNA. This is supported by the model membranes interaction study, as copolymer – DNA complexes were less able to displace or disturb the fluorescent probe DPH from the membrane model compared to the DMA homopolymer – DNA complexes. Among all the copolymer systems studied, DMA<sub>100</sub>MPC<sub>30</sub> – DNA complexes had the highest cellular association and transfection ability. Again, this is consistent with the model membranes interaction study as DMA<sub>100</sub>MPC<sub>30</sub> – DNA complexes demonstrated the greatest interaction with model membranes within all copolymers studied. This system also has the highest ability to protect DNA from enzymatic degradation. However, the cellular association and transfection efficiency were still only about 25% and 10% of those obtained for DMA homopolymer – DNA complexes, respectively. The results hence demonstrate that MPC-rich copolymers have low non-specific

cellular association and transfection efficiency. This can be attributed to the steric barrier around the complexes, created by the hydrophilic MPC blocks, which prevents adhesion to the cellular surface, as suggested in the model membranes interaction study. Additionally, the MPC surface layer shields possible positive charges arising from the polycation groups, as suggested by the zeta potential study presented in chapter 4.

The effect of the hydrophilic component on the transfection efficiency *in vitro* has been a matter of a debate. It is not clear how exactly the hydrophilic polymer, such as the frequently used PEG, affects the cellular association and transfection efficiency of the DNA complexes. It has been suggested that PEG is membrane active, thus increasing the cellular association and subsequently the transfection efficiency of PEG containing DNA complexes such as PLL-PEG (Toncheva *et al.*, 1998) and PEI-PEG (Ahn *et al.*, 2002). The authors suggested that PEG may act locally to dehydrate the membrane, thereby promoting entry of the complexes into the cells. In contrast, there is also evidence showing that PEO or PEG modified PEI or PLL – DNA complexes had much lower transfection efficiency compared to the unmodified controls (Choi *et al.*, 1998, Nguyen *et al.*, 2000). Nevertheless, it has also been pointed that the transfection efficiency of PEG containing systems might be dependent on cell lines and the molecular weight of PEG (Park *et al.*, 2005), therefore the effect of hydrophilic PEG is not certain at this stage. For DMA based delivery systems, the incorporation of PEG polymer was shown to reduce cellular interaction and transfection efficiency (Zuidam *et al.*, 2000, Rungsardthong *et al.*, 2001), possibly due to the charge shielding effect or steric barrier around the complexes that inhibits interaction with the cells. It appears that the effect of MPC is very similar to PEG, as both of these molecules are extremely hydrophilic, and the MPC and PEG modified DMA – DNA complexes shared similar biological properties.

The relatively poor cellular association and low transfection efficiency achieved using the DMA-MPC diblock copolymers is indeed essentially beneficial for the design of an effective gene delivery system, provided that

adequate DNA condensation is achieved. The ultimate goal of gene delivery is to deliver therapeutic DNA to specific target cells with minimal promiscuous non-specific cellular interaction and transfection. It is therefore important that the delivery vector does not disturb the balance of the cell membrane. Thus, provided that specific cells can be targeted by conjugation of an appropriate ligand, these DMA-MPC copolymers will be promising candidates as synthetic vectors for gene therapy applications. In fact, a novel folate conjugated DMA-MPC copolymer system has been developed recently and the evaluation of this functionalised copolymer system is described in the following chapter.

## 5.5 CONCLUSIONS

This chapter examined the biological properties of DMA-MPC copolymer for gene delivery. With the addition of polyanions, DNA – complexes formed by the homopolymer and copolymer can be dissociated to release the DNA, which is an essential process for successful transfection. The enzymatic degradation study shows that the DMA homopolymer can effectively protect and preserve the DNA from DNase I activity. However, the presence of a high proportion of MPC in the copolymers reduced their ability to protect DNA from enzymatic degradation, probably due to the formation of less well condensed structures. In addition, high proportions of MPC also reduce cellular association and consequently the transfection efficiency. It is possible that the steric barrier formed by the hydrophilic MPC prevents the interaction between the DNA complexes and the phospholipid bilayer of the cell membrane, as suggested by the model membranes interaction study. The goal of gene delivery is to transfer the DNA into target cells only, with minimal interaction with non-specific cells. The low cellular association and transfection efficiency of the DMA-MPC copolymer system is in fact desirable in the design of such gene delivery systems as any non-specific interaction is minimized, whereas specific targeting could possibly be achieved by conjugation of appropriate ligands.

## CHAPTER 6

# CELLULAR UPTAKE OF DMA HOMOPOLYMER – DNA COMPLEXES

### 6.1 INTRODUCTION

A number of different endocytic pathways have been identified in eukaryotic cells that may be involved in the cellular uptake of DNA complexes. The two main pathways that are believed to be involved in polycation delivery are the clathrin coated pits mediated pathway and the caveolae mediated pathway (Zuidam *et al.*, 2000, Jones *et al.*, 2003). The subsequent intracellular routes and eventual fate of substances internalized by these two different pathways are very distinct. Therefore, the mode of internalisation of DNA complexes might affect the kinetics of their intracellular processing, and thus the transfection efficiency. In order to improve our understanding and to assist the rational design of a non-viral gene delivery system, it is essential to elucidate the mechanism of uptake of DNA – complexes.

#### 6.1.1 Endocytosis

The plasma membrane is the interface between cells and their external environment. Uptake of nutrients and communication between cells and their environment occurs through this dynamic interface. Endocytosis is the process by which cells ingest extracellular materials by trapping them in invaginations of the plasma membrane, which then pinch off to form intracellular transport vesicles. A number of endocytic pathways are distinguished and they fall into two broad categories, namely phagocytosis (the uptake of large particles) and pinocytosis (the uptake of fluid and

solutes). The latter includes four distinct mechanisms, including clathrin-mediated endocytosis, caveolae-mediated endocytosis, macropinocytosis, and clathrin- and caveolin-independent endocytosis. Each of these mechanisms are utilised by the cells to accomplish different tasks (Kirkham and Parton, 2005). Certain cell treatments can inhibit cellular internalization via endocytosis, which is useful in determining the uptake pathways of different system. Commonly used cell treatments are summarised in table 6.1.

It has been demonstrated that some polymeric gene delivery vectors are able to transfect cells. However, the uptake mechanisms that these systems employ to gain entry into the cells are not clearly understood. Two mechanisms are generally believed to be involved in the uptake of polymer based delivery system, the clathrin-mediated endocytosis and caveolae-mediated endocytosis (Rejman *et al.*, 2005). Each of these mechanisms is described in more detail below.

**Table 6.2 Effect of different cell treatments on cellular uptake mechanism.**

<b>Treatment</b>	<b>Effect</b>	<b>Mechanism</b>	<b>Reference</b>
Low temperature	General inhibitor of endocytosis	Energy depletion	Lamaze and Schmid (1995)
Potassium depletion	Specific inhibitor of clathrin-mediated endocytosis	Dissociation of clathrin coats	Hansen <i>et al.</i> (1993)
Hypertonic medium (e.g. sucrose)	Specific inhibitor of clathrin-mediated endocytosis	Dissociation of clathrin coats	Hansen <i>et al.</i> (1993)
Low pH treatment	Specific inhibitor of clathrin-mediated endocytosis	Dissociation of clathrin coats	Hansen <i>et al.</i> (1993)
Chlorpromazine	Specific inhibitor of clathrin-mediated endocytosis	Causes clathrin to localize and accumulate in late endosomes	Wang <i>et al.</i> (1993)
Concanavalin A	Specific inhibitor of clathrin-mediated endocytosis	Prevents coated pits assembly	Smith <i>et al.</i> (2001)
Brefeldin A	Specific inhibitor of clathrin-mediated endocytosis	Interfere with the assembly of clathrin coats	Brodsky <i>et al.</i> (2001)
Nystatin	Specific inhibitor of caveolae-mediated endocytosis	Sequester cholesterol	Lamaze and Schmid (1995)
Filipin	Specific inhibitor of caveolae-mediated endocytosis	Cholesterol binding	Schnitzer <i>et al.</i> (1994)
Methyl- $\beta$ -cyclodextrin	Specific inhibitor of caveolae-mediated endocytosis	Deplete cholesterol	Lamaze and Schmid (1995)
Genestein	Inhibitor of caveolae-mediated endocytosis	Tyrosine kinase inhibitor	Orlandi and Fishman (1999)
Colchicine	Inhibitor endocytosis	Microtubule depolymerisation	Margolis <i>et al.</i> (1980)
Vinblastine	Inhibitor of endocytosis	Microtubule depolymerisation	Wang and MacDonald (2004)
Nicodazole	Inhibitor of endocytosis	Microtubule depolymerisation	Wang and MacDonald (2004)
Cytochalasin D	Inhibitor of endocytosis and macropinocytosis	Actin depolymerisation	Parton <i>et al.</i> (1994)
Latruncubin B	Inhibitor of endocytosis and macropinocytosis	Inhibits actin polymerisation and disrupts microfilament organisation	Spector <i>et al.</i> (1983)
Chloroquine	Disruption of endosomes and lysosomes	Prevents endosomes acidification and causes swelling to endosomes and lysosomes	Wattiaux <i>et al.</i> (2000)



### 6.1.2 Clathrin-mediated endocytosis

Clathrin-mediated endocytosis is a process by which virtually all eukaryotic cells internalise nutrients, antigens, growth factors, pathogens and recycling receptors (Mellman, 1996, Hirst and Robinson, 1998, Lakadamyali *et al.*, 2004). It usually occurs at specialized sites on the plasma membrane. The most prominent feature of clathrin-mediated endocytosis is the formation of coated pits, which cover 0.5 – 2% of the cell surface (Brown and Petersen, 1999). The most abundant proteins found in coated pits are clathrin and adaptor protein 2 (AP-2). Internalization occurs either constitutively or in response to certain stimuli. The constitutive pathway is mainly involved in the uptake of receptors that undergo continuous internalization and recycling. It is also responsible for ligand-independent internalisation of signalling receptors (Parent *et al.*, 2001, Waterman and Yarden, 2001). The uptake of macromolecules and certain viruses, and the regulation of a number of proteins in the circulation rely on the constitutive pathway. The signal induced pathway is responsible for the control of signalling potency of the receptor by regulating events that occur at the level of internalisation, which in turn determine the post-endocytic fate, i.e. recycling or degradation of the receptor (Mousavi *et al.*, 2004).

The process of clathrin-mediated endocytosis is summarized in figure 6.1. Three main stages are identified during the formation of clathrin coated vesicles: (1) Assembly of clathrin into a polygonal lattice and formation of coated pits, (2) invagination of coated pits, and (3) pinching-off the coated vesicles. During the process, clathrin is assembled on the cytoplasmic face of the plasma membrane by the recruitment of AP-2 to form a characteristic invagination or coated pits, which are typically 100-150 nm (Takei and Haucke, 2001, Mousavi *et al.*, 2004). Following the release of clathrin coated vesicles from the plasma membrane, the internalised molecules are delivered to early endosomes where clathrin is subsequently released. Molecules such as recycling receptors are rapidly recycled back to the plasma membrane for reutilization. The rest are transported to the increasingly

acidic milieu of the late endosomes and lysosomes for degradation (Gruenberg 2001).

There are number of ways to inhibit clathrin-mediated endocytosis. Approaches such as hypertonic challenge (using sucrose), intracellular potassium depletion and low pH shock treatment have been traditionally used to disrupt clathrin-mediated endocytosis by dissociation of clathrin coats from the plasma membrane (Hansen *et al.*, 1993, Brodsky *et al.*, 2001). Chemical agents such as concanavalin A (conA), chlorpromazine and brefeldin A (BFA) are also frequently employed as alternatives to inhibit clathrin-mediated endocytosis (Wang *et al.*, 1993, Brodsky *et al.*, 2001, Smith *et al.*, 2001).

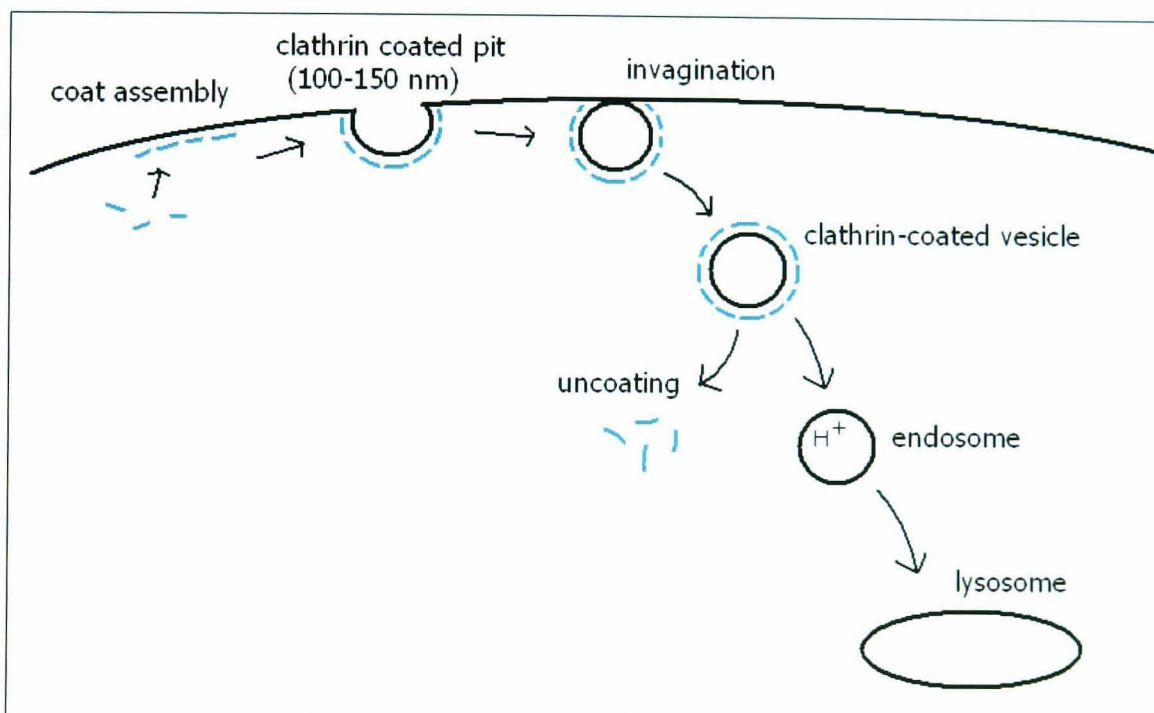


**Figure 6.1 Schematic diagram of clathrin-mediated endocytosis.** Clathrin is first assembled at the intracellular surface of the plasma membrane. Clathrin coated pit is formed and the invagination of the coated pit occurs. The deeply invaginated coated pits pinch off from the plasma membrane to form clathrin coated vesicle. The vesicle loses its clathrin coat and progress to endosomes which are acidified. The endosomes are then transported to lysosomes where the internalised material is degraded.

### 6.1.3 Caveolae-mediated endocytosis

Caveolae are flask-shaped, cholesterol and sphingolipid rich invaginations of the plasma membrane on the surface of endothelial cells. They belong to a sub domain of the biochemically defined glycolipid raft (Anderson, 1998, Nabi and Le, 2003). Not all cell types have caveolae. Caveolae are smaller than clathrin coated vesicles, with a diameter of 50-100 nm. Up to 30% of the cell surface can be occupied by caveolae (Parton and Richards, 2003). The most characterized protein component of caveolae is the caveolin-1 (Rothberg *et al.*, 1992), which are widely used as markers for caveolae. Caveolin-1 is essential for the formation and stability of caveolae. Caveolae cannot be detected in cells that lack caveolin-1. However, introduction of caveolin-1 to these cells induces the formation of caveolae at the plasma membrane (Fra *et al.*, 1995). A number of substances are known to internalise into the cells through this pathway, including membrane components (e.g. glycosphingolipids and glycosylphosphatidylinositol-anchored proteins), extracellular ligands (e.g. folic acid), bacterial toxin (e.g. cholera toxin), and non-enveloped viruses (e.g. simian virus 40) (Rothberg *et al.*, 1990, Parton *et al.*, 1994, Anderson *et al.*, 1996, Nichols *et al.*, 2001, Duncan *et al.*, 2002).

The process of caveolae-mediated endocytosis is summarized in figure 6.2. In contrast to clathrin-mediated endocytosis, internalization *via* caveolae is not a constitutive process and only occurs upon cell stimulation (Thomsen *et al.*, 2002, Pelkmans and Helenius 2003). In addition, internalisation *via* caveolae occurs at a much slower rate compared to the clathrin-mediated pathway (Tran *et al.*, 1987, Anderson *et al.*, 1996, Pelkmans and Helenius 2003). It is also a more tightly regulated process. One interesting aspect of caveolae-mediated endocytosis is that the internalized caveolae bypass the acidic endosomes and lysosomes. Instead, they are transported to a specific endosomal compartment with neutral internal pH, which is often referred as caveosomes (Pelkmans *et al.*, 2001). The internalised material could reside, be sorted to the Golgi complex or to the endoplasmic reticulum. For this

reason, the caveolar internalisation pathway has potential advantages for targeted drug or gene delivery (Bathori *et al.*, 2004).

Several drugs have been reported to selectively inhibit caveolae-mediated endocytosis. Cholesterol is a very important component of caveolae and is required to maintain the structural integrity of these vesicles. Caveolae disappear in cells that are depleted of cholesterol. Therefore, the most effective way to disrupt caveolar function is to use sterol-binding drugs which remove cholesterol from the plasma membrane and cause disassembly of caveolae. Such drugs include methyl- $\beta$ -cyclodextrin, filipin and nystatin (Rothberg *et al.*, 1992, Schnitzer *et al.*, 1994, Orlandi and Fishman, 1998), none of which typically affect clathrin-mediated endocytosis. These drugs have been frequently used in the study of uptake of simian virus (SV40), which is well known to be internalised through caveolae dependent pathway (Anderson *et al.*, 1996, Sieczkarski and Whittaker, 2002, Pelkmans and Helenius, 2003).

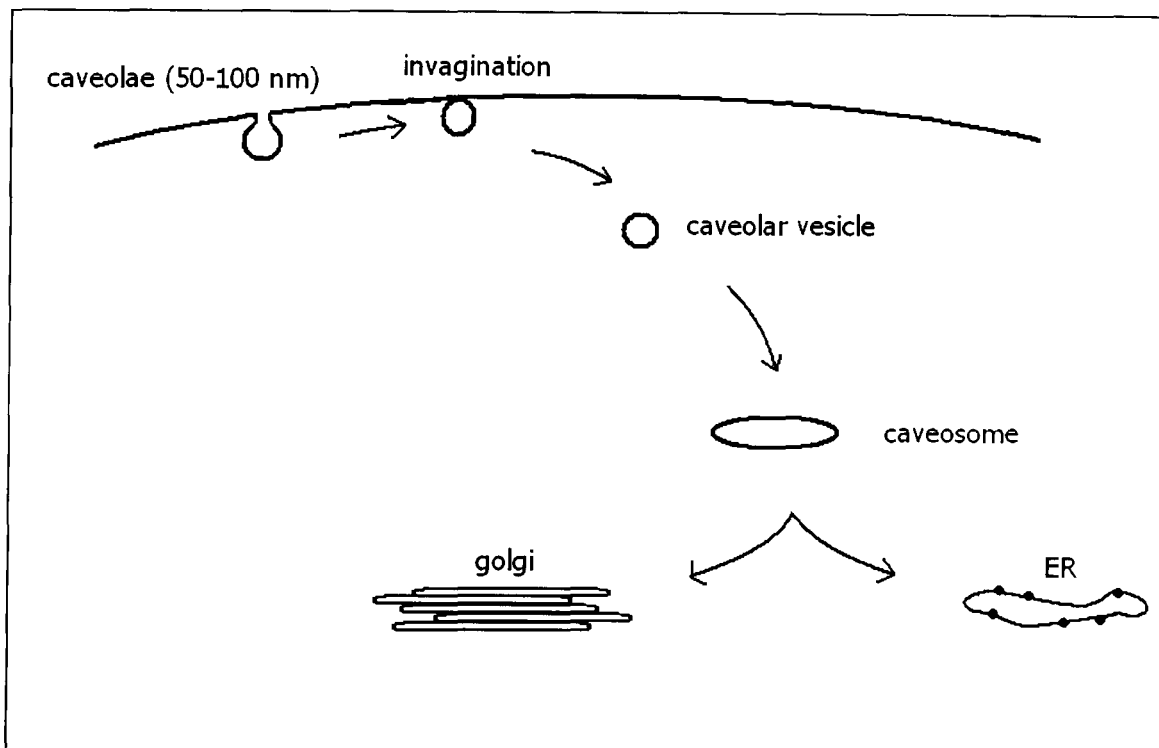


**Figure 6.2 Schematic diagram of caveolae-mediated endocytosis.** Caveolae appear as flask-shaped vesicles at plasma membrane, which subsequently invaginate and bud into the cytoplasm. The internalised caveolar vesicles fuse to form caveosomes which have neutral pH. Without being transported into the lysosomes, the internalised materials are sorted to golgi complex or endoplasmic reticulum.

#### 6.1.4 Involvement of microtubules and actin filaments in endocytosis

Both microtubules and actin filaments are known to be involved in the endocytosis process (Cole and Lippincott-Schwartz *et al.*, 1995, Qualmann *et al.*, 2000, Murray and Wolkoff, 2003). However, they are involved in different stages of the process. Microtubules, a component of the cytoskeleton, consist of tubulin and several associated proteins. The protein filaments stretch across cells and provide a mechanical basis for chromosome sorting, cell polarity and organelle localization among other functions. The transport of endocytic contents from early to the late endosomes is dependent on microtubules which also promote fusion and fission of endocytic vesicles (Aniento *et al.*, 1993, Elkjaer *et al.*, 1995, Harada *et al.*, 1995). Colchicine, vinblastine and nocodazole are well known microtubules depolymerising agents that bind specifically to tubulin and inhibit its polymerization (Margolis *et al.*, 1980, Wang and MacDonald 2004).

Filamentous actin is also a major component of cytoskeleton. However, its involvement in endocytosis is less well defined. It is believed that the actin filaments are important for events that take place during the invagination of the vesicles, but not the trafficking of vesicles within the cells (Salas *et al.*, 1986, Lamaze *et al.*, 1997, Zegers *et al.*, 1998, Mundy *et al.*, 2002). Commonly used actin filament disrupting drugs include cytochalasin D and latrunculin B (Spector *et al.*, 1983, Cooper, 1987, Coue *et al.*, 1987, Sampath and Pollard, 1991, Morton *et al.*, 2000). Cytochalasin D is a fungal alkaloid that binds to the positive end of the actin filaments and prevents elongation. Latrunculin B is a marine toxin which inhibits actin polymerization and disrupts microfilament organization as well as microfilament-mediated processes. Both agents are frequently used to investigate the internalization pathway of bacteria (Murai *et al.*, 1993, Wells *et al.*, 1998, van de Walle *et al.*, 2001, Biswas *et al.*, 2003), but are less commonly used in the study of gene delivery system.

### 6.1.5 Aims

The purpose of this work was to establish the mechanism of internalisation and intracellular trafficking of DNA complexes formed with DMA homopolymer, which has been previously demonstrated to be able to transfect several different cell lines (Desphande *et al.*, 2004). The luciferase assay was performed on A549 cells at different time point post transfection in order to create a time profile of gene expression of the DMA homopolymer – DNA complexes as a control. Various endocytic inhibitors with effects on different routes and stages of endocytosis were also employed in the transfection study in order to examine the mechanism of cellular uptake of the DNA complexes. In addition, a confocal microscopy study was performed to assist the understanding of the route of uptake as well as intracellular trafficking of the DNA complexes.

## **6.2 MATERIALS AND METHODS**

### **6.2.1 Materials**

Materials used were as described in Chapter 2, Section 2.1 unless otherwise specified below.

OptiMEM-I was purchased from Gibco, UK. Lipofectamine™ was purchased from Invitrogen, USA. Luciferase assay system was purchased from Promega, USA. YOYO-1 iodide and CellTracker Orange were purchased from Molecular Probes, Oregon, USA.

### **6.2.2 Cell lines and subculture**

A549 cells (human lung carcinoma) were used. They were cultured and maintained as described in Chapter 2, section 2.2.2.

### **6.2.3 Transfection study at different time point**

A transfection study was carried out as described in Chapter 5, section 5.2.5 with minor modifications. After the cells were incubated with DNA complexes for 4 h, the complexes were removed, replaced with RMPI-1640 medium and incubated at 37°C and 5% CO<sub>2</sub>. The cells were analysed at 4, 8, 12, 24, 36, 48 and 72 h post transfection. The detection of luciferase and determination of cellular proteins were carried out as described in Chapter 5, sections 5.2.6.1 and 5.2.6.2 respectively.

**6.2.4 Transfection with inhibitors**

The transfection study was carried out as described in Chapter 5, section 5.2.6 with minor modifications. Prior to the transfection study, six well plates were seeded with  $1 \times 10^5$  cells per well and the cells were incubated at 37 °C and 5% CO<sub>2</sub> for 24 h. The cells were pre-treated with colchicine (1-25 µg/ml), cytochalasin D (1-25 µg/ml), chlorpromazine (1-25 µg/ml), conA (1-250 µg/ml), nystatin (1-25 µg/ml) or filipin (1-10 µg/ml) for 1 h at 37°C. Subsequently the cells were washed and incubated with polymer – DNA complexes (4 µg DNA / well) at 37°C and 5% CO<sub>2</sub> for 4 h (with or without inhibitors). Following incubation, the complexes were removed and replaced with serum supplemented RPMI-1640 medium (with or without inhibitors). The cells were incubated with 5% CO<sub>2</sub> at 37°C for the required time before analysis. The detection of luciferase and determination of cellular proteins were carried out as described in Chapter 5, section 5.2.6.1 and 5.2.6.2 respectively.

**6.2.5 Confocal microscopy study**

In the intracellular trafficking study,  $1 \times 10^5$  A549 cells were seeded on a Mattek dish (Mattek Corp. Ashland MA, USA). The cells were incubated at 37°C and 5% CO<sub>2</sub> for 24 h. After 24 h, the medium was removed and replaced with DMA homopolymer – DNA complexes. The complexes were prepared at 2:1 monomeric unit: nucleotide ratio in OptiMEM-I and the plasmid DNA was labelled with YOYO-1 iodide (1 molecule of the dye per 300 base pairs of the nucleotide) according to the manufacturer's protocol. The excitation and emission wavelengths for YOYO-1 are 491 and 509 nm, respectively. The cells were incubated at 37°C and 5% CO<sub>2</sub> in a heated Perspex box throughout the experiment. Confocal imaging was performed on the same sample at 5, 30, 60, 90 and 150 min after the addition of DNA complexes.



For other confocal studies, A549 cells were seeded and incubated in the Mattek dish as described above. After 24 h of incubation, the medium was removed from the cells and the cytoplasm of the cells were labelled with CellTracker Orange according to the manufacturer's protocol. The excitation and emission wavelengths for CellTracker Orange probe are 541 and 565 nm respectively. The cells were then treated with inhibitors if needed for 1 h. The cells were then washed with PBS before the addition of DMA homopolymer – DNA complexes (with the presence of inhibitors if needed). The complexes were prepared at 2:1 monomeric unit: nucleotide ratio in OptiMEM-I and the plasmid DNA was labelled with YOYO-1 iodide. DNA complexes were incubated with the cells at 37°C and 5% CO<sub>2</sub> in the incubator for 240 min. Confocal imaging was then performed. The cells were incubated at 37°C and 5% CO<sub>2</sub> in a heated Perspex box during imaging.

Confocal laser scanning microscopy (Zeiss Axiovert 100 with a Zeiss LSM510uv META Combi confocal system, Germany) was used for optical sectioning of cells to visualize the cellular uptake and intracellular trafficking of DNA complexes. 63X Zeiss Plan Apochromat objective lens was used. An argon laser at 488 nm with a BP505-530 filter and a helium-neon laser at 543 nm with a LP560 filter were used to induce fluorescence of YOYO-1 probe and CellTracker Orange probe respectively. Image analysis was performed on all the images to determine their relative position from the cell surface using Zeiss LSM Image Browser Version 3.5.0.376 (Carl Zeiss GmbH, Jena, 1997-2005).

## 6.3 RESULTS

### 6.3.1 Transfection study at different time points

The first part of the study was to investigate the expression of the reporter gene luciferase at various times post-transfection. DMA homopolymer – DNA complexes (2:1 monomeric unit: nucleotide ratio) were incubated with A549 cells and the luciferase assay was carried out at various time, starting from 4 to 72 hours post-transfection. The results are shown in figure 6.3. It was found that expression of the luciferase plasmid was observed as early as 4 h post-transfection, and the level of gene expression increased considerably over time, with the peak level of transfection efficiency seen at 16 hours post-transfection. The transfection efficiency remained steady at the maximum level for next 20 hours. From 48 hours post-transfection and onwards, the transfection efficiency was reduced gradually.

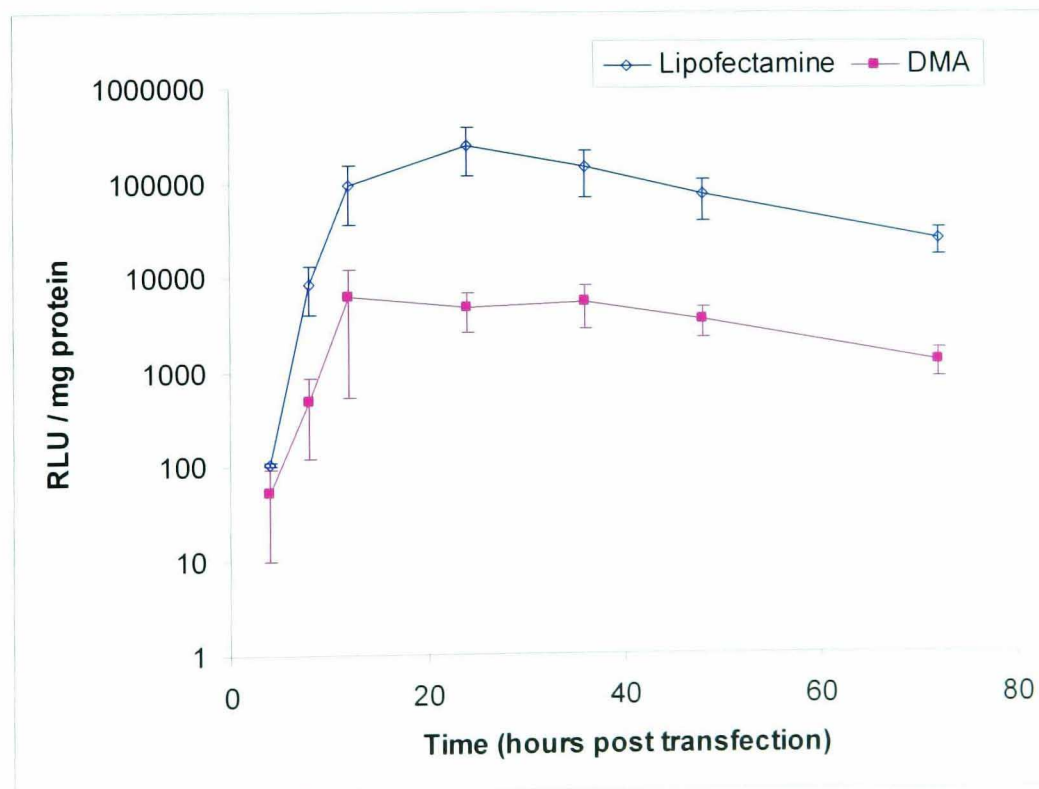


**Figure 6.3** Transfection efficiency of DMA homopolymer – DNA complexes on A549 cells measured at different time post-transfection. DNA complexes were prepared at 2:1 monomeric unit: nucleotide ratio. The luciferase assay was carried at 4, 8, 12, 24, 36, 48 and 72 h post-transfection. Lipofectamine™ was used as control (n=3).

### 6.3.2. Transfection with tubulin / actin inhibitors

In order to investigate the contribution of microtubules and actin filaments to the transport of DMA homopolymer – DNA complexes, the effects of two different inhibitors, colchicine, a microtubule inhibitor (Margolis *et al.*, 1980), and cytochalasin D, a microfilament inhibitor (Cooper, 1987, Sampath and Pollard, 1991), on transfection efficiency in A549 cells were examined by luciferase assay.

When the cells were pre-treated with colchicine (figure 6.4), the transfection efficiency was significantly inhibited by almost 80% relative to the untreated control at 16 hours post-transfection for all concentrations. At 24 hours post-transfection, the gene expression was restored and there was no significant difference in transfection efficiency compared to the control ( $p>0.05$ ). As the time increased, the transfection efficiency continued to increase. At 36 hours post-transfection, the inhibitor caused a 10-fold increase in transfection and at 48 hours post-transfection, the gene expression was enhanced dramatically by 20- to 40-fold in a dose dependent manner. A similar pattern was observed in both situations when the cells were pre-treated and incubated with colchicine throughout the experiment (figure 6.6). A much higher transfection level was observed at 48 hours post-transfection, with 40- to 50-fold increase observed in a dose dependent manner. Recovery protein level of the cells was used as an indicator of the health status of colchicine treated cells. The protein level of the cells decreased gradually as the time of exposure and the concentration of inhibitor increased (figure 6.5 and 6.7).

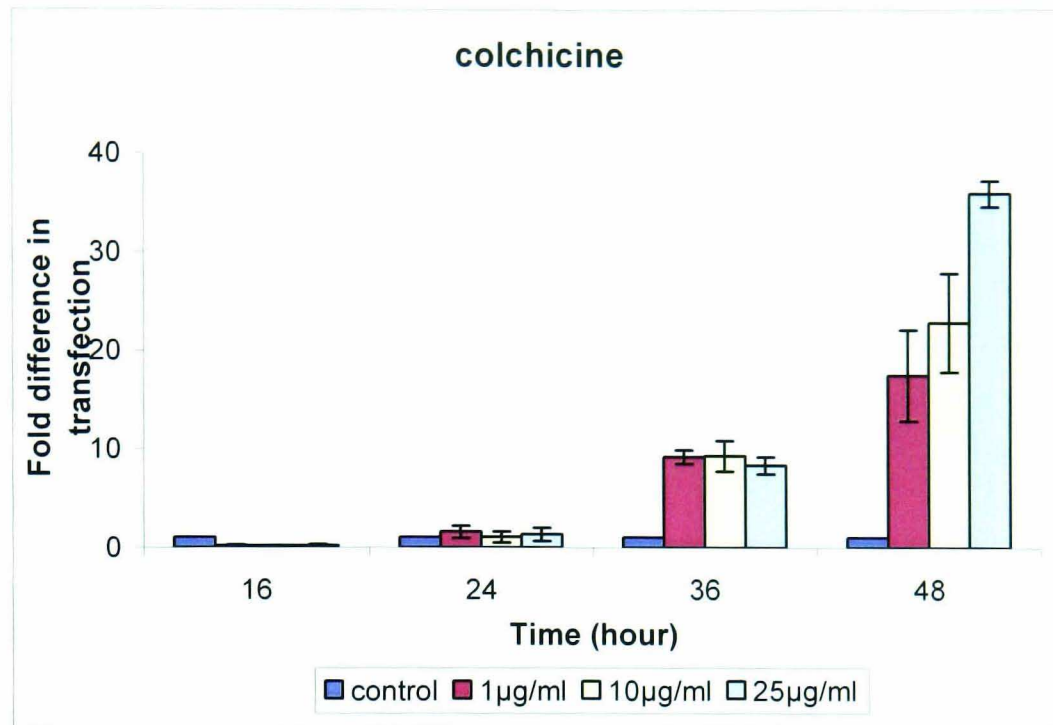


**Figure 6.4** Transfection efficiency of DMA homopolymer – DNA complexes on colchicine pre-treated A549 cells. The complexes were prepared at 2:1 monomeric unit: nucleotide ratio. The transfection activities were measured at different time post-transfection and the results were expressed as fold difference compared to control (without inhibitor) which is equal to 1 at all time (n=3).

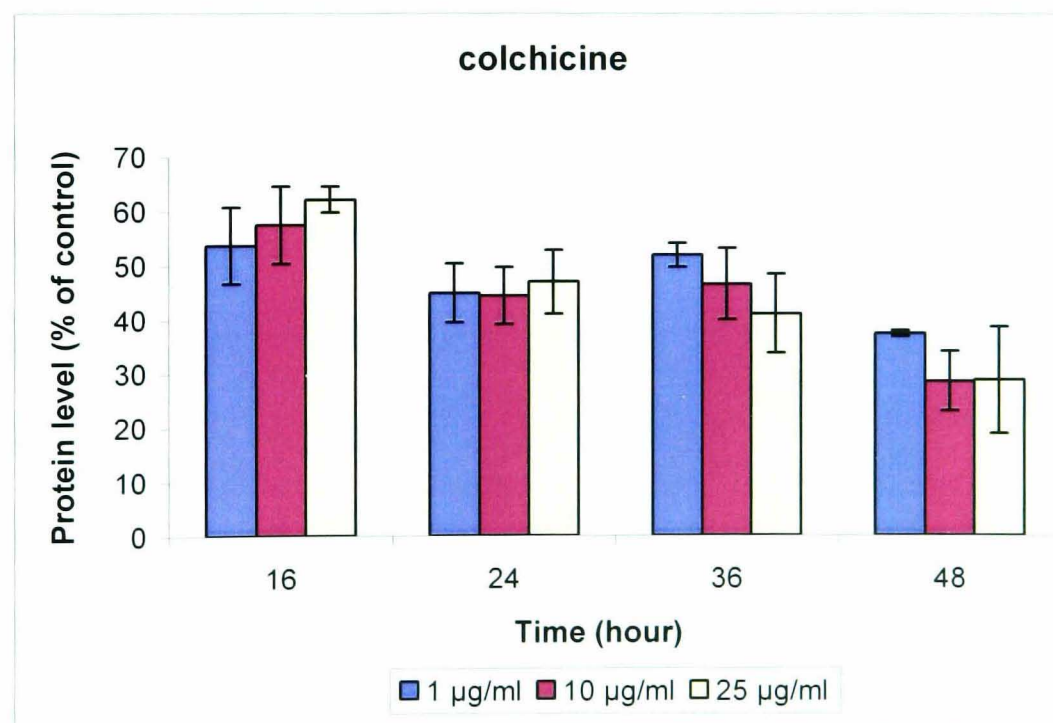


**Figure 6.5** Protein level of colchicine pre-treated A549 cells in the luciferase assay. The cells were incubated with colchicine at various concentrations 1 h prior to complexes addition. The protein level was determined using Bradford assay. The results were expressed as % compare to the control (without inhibitor) (n=3).

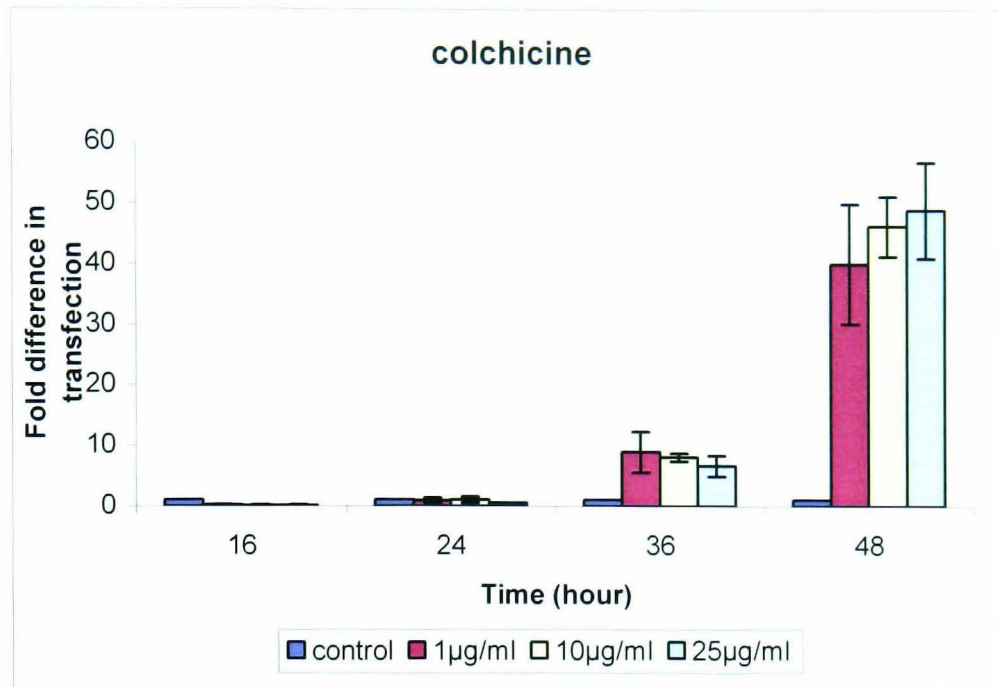


**Figure 6.6** Transfection efficiency of DMA homopolymer – DNA complexes on colchicine pre-treated A549 cells, with colchicine present during the experiment. The complexes were prepared at 2:1 monomeric unit: nucleotide ratio. Transfection activities were measured at different time post-transfection. The results were expressed as fold-difference compare to control (without inhibitor) which is equal to 1 at all time (n=3).

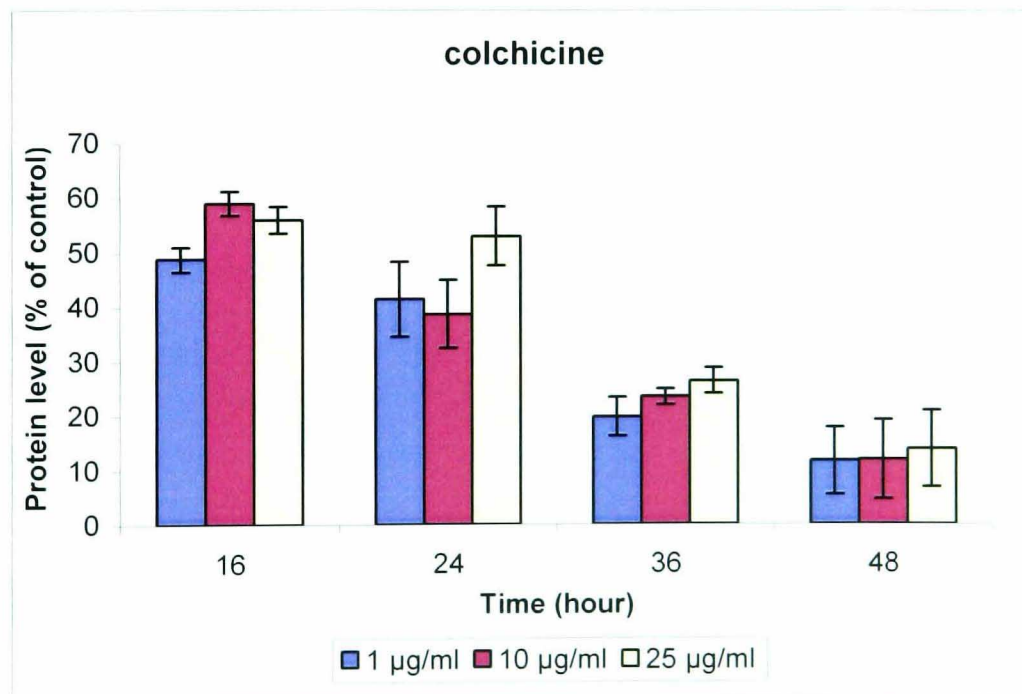


**Figure 6.7** Protein level of colchicine treated A549 cells in the luciferase assay. The cells were incubated with colchicine at various concentrations 1 h prior to complexes addition and during the experiment. The protein level was determined using Bradford assay. The results were expressed as % compare to the control (without inhibitor) (n=3).

Cytochalasin D was incubated with the cells one hour prior to the addition of the DNA complexes and was then removed. It was clearly shown that the transfection efficiency of DMA homopolymer – DNA complexes was effectively inhibited by cytochalasin D (figure 6.8). At 24 hours post-transfection, the transfection efficiency was decreased significantly compared to the untreated control ( $p < 0.05$ ) in a dose dependent manner. At 48 hours post-transfection, the level of gene expression was inhibited to approximately 35% of the control. However, there was no significant difference of transfection efficiency between different concentrations of the inhibitor ( $p > 0.05$ ). Again, the recovery protein level of the cells was used as an indicator of the health status of cytochalasin D treated cells. It was found that the protein level reduced with increasing concentration of inhibitor (figure 6.9).

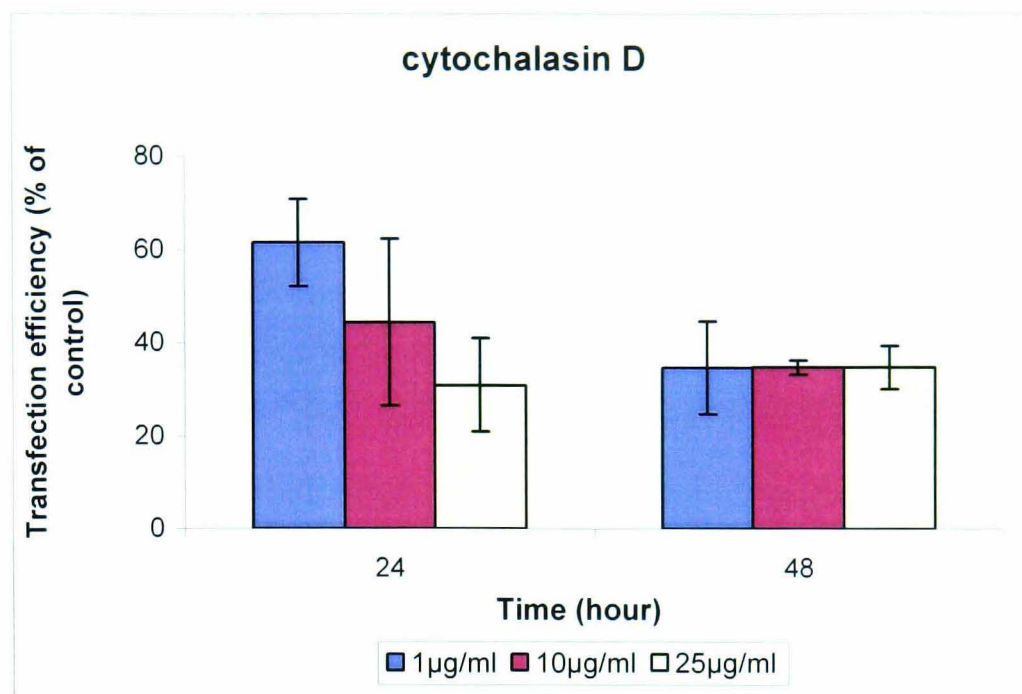


**Figure 6.8** Transfection efficiency of DMA homopolymer – DNA complexes on cytochalasin D pre-treated A549 cells. The complexes were prepared at 2:1 monomeric unit: nucleotide ratio. The transfection activities were measured at different time post transfection and the results were expressed as percentage compare to the control (without inhibitor) (n=3).

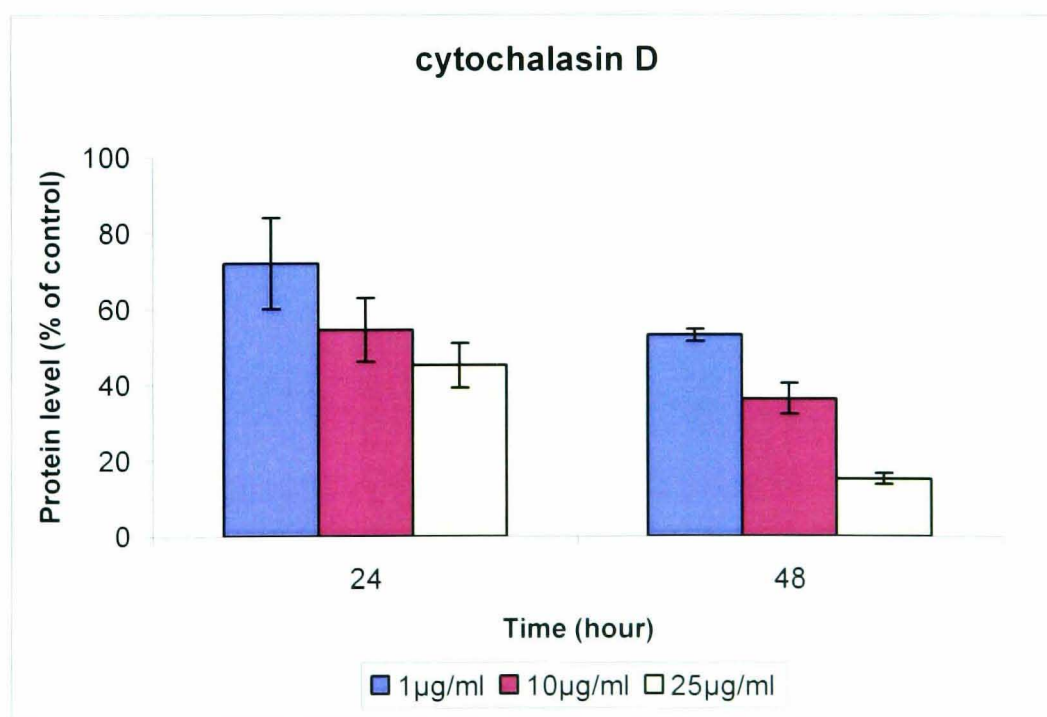


**Figure 6.9** Protein level of cytochalasin D pre-treated A549 cells in the luciferase assay. The cells were incubated with cytochalasin D at various concentrations 1 h prior to complexes addition. The protein level was determined using Bradford assay and the results were expressed as % compared to the control (without inhibitor) (n=3).

### 6.3.3 Transfection with clathrin / caveolae inhibitors

In order to explore the role of the two types of cellular uptake mechanism (clathrin-mediated and caveolae-mediated endocytosis) in transfection, both mechanisms were investigated using respective inhibitors. ConA and chlorpromazine are inhibitors of clathrin-mediated endocytosis (Smith *et al.*, 2001, Brodsky *et al.*, 2001), whereas filipin and nystatin are inhibitors of caveolae-mediated endocytosis (Rothberg, *et al.*, 1992, Orlandi and Fishman, 1998). Transfection experiments were carried out on A549 cells. When the cells were treated with conA or chlorpromazine, the transfection efficiency was markedly reduced with increasing concentration of the inhibitors (figure 6.10 and 6.11). The transfection efficiency was reduced to approximately 20% and 30% of the untreated control when 250  $\mu\text{g/ml}$  of conA and 25  $\mu\text{g/ml}$  of chlorpromazine were used respectively. When the cells were treated with filipin or nystatin, the transfection of the cells were also inhibited, but to a lesser extent when compared to those treated with conA or chlorpromazine (figure 6.12 and 6.13). The transfection efficiency was decreased to approximately 40% of the untreated control when 10  $\mu\text{g/ml}$  of filipin or 25  $\mu\text{g/ml}$  of nystatin was incubated with the A549 cells.



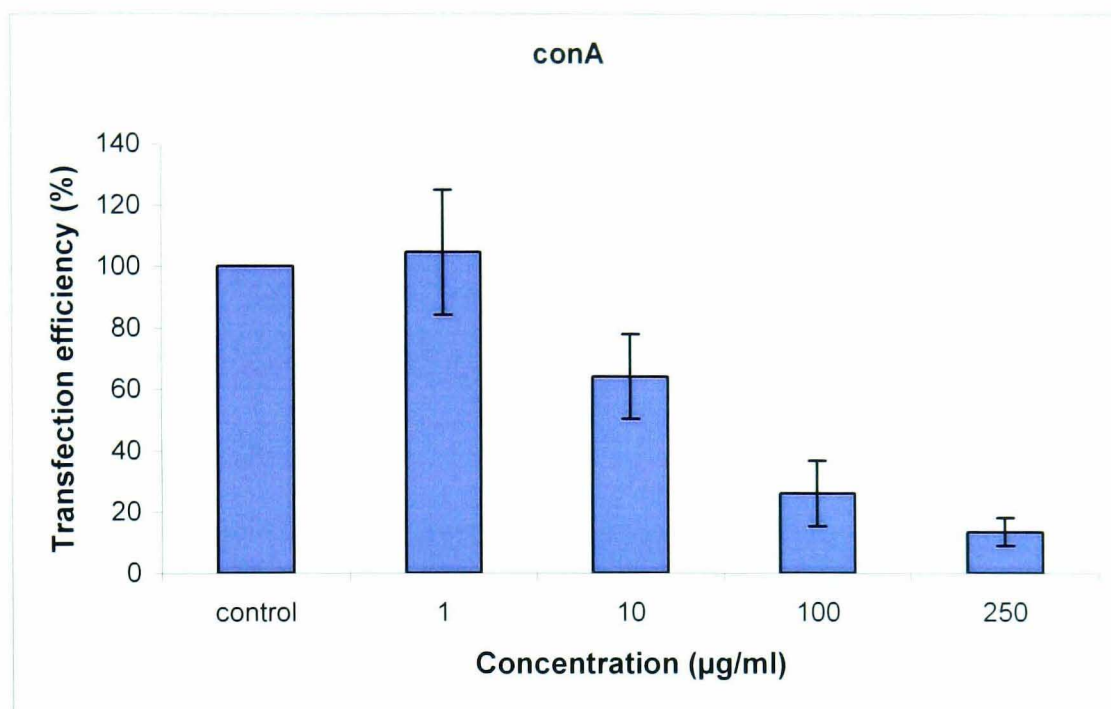


**Figure 6.10** Transfection efficiency of DMA homopolymer – DNA complexes on conA pre-treated A549 cells, with conA present during the entire experiment. The complexes were prepared at 2:1 monomeric unit: nucleotide ratio. The transfection activities were measured 24 h post transfection and the results were expressed as percentage compare to the control (without inhibitor) (n=3).

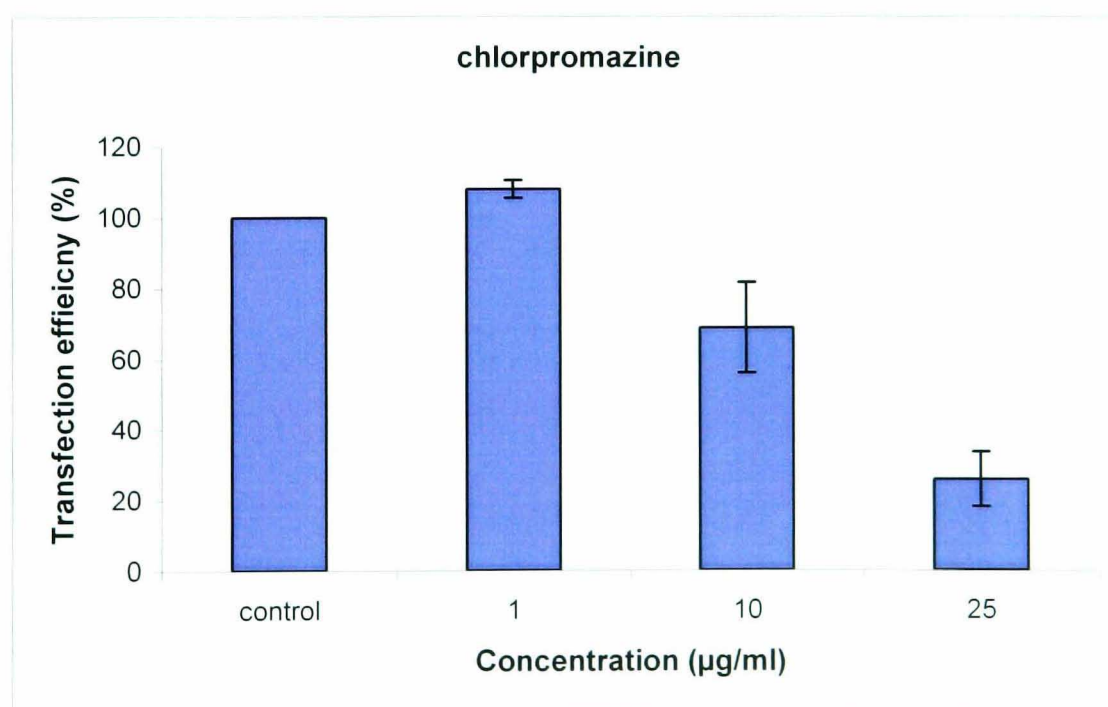


**Figure 6.11** Transfection efficiency of DMA homopolymer – DNA complexes on chlorpromazine pre-treated A549 cells, with chlorpromazine present during the experiment. The complexes were prepared at 2:1 monomeric unit: nucleotide ratio. The transfection activities were measured 24 h post transfection and the results were expressed as percentage compare to control (without inhibitor) (n=3).

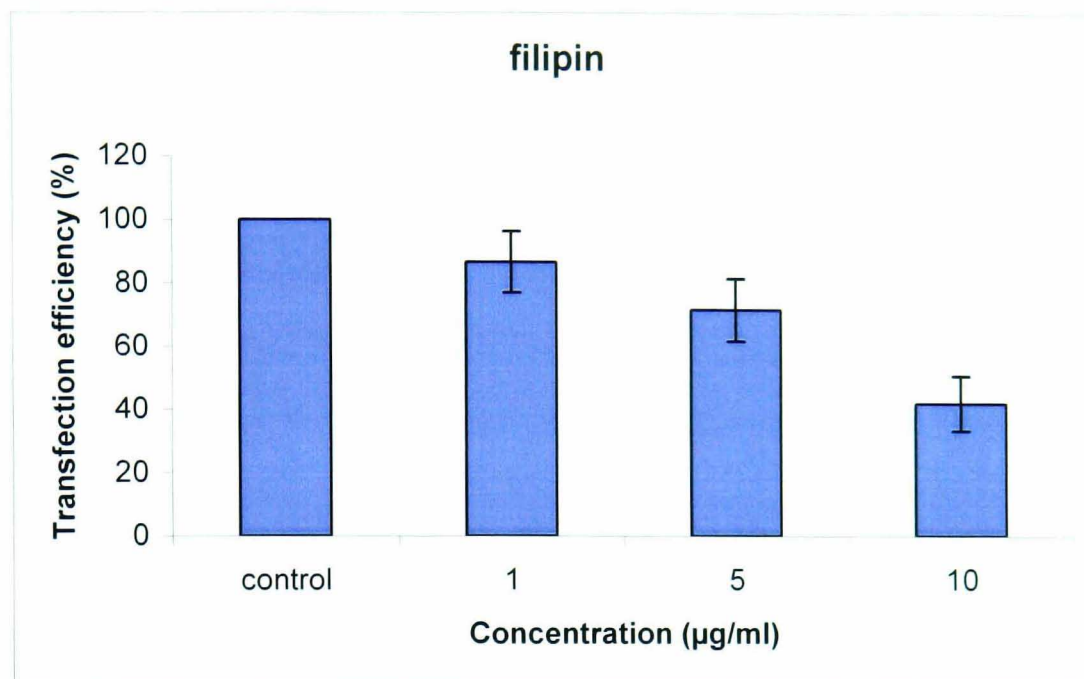


**Figure 6.12** Transfection efficiency of DMA homopolymer – DNA complexes on filipin pre-treated A549 cells, with filipin present during the experiment. The complexes were prepared at 2:1 monomeric unit: nucleotide ratio. The transfection activities were measured 24 h post transfection and the results were expressed as percentage compare to control (without inhibitor) (n=3).

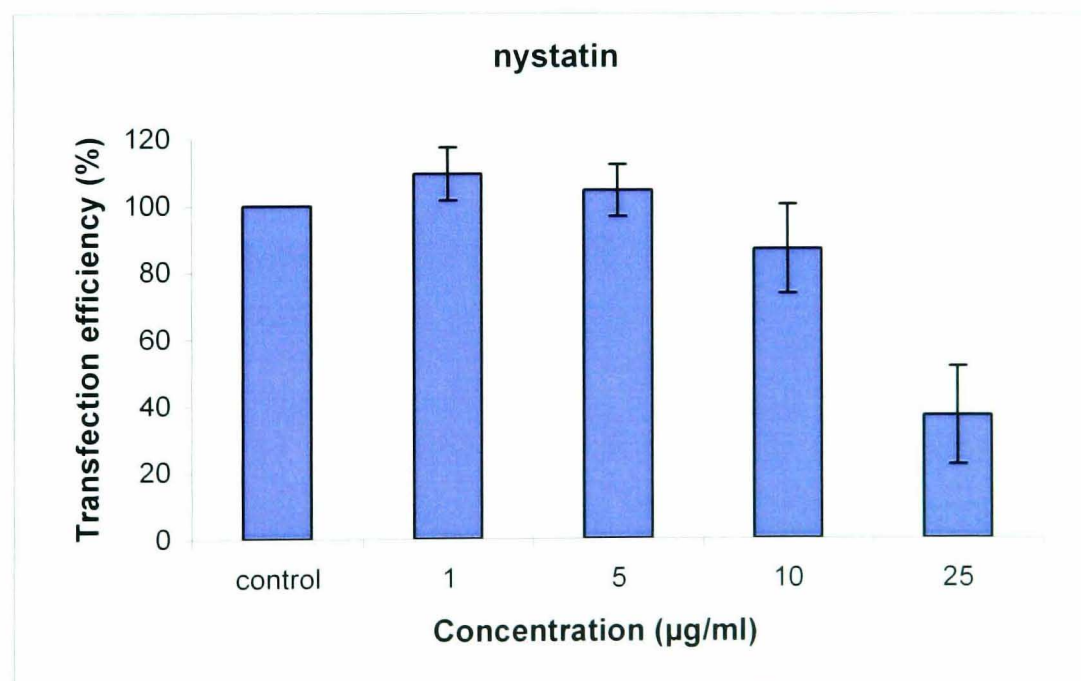


**Figure 6.13** Transfection efficiency of DMA homopolymer – DNA complexes on nystatin pre-treated A549 cells, with nystatin present during the experiment. The complexes were prepared at 2:1 monomeric unit: nucleotide ratio. The transfection activities were measured 24 h post transfection and the results were expressed as percentage compare to control (without inhibitor) (n=3).

### 6.3.4 Confocal microscopy study

In the first part of this study, the confocal microscopy was used to investigate the intracellular trafficking of DMA homopolymer – DNA complexes in A549 cells over a period of time. The confocal images were captured on the same living cells at  $T=5, 30, 60, 90$  and  $150$  min. All the images were taken at the same  $xy$  position and same  $z$  height throughout the experiment. The confocal images are shown in figure 6.14. At  $t=5$  min, a speck of dim fluorescence was observed at the periphery of the cell. As the time progressed, the fluorescence appeared to move towards the centre of the cells. In addition, more fluorescent spots could be detected inside the cell. At  $t=150$  min, several fluorescent spots were observed surrounding the nucleus of the cell. The fluorescence was not uniform throughout the cell, but rather present at distinct points inside the cell.

These first set of confocal images demonstrated the movement of DNA complexes into the cell over time. In order to confirm whether the DNA complexes were indeed located inside of the cells, the cytoplasm of the cells were fluorescently labelled in the second study. Since the DNA was also fluorescently labelled, one is able to tell whether the DNA complexes were taken up into the interior of the cells by comparing the relative position of the fluorescently labelled DNA to the cytoplasm of the cell through analysing the image in  $xz$  and  $yz$  planes. In this set of experiments, the A549 cells were labelled with the CellTracker Orange (red) and the plasmid DNA was labelled with YOYO-1 iodide (green). The cells were imaged 240 min after the addition of DNA complexes. The trans-section confocal image is shown in figure 6.15. Figure a and b show the same cells with the fluorescence located at different position in the cell (as indicated by the arrow). The images clearly show that the DNA complexes were situated inside the cell, as revealed by the analysis of the image in the  $xz$  (right panel) and  $yz$  (top panel) planes.

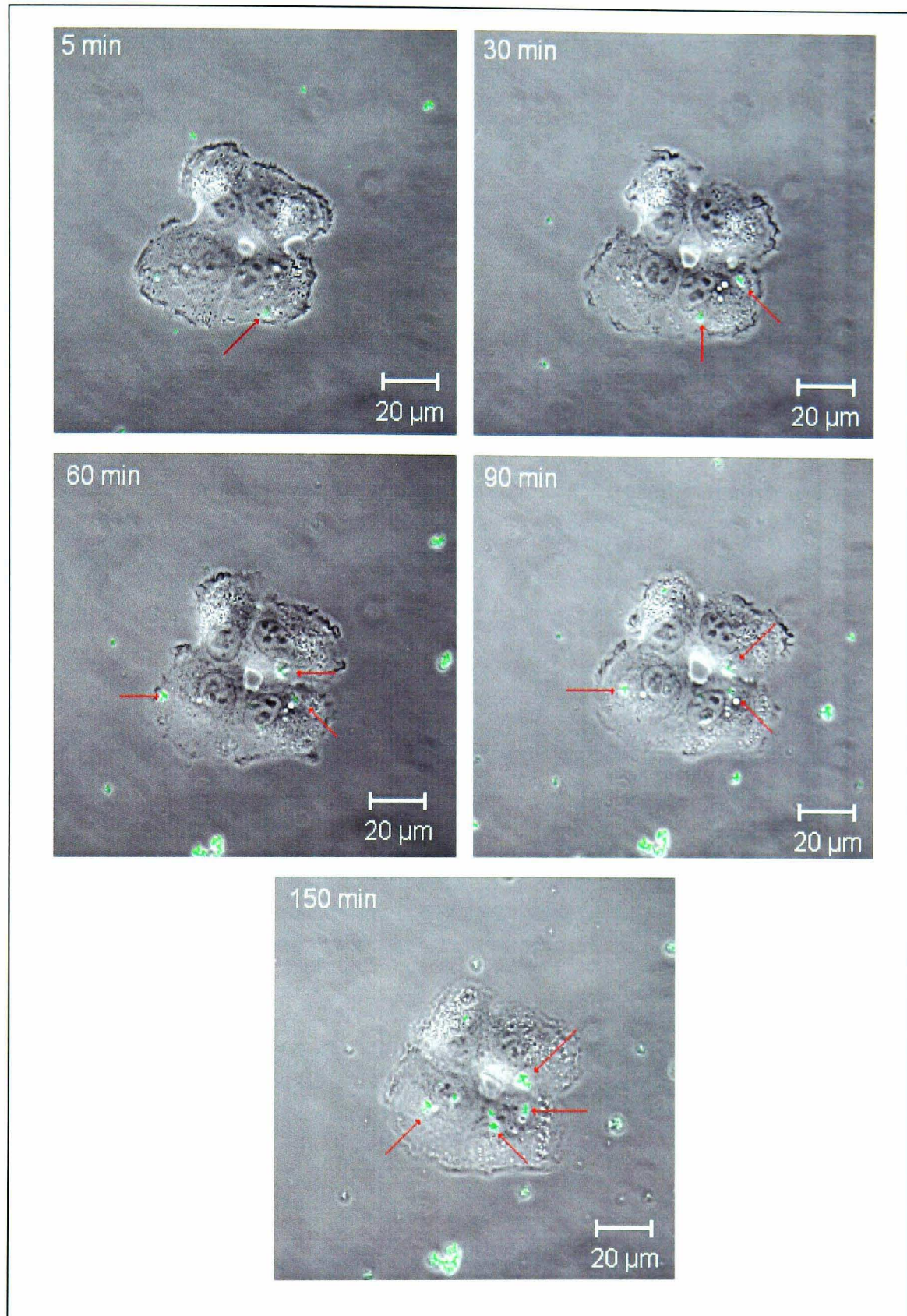


**Figure 6.14** Confocal images showing intracellular trafficking of DMA homopolymer – DNA complexes on A549 cells at various time intervals. DNA complexes were prepared at 2:1 monomeric unit: nucleotide ratio. Plasmid DNA was labelled with YOYO-1 fluorescence probe (green). The arrows indicate the position of DNA complexes in the cell. All the images were taken at the same  $z$  height. The cells were kept at 37°C with 5% CO<sub>2</sub> throughout the entire experiment.

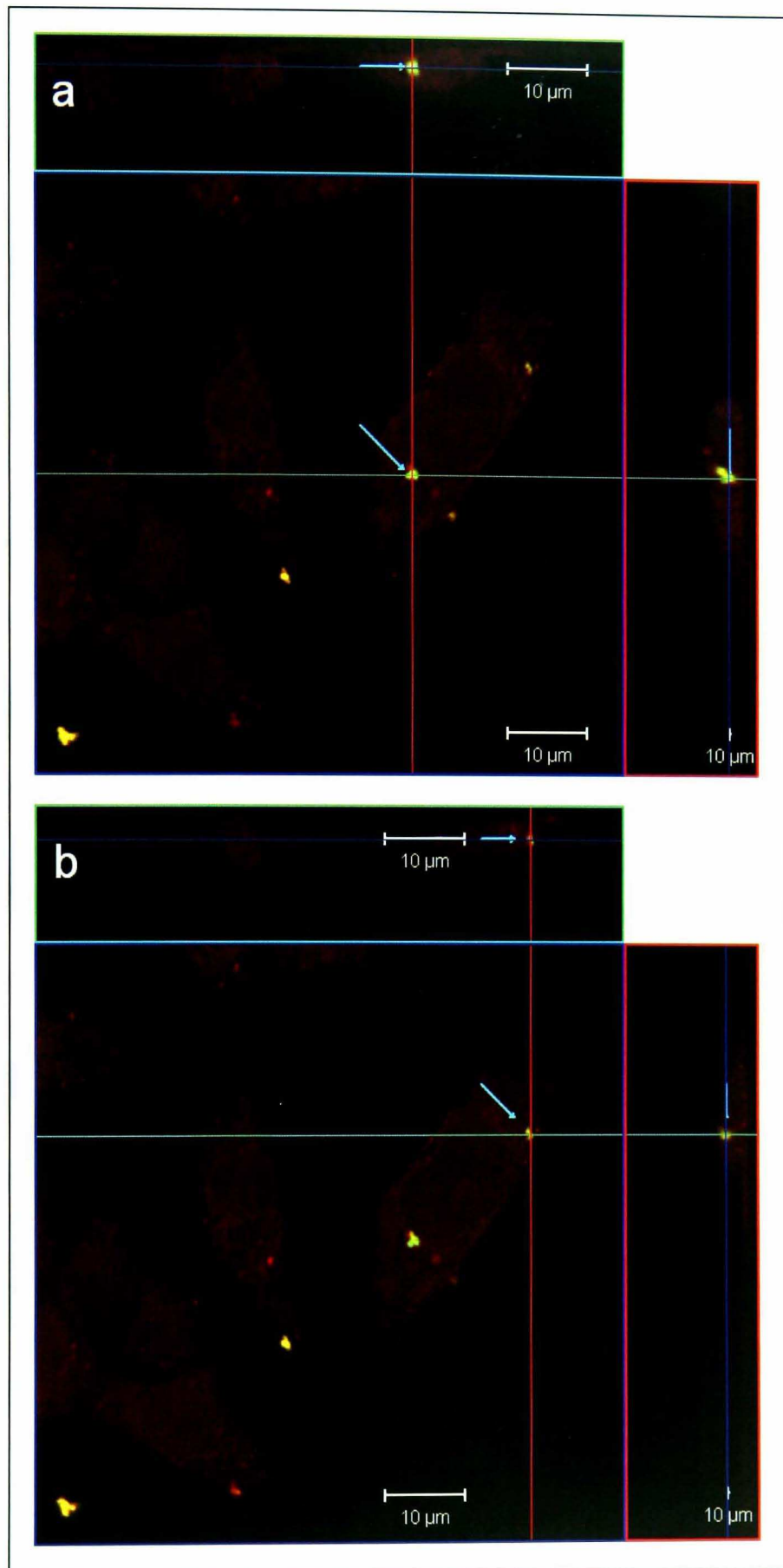


**Figure 6.15** Trans-sectional confocal images of A549 cells at 240 min following the addition of DMA homopolymer – DNA complexes. DNA complexes were prepared at 2:1 monomeric unit: nucleotide ratio. Plasmid DNA was labelled with YOYO-1 fluorescent probe (green) and the cell was labelled with CellTracker Orange (red). The arrows indicate the position of DNA complexes.

In order to explore the routes of cellular uptake of the DNA complexes in A549 cells, conA and nystatin were employed to inhibit clathrin-mediated endocytosis and caveolae-mediated endocytosis respectively in the confocal study. The cells were incubated with the inhibitors one hour before the addition of DNA complexes and throughout the entire experiments. The confocal images were taken 240 min after the complexes were added to the cells.

When the cells were treated with conA (figure 6.16 and 6.17), the DNA complexes were found to be located outside the cells. In figure a, the image was captured at a  $z$  height which was at the top surface of the cells. Green fluorescence (YOYO-1 labelled DNA) was seen to be located at the surface of the cells. When the image was captured at a different  $z$  height which was across the mid section of the same cells (figure b), green fluorescence could not be observed, suggesting the DNA complexes did not enter into the cells. Figure c shows the tran-sectional view of the cells. It was clearly demonstrated that the green fluorescence (indicated by the arrows) was located at the outer surface of the cells, as shown by the analysis of the image in the  $xz$  (right panel) and  $yz$  (top panel) planes. When the cells were treated with nystatin, the green fluorescence (indicated by arrows) could be seen inside of the cells as illustrated in the  $xz$  (right panel) and  $yz$  (top panel) planes in figure 6.18.

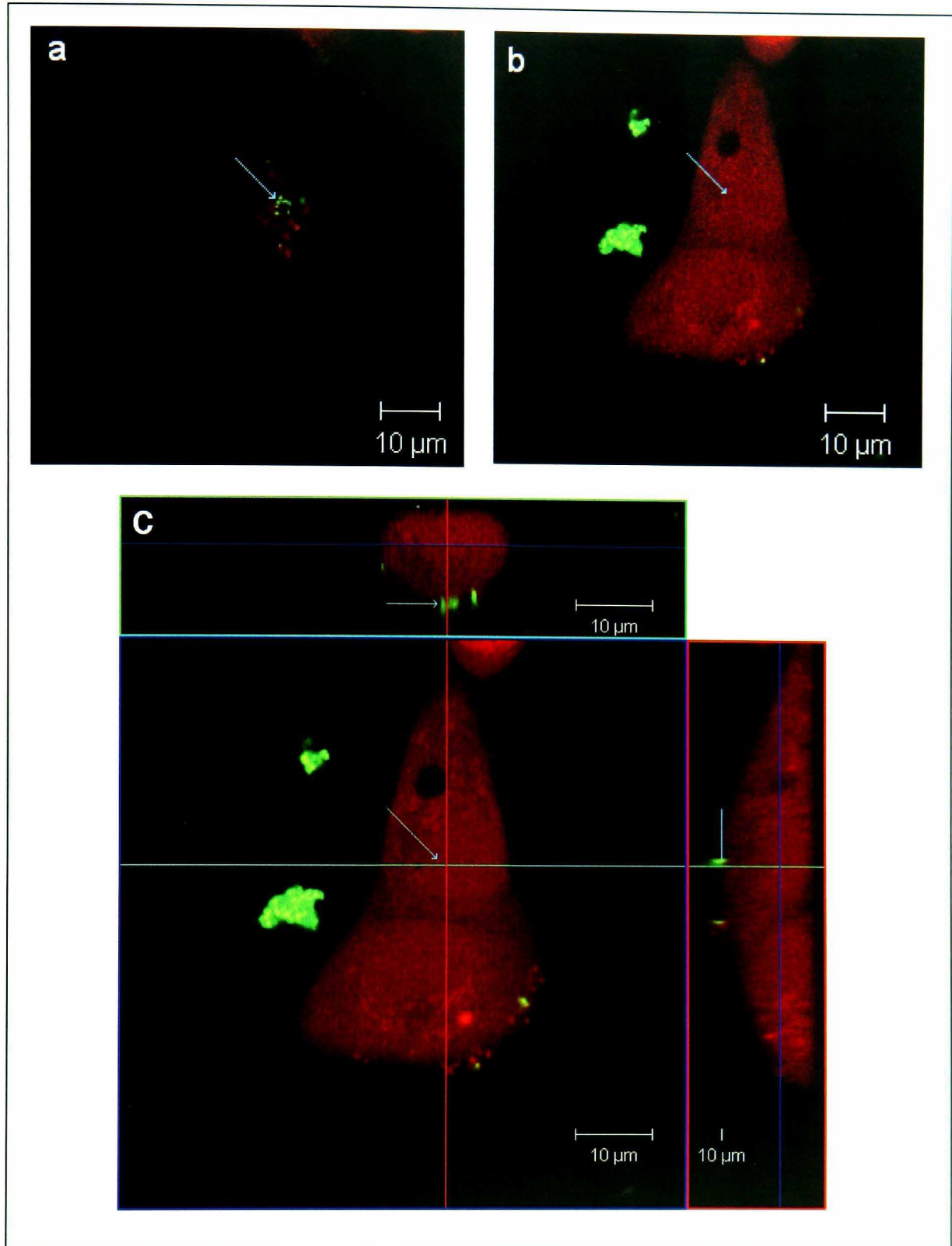


**Figure 6.16** Confocal images of conA treated A549 cells at 240 min following the addition of DMA homopolymer – DNA complexes (1). DNA complexes were prepared at 2:1 monomeric unit: nucleotide ratio. The cells with incubated with conA (250 μg/ml) one hour prior the addition of DNA complexes and during the experiment. Plasmid DNA was labelled with YOYO-1 fluorescent probe (green) and the cell was labelled with CellTracker Orange (red). The arrow indicates the position of DNA complexes. (a) Image captured at the surface of the cell, (b) image captured at the centre of the cell and (c) Trans-sectional view of the cell.

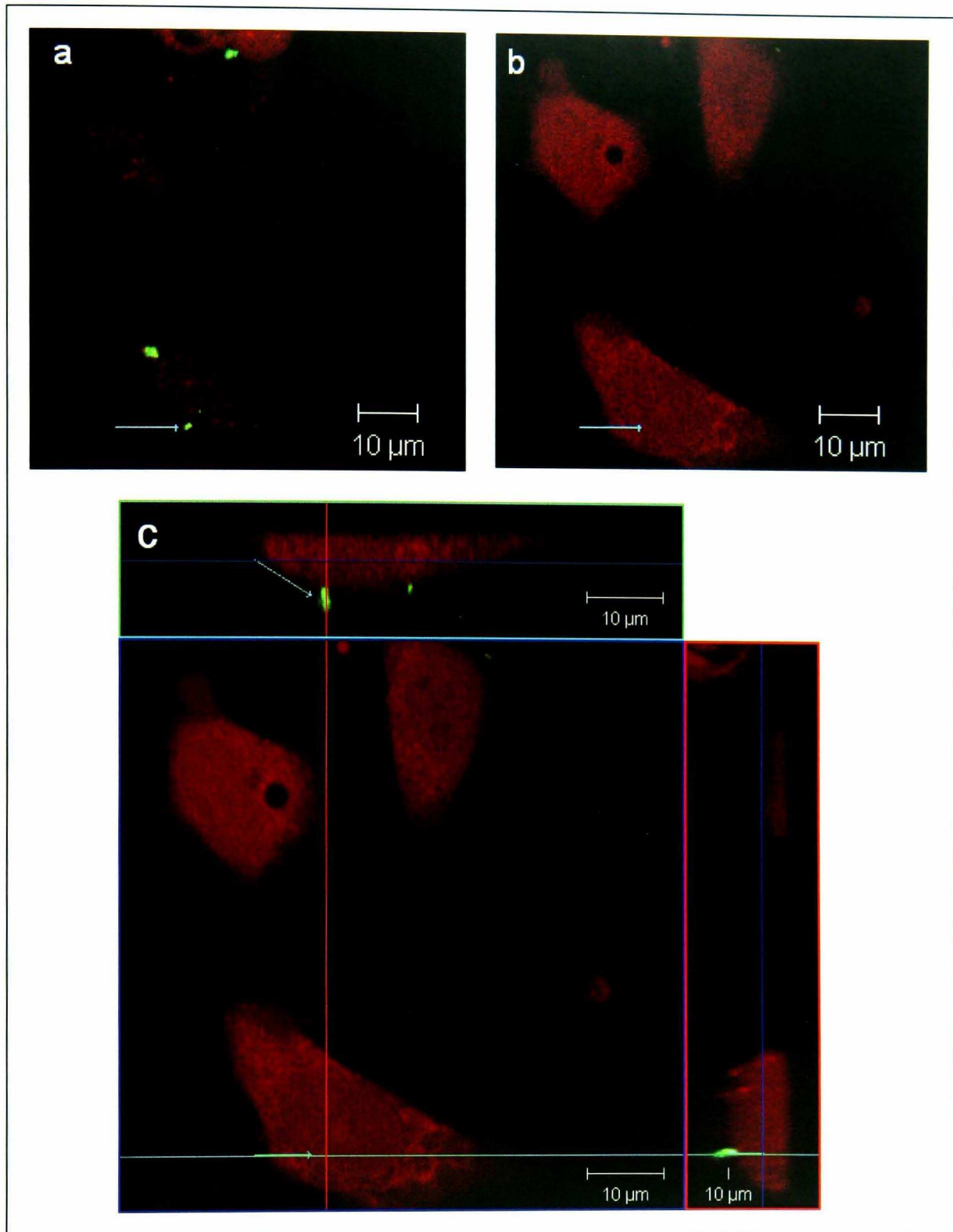


**Figure 6.17** Confocal images of conA treated A549 cells at 240 min following the addition of DMA homopolymer – DNA complexes (2). DNA complexes were prepared at 2:1 monomeric unit: nucleotide ratio. The cells with incubated with conA (250 μg/ml) one hour prior the addition of DNA complexes and during the experiment. Plasmid DNA was labelled with YOYO-1 fluorescent probe (green) and the cell was labelled with CellTracker Orange (red). The arrow indicates the position of DNA complexes. (a) Image captured at the surface of the cell, (b) image captured at the centre of the cell and (c) Trans-sectional view of the cell.



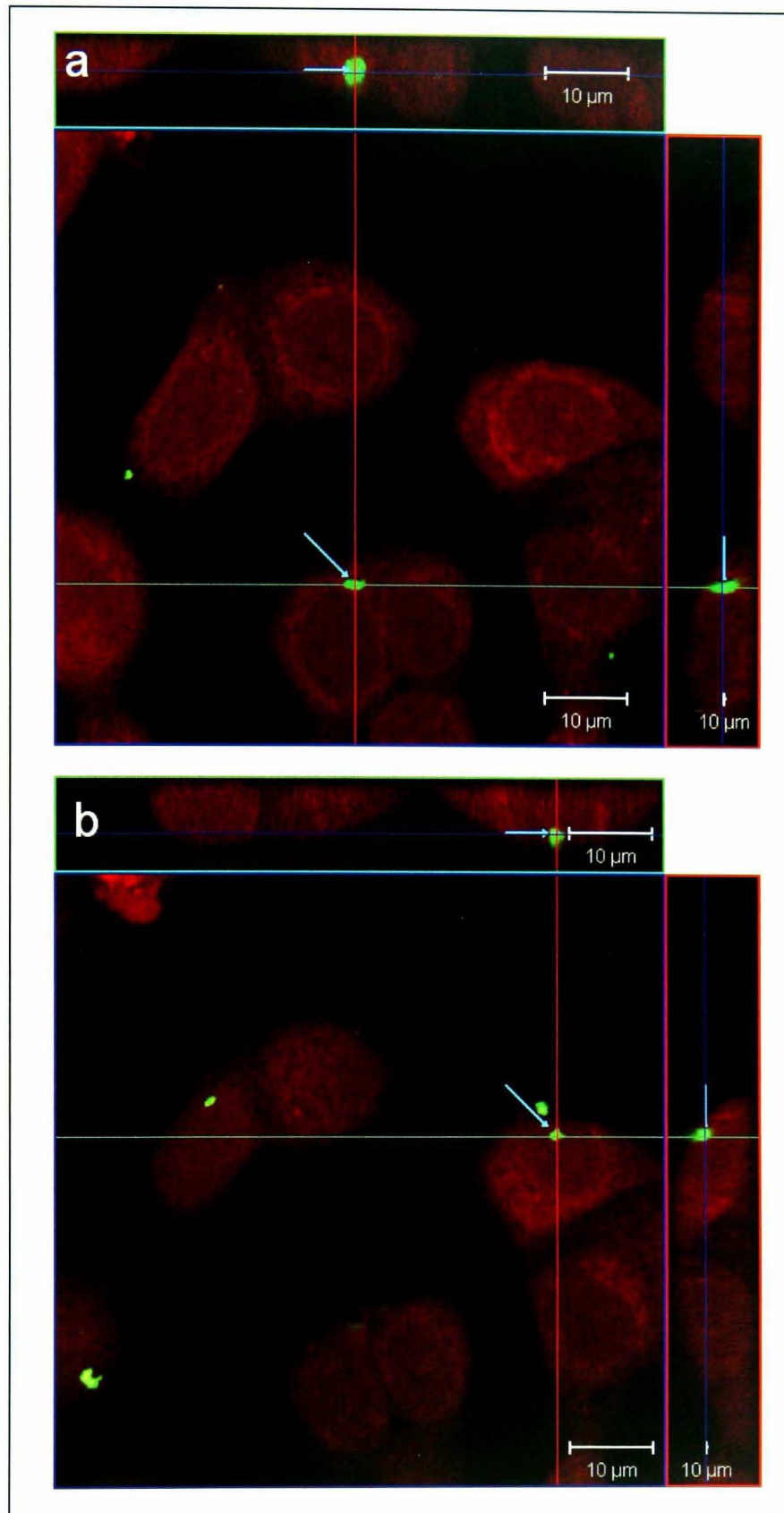


**Figure 6.18** Trans-sectional confocal images of nystatin treated A549 cells at 240 min following the addition of DMA homopolymer – DNA complexes. DNA complexes were prepared at 2:1 monomeric unit: nucleotide ratio. The cells were incubated with nystatin (10 μg/ml) one hour prior to the addition of DNA complexes and during the experiment. Plasmid DNA was labelled with YOYO-1 fluorescent probe (green) and the cell was labelled with CellTracker Orange (red). The arrows indicate the position of DNA complexes.

## 6.4 DISCUSSION

To investigate the cellular uptake pathway of DMA homopolymer – DNA complexes, inhibitors were used in cell culture to evaluate their effects on the uptake and the level of gene expression. The profile of time course effect on transfection efficiency of the DNA complexes was performed as a control. It was noticed that in the absence of inhibitors, the expression of the luciferase reporter gene was detected within a few hours after the addition of the DNA complexes to the cells, and a peak level of transfection was observed after 16 to 36 hours. Between the cellular uptake of the DNA and the synthesis of protein, the DNA has to travel from the site of internalisation at the cell membrane, into the nucleus where the transcription takes place. Indeed, the intracellular trafficking of the DNA complexes is recognised as one of the major barriers to efficient gene delivery. However, the mechanism by which the DMA homopolymer – DNA complexes are taken up into the cells are not clearly understood.

The importance of microtubules and actin filaments in the uptake of DMA homopolymer – DNA complexes was investigated. These two types of protein filaments are involved in the different stages of endocytosis. The former is important in transport of vesicles within the cells whereas the latter is believed to be involved in the formation and invagination of vesicles (Harada *et al.*, 1995, Mundy *et al.*, 2002, Murray and Wolkoff, 2003). It has recently been reported that microtubule inhibitor such as nocodazole and colchicine enhanced the expression of genes using cationic lipid or liposome based gene delivery system (Hasegawa *et al.*, 2001, Lindberg *et al.*, 2001, Nair *et al.*, 2002, Wang and MacDonald, 2004). In their studies, the magnitude of enhancement varied from 2- to 30-fold compared to the untreated control, depending on the cell types, the choice and the concentration of inhibitors. The gene expression assay was carried out 24 hours post-transfection in the majority of these studies. Since the microtubule is the major contributor to the trafficking in the endosomal /

lysosomal pathway, it was logical to expect that these inhibitors might block the transfer of DNA from the endosomes to the lysosomes, thus preventing degradation of DNA, resulting in an increase of transfection efficiency (Chowdhury *et al.*, 1996).

Our results showed that the transfection efficiency of DMA homopolymer – DNA complexes was inhibited by the microtubule inhibitor, colchicine, to approximately 20% when the luciferase assay was carried out 16 hours post-transfection. However, the level of gene expression increased as the time increased. A dramatic increase in transfection efficiency compared to the untreated control was observed from 36 hours and onwards. Interestingly, van der Aa *et al.* have demonstrated that when cells were treated with another microtubule inhibitor, nocodazole, gene expression of DMA homopolymer – DNA complexes was reduced to 20% after 24 hours post transfection. However, other time points were not investigated in their study (van der Aa *et al.*, 2005).

Based on the results of our studies, it appears that the course of time was an important factor in determining the level of gene expression. This time course effect has not been reported in the literature before. One of the possible explanations of our results is that, initially, the intracellular transport of the internalised vesicles containing the DNA complexes was impeded due to the destruction of microtubules by the colchicine. This could possibly lead to the accumulation of vesicles at the periphery of the cells, which slowly diffused towards the nucleus of the cells. The DNA complexes might therefore require a longer time to travel into the nucleus, resulting in a delay of the transcription and hence the translation process. Thus, a reduction of transfection level was observed at early stage. Since the internalised DNA complexes were not transported to the endosomes / lysosomes for destruction, the transfection efficiency was significantly improved at a later stage. Techniques such as fluorescence microscopic study at real time will be helpful to explore this hypothesis.

Another possible hypothesis is that the time course effect of colchicine may affect the intracellular transport of the DNA complexes. Colchicine is a reversible microtubule inhibitor. It has been reported that when colchicine was injected into rats, disruption of microtubular structures was noticed in the hepatocytes within an hour, with maximum disruption was observed after two hours. The microtubular network were partially regenerated at 24 hours and fully regenerated after 48 hours of administration (Chowdhury *et al.*, 1996).

In our case, it is possible that the disruption of microtubules in the early stage impaired the movement of DNA complexes within the cells, resulting in an inhibition of transfection efficiency initially. As time progressed, the microtubules started to regenerate, assisting the movement of the DNA complexes towards the nucleus, restoring the transfection efficiency. However, as the recovery of the microtubules was not fully complete, some of the vesicles failed to be transported along the endosomes / lysosomes pathway for degradation, resulting in an increase in the level of gene expression.

It must be noted that for both hypotheses, an assumption has been made in the very first place that the escape from endosomes / lysosomes was a limiting factor for the efficient delivery of DMA homopolymer – DNA complexes. In fact this is an important barrier to most non-viral gene delivery systems (Lechardeur *et al.*, 2005). Although some polymeric delivery systems such as PEI (Boussif *et al.*, 1996) and polyamidoamine (Tang *et al.*, 1996) have the ability to escape from the acidic endosomes (proton sponge property), recent study has indicated that DMA homopolymer does not possess this desirable property (Jones *et al.*, 2004) (further discussion later in this section).

Whether the cells were only pre-treated with colchicine or incubated with it throughout the experiment, there was no significant difference in the terms of the trend of transfection level over time, although the enhancement of gene

expression appeared to be augmented. In fact, it has been suggested that multi-drug resistance (MDR) could be developed over time when the cells were treated with a variety of hydrophobic drugs, including colchicine (Ford and Hait, 1990). This may be developed as a result of overexpression of membrane P- glycoprotein (PGP), which acts as a defence mechanism against potentially harmful substances by exporting these substances from the cell (Ford and Hait, 1990, Nair *et al.*, 2002). It has been demonstrated that treatment of cells with colchicine together with glucocorticoid, which is a known substrate for PGP (Rao *et al.*, 1994), resulted in efficient blockage of colchicine efflux, and the gene expression of liposomes – DNA was further enhanced compared to treatment with colchicine alone. This could explain why prolonged incubation of the cells with colchicine might not have further effects on the structure of microtubule, but might continue to contribute to the toxicity towards the cells.

The studies conducted up to this point confirmed that microtubules play a role in the uptake of DMA homopolymer – DNA complexes. The effect of actin filaments on the uptake of the DNA complexes was also explored. With the treatment of a microfilament depolymerising agent, cytochalasin D, transfection efficiency of DMA homopolymer – DNA complexes was effectively inhibited, indicating the involvement of actin filaments in the uptake of the DNA complexes. Since actin filaments are known to be involved in endocytosis, the results confirmed that the DNA complexes were taken up into the cells through endocytotic process. This agrees with an earlier study by another group, who showed that DMA homopolymer – DNA complexes entered cells through endocytosis as the uptake process was inhibited at 4°C (Zuidam *et al.*, 2000). However, since both clathrin – dependent and clathrin – independent endocytosis are both inhibited by cytochalasin D in different cell types (Gottlieb *et al.*, 1993, Jackman *et al.*, 1994, Durrbach *et al.*, 1996), more specific inhibitors are hence required to differentiate between the two pathways.

Inhibitors of clathrin-mediated endocytosis and caveolae-mediated endocytosis were used to examine the relative importance of clathrin coated pits and caveolae in mediating the uptake of the DNA complexes on A549 cells. From the transfection data, it was found that conA, a well-characterised clathrin-mediated endocytosis inhibitor, significantly inhibited transfection efficiency by almost 80%. ConA binds to cell surface glycoproteins and impairs their mobility within the membrane bilayer, thereby blocking the movement of proteins into coated pits and coated pits assembly (Smith *et al.*, 2001). Chlorpromazine is another frequently used inhibitor of clathrin-mediated endocytosis. It causes coated pits to disappear from the cell surface and reappear on endosomal membranes, probably due to the reverse of an on/off switch that controls AP-2 binding to membrane (Brodsky *et al.*, 2001). Transfection efficiency was effectively reduced by 70% when the cells were treated with 25 µg/ml of chlorpromazine. These results hence clearly demonstrate that DMA homopolymer – DNA complexes recruited the coated pits for the entry into the cell. The confocal images also show that incubation of the cells with conA blocked the entry of the DNA complexes into the cells, supporting the transfection data.

Nystatin and filipin are sterol-binding agents that effectively disrupt caveolar structure, hence inhibiting caveolae mediated uptake (Rothberg *et al.*, 1992, Orlandi and Fishman, 1998, Stuart *et al.*, 2003). It was found that both agents were also able to inhibit transfection efficiency, though to a lesser extent compared to clathrin inhibitors. With 5 µg/ml of filipin or 10 µg/ml of nystatin, the commonly used concentrations to inhibit caveolar function, the transfection efficiency was reduced by about 20% relative to the control. In the confocal study, it was found that 10 µg/ml nystatin did not appear to affect the cellular uptake of DMA homopolymer – DNA complexes. Since the transfection efficiency was only slightly inhibited by nystatin, it was not surprising that DNA complexes were found to be taken up into the cells.

It is apparent that the DMA homopolymer – DNA complexes were internalized primarily through a clathrin-mediated pathway, with a minor fraction possibly entered cells *via* caveolae. This can be concluded as transfection efficiency and the uptake of the DNA complexes was more effectively inhibited by the clathrin inhibitors than by the caveolae inhibitors. However, it cannot be ignored that other combinations of pathways, such as phagocytosis and pinocytosis, might also be involved as none of the inhibitors could completely abolish the uptake of the DNA complexes.

Although a number of pathways are believed to be involved in the uptake of DNA complexes, the determination of the route of uptake is indeed poorly understood. It is reported that the size of the particles play an important role in the choice of entry pathway (Rejman *et al.*, 2004). With the use of liposomes as delivery vector on non-phagocytotic mammalian cells in the study, it was suggested that particles that were less than 200 nm were predominantly internalised through the clathrin-mediated pathway. With increasing particle size, a shift to a mechanism that relied on the caveolae-mediated pathway became apparent, and became the major route of entry for particles of 500 nm in size. This finding is interesting as current general understanding considers that the typical size of caveolae (50-100 nm) is far too small to accommodate particles as large as 500 nm. Certain bacteria, such as Fim-H expressing *E coli.* and *Mycobacterium bovis*, utilize caveolae for entry into the host cells (Shin and Abraham, 2001) although their size exceeds 1  $\mu\text{m}$ . However, a clear explanation of this phenomenon is lacking.

In contrast, a conflicting result was observed by another research group (Grosse *et al.*, 2005) using polycations to deliver genes. It was reported polyplexes with size ranged from 100 – 200 nm were taken up primarily through clathrin coated pits. However, caveolae were involved in the uptake of polyplexes only when the particle size was less than 100 nm, which in fact is consistent with the size of caveolae. When the particle size was over 200 nm, the polyplexes were found to be taken up through macropinocytosis. Although from all these results, the effect of particle size on the route of

cellular uptake was uncertain, it is apparent that the particle size does play a role here.

For the case of DMA homopolymers, the DNA complexes formed were in fact aggregates with particle size of over 1  $\mu\text{m}$ , as measured by the photon correlation spectroscopy (as shown in chapter 3, table 3.2). However, it is not clear how strong the aggregated complexes were associated with each other. It is possible that when DNA complexes were added to the cells *in vitro*, some of the loosely aggregated complexes break down into smaller fragments to the size around 200 nm and gained entry into the cells through clathrin-mediated endocytosis, while smaller or larger complexes entered the cells through other pathways, including the caveolae-mediated pathway. Indeed, it was noticed from the confocal image that the DNA complexes were present inside the cells appeared as small discrete particles (figure 6.19), whereas large clumps of complexes remained outside of the cells throughout the experiment (figure 6.20).



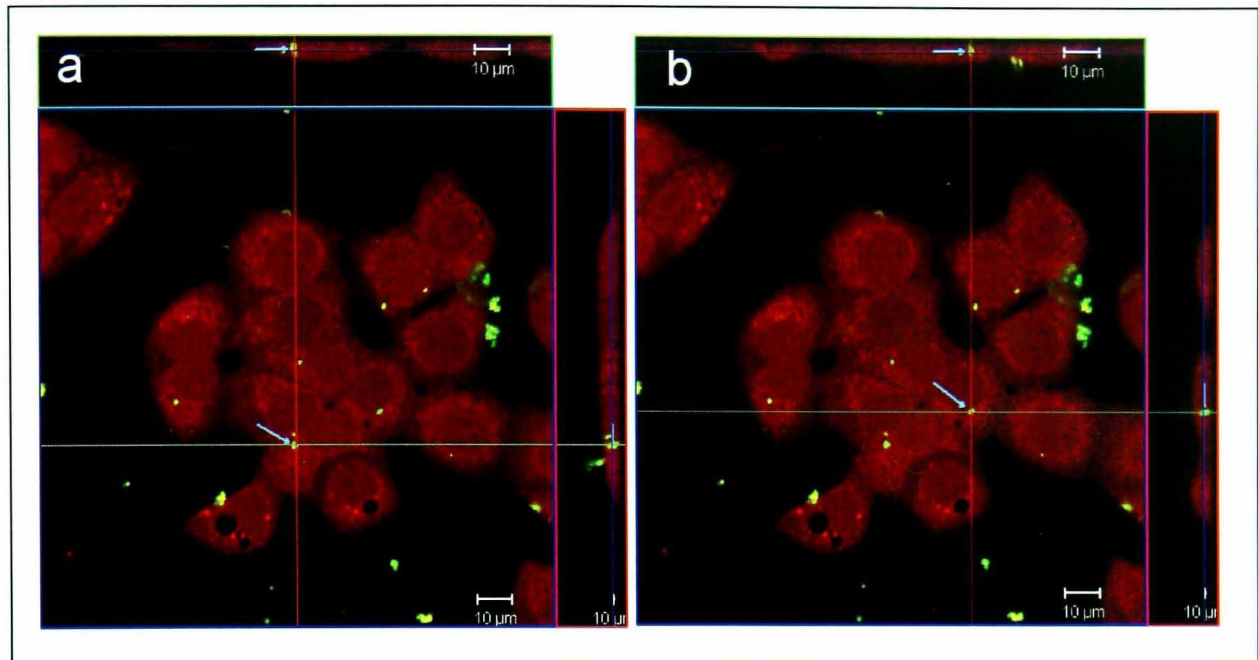


**Figure 6.19** Confocal images of DMA homopolymer – DNA complexes that entered the cells appeared as discrete particles. DNA complexes were prepared at 2:1 monomeric unit: nucleotide ratio and the images were taken at 240 min after addition of complexes on A549 cells. Plasmid DNA was labelled with YOYO-1 fluorescent probe (green) and the cell was labelled with CellTracker Orange (red). Both (a) and (b) images were taken at different  $z$  height on the same cells. The arrows indicate the different DNA complexes inside the cells, as revealed by the  $xz$  (right panel) and  $yz$  (top panel) planes.

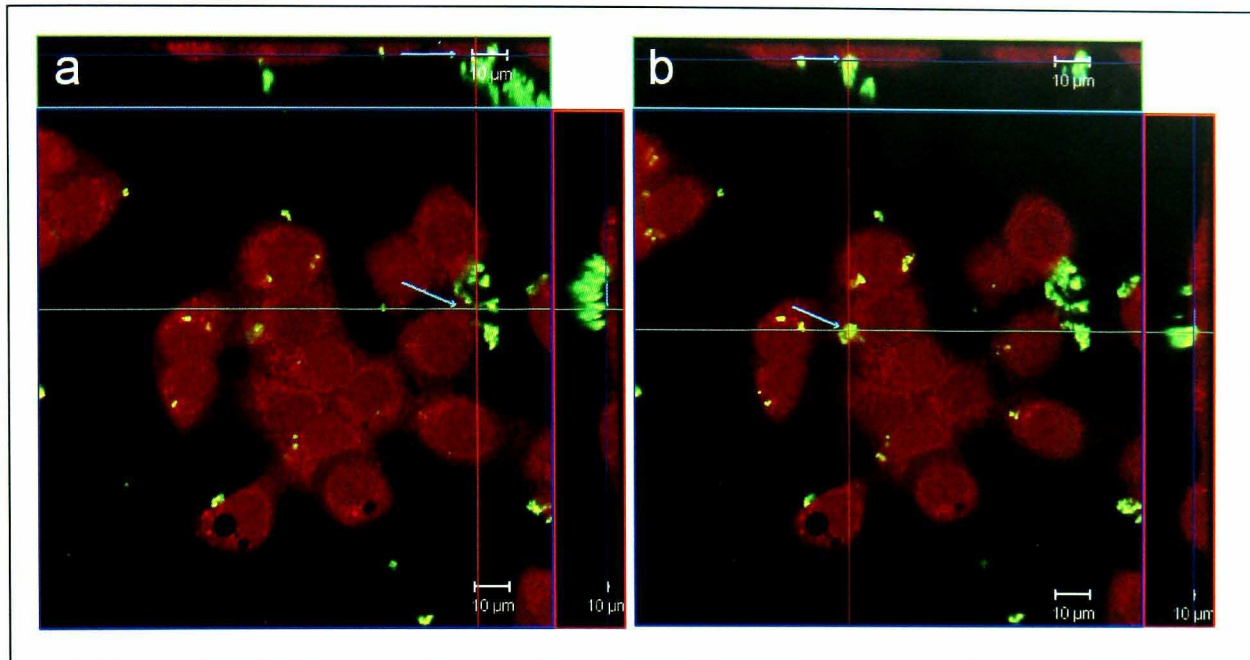


**Figure 6.20** Confocal images of DMA homopolymer – DNA complexes that remained outside the cells appeared as aggregates. DNA complexes were prepared at 2:1 monomeric unit: nucleotide ratio and the images were taken at 240 min after addition of complexes on A549 cells. Plasmid DNA was labelled with YOYO-1 fluorescent probe (green) and the cell was labelled with CellTracker Orange (red). Both (a) and (b) images were taken on the same cells. The arrows indicate the different DNA complexes aggregates outside the cells, as revealed by the  $xz$  (right panel) and  $yz$  (top panel) planes.

The two different routes of endocytosis lead to different intracellular fate of the polymer – DNA complexes. For the clathrin-mediated pathway, the internalised materials are normally transported to endosomes where there is a reduction of pH and consequently fusion with lysosomes where the degradation of the materials takes place. However, there are also exceptions. It is well known that the cationic polymer polyethylenimine (PEI) possesses substantial buffering capacity below physiological pH. PEI contains protonable nitrogen atoms, making it possible to buffer the endosomal environment, prompting the osmotic swelling and rupture of the vesicle, which leads to the liberation of the polymeric system to the cytoplasm. This phenomenon is known as the ‘proton sponge’ effect (Bohr 1994, Boussif *et al.*, 1995). For this reason, the PEI based system is believed to successfully escape from endosomal / lysosomal degradation.

In the case of DMA polymer system, it was at first thought that this polymer might act like PEI to have the ability to cause a disruption of the endosomes (van de Wetering *et al.*, 1999). This was because DMA has an average pK(a) value of 7.5 and is partially protonated at physiological pH, and thus it might behave as a proton sponge. It was also found that with the addition of endosomolytic agent, chloroquine, the transfection efficiency of DMA homopolymer – DNA complexes was not enhanced (van de Wetering *et al.*, 1997, Deshpande, 2002), suggesting that the endosomal escape might not be a limiting step to transfection efficiency of the system, although cytotoxicity associated with chloroquine could also be the explanation. Recent work indicated that the uncomplexed DMA homopolymer did not physically disrupt the endosomes (Jones *et al.*, 2004), though the polymer was found to induce changes in the morphology of the late endosomes / lysosomes. Although one may argue that the ability of the polymer – DNA complexes to disrupt endosomes may be greater than the uncomplexed polymer, a confocal study conducted by other groups has shown that the polymer – DNA complexes were not present outside the endocytic vesicles up to 48 hours after uptake by the cells (Zuidam *et al.*, 2000), suggesting that the intracellular trafficking from the endosomes to the nucleus is indeed very

inefficient. On the other hand, particles that entered the cells *via* caveolae-mediated uptake could avoid the acidic endosomes and lysosomes. They were believed to be delivered to vesicles called caveosomes, which are neutral compartments (Pelkmans and Helenius, 2002). For this reason, the caveolae-dependent pathway is becoming an attractive route for drug and gene delivery (Bathori *et al.*, 2004). However, both transfection and confocal studies suggested that caveolae-dependent uptake mechanism was not the major route of entry of the DMA homopolymer – DNA complexes.

Interestingly, it has been reported recently by another group using the same polymer system, that DMA homopolymer – DNA complexes were taken up by both the clathrin- and caveolae – mediated pathway, but the latter was found to be the major route of uptake leading to ultimate expression of the delivered gene (van der Aa *et al.*, 2005). In their work, the transfection efficiency of the DNA complexes was almost completely inhibited by the caveolae inhibitor, genistein, but not by affected by the clathrin inhibitor, chlorpromazine. Their results appeared to conflict with our data. The different composition of the polymer – DNA complexes, choice of cell lines and inhibitors might contribute to the discrepancy of the results. In fact, genistein is a tyrosine kinase inhibitor, which has a different mechanism to filipin in blocking caveolae function. It should be noted that many of these inhibitors may have a different secondary effect to the cells. For example, it is known that chlorpromazine targets other intracellular enzymes, leading to multiple effects on cell function. Therefore the specificity of inhibitors should be taken in consideration. Nevertheless, the clathrin-mediated pathway does not appear to be an effective route of gene delivery, especially when the system lacks the ability to escape from the acidic endosomes / lysosomes.

It might be advantageous to target the delivery of the DNA complexes through caveolae-mediated pathway. As mentioned earlier, size of particles appeared to play a crucial role in determining the route of entry. An appropriate tailoring of particle size might be useful to control the route of

entry. However, this does not seem to be feasible for DMA homopolymer – DNA complexes as their size is not easily adjusted. In addition, the effect of size on the route of entry is still controversial. Alternatively, the particles can be attached to ligands for caveolar receptors, such as folic acid (Rothberg *et al.*, 1990, Rijnboutt *et al.*, 1996), or antibodies developed against caveolar proteins, such as interleukin-2 (IL2) (Lamaze *et al.*, 2001). However, further studies are required to explore the possibility of these strategies.

## **6.5 CONCLUSIONS**

In this chapter, the cellular uptake and intracellular route of DMA homopolymer – DNA complexes were investigated. It was found that the uptake of the DNA complexes took place within 30 minutes and optimum transfection efficiency was observed after 16 to 36 hours post-transfection. The uptake pathway of DMA homopolymer – DNA complexes was investigated by transfection study using different inhibitors, with the assistance of confocal microscopy study. Especially the effect of time course in transfection efficiency with the use of inhibitors is first reported here. Our results indicated that microtubules and actin filaments were both involved in the uptake of DNA complexes, suggesting that the complexes were internalised by means of endocytosis. Both the clathrin- and caveolae-mediated pathways were responsible for the uptake of DMA homopolymer – DNA complexes, whereby the former appears to be the major route of uptake. The escape from the acidic endosomes / lysosomes is one of the major limiting factors in the clathrin – mediated endocytosis of non-viral delivery system. Since the caveolae – mediated pathway bypasses this potential problem, it became an attractive route of targeting gene delivery for future investigation.

## CHAPTER 7

### FOLATE CONJUGATED GENE DELIVERY SYSTEM

#### 7.1 INTRODUCTION

The two major problems associated with polycation gene delivery systems are low efficiency and lack of specificity. Incorporation of suitable ligand to the delivery system to achieve specific targeting has been widely investigated in order to tackle the later problem (Varga *et al.*, 2000, Marcucci and Lefoulon, 2004). With this approach, the uptake of the ligand conjugated system to the receptor expressing target cells can be enhanced through receptor-mediated uptake mechanisms. Among the possible targeting agents, folic acid has been employed frequently to target therapeutic agents into a wide range of cancer cells (Leamon *et al.*, 1999, Guo and Lee, 2001, Ward *et al.*, 2002, Zhou *et al.*, 2002, Saul *et al.*, 2003).

##### 7.1.1 Folic acid

Folic acid (figure 7.1) is one of the many ligands being examined for specific targeting in gene delivery. It is a low molecular weight vitamin which is essential for the biosynthesis of nucleotide bases and a number of amino acids (Blakley and Whitehead, 1986). Since mammalian cells lack the key enzymes to synthesise this vitamin, efficient routes of uptake have been evolved in mammalian cells to capture folate exogenously. There are two major pathways responsible for folate internalization. The first one involves the use of reduced-folate carrier (RFC), which is the major route of folate uptake in normal cells (Sirotnak and Tolner, 1999). RFC is highly specific for reduced forms of folic acid such as 5-methyl-tetrahydrofolate, and

methotrexate, but has a low affinity for folic acid ( $K_d \sim 1-5 \mu\text{M}$ ) (Antony 1992). Therefore, folate conjugates will not be taken up by RFC. The second route involves the membrane bound folate receptors (FRs), which have a high affinity for folic acid ( $K_d \sim 100 \text{pM}$ ) (Kamen and Capdevia 1986). FRs are significantly overexpressed in many types of cancer cells, such as ovarian, breast, kidney, brain and endometrium tumours (Ross *et al.*, 1994, Weitman *et al.*, 1994, Toffoli *et al.*, 1997, Bueno *et al.*, 2001), but are only limited in a number of normal tissues. As a result, FRs have become attractive sites for specific targeting to tumour tissues.

It is believed that FRs mediate the uptake of folic acid through endocytosis (Kamen and Capdevila, 1986). Simple covalent attachment of folic acid to virtually any macromolecule produces conjugates that can be internalised into the cells in the same way as free folic acid (Leamon and Low, 1991, Reddy and Low, 1998, Sudimack and Lee, 2000). There is evidence suggesting that conjugation of molecules to folic acid does not normally interfere with the high affinity of folate for its receptors or with its endocytosis into the cell (Leamon and Low 1993, Turek *et al.*, 1993).

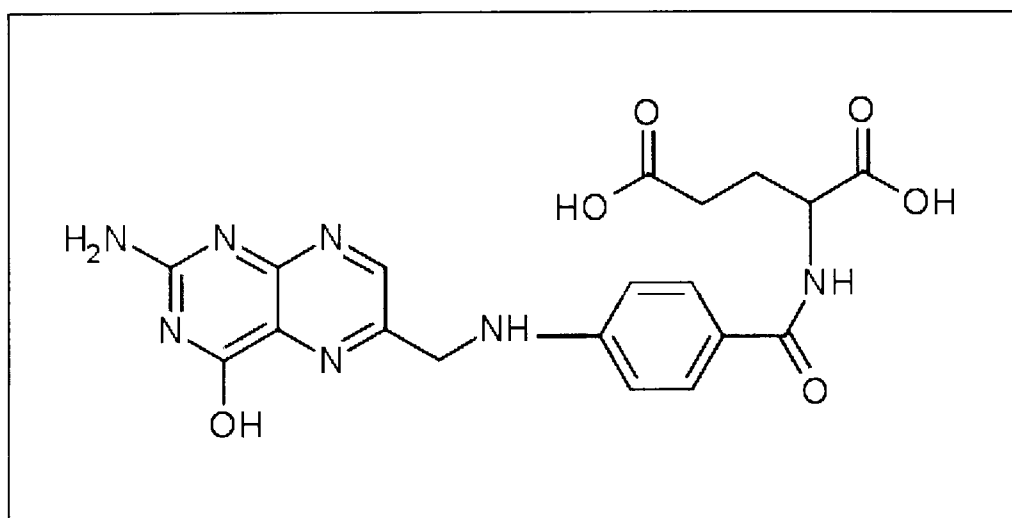


Figure 7.1 Chemical structure of folic acid



Folic acid has additional advantages over other targeting ligands. First of all, folic acid is taken into cells for essential functions. It has been suggested that most of the folate conjugates are released into the cytosol, instead of being delivered to lysosomes for destruction (Turek *et al.*, 1993). Secondly, because of the high affinity of folic acid and its conjugates for FRs, folate conjugates can be administered at low concentrations in order to saturate all accessible FR. Folic acid is also inexpensive and relatively easily coupled to a wide variety of therapeutic agents (Leamon and Reddy, 2004). Furthermore, since folic acid is naturally found in the body, it is non-immunogenic (Low, 2004).

Folic acid has been employed as targeting moiety in the delivery of a wide variety of therapeutic agents, such as imaging agents (Wang *et al.*, 1996, Konda *et al.*, 2000), protein toxins (Ward *et al.*, 2000), chemotherapeutic agents (Ladino *et al.*, 1997, Lee *et al.*, 2002, Aronov *et al.*, 2003, Reddy *et al.*, 2006), antisense oligonucleotides (Citro *et al.*, 1994, Li *et al.*, 1998, Jeong *et al.*, 2005), liposomal drug carriers (Lee and Low, 1994, Gabizon *et al.*, 1999) and gene delivery vectors (Mislick *et al.*, 1995, Leamon *et al.* 1999, Hofland *et al.*, 2002, Benns *et al.*, 2002, Hattori and Maitani, 2004). In addition, the folate-targeted therapeutic drug and folate-linked imaging agents are currently under evaluation in clinical trials (Paulos *et al.*, 2004).

### 7.1.2. Aims

Folic acid conjugated DMA-MPC diblock copolymer system was developed recently (Licciardi *et al.*, 2005), in which the folic acid is covalently attached to the terminus of the MPC block. In the previous chapters, it has been demonstrated that certain compositions of the DMA-MPC copolymer have the ability to condense DNA efficiently to form colloiddally stable complexes with minimal non-specific cellular association. Here, the DMA<sub>50</sub>MPC<sub>30</sub> copolymer, which fulfilled the above characteristics, was employed to conjugate with folic acid (DMA<sub>50</sub>MPC<sub>30</sub> – FA). This copolymer composition

was selected based on the results of previous studies (chapter 3 and 4) which have suggested that at least 30 units of MPC are required to achieve sufficient steric stabilization of the complexes, and no less than 40 units of DMA are needed to condense DNA efficiently when 30 units of MPC were attached. In addition, a binary polymer system which consisted of DMA<sub>50</sub>MPC<sub>30</sub> – FA / DMA homopolymer (50/50 monomer/monomer) as a delivery vector was introduced here. The purpose of blending the two types of polymer was in the attempt to produce more condensed structure with higher ability to protect DNA from enzymatic degradation compared to the diblock copolymer on its own, and also to provide steric stabilization effect that was deficient in DMA homopolymer. Both physicochemical and biological properties of this novel folate conjugated system are described in this chapter.

## 7.2 MATERIALS AND METHODS

### 7.2.1 Materials

Materials used were as described in Chapter 2, Section 2.1 unless otherwise specified below.

DMA<sub>50</sub>-MPC<sub>30</sub>-FA functionalised diblock polymers were synthesised by the group of Professor S. Armes (Department of Chemistry, The University of Sheffield, UK) according to the methods described in the literature (Armes *et al.*, 2001; Licciardi *et al.*, 2005). The properties and the chemical structures of DMA<sub>50</sub>-MPC<sub>30</sub>-FA functionalised diblock polymers are shown in table 7.1 and figure 7.2 respectively. All polymers were supplied as freeze-dried solids which were subsequently dissolved in ELGA water (1-10 mg/ml) and subsequently stored at -20°C.

The binary polymer system consisted of DMA<sub>50</sub>MPC<sub>30</sub> – FA and DMA homopolymer was prepared by mixing the two polymers according to the following equation (6):

$$\text{Amount of polymer 1} = \frac{\text{Polymer 1 monomer Mw} \times \text{ratio} \times \text{Amount of polymer 2}}{\text{Polymer 2 monomer Mw}} \quad (6)$$

**Table 7.1. Summary of molecular weight data and folic acid content for DMA-MPC-FA functionalized diblock copolymers**

Polymer	% of conjugated folic acid		residual free folic acid (wt %)	M <sub>n</sub>	M <sub>w</sub> /M <sub>n</sub>
	wt ratio %	mol ratio %			
DMA <sub>50</sub> -MPC <sub>30</sub> -FA	2.33	100	< 0.01	20,300	1.32

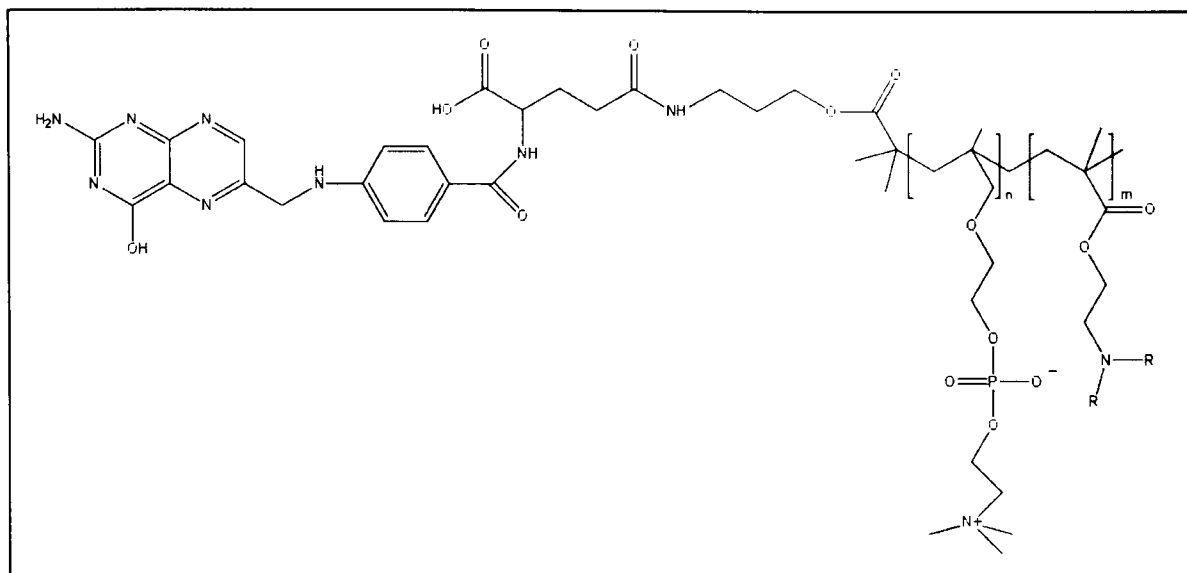


**Figure 7.2** Chemical structures of  $\text{DMA}_m\text{-MPC}_n\text{-FA}$  functionalised diblock polymers.

### 7.2.2 Preparation of polymer – DNA complexes

The polymer – DNA complexes were prepared as described in Chapter 2, section 2.2.1. For the binary polymer system, DNA complexes were produced *via* a single addition of mixed binary polymer solution to DNA in the same fashion as described in section 2.2.1.

### 7.2.3 Gel retardation assay

The DNA binding ability of  $\text{DMA}_{50}\text{-MPC}_{30}\text{-FA}$  polymer and the binary polymer system was assessed by gel retardation assay as described in Chapter 3, section 3.2.3.

#### **7.2.4 Particle size analysis**

Particle size of DNA complexes formed with DMA<sub>50</sub>-MPC<sub>30</sub>-FA polymer and the binary polymer system was determined using proton correlation spectroscopy (PCS), as described in Chapter 3, section 3.2.5. DNA complexes were prepared at monomeric unit: nucleotide ratio 0.5:1, 1:1, 2:1 and 5:1.

#### **7.2.5 Morphology study**

The morphology of DNA complexes formed with DMA<sub>50</sub>-MPC<sub>30</sub>-FA polymer and binary polymer system was examined using transmission electron microscope (TEM), as described in Chapter 4, section 4.2.2. DMA<sub>50</sub>-MPC<sub>30</sub>-FA polymer – DNA complexes were prepared at monomeric unit: nucleotide ratio 1:1, 2:1 and 5:1, and binary polymer – DNA complexes were prepared at nucleotide ratio 2:1 and 5:1.

#### **7.2.6 Enzymatic degradation assay**

The ability of DMA<sub>50</sub>MPC<sub>30</sub> – FA and the binary polymer system to protect DNA from enzymatic degradation was assessed by gel electrophoresis, as described in Chapter 5, section 5.2.3.

#### **7.2.7 Cell lines and routine subculture**

A549 cells (human lung carcinoma) were provided by the Experimental Cancer Chemotherapy Group, University of Nottingham, UK. MCF-7 cells (human breast carcinoma) were provided by Tissue Engineering Group, School of Pharmacy, University of Nottingham, UK. KB cells (human oral carcinoma) were purchased from American Type Culture Collection (ATCC).

USA. All cell lines used in this chapter were maintained in folic acid free RPMI-1640 medium supplemented with 100 U/ml penicillin, 100 µg/ml streptomycin, and 10% FCS which was the only source of folate for the cells. The cells were cultured in humidified atmosphere with 5% CO<sub>2</sub> at 37°C. The cells were sub-cultured twice a week at a 1:10 ratio, using Trypsin – EDTA as dissociating agent.

### **7.2.8 Flow cytometry study**

The flow cytometry was used to investigate the cellular association of the folate conjugated system. Three different cell lines, A549, MCF-7 and KB cells were used. The experiment was carried out as described in Chapter 5, section 5.2.5, with one modification. Instead of using the optiMEM-I, the DNA complexes were prepared in folic acid free and serum free RPMI-1640 medium. Free folic acid (1 mM) was added to the cells together with the DNA complexes when required.

### **7.2.9 Transfection study**

The transfection study of folate conjugated system was carried out on A549, MCF-7 and KB cells, as described in Chapter 5, section 5.2.6, with minor modification. Instead of using the optiMEM-I buffer, the DNA complexes were prepared in folic acid free and serum free RPMI-1640 medium. After the cells were incubated with the DNA complexes for 4 h, the complexes were removed and replaced with folic acid free RPMI-1640 medium (supplemented with 10% FCS) and the cells were incubated for a further 48 h before analysis. Free folic acid (1 mM) was added to the cells together with the DNA complexes when required.

## 7.3 RESULTS

### 7.3.1 Gel retardation assay

The gel retardation assay of DMA<sub>50</sub>MPC<sub>30</sub> – FA – DNA complexes is showed in figure 7.3a. Free DNA band could be seen in the upper image at low monomeric unit: nucleotide ratio. As the ratio increased, DNA bands gradually became fainter. At ratio 1.25:1, no DNA bands could be observed but fluorescence could still be detected in the loading well. As the ratio further increased, fluorescence could no longer be seen at all, indicating that the binding sites of the plasmid DNA were mostly occupied by the copolymer. Polymer band could be seen in the lower image at ratio 2:1, suggesting the presence of free polymer within the system. The gel retardation assay of the binary polymer system, DMA<sub>50</sub>MPC<sub>30</sub> – FA / DMA (50/50), is shown in figure 7.3b. The general pattern of the gel was very similar to the DMA<sub>50</sub>MPC<sub>30</sub> – FA system, with DNA bands disappearing at a lower ratio of 0.75:1, suggesting a higher DNA binding efficiency with the binary polymer system. Free uncomplexed polymer with the binary system also appeared at a lower ratio of 1.5:1, indicating that less polymer is needed to achieve complete binding of the plasmid DNA.

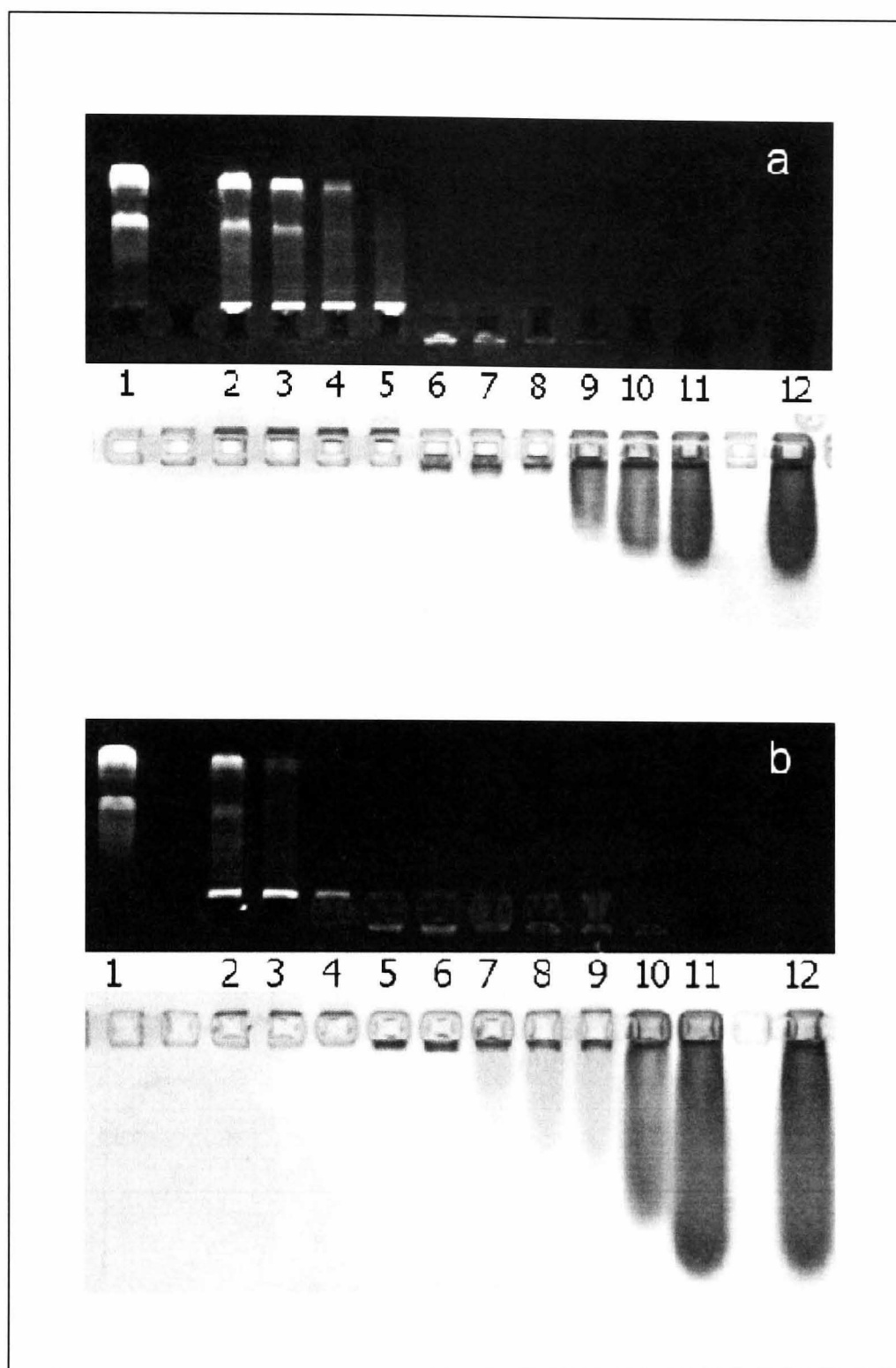


**Figure 7.3** Agarose gel retardation assay of folate conjugated systems. Lane 1 is the DNA control. Lanes 2-11 correspond to 0.25:1, 0.5:1, 0.75:1, 1:1, 1.25:1, 1.5:1, 1.75:1, 2:1, 5:1 and 10:1 monomeric unit: nucleotide ratio. Lane 12 is polymer control. (a) DMA<sub>50</sub>MPC<sub>30</sub>-FA (b) The binary polymer system, DMA<sub>50</sub>MPC<sub>30</sub>-FA /DMA (50/50).



### 7.3.2 Particle size analysis

Photon correlation spectroscopy (PCS) was used to measure the particle size of DMA<sub>50</sub>MPC<sub>30</sub> – FA – DNA complexes and the binary polymer – DNA complexes. The average diameter, scattering intensity and polydispersity of the complexes were measured. The results are shown in tables 7.2 and 7.3 respectively. For the DMA<sub>50</sub>MPC<sub>30</sub> – FA system, the complexes formed were well below 200 nm, with decreasing particle size as the ratio increased. At ratio 5:1, the complexes formed were approximately 100 nm. The scattering intensity of the complexes increased with the ratios, indicating the formation of more condensed and compact particles. The polydispersity of the particles was approximately 0.5 at all ratios. For the binary polymer system, it was found that the complexes were highly aggregated at ratio 0.5:1, with particle size measured at over 1 µm. The high scattering intensity also indicated the agglomeration of complexes. As the ratio increased, the particle size gradually decreased. The particle size of the DNA complexes was approximately 200 nm and 120 nm at ratio 2:1 and 5:1 respectively. The scattering intensity decreased as the ratio increased, suggesting the formation of colloiddally stable complexes which were more ‘soluble’ and less dense than the aggregating complexes at low ratio. The polydispersity of the complexes also decreased when the ratio increased.

**Table 7.2 Average particle size, scattering intensity and polydispersity of DMA<sub>50</sub>MPC<sub>30</sub> – FA – DNA complexes measured by PCS.** DNA complexes were prepared at 0.5:1, 1:1, 2:1 and 5:1 monomeric unit: nucleotide ratio in 10% (v/v) PBS (n=6).

Monomeric unit : nucleotide ratio	Average diameter (nm) ± SD	Scattering intensity (KCps) ± SD	Polydispersity ± SD
0.5:1	165 ± 20	275 ± 11	0.63 ± 0.11
1:1	159 ± 1	672 ± 7	0.44 ± 0.01
2:1	125 ± 2	719 ± 17	0.49 ± 0.01
5:1	103 ± 3	796 ± 26	0.43 ± 0.04

**Table 7.3 Average particle size, scattering intensity and polydispersity of DMA<sub>50</sub>MPC<sub>30</sub>-FA/DMA binary polymer – DNA complexes measured by PCS.** DNA complexes were prepared at 0.5:1, 1:1, 2:1 and 5:1 monomeric unit: nucleotide ratio in 10% (v/v) PBS (n=6).

Monomeric unit : nucleotide ratio	Average diameter (nm) ± SD	Scattering intensity (KCps) ± SD	Polydispersity ± SD
0.5:1	1742 ± 400	2006 ± 144	1.0 ± 0
1:1	209 ± 8	1579.3 ± 27	0.59 ± 0.03
2:1	191 ± 8	1433 ± 63	0.52 ± .004
5:1	119 ± 1	871 ± 14	0.34 ± 0.01

### 7.3.3 Morphology study

The morphology of the DNA complexes was examined under transmission electron microscope (TEM). The TEM images of DMA<sub>50</sub>MPC<sub>30</sub> – FA – DNA complexes are shown in figure 7.4-6 and the measurement of the complexes are shown in table 7.4. At 1:1 monomeric unit: nucleotide ratio, it appeared that DNA was not well condensed as strands of uncondensed DNA could be seen. At ratio 2:1, particulate DNA complexes were formed; they appeared as highly condensed compact particles with either spherical or oval shape. At ratio 5:1, the majority of the complexes appeared as short, thick rods or oval shape particles. A small amount of toroids can also be seen. The complexes formed at ratio 5:1 were slightly smaller than those formed at 2:1 (43± 9 nm and 55 ± 12 nm, respectively, n=50) (table 7.4), which is consistent with the size measured using PCS. However, the particle size measured under the TEM is considerably smaller than that measured with PCS, probably due to the dehydration effect in TEM.

The TEM images of DMA<sub>50</sub>MPC<sub>30</sub> – FA / DMA (50/50) – DNA complexes are shown in figure 7.7 and 7.8. At 2:1 monomeric unit: nucleotide ratio, the majority of the DNA complexes formed were of spherical or oval shape. The complexes were seen aggregating in clumps. This is consistent with the PCS

results, which also suggests that slight aggregation occurred at this ratio. At ratio 5:1, colloidal DNA complexes were formed, and aggregation was no longer observed. The complexes appeared as either rods or oval shaped particles, similar to those observed with DMA<sub>50</sub>MPC<sub>30</sub> – FA – DNA complexes at the same ratio.

**Table 7.4 Average particle size of DMA<sub>50</sub>MPC<sub>30</sub> – FA – DNA complexes and DMA<sub>50</sub>MPC<sub>30</sub> – FA/ DMA binary system – DNA complexes measured under the TEM.** The complexes were prepared in 10% (v/v PBS) and stained with uranyl acetate. The bracket indicates the monomer unit: nucleotide ratio of the complexes (n=50).

System	Average article size (nm) ± SD
DMA <sub>50</sub> MPC <sub>30</sub> – FA (2:1)	55 ± 13
DMA <sub>50</sub> MPC <sub>30</sub> – FA (5:1)	43 ± 9
DMA <sub>50</sub> MPC <sub>30</sub> – FA / DMA (5:1)	52 ± 11

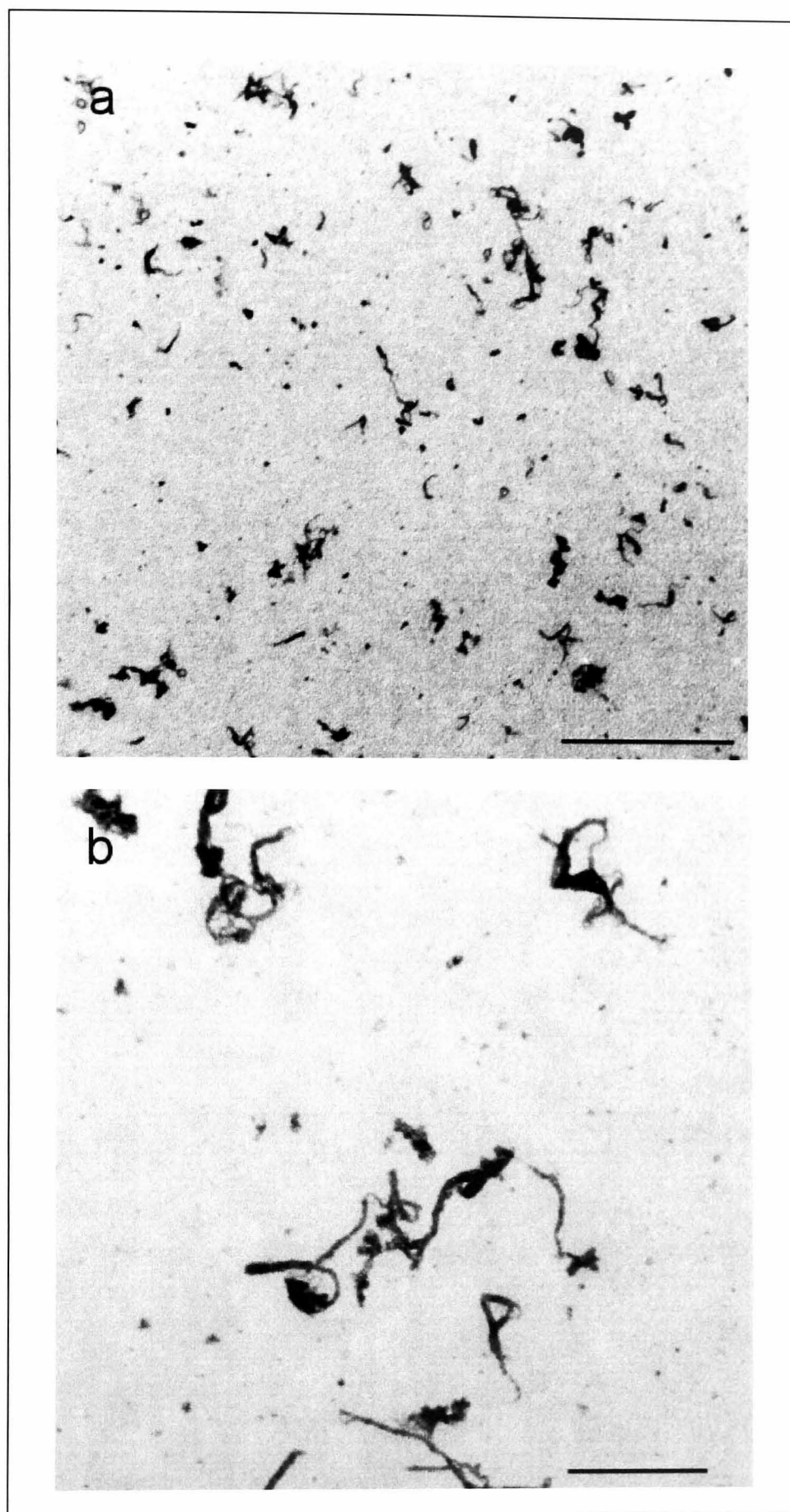


**Figure 7.4** TEM images of DMA<sub>50</sub>MPC<sub>30</sub>-FA – DNA complexes at 1:1 monomeric unit: nucleotide ratio. Complexes were prepared in 10% (v/v) PBS and stained with uranyl acetate. The bars represent (a) 1000 nm and (b) 200 nm.

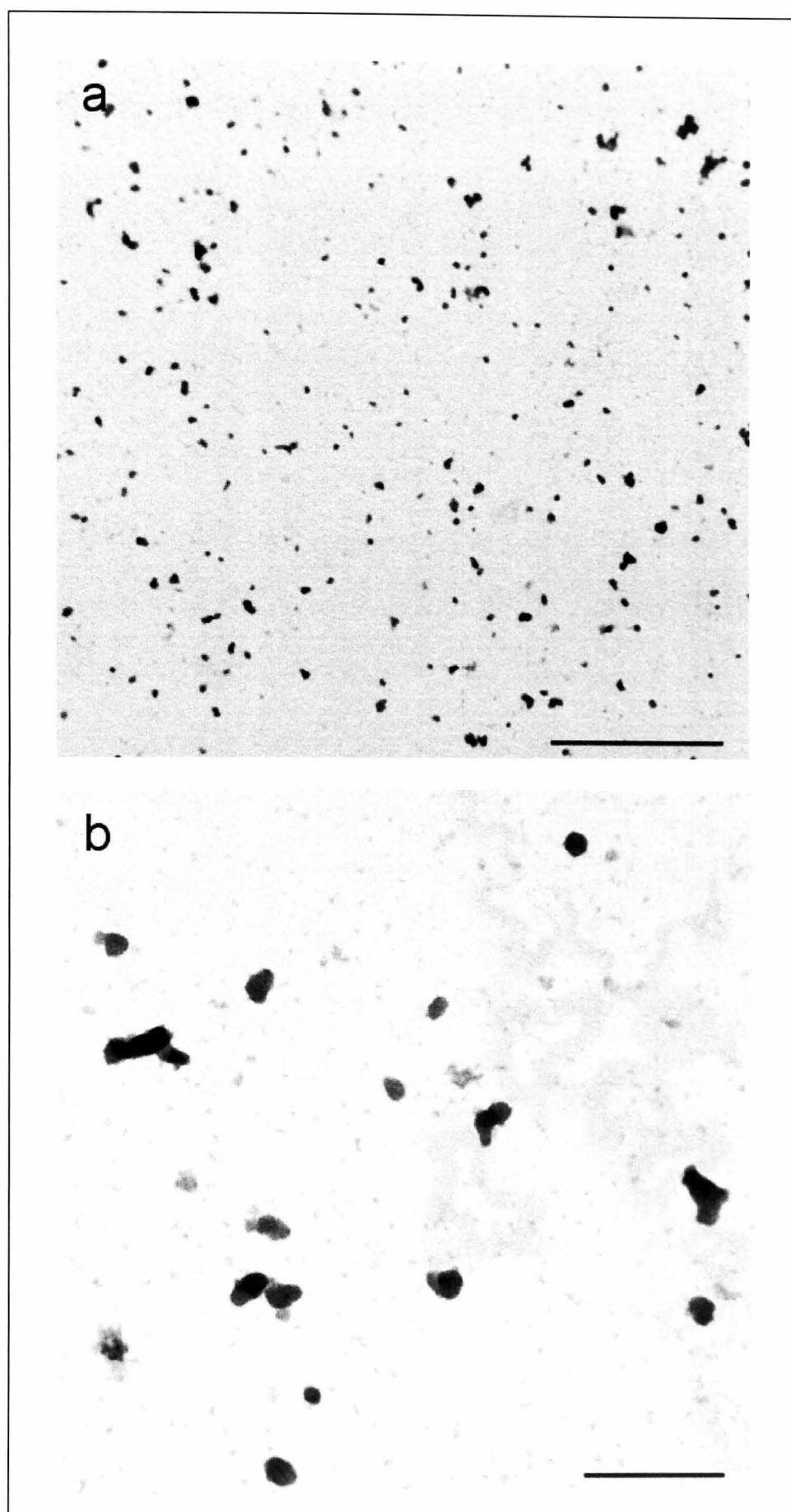


**Figure 7.5** TEM images of DMA<sub>50</sub>MPC<sub>30</sub>-FA – DNA complexes at 2:1 monomeric unit: nucleotide ratio. Complexes were prepared in 10% (v/v) PBS and stained with uranyl acetate. The bars represent (a) 1000 nm and (b) 200 nm.

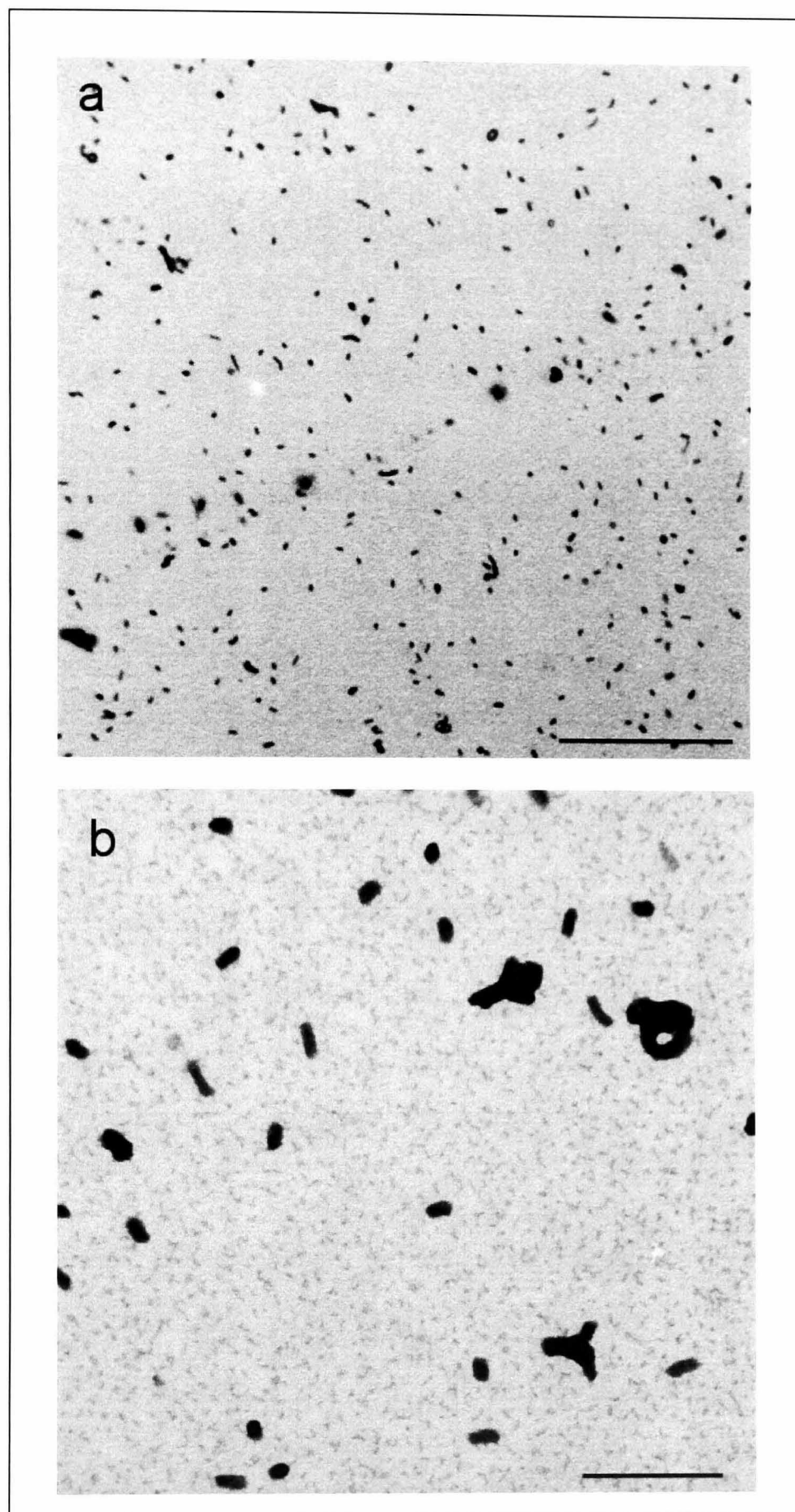


**Figure 7.6** TEM images of DMA<sub>50</sub>MPC<sub>30</sub>-FA - DNA complexes at 5:1 monomeric unit: nucleotide ratio. Complexes were prepared in 10% (v/v) PBS and stained with uranyl acetate. The bars represent (a) 1000 nm and (b) 200 nm.

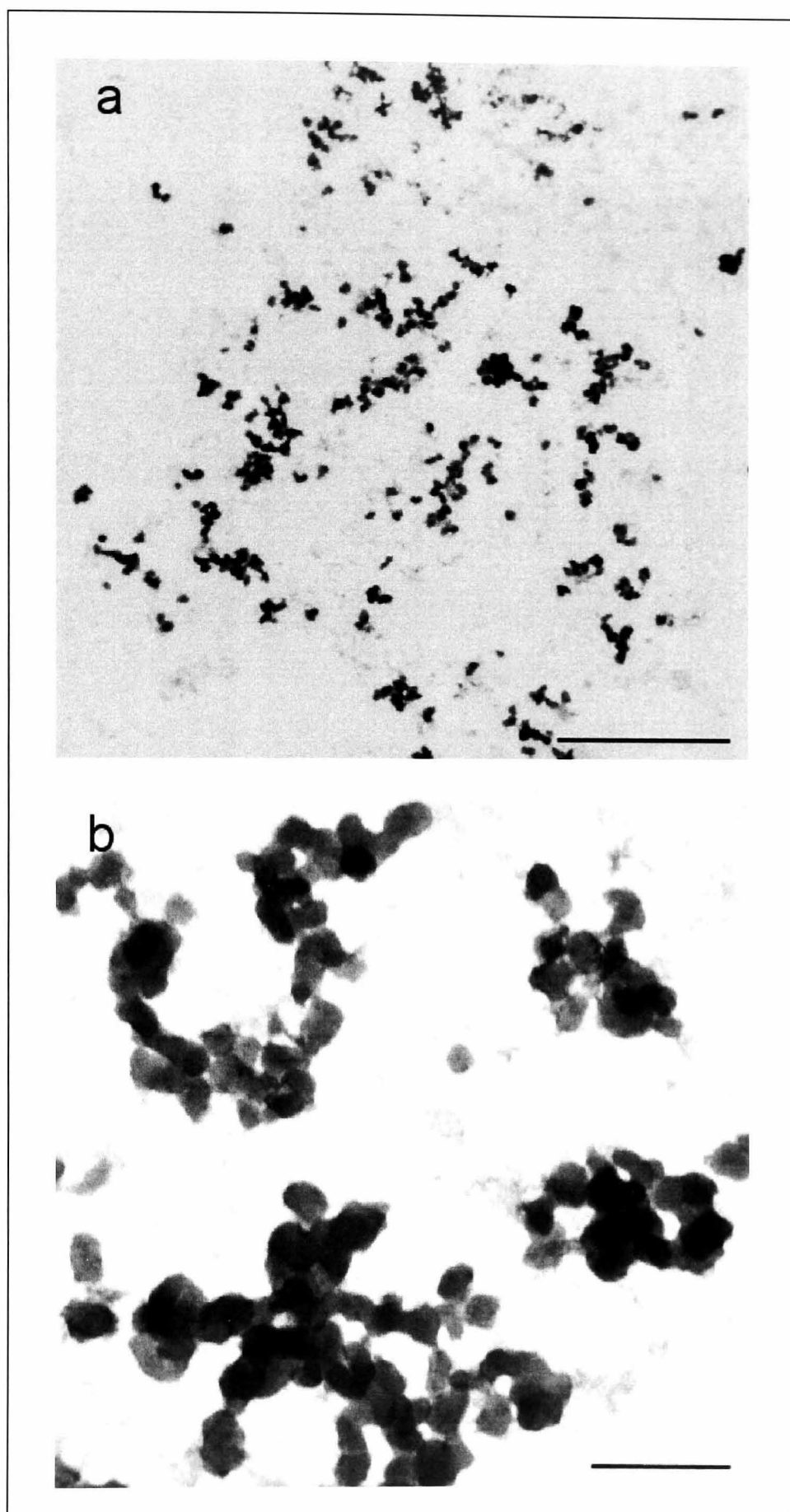


**Figure 7.7** TEM images of DMA<sub>50</sub>MPC<sub>30</sub>-FA / DMA binary polymer – DNA complexes at 2:1 monomeric unit: nucleotide ratio. Complexes were prepared in 10% (v/v) PBS and stained with uranyl acetate. The bars represent (a) 1000 nm and (b) 200 nm.

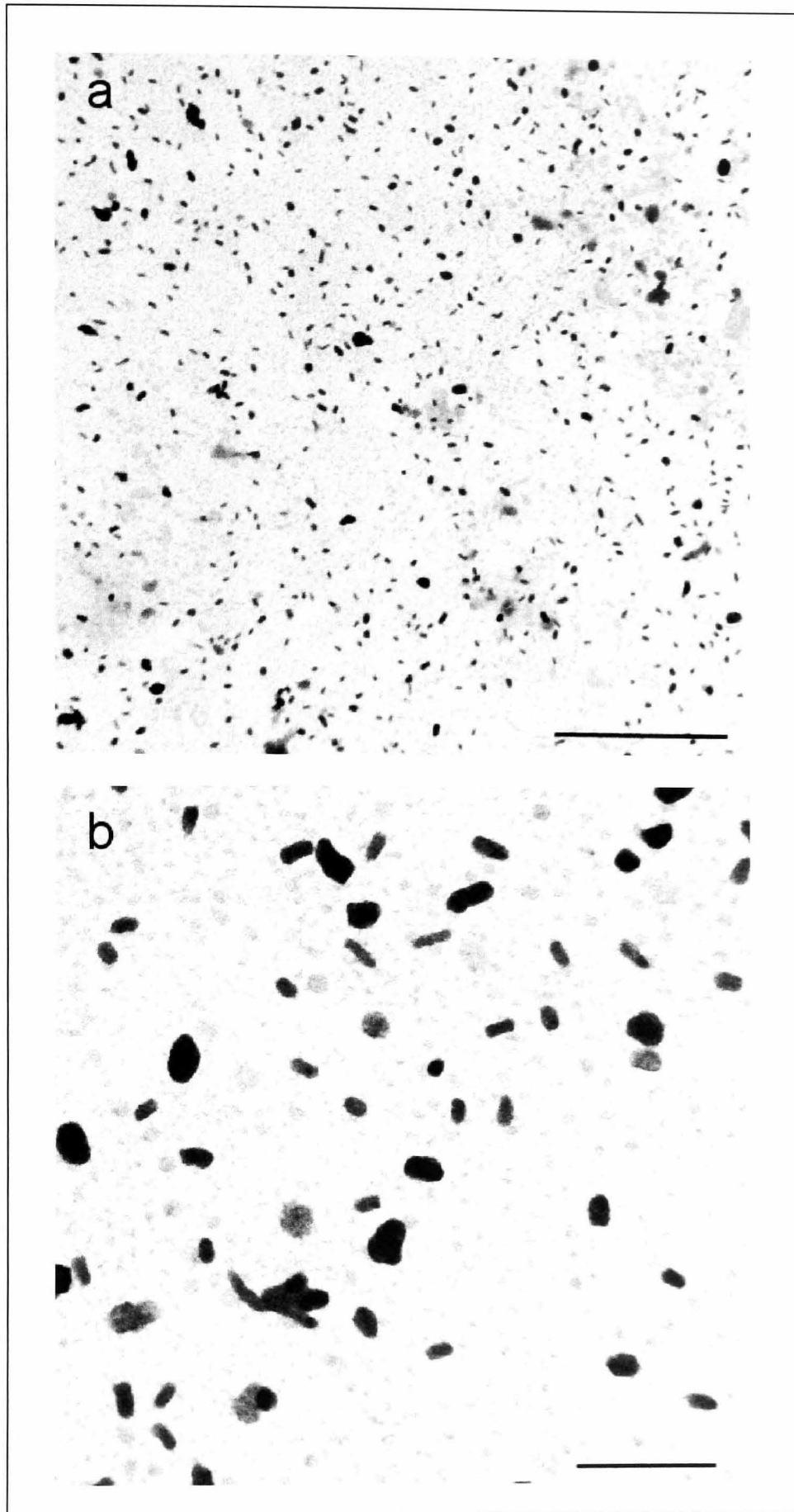


**Figure 7.8** TEM images of DMA<sub>50</sub>MPC<sub>30</sub>-FA / DMA binary polymer – DNA complexes at 5:1 monomeric unit: nucleotide ratio. Complexes were prepared in 10% (v/v) PBS and stained with uranyl acetate. The bars represent (a) 1000 nm and (b) 200 nm.



### 7.3.4 Enzymatic degradation assay

The ability of the folate conjugated system to protect DNA from enzymatic degradation was assessed by gel electrophoresis and the results are shown in figure 7.9. For both the DMA<sub>50</sub>MPC<sub>30</sub> – FA copolymer and the binary polymer system, the DNA complexes were dissociated with pAsp, as the DNA band with molecular weight similar to the DNA control can be seen on the gel after the addition of the polyanion.

Following the complexes incubation with DNase I, the systems were shown to protect DNA from degradation to a different extent. For DMA<sub>50</sub>MPC<sub>30</sub> – FA, small molecular weight DNA, instead of the original DNA band, was observed at the top side of the gel at low monomeric unit: nucleotide ratios, indicating the partial breakdown of the plasmid DNA. As the ratio increased, the fluorescence intensity appeared to be brighter, and the DNA band which had the same molecular weight with the DNA control could be seen at ratio 10:1. The results hence indicate that the protection of DNA from enzymatic degradation could be better prevented at high ratio, even though the protection was still not complete, as the released DNA band was dimmer than the control and fragments of small molecular weight DNA could be seen at the top side of the gel.

For DMA<sub>50</sub>MPC<sub>30</sub> – FA / DMA binary polymer system, it was found that protection of DNA could be achieved at a much lower monomeric unit: nucleotide ratio. The DNA bands with molecular weight similar to the control could be observed at ratio as low as 1:1. This was probably due to the presence of DMA homopolymer within the binary polymer system and hence formation of more condensed complexes. Again, the full protection was not achieved as fragments of DNA with small molecular weight can be observed on the gel as partial breakdown of plasmid occurred.

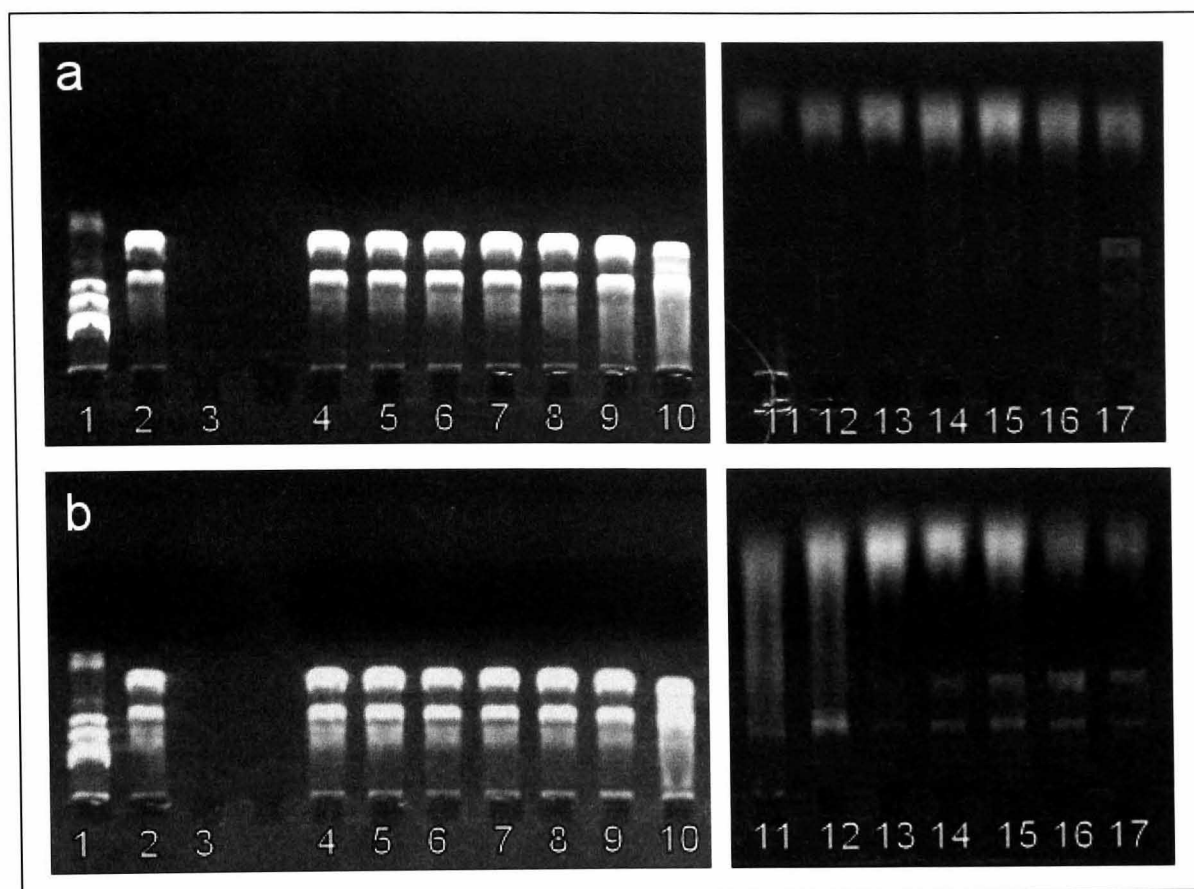


**Figure 7.9** Gel electrophoresis of folate conjugated systems in enzyme degradation assay. Lane 1 = DNA ladder, lane 2 = control DNA, lane 3 = naked DNA following DNase I incubation. Lane 4-10 contain DNA complexes at ratios 0.25:1, 0.5:1, 1:1, 1.5:1, 2:1, 5:1 and 10:1 respectively, after dissociation with pAsp. Lane 11-17 contain DNA complexes at ratios 0.25:1, 0.5:1, 1:1, 1.5:1, 2:1, 5:1 and 10:1, respectively, after incubation with DNase I at 37°C for 10 min followed by dissociation of complexes with pAsp (a) DMA<sub>50</sub>MPC<sub>30</sub>-FA (b) DMA<sub>50</sub>MPC<sub>30</sub>-FA/DMA binary polymer system.

### 7.3.5 Flow cytometry study

In this study, flow cytometry was employed to investigate the cellular association of the folate conjugated systems (DMA<sub>50</sub>MPC<sub>30</sub> – FA and DMA<sub>50</sub>MPC<sub>30</sub> – FA / DMA binary polymer). Three different cell lines were used: A549, MCF-7 and KB cells. A549 cells have a low level of folate receptors (Too and Park, 2004, Cho *et al.*, 2005), whereas MCF-7 and KB cells have been reported to have overexpression of folate receptors (Leamon and Low, 1991, Hattori and Maitani, 2004). The aim of this study was to

investigate whether there was selective uptake of folate conjugated DNA delivery system by the folate receptors expressing cells. DMA homopolymer and a non-conjugated diblock copolymer with comparable composition to the folate conjugated copolymer, DMA<sub>60</sub>MPC<sub>30</sub>, were used as controls.

The average fluorescence intensity measured from flow cytometry of both DMA<sub>50</sub>MPC<sub>30</sub> – FA and the binary polymer system on the three cell lines are shown in figure 7.10. The fluorescence intensity for all MPC containing copolymer (both folate conjugated and non-conjugated) and binary polymer system was lower than DMA homopolymer on all cell lines, suggesting a decrease in non-specific cellular association.

For A549 cells, there were no significant differences in fluorescence intensity between the non conjugated DMA<sub>60</sub>MPC<sub>30</sub>, the folate conjugated DMA<sub>50</sub>MPC<sub>30</sub> and the binary polymer system. Similar results were observed with MCF-7 cells. Although MCF-7 cells were reported to have overexpression of folate receptors, there were no significant differences in fluorescence intensity between the folate conjugated and non-conjugated system ( $p > 0.05$ ). For KB cells, which are the most commonly used cell lines in the study of folate conjugated delivery system, there was a significant increase in fluorescence intensity for DMA<sub>50</sub>MPC<sub>30</sub> – FA system at both ratios (2:1 and 5:1) compared to the non-conjugated DMA<sub>60</sub>MPC<sub>30</sub> system ( $p < 0.05$  in each case). However, for the folate conjugated binary polymer system, there was no significant difference in fluorescence intensity with the non – conjugated system ( $p > 0.05$ ).

In order to investigate whether the increase of cellular association of the folate conjugate copolymer system on the folate receptor expression KB cells were due to specific receptor interaction, the DMA<sub>50</sub>MPC<sub>30</sub> – FA – DNA complexes (ratio 5:1) were incubated with KB cells in the presence of 1 mM of free folic acid. The results (figure 7.11) showed that there was a significant reduction of fluorescence intensity when the free folic acid was present, suggesting that the free folic acid reduced the cellular association of

the folate conjugated system by competing with the DNA complexes for the folate receptors.

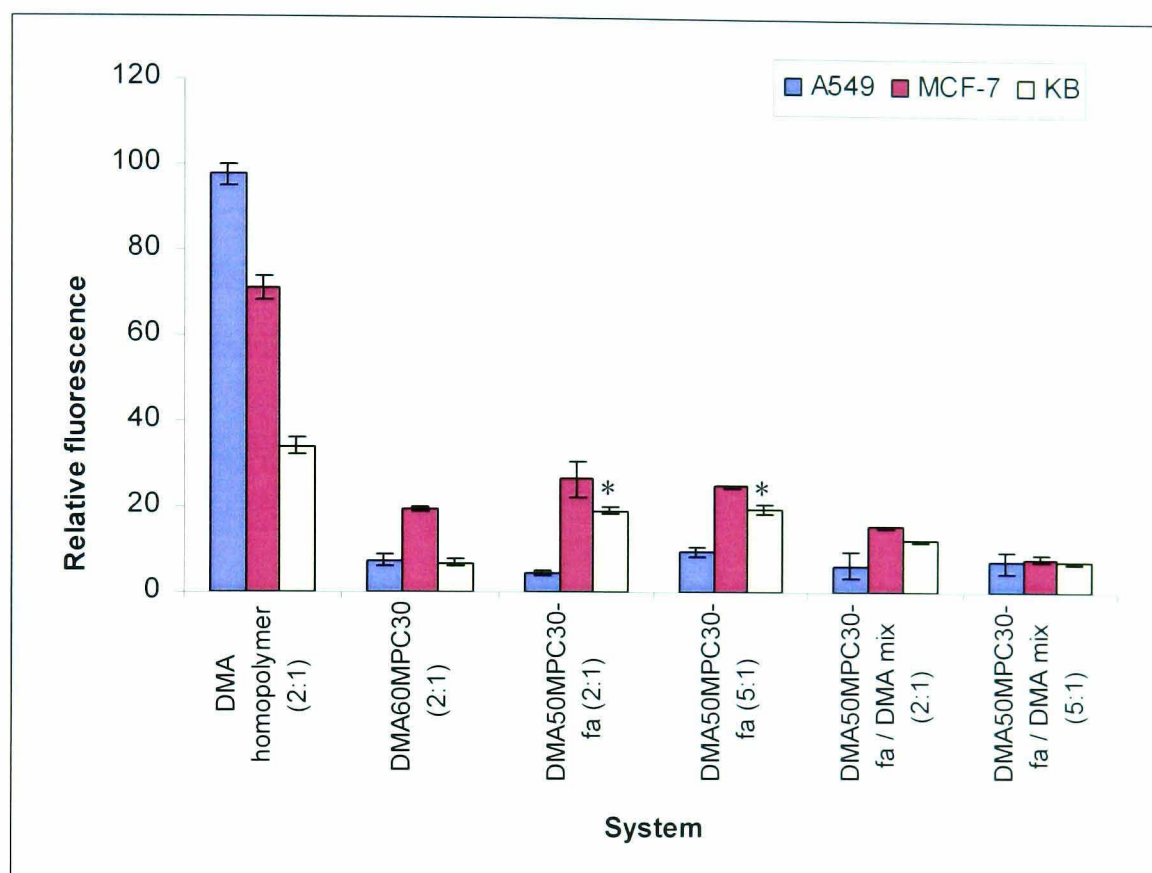


**Figure 7.10 Average fluorescent intensity associated with A549, MCF-7 and KB cells using folate conjugated system in flow cytometry study.** DMA homopolymer and non-conjugated DMA<sub>60</sub>-MPC<sub>30</sub> diblock copolymer system were used as control (n=6). \*  $P < 0.05$  when compared with DMA<sub>60</sub>-MPC<sub>30</sub> system on KB cells.

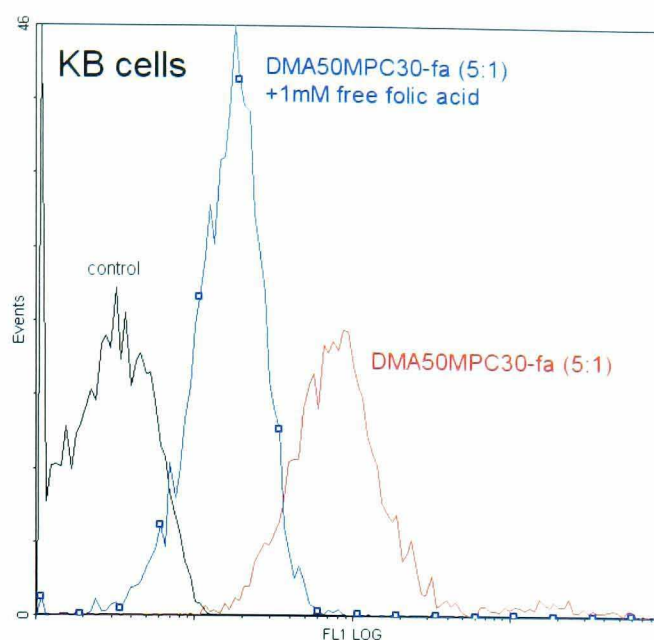


**Figure 7.11 Cellular association of DMA<sub>50</sub>MPC<sub>30</sub>-FA – DNA complexes on KB cells, with the presence or absence of free folic acid in flow cytometry study.** DNA complexes were prepared at 5:1 monomeric unit: nucleotide ratio. The untreated KB cells were used as control.

### 7.3.6 Transfection study

The transfection efficiency of both DMA<sub>50</sub>MPC<sub>30</sub> – FA and the binary polymer system on the three cell lines are shown in figure 7.12. For the A549 cells, although the transfection efficiency of the folate conjugated systems had been enhanced compared to the non-conjugated DMA<sub>60</sub>MPC<sub>30</sub> ( $p < 0.05$ ), the overall level of gene expression was still very low. For both folate receptor expressing MCF-7 and KB cells, a significant increase in transfection efficiency was observed for the folate conjugated system compared to the non-conjugated copolymer ( $p < 0.05$  in each system). Also, for both folate conjugated system (DMA<sub>50</sub>MPC<sub>30</sub> – FA and the binary polymer system), DNA complexes formed at 5:1 ratio had a higher transfection efficiency than those formed at 2:1 ratio. In addition, the DMA<sub>50</sub>MPC<sub>30</sub> – FA system had a higher transfection efficiency than the binary polymer system at respective ratio. However, the transfection efficiency on all the folate conjugated systems on the two folate receptor

expressing cells were still significantly lower than that of the DMA homopolymer ( $p < 0.05$ ).

To decide whether the increase in gene expression of the folate conjugated system on MCF-7 and KB cells were due specific receptor interaction, the transfection experiments were also carried out in the presence of 1mM free folic acid using the DMA<sub>50</sub>MPC<sub>30</sub> – FA – DNA complexes prepared at both ratios 2:1 and 5:1 (figure 7.13). For the non-conjugated DMA<sub>60</sub>MPC<sub>30</sub> system, there was no significant difference in transfection efficiency when the free folic acid was present or absent in the culture medium ( $p > 0.05$ ). On MCF-7 cells, a significant reduction of transfection efficiency was observed for the folate conjugated system at ratio 5:1 ( $p < 0.05$ ) when the folic acid was present in the medium. However, no significant difference was observed at ratio 2:1 ( $p > 0.05$ ). On KB cells, a significant reduction of transfection efficiency was observed for the folate conjugated system at both ratios when free folic acid was present ( $p < 0.05$  at both ratios). The reduction of transfection efficiency could be attributed to the blocking of the folate receptor on KB cells by the free folic acid, resulting in reduction of cellular uptake of complexes (which is consistent with the flow cytometry results), and consequently a lower transfection efficiency.

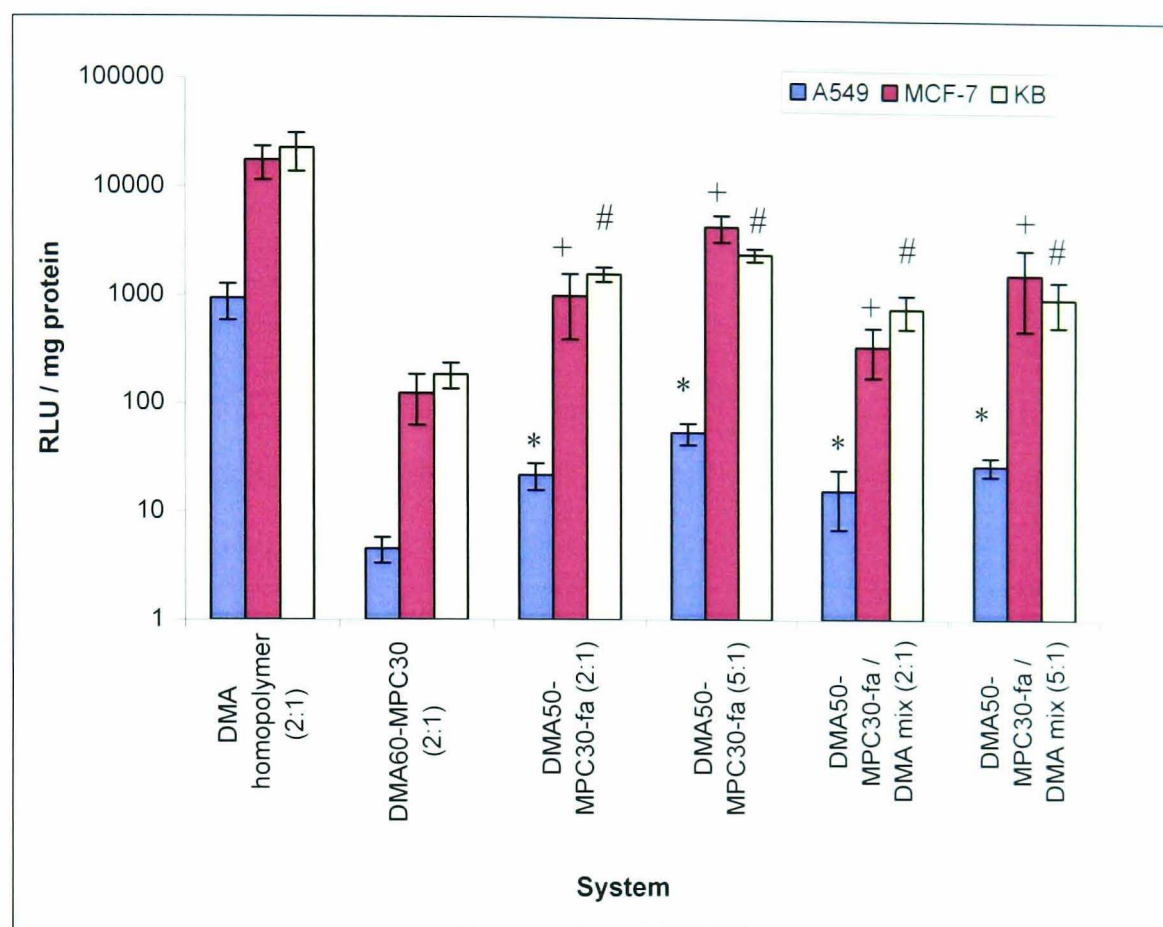


**Figure 7.12** Transfection efficiency of folate conjugated systems on A549, MCF-7 and KB cells. DMA-MPC diblock copolymer and the binary polymer system were prepared at monomeric unit: nucleotide ratio 2:1 and 5:1. Data were presented in terms of relative light unit (RLU) / mg protein. DMA homopolymer and non folate conjugated DMA-MPC diblock copolymer were used as control (n=6). \*  $P < 0.05$  when compared with DMA<sub>60</sub>-MPC<sub>30</sub> system on A549 cells. +  $P < 0.05$  when compared with DMA<sub>60</sub>-MPC<sub>30</sub> system on MCF-7 cells. #  $P < 0.05$  when compared with DMA<sub>60</sub>-MPC<sub>30</sub> system on KB cells.

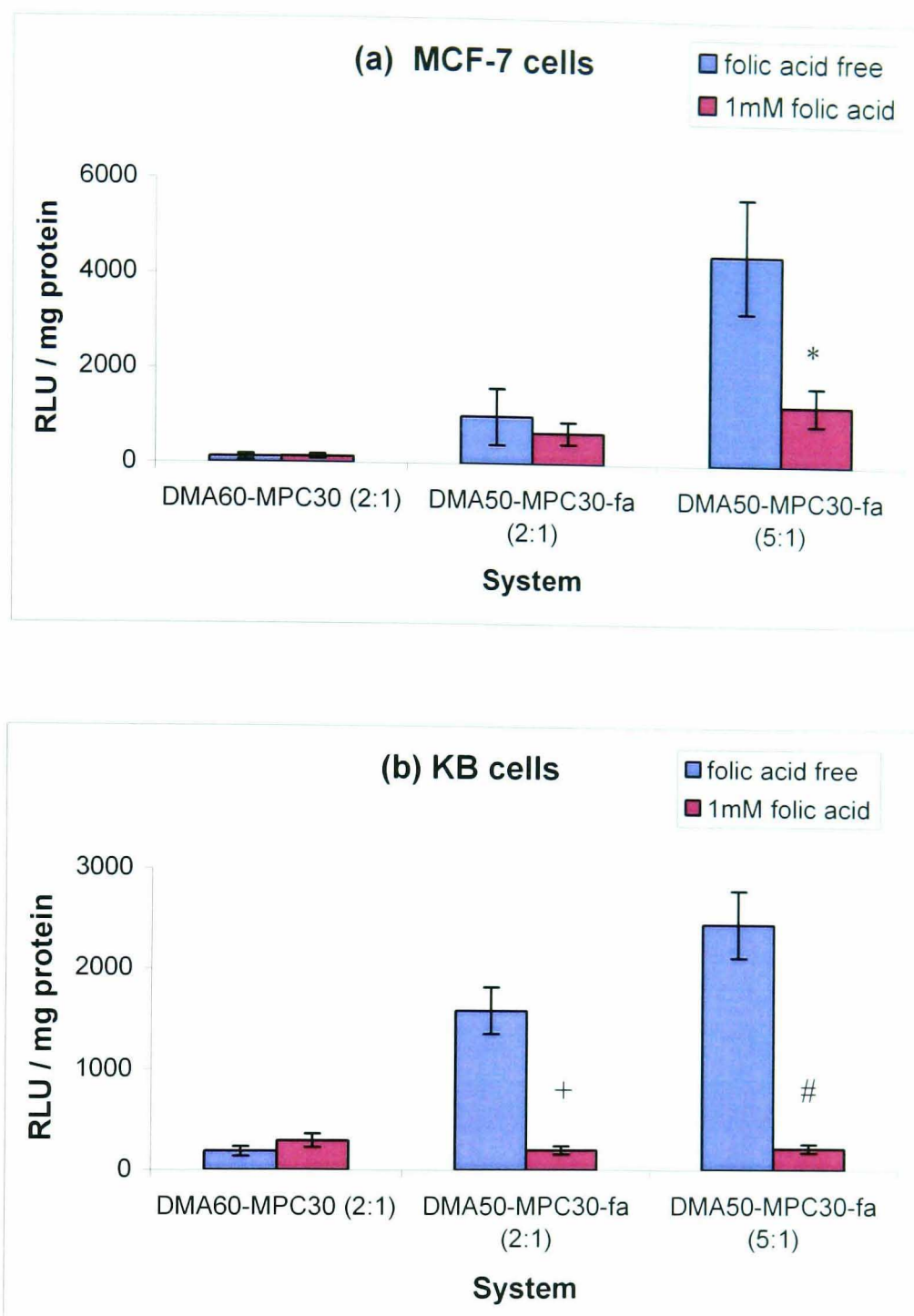


**Figure 7.13** Transfection efficiency of DMA<sub>50</sub>-MPC<sub>30</sub>-FA on (a) MCF-7 and (b) KB cells, in the presence or absence of free folic acid. Non - conjugated DMA<sub>60</sub>-MPC<sub>30</sub> diblock copolymer was used as control. (n=6). \*  $P < 0.05$  when compared with folic acid free medium at the same ratio on MCF-7 cells. +  $P < 0.05$  when compared with folic acid free medium at the same ratio on KB cells. #  $P < 0.05$  when compared with folic acid free medium at the same ratio on KB cells



## 7.4 DISCUSSION

An ideal gene delivery vector should be able to achieve specific targeting with minimal non-specific cellular interaction. The hydrophilic MPC has been demonstrated to provide steric stabilization for the DNA complexes, as well as reducing non-specific cellular interaction by providing steric hindrance, as described previously in chapter 3 and 5. However, the transfection efficiency of the DMA-MPC diblock copolymer remains relatively low, due to minimal cell surface interaction. In order to improve the efficiency of this system, a folic acid ligand is covalently attached to the MPC of the copolymer system in order to enhance gene expression *via* folate receptor mediated endocytosis.

First of all, a series of physicochemical evaluations of the folate conjugated system was carried out to investigate whether the attachment of folic acid affects the physicochemical property of the DNA complexes. The results indicate that DMA<sub>50</sub>MPC<sub>30</sub> – FA was able to condense DNA effectively to produce colloiddally stable complexes with small particle size approximately 120 nm diameter at monomeric unit: nucleotide ratio 2:1 or above. However, the enzymatic degradation assay shows that the ability of this system to protect DNA from nuclease attack was not entirely satisfactory. A high ratio of 10:1 was required in order to preserve the structure of the plasmid DNA. At this ratio, there was an abundance of free folate conjugated copolymer available in the solution as shown in gel retardation assay. This is not desirable as the uncomplexed folate conjugated copolymer may compete with the DMA<sub>50</sub>MPC<sub>30</sub> – FA – DNA complexes for the folate receptor on the cell surface. It has been reported that other folate conjugated delivery system, such as PLL – PEG – FA, a high polymer – DNA ratio would in fact lead to substantial reduction of transfection efficiency possibly due to competition for receptors between uncomplexed polymer and DNA complexes (Cho *et al.*, 2005).

The binary polymer system, which consists of DMA<sub>50</sub>MPC<sub>30</sub> – FA / DMA, was also investigated. This system formed DNA complexes which were aggregating at low monomeric unit: nucleotide ratios, as shown in the PCS data and morphology study. This is probably due to insufficient steric stabilization provided by the hydrophilic MPC. As the ratio increased, colloiddally stable complexes were formed, with average particle size approximately 200 nm and 120 nm in diameter for ratio 2:1 and 5:1 respectively. The TEM images also show discrete well condensed particles at ratio 5:1. It appeared that the binary polymer system can condense DNA more efficiently compared to DMA<sub>50</sub>MPC<sub>30</sub> – FA, as demonstrated by the gel retardation assay. The enzymatic degradation assay also revealed that the binary polymer system was superior to DMA<sub>50</sub>MPC<sub>30</sub> – FA in protecting DNA from enzymatic degradation, probably due to the more efficient condensing property of the binary polymer system to produce complexes with tighter and more compact structure.

However, it is worth to mention that since the two polymers (DMA homopolymer and DMA<sub>50</sub>MPC<sub>30</sub> – FA copolymer) in the binary polymer system are not covalently attached to each other, there is a possibility that some DMA<sub>50</sub>MPC<sub>30</sub> – FA polymers are excluded from the DNA complexes during condensation of DNA, as DMA homopolymer has a higher affinity to DNA compare to DMA<sub>50</sub>MPC<sub>30</sub> – FA polymer, suggested by EtBr displacement and gel retardation assays as shown previously in chapter 3. Although the improvement of steric stabilization (as shown in PCS particle size and morphology studies) in the binary polymer system has indicated that the DMA<sub>50</sub>MPC<sub>30</sub> – FA polymer was actually present in the binary polymer – DNA complexes, it is uncertain if the ratio between the two polymers was indeed 50 : 50 (monomer: monomer). The observation that the binary polymer system is more superior ( in terms of DNA binding/condensation and enzymes protection) than the DMA<sub>50</sub>MPC<sub>30</sub> – FA is valid only if DMA<sub>50</sub>MPC<sub>30</sub> – FA is present in the binary polymer – DNA complexes at the stated ratio. Nevertheless, the initial physicochemical results showed the

both folate conjugated system can condense DNA efficiently to form colloiddally stable complexes and provide a certain level of DNA protection against enzymatic degradation. Apparently, the conjugation of the folic acid ligand does not seem to affect the physicochemical properties of the DMA-MPC copolymer system.

In order to find out whether the incorporation of folic acid could improve the specificity of the delivery system, it is important to evaluate the biological properties of the system *in vitro* in the first step. In all three cell lines investigated, the cellular association and transfection efficiency were significantly reduced when hydrophilic MPC was incorporated in the system, compared to the DMA homopolymer. The non-specific cellular interaction has been successfully reduced due to steric hindrance provided by the MPC. Any increase in cellular association and transfection efficiency with the folate conjugated system are expected to be the result of folate receptor mediated endocytosis.

On A549 cells, the level of cellular association of folate containing system does not seem to be affected by the conjugation of folic acid. However, the transfection efficiency seems to be slightly improved. Although the A549 cells do not have overexpression of folate receptors (Cho *et al.*, 2005), the small amount of folate receptors on the cell surface may be responsible for the enhancement of gene expression. Even though the transfection efficiency has been increased on this cell line, the level of gene expression still remained very low, which was about 200- to 500-fold reduction compared to DMA homopolymer.

On MCF-7 and KB cells, it was found that transfection efficiency was increased by at least 10-fold when folic acid was conjugated to the copolymer. When free folic acid was incubated together with the DNA – complexes, the transfection level was inhibited. This suggests that folate conjugated system was internalised through folate receptors. On both type of cells, DNA – complexes prepared at 5:1 ratio has higher transfection efficiency than those

prepared at 2:1. One of the possible explanations is that at a higher ratio, there may be a higher number of ligands present at the surfaces of the DNA complexes, increasing the chance of the complexes to be recognised by the receptors on the cell surface. In addition, the DMA<sub>50</sub>MPC<sub>30</sub> – FA system was found to have a higher level of transfection compared to the binary polymer system at the respective ratio. This may be due to a number of reasons. First, the complexes formed by the binary polymer system may have fewer ligands per complex compared to DMA<sub>50</sub>MPC<sub>30</sub> – FA at the same monomeric unit: nucleotide ratio, thereby reducing receptor mediated uptake. Secondly, since the binary polymer system was more efficient in binding with DNA, less polymer was required, to condense DNA at the same ratio. Consequently, more free uncomplexed polymer may be present in the solution (as shown by the gel retardation assay), leading to their competition for the folate receptors with the DNA complexes. Thirdly, with the binary system, the orientation of the ligand on the complexes may be less exposed to the surface, compared to that of DMA<sub>50</sub>MPC<sub>30</sub> – FA. The trapped ligands may be more difficult to be recognised by the folate receptor on the cell surface, thereby reducing cellular association and hence transfection efficiency. Furthermore, the size of DNA complexes also appeared to affect the transfection efficiency. DMA<sub>50</sub>MPC<sub>30</sub> – FA system formed smaller complexes with DNA than the binary polymer system at respective ratio. For both DMA<sub>50</sub>MPC<sub>30</sub> – FA system and binary polymer system, smaller DNA complexes were formed at a high monomeric unit: nucleotide ratio. DNA complexes with smaller size in general displayed a better transfection efficiency.

Although the level of gene expression of folate conjugated system was enhanced on MCF-7 and KB cells by 10- to 50-fold, the increase of cellular association with the DNA complexes did not follow the same trend. One of the possible explanations is that a more efficient route of intracellular trafficking exists when DNA complexes are taken up through folate receptor mediated endocytosis. It has been suggested that once internalised inside the cell, the folic acid and its conjugates are released into the cytosol before being transported into lysosomes for degradation (Leamon and Low, 1992).

This could mean that high transfection efficiency of folate conjugated system is not necessary accompanied with high cellular association or uptake. Folic acid has been used by other groups as a targeting ligand attached to PEG which was conjugated to polycation for gene delivery (Leamon *et al.*, 1999, Ward *et al.*, 2002, van Steenis *et al.*, 2003). It has been demonstrated by Ward *et al.* that the level of gene expression of folate – PEG – PLL – DNA complexes was independent of level of internalised DNA (Ward *et al.*, 2002). The folate conjugated systems that showed a lower cellular uptake were actually more transfection active. They also showed that the transfection efficiency of the systems with low cellular uptake was not increased by the presence of the endosomolytic agent chloroquine, suggesting that endosomal escape may not be a limiting factor of folate conjugated complexes. In contrary, a conflicting result was observed by another group (Mislick *et al.*, 1995), who demonstrated that following the uptake of folate conjugated PLL – DNA complexes, they were eventually delivered into the lysosomes. Further investigation, such as confocal microscopy study, maybe useful in confirming the uptake mechanism. Nevertheless, it is well understood that an efficient intracellular trafficking route is important in improving transfection efficiency.

The initial *in vitro* data suggests that both DMA<sub>50</sub>MPC<sub>30</sub> – FA and DMA<sub>50</sub>MPC<sub>30</sub> – FA / DMA binary polymer system improve transfection efficiency compare to the non-folate conjugated DMA<sub>60</sub>-MPC<sub>30</sub> copolymer on MCF-7 and KB cells, the folate receptor expressing cells. The transfection efficiency on A549 cells remained at low level, suggesting that these systems show minimal non-specific cellular interaction. However, none of the folate conjugated system had transfection efficiency that was comparable to DMA homopolymer on both MCF-7 and KB cells. The design of this MPC based folate conjugated system is still at its infancy stage. The structure and the composition of this system must be further investigated and optimized in order to maximize gene transfection efficiency in targeting cells.

First of all, it is highly desirable for the targeting ligand to be exposed on the surface of the complexes (figure 7.14a). Proper ligand positioning is important for accessibility of the ligand to the receptor since polymers carrying bulky moieties may reduce interaction of the complexes with cell receptors. MPC is a very flexible hydrophilic molecule (Murphy and Lu, 2000), and the ligand that is attached at the end of this molecule may be trapped or hidden within the hydrophilic chains of the complexes (figure 7.14b), reducing its chance to be brought in contact and bind to the receptor. Further investigations, such as biochemical analysis or surface analysis technique, such as surface plasmon resonance (SPR) (Pattnaik, 2005) and dual polarization interferometry (DPI) (Swann *et al.*, 2004) may be helpful in examining the surface properties of the complexes, thereby assisting the design of a system with ligands that would orient themselves outward towards the bulk solution. With other polycation – PEG – FA system developed, it was discovered that the chain length of the steric stabilizer PEG has played a crucial role in successful delivery of DNA into the target cells (Leamon *et al.*, 1999, Ward *et al.*, 2002, Zhou *et al.*, 2002). It is believed that PEG within the conjugates act not only as steric stabilizer, but also as an extended linker arm to allow the ligand to optimally bind to its cell surface receptor. The optimal length of MPC in our system should also be investigated to optimise its efficiency.

Secondly, the quantity of ligands attached to each complex must be controlled. Polyplexes are formed by spontaneous electrostatic interaction and it is uncertain how many polymer molecules interact with one plasmid. Consequently, it is difficult to monitor the number of ligands attached to each complex. Too few ligands on the complexes lead to decreasing opportunity of ligand – receptor interaction. Leamon *et al.* (1999) found that in PLL – PEG – FA system, the number of PEG-FA group per PLL chain is an important factor in determining the level of gene expression. When there were too few or too many PEG-FA groups per PLL chain, the transfection efficiency decreased significantly. For this reason, the optimum number of ligands per polymer system must be determined.

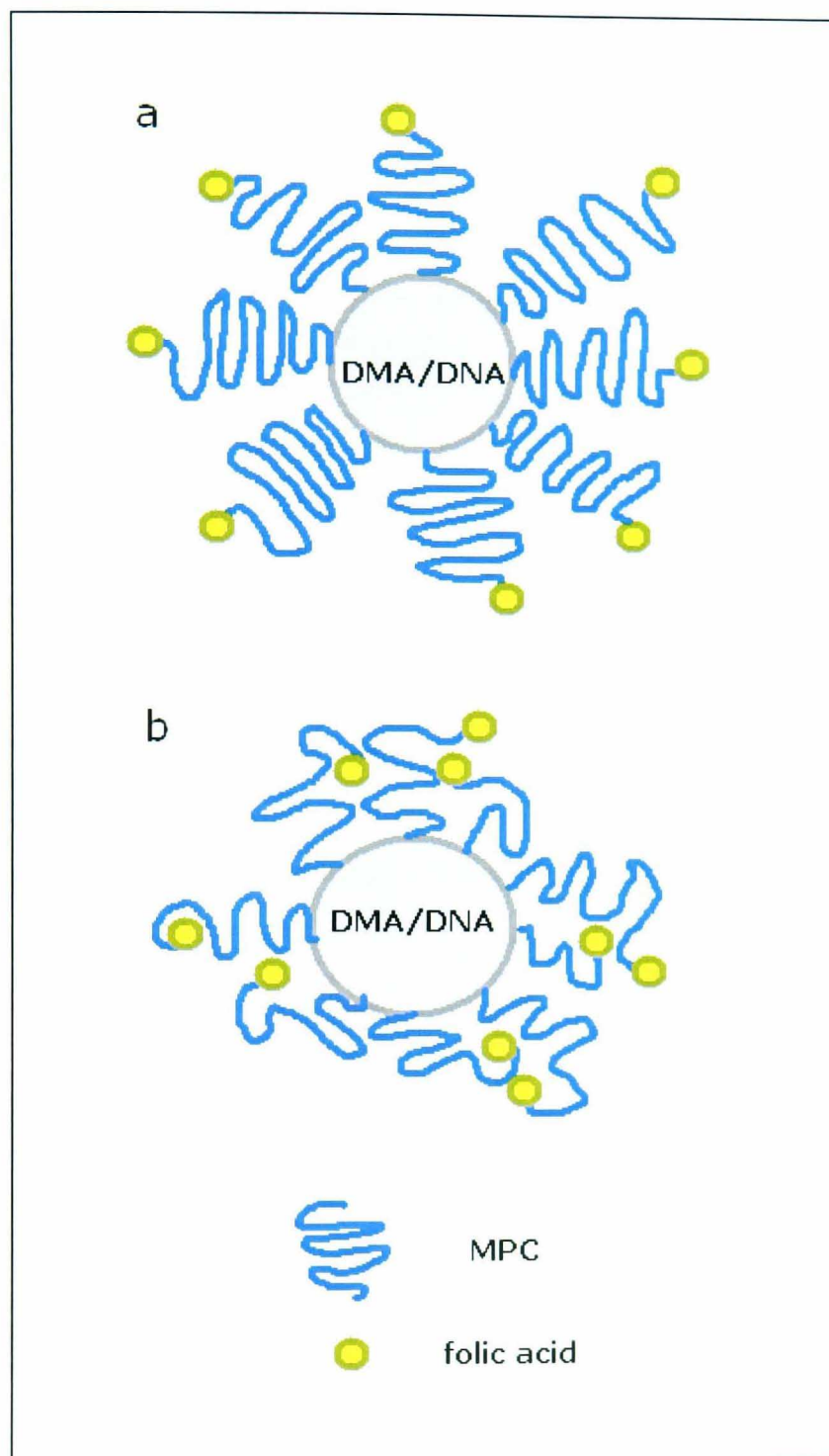


**Figure 7.14** Schematic diagram of the proposed structure of folate conjugated DNA complexes (a) with ligands exposing at the surface of the complexes (b) with ligands being trapped or hiding within the hydrophilic chains of the complexes.

Furthermore, the composition of the functionalised polymer must be carefully balanced to maximise its efficiency. The initial data shows that folate conjugated DMA-MPC diblock has demonstrated an enhancement of transfection efficiency on folate receptor expressing cells, but its capability to protect DNA from nuclease attack was less satisfactory. On the contrary, the binary polymer system was more effective in protecting DNA from enzymatic degradation, but the transfection efficiency was somewhat lower than DMA<sub>50</sub>MPC<sub>30</sub> – FA. Therefore, the composition of system must be optimised to create a well balanced effect

Although the use of folic acid as targeting ligand in the delivery of drug and imaging agents to cancer cells has been studied for a long time (Lu and Low, 2002, Leamon and Reddy, 2004, Ke *et al.*, 2004, Lu *et al.*, 2004, Gabizon *et al.*, 2004), the experience with the use of folic acid in polymer based gene delivery systems is still very limited and most of the results with these systems are restricted to *in vitro* study only. The majority of the systems are formulated with PEG in order to prolong systemic circulation. Interestingly, most of the system currently being investigated involve the surface coating of the folate-PEG component, by means of covalent or non-covalent coupling, to the pre-formed polyplexes (Ward *et al.*, 2002, van Steenis *et al.*, 2003, Cho *et al.*, 2005, Kim *et al.*, 2005). There is very little literature reporting direct incorporation of folic acid molecules to the copolymer system (Leamon *et al.*, 1999) like our DMA-MPC-FA system, which allows the targeting ligand to be firmly anchored to the backbone of the polymer. The coating of hydrophilic component to the pre-formed polyplexes (with or without ligand attachment) was claimed to produce more stable complexes that can extend circulation times *in vivo* (Ward *et al.*, 2002, Verbaan *et al.*, 2004). However, no direct comparison between the two types of preparation methods of folate conjugated system was available. In fact, our DMA-MPC-FA system requires one step less in the production of complexes compared to the coating system, thus potentially better control could be achieved during complexes formation with less batch to batch variation.



## 7.5 CONCLUSIONS

In this chapter, it has been demonstrated that conjugation of folic acid can successfully enhance level of gene expression of DMA-MPC-FA copolymer - DNA system on folate receptor expressing cancer cells. The transfection efficiency of the folate conjugated system was significantly inhibited by the presence of free folic acid, indicating that the uptake of the DNA complexes was associated with folate receptor function. The increase in transfection efficiency of the folate conjugated system was not always accompanied with the increase in cellular association, suggesting that the folate receptor mediated uptake pathway may possibly provide a more efficient intracellular trafficking route with less complexes delivered into endosomes / lysosomes for destruction. The concept of blending of two polymer systems (DMA<sub>50</sub>MPC<sub>30</sub> – FA and DMA homopolymer) to form new binary polymer system seems to be beneficial as the ability to protect DNA from enzymatic degradation was improved. However, parameters such as the optimum length of MPC component, number of ligands per DNA complex and the composition of the binary polymer system need to be further investigated in order to maximize the transfection efficiency. *In vivo* study will be the next stage to evaluate the efficacy and safety of this novel system. Nevertheless, this study presents an important step toward the design of non-viral vectors with low non-specific transfection and the ability to target therapeutic genes to various tumours.

## CHAPTER 8

### GENERAL CONCLUSIONS AND FUTURE DIRECTIONS

The development of a safe and efficient gene delivery vector is considered to be a bottle-neck and challenge to the success of gene therapy. Although viral vector is the most efficient method to deliver gene into human cells, the concerns over safety issue and immunological problems has led to the development of non-viral vectors as a potentially safer alternative. Cationic polymers have been intensively investigated in recent years for gene delivery. However the major problem associated with cationic polymers is poor efficiency compared to viral vectors. Strategy such as the design of a polycation based multifunctional gene delivery system can improve the efficiency.

The overall objective of this thesis was to evaluate the potential of the novel DMA-MPC diblock copolymer structure as non-viral gene delivery vector, with the phosphorylcholine based hydrophilic MPC polymer being proposed for the first time as a new steric stabilizer for the gene delivery system. Both physicochemical and biological properties of the system were examined. In order to achieve specific targeting, folic acid was covalently attached to MPC component of the copolymer and the properties of this folate conjugated system were evaluated. Furthermore, the route of cellular uptake and intracellular trafficking of the DMA homopolymer – DNA complexes were also investigated.

DMA-MPC diblock copolymers with different chain length of DMA and MPC were synthesized by the group of Professor S. Armes (Department of Chemistry, The University of Sheffield, UK). First, the effect of different compositions of these diblock copolymers on the interaction with DNA.

and the physicochemical properties of the resulting complexes were investigated. It is known that DMA homopolymer is able to condense and form complexes with DNA but the highly aggregating complexes are considered to be obstacles to the system for *in vivo* use. In our study, it was demonstrated that the hydrophilic MPC block, with a minimum length of 30 monomeric units, could effectively prevent self – aggregation of DNA complexes by providing a steric barrier to the system. However, the presence of this hydrophilic moiety was shown to hinder the electrostatic interaction between the cationic DMA and the negatively charged DNA, as the copolymer with high proportion of MPC was found to have a lower affinity to DNA. Therefore the composition of the diblock copolymer must be carefully adjusted so that DNA condensing and steric stabilizing effects could be achieved simultaneously.

For the purpose of improving long term stability of polymer – DNA complexes, the complexes were subjected to freeze-drying. However, the aggregation of the freeze-dried DNA complexes following rehydration was reported to be the major problem associated with freeze-dried formulations. Therefore lyoprotectants were frequently employed in order to tackle this problem. In our study, DMA<sub>60</sub>MPC<sub>30</sub> – DNA complexes were freeze-dried using sucrose or glucose as lyoprotectant. The results showed that both sucrose and glucose were effective in maintaining the size of polymer – DNA complexes during freeze drying. In addition, the sequence of the addition of sugar (sucrose or glucose) was found to be the key factor in maintaining the particle size during freeze-drying. The size of the DNA complexes were better preserved when sugar was added after the formation of complexes, and the size of complexes that were comparable to the unfrozen control could be achieved at 1000:1 sugar: DNA (w/w) ratio.

To enhance our understanding of DNA condensation, the morphology of DNA complexes formed with DMA-MPC was investigated using TEM and AFM. Surprisingly, the TEM and AFM images of the DNA complexes

were drastically different. The structures observed under the TEM appeared to be better condensed compared to AFM. One of the reasons is that dehydrated samples were studied under TEM whereas hydrated samples were studied under AFM. Since MPC is a very hydrophilic polymer, dehydration of the DNA complexes during drying would have a dramatic impact on the morphology of the MPC chain and consequently the complex morphology. Moreover, the different sample preparation and environment may also affect the resulting morphology observed in TEM and AFM. Nevertheless, both imaging techniques have provided useful insights into the process of DNA condensation. In general, both imaging techniques show that as the length of DMA in the copolymer increased, better condensation of DNA was achieved as more condensed structures of DNA condensates were observed. In contrast, a copolymer with a high proportion of MPC appeared to hinder interaction between the DNA and the copolymer, resulting in the formation of loosely condensed structures. Furthermore, the TEM images also demonstrated that MPC can effectively prevent aggregation of DNA complexes, leading to the formation of discrete complexes.

One of the important features of a non-viral system is the ability to protect DNA from nuclease activity. The enzymatic degradation study has revealed that the ability of the copolymer to protect DNA from nuclease attack was highly dependent on its composition. Only DNA complexes formed with DMA homopolymer or copolymer with a high proportion of DMA block (DMA<sub>40</sub>MPC<sub>10</sub> and DMA<sub>100</sub>MPC<sub>30</sub>) were able to preserve the structure of DNA following incubation with DNase I. Other copolymers with a high proportion of MPC failed to protect DNA from enzymatic degradation, probably due to the formation of loosely condensed complexes (as shown in the AFM images), and the exposure of uncondensed DNA within these complexes may become the site of enzymatic attack.

The biological study revealed that the presence of MPC has significantly reduced cellular association and transfection efficiency of the copolymer – DNA complexes. It is believed that the steric barrier formed by the hydrophilic MPC prevents the interaction between the complexes and the phospholipid membranes, as suggested by the model membranes study. In fact, the reduction of cellular interaction and consequently the low transfection efficiency of DMA-MPC copolymer system are desirable properties for a gene delivery systems, as an ideal gene delivery vector should display minimum non-specific cellular interaction. On the other hand, specific targeting and uptake could possibly be achieved *via* the conjugation of appropriate ligands.

While DMA homopolymer – DNA complexes showed considerable cellular association and transfection efficiency, the route of uptake and intracellular trafficking of this system were studied. The effects of different endocytotic inhibitors on the uptake of the DNA complexes were examined. Both actin and microtubulin filaments were indicated to be involved in the uptake of DMA homopolymer – DNA complexes, suggesting that the complexes were internalised by means of endocytosis. Two major endocytosis pathways, the clathrin – mediated endocytosis and the caveolae – mediated endocytosis, are generally believed to be responsible for the uptake of polymer – DNA complexes. It is important to determine the mechanism of entry as the eventual fate of substance internalised by these two routes are very different. The clathrin – mediated endocytosis often leads to degradation of substances in the endosomes / lysosomes unless the substance possess endosomolytic activity. On the other hand, substances that enter the cell through caveolae – mediated endocytosis are delivered into non-destructive caveosomes and subsequently released into the cytosol. Our results from transfection study in the presence of appropriate inhibitors and relevant confocal study indicated that both pathways are involved in the uptake of DMA

homopolymer – DNA complexes, whereby the former appears to be the major route of uptake.

Finally, in order to improve the cell specific uptake of the DMA-MPC copolymer system, a targeting ligand was covalently attached to the MPC polymer. Folic acid is an attractive ligand for this role due to the significant overexpression of folate receptors in a wide variety of cancer cells. Moreover, folic acid is inexpensive and non-immunogenic. DMA-MPC-FA and a binary polymer which consists of DMA-MPC-FA and DMA homopolymer were investigated. Physicochemical study showed that the attachment of folic acid to the terminal of MPC did not appear to affect the DNA binding ability of the folate conjugated systems, and colloiddally stable DNA complexes were formed at monomeric unit: nucleotide ratio 2:1 and 5:1 for DMA-MPC-FA and binary polymer system respectively. Moreover, the binary polymer system also demonstrated ability to protect DNA from enzymatic degradation.

*In vitro* transfection study has shown that conjugation of folic acid could successfully enhance the transfection efficiency of the copolymer system in folate receptors expressing cells. Folate receptors were responsible for the uptake of the folate conjugated system as the presence of free folic acid was found to inhibit transfection in these cell lines. Interestingly, the increase in transfection efficiency of the folate conjugated system was not accompanied with the increase in cellular association, suggesting that the folate receptor mediated uptake pathway may possibly provide a more efficient intracellular trafficking route with less complexes delivered into endosomes / lysosomes for degradation. However, the optimum composition of folate conjugated DMA-MPC system remains to be determined.

In summary, the novel DMA-MPC copolymer has demonstrated desirable properties to remain a potential candidate for gene delivery. With

appropriate composition, the copolymer is able to condense DNA to form colloiddally stable DNA complexes with minimal non-specific cellular interaction. Moreover, the initial results from folate conjugated system have shown that selective uptake to folate receptors expressing cells could be achieved.

The future work should focus on the optimization of the DMA-MPC system by varying the composition of the diblock copolymer. For example, by increasing the length of DMA block of the copolymer so that better DNA condensation could be achieved, resulting in the formation of more compact DNA complexes that are more resistant to enzymatic degradation. Other components such as endosomolytic agent and nuclear localizing signal could be considered and included in the system so that efficiency could be further enhanced.

*In vivo* study will be the next step to evaluate the efficacy and safety of the system. Work presented in this thesis has proven that MPC is able to provide steric stabilization and reduce cellular association *in vitro*. It would be of great interest to conduct *in vivo* studies in attempt to correlate these with *in vitro* prediction. For example, an *in vivo* biodistribution study would be necessary to confirm whether the presence of MPC could in fact prolong systemic circulation of the gene delivery system. In the case of folate conjugated system, parameters such as the number of ligand per complex and the length of the MPC spacer should be optimized. The particle surface of the system can be characterized to ensure that the ligands are properly positioned for easy access to the receptors. Again, it would be of particular interest to investigate whether cell specific uptake of the folate conjugated system could be achieved *in vivo*. Furthermore, specificity could be further enhanced by designing the therapeutic gene consisting of cell type specific promoters so that the gene is only expressed through activation by responsive elements.

## REFERENCE

- Abdelhady, H.G., Allen, S., Davies, M.C., Roberts, C.J., Tendler, S.J.B. and Williams, P.M. (2003) Direct real-time molecular scale visualisation of the degradation of condensed DNA complexes exposed to DNase I. *Nucleic Acid Research* **31**, 4001-4005
- Adami, R., Collard, W.T., Gupta, S.A., Kwok, K.Y., Bonadio, J., and Rice, K.G. (1998) Stability of peptide-condensed plasmid DNA formulations. *Journal of Pharmaceutical Sciences* **87**, 678-683
- Adams, M.L., Lavasanifar, A. and Kwon, G.S. (2003). Amphiphilic Block Copolymers for Drug Delivery. *Journal of Pharmaceutical Sciences* **92**, 1343-1355
- Ahn, C-H., Chae, S.Y., Bae, Y.H. and Kim, S.W. (2002). Biodegradable poly(ethylenimine) for plasmid DNA delivery. *Journal of Controlled Release* **80**, 273-282
- Albert, B., Bray, D., Lewis, J., Raff, M., Roberts, K. and Watson, D.J. (2002) *Molecular Biology of Cell (4<sup>th</sup> ed.)* Garland Science, New York.
- Allison, S.D., Molina, M.D.C. and Anchordoquy, T.J. (2000) Stabilization of lipid/DNA complexes during the freezing step of the lyophilization process: the particle isolation hypothesis. *Biochimica et Biophysica Acta* **1468**, 127-138
- Amiji, M.M. (1996) Surface modification of chitosan membranes by complexation – interpenetration of anionic polysaccharides for improved blood compatibility in hemodialysis. *Journal of Biomaterials Science - Polymer Edition* **8**, 281-298
- Amos, W.B. and White, J.G. (2003) How the confocal laser scanning microscope entered biological research. *Biology of the cell* **95**, 335-342
- Anchordoquy, T.J., Carpenter, J.F. and Kroll, D.J. (1997) Maintenance of transfection rates physical characterization of lipid/DNA complexes after freeze-drying and rehydration. *Archives of Biochemistry and Biophysics* **348**, 199-206
- Anchordoquy, T.J., Girouard, L.G., Carpenter, J.F. and Kroll, D.J. (1998) Stability of lipid/ DNA complexes during agitation and freeze-thawing. *Journal of Pharmaceutical Sciences* **87**, 1046-1051
- Anchordoquy, T.J. and Koe, G.S. (1999) Physical stability of nonviral plasmid – based therapeutics. *Journal of Pharmaceutical Sciences* **89**, 289-296
- Anchordoquy, T.J., Allison, A.D., Molina, M.D.C., Girouard, L.G. and Carson, T.K. (2001) Physical stabilization of DNA-based therapeutics. *Drug Discovery Today* **6**, 463-470
- Anderson, H.A, Chen, Y. and Norkin, L.C. (1996) Bound simian virus 40 translocates to caveolin-enriched membrane domains, and its entry is inhibited by drugs that selectively disrupt caveolae. *Molecular Biology of the Cell* **7**, 1825-1834
- Anderson, R.G. (1998) The caveolae membrane system. *Annual Review of Biochemistry* **67**, 188-225



- Aniento, F., Emans, N., Griffiths, G. and Gruenberg, J. (1993) Cytoplasmic dynein-dependent vesicular transport from early to late endosomes. *Journal of Cell Biology* **123**, 1373-1387
- Antony, A.C. (1992) The biological chemistry of folate receptors. *Blood* **79**, 2807-2820
- Anwer, K., Rhee, B.G. and Mendiratta, K. (2003) Recent progress in polymeric gene delivery systems. *Critical Reviews in Therapeutic Drug Carrier Systems* **20**, 249-293
- Arigita, C., Zuidam, N.J., Crommelin, D.J.A. and Hennink, W.E. (1999) Association and dissociation characteristics of polymer/DNA complexes used for gene delivery. *Pharmaceutical Research* **16**, 1534-1541
- Armstrong, T.K.C., Girouard, L.G. and Anchordoquy T.J. (2002) Effects of PEGylation on the preservation of cationic lipid/DNA complexes during freeze-thawing and lyophilization. *Journal of Pharmaceutical Sciences* **91**, 2549-2558
- Arnold, L.J. (1985) Polylysine-drug conjugates. *Methods in Enzymology* **112**, 270-285
- Aronov, O., Horowitz, A.T., Gabizon, A., and Gibson, D. (2003) Folate-targeted PEG as a potential carrier for Carboplatin analogs. Synthesis and in vitro studies. *Bioconjugate Chemistry* **14**, 563-574
- Baque, P., Pierrefite-Carle, V., Gavelli, A., Brossette, N., Benchimol, D., Bourgeon, A., Staccini, P., Saint-Paul, M.C. and Rossi, B. (2002) Naked DNA injection for liver metastases treatment in rats. *Hepatology* **35**, 1144-1152
- Baru, M., Axelrod J., and Nur, I. (1995) Liposome-encapsulated DNA-mediated gene transfer and synthesis of human factor IX in mice. *Gene* **161**, 143-150
- Bathori, G., Cervenak, L., and Karadi, I. (2004) Caveolae – an alternative endocytotic pathway for targeted drug delivery. *Critical Reviews in Therapeutic Drug Carrier Systems* **21**, 67-95
- Becheran-Maron, L., Peniche, C. and Argüelles-Monal, W. (2004) Study of the interpolyelectrolyte reaction between chitosan and alginate: influence of alginate composition and chitosan molecular weight. *International Journal of Biological Macromolecules* **34**, 127-133
- Behr, J.P. (1994) Gene transfer with synthetic cationic amphiphiles: prospects for gene therapy. *Bioconjugate Chemistry* **5**, 382-389
- Benns, J.M., Mahato, R.I. and Kim, S.W. (2002) Optimization of factors influencing the transfection efficiency of folate-PEG-graft-polyethylenimine. *Journal of Controlled Release* **79**, 255-269
- Bielinska, A.U., Kukowska-Latallo, J.F. and Baker, J. (1997) The interaction of plasmid DNA with polyamidoamine dendrimers: Mechanism of complex formation and analysis of alterations induced in nuclease sensitivity and transcriptional activity of the complexed DNA. *Biochimica et Biophysica Acta* **1353**, 180-190
- Bielinska, A.U., Yen, A., Wu, H.L., Zahos, K.M., Sun, R., Weiner, N.D., Baker, J.R. and Roessler, B.J. (2000) Application of membrane-based dendrimer / DNA complexes for solid phase transfection *in vitro* and *in vivo*. *Biomaterials* **21**, 877-887

- 
- Binnig, G. and Quate, C.T. (1986) Atomic force microscope. *Physical Review Letters* **56**, 930-933
- Biswas, D., Itoh, K. and Sasakawa, C. (2003) Role of microfilaments and microtubules in the invasion of INT-407 cells by *Campylobacter jejuni*. *Microbiology and Immunology* **47**, 469-473
- Blakley, R.L. and Whitehead, V.A. (1986) *Folate and Pterins: nutritional pharmacological and physiological aspects*. John Wiley and Sons, New York.
- Blessing, T., Kursa, M., Holzhauser, R., Kircheis, R. and Wagner, E. (2001) Different strategies for formation of pegylated-EGF-conjugated PEI/DNA complexes for targeted gene delivery. *Bioconjugate Chemistry* **12**, 529-537
- Bloomfield, V.A. (1991) Condensation of DNA by multivalent cations – considerations on mechanism. *Biopolymers* **31**, 1471-1481
- Bloomfield, V.A. (1996) DNA condensation. *Current Opinion in Structural Biology* **6**, 334-341.
- Bloomfield, V.A. (1997) DNA condensation by multivalent cations. *Biopolymers* **44**, 269-282
- Boletta, A., Benigni, A., Lutz, J., Remuzzi, G., Soria, M.R. and Monaco, L. (1997) Nonviral gene delivery to the rat kidney with polyethylenimine. *Human Gene Therapy* **8**, 1243-1251
- Boulikas, T. (1993). Nuclear localization signals (NLS). *Critical Reviews in Eukaryotic Gene Expression* **3**, 193-227
- Boussif, O., Lezoualch, F., Zanta, M.A., Mergny, M.D., Scherman, D., Demeneix, B. and Behr, J.P. (1995) A versatile vector for gene and oligonucleotides transfer into cells in culture and in vivo: polyethylenimine. *Proceedings of the National Academy of Sciences of USA* **92**, 7297-7301
- Boussif, O., Zanta, M.A. and Behr, J.P. (1996) Optimized galenics improve *in vitro* gene transfer with cationic molecules up to 1000-fold. *Gene Therapy* **3**, 1074-1080
- Bradford, M.M. (1976) A rapid and sensitive method for the quantitation of microgram quantities of microgram quantities of protein utilising the principle of protein dye binding. *Analytical Biochemistry* **72**, 248-254
- Branden, L.J., Mohamed, A.J. and Smith, C.I. (1999) A peptide nucleic-acid-nuclear localization signal fusion that mediates nuclear transport of DNA. *Nature Biotechnology* **17**, 784-787
- Braun, C.S., Vetro, J.A., Tomalia, D.A., Koe, G.S., Koe, J.G. and Middaugh, C.R. (2005) Structure/function relationships of polyamidoamine / DNA dendrimers as gene delivery vehicles. *Journal of Pharmaceutical Sciences* **94**, 423-436
- Brine, C.J., Sandford, P.A. and Zikakis, J.P. (1992) *Advances in Chitin and Chitosan*. Elsevier Applied Science, London.
- Brisson, M., Tseng, W.C., Almonte, C., Watkins, S. and Huang, L. (1999) Subcellular trafficking of the cytoplasmic expression system *Human Gene Therapy* **10**, 2601-2613

- Brodsky, F.M., Chen, C.Y., Knuehl, C., Towler, M.C. and Wakeham, D.E. (2001) Biological basket weaving: formation and function of clathrin-coated vesicles. *Annual Review of Cell and Developmental Biology* **17**, 517-568
- Brown, C.M. and Petersen, N.O. (1999) Free clathrin triskelions are required for the stability of clathrin-associated adaptor protein (AP-2) coated pit nucleation sites. *Biochemistry and Cell Biology* **77**, 439-448
- Brunner, S., Sauer, T., Carotta, S., Cotton, M., Saltik, M. and Wagner, E. (2000) Cell cycle dependence of gene transfer by lipoplex, polyplex and recombinant adenovirus. *Gene Therapy* **7**, 401-407
- Brunner, S., Furtbauer, E., Sauer, T., Kursu, M. and Wagner, E. (2002) Overcoming the nuclear barrier: cell cycle independent non-viral gene transfer with linear polyethylenimine or electroporation. *Molecular Therapy* **5**, 80-86
- Brus, C., Kleemann, E., Aigner, A., Czubayko, F. and Kissel, T. (2004) Stabilization of oligonucleotide-polyethylenimine complexes by freeze-drying: physicochemical and biological characterization. *Journal of Controlled Release* **95**, 119-131
- Bueno, R., Appasani, K., Mercer, H., Lester, S. and Sugarbaker, D. (2001) The alpha folate receptor is highly activated in malignant pleural mesothelioma. *Journal of Thoracic and Cardiovascular Surgery* **121**, 225-233
- Bunnell, B.A. and Morgan, R.A. (1998) Gene therapy for infectious diseases. *Clinical Microbiology Reviews* **11**, 42-56
- Carlisle, R.C., Etrych, T., Briggs, S.S., Preece, J.A., Ulbrich, K. and Seymour, L.W. (2004) Polymer-coated polyethylenimine / DNA complexes designed for triggered activation by intracellular reduction. *Journal of Gene Medicine* **6**, 337-344
- Cavazzana-Calvo, M., Hacein-Bey, S., Basile, C.D., Gross, F., Yvon, E., Nusbaum, P., Selz, F., Hue, C., Certain, S., Casanova, J.L., Bousso, P., Le Deist, F., and Fisher, A. (2000) Gene therapy of human severe combined immunodeficiency (SCID)- X1 disease. *Science* **288**, 669-672
- Chen, C., Lumsden, A.B. and Ofenloch, J.C. (1997) Phosphorylcholine coating of ePTFE grafts reduced neointimal hyperplasia in canine model. *Annals of Vascular Surgery* **11**, 74-79
- Cheng, S., Merlino, G.T. and Pastan, I.H. (1983) A versatile method for the coupling of protein to DNA: synthesis of  $\alpha_2$  macroglobulin-DNA conjugates. *Nucleic Acids Research* **11**, 695-669
- Cherng, J Y, van de Wetering, P, Talsma, H, Crommelin, D J and Hennink W E (1996). Effect of size and serum proteins on transfection efficiency of poly((2-dimethylamino)ethyl methacrylate)-plasmid nanoparticles (1996). *Pharmaceutical Research* **13**, 1038-1042
- Cherng, J.Y., van de Wetering, P., Talsma, H., Crommelin, D.J.A. and Hennink, W.E. (1997) Freeze-drying of poly((2-dimethylamino)ethyl methacrylate)- based gene delivery systems. *Pharmaceutical Research* **14**, 1838-1841
- Cherng, J., Talsma, H., Crommelin, D. and Hennink, W. (1999). Long term stability of poly((2-dimethylamino)ethyl methacrylate)-based gene delivery systems. *Pharmaceutical Research* **16**, 1417-1423

- Cho, K.C., Kim, S.H., Jeong, J.H. and Park, T.G. (2005) Folate receptor-mediated gene delivery using folate-poly(ethylene glycol)-poly(l-lysine) conjugate. *Macromolecular Bioscience* **5**, 512-519
- Choi, Y.H., Liu, F., Kim, J.S., Choi, Y.K., Park, J.S. and Kim, S.W. (1998) Polyethylene glycol-grafted poly-L-lysine as polymeric gene carrier. *Journal of Controlled Release* **54**, 39-48
- Chonn, A. and Cullis, P.R. (1995) Recent advances in liposomal drug-delivery systems. *Current Opinion in Biotechnology* **6**, 698-708
- Chonn, A. and Cullis, P.R. (1998) Recent advances in liposome technologies and their applications for systemic gene delivery. *Advanced Drug Delivery Reviews* **30**, 73-83
- Choosakoonkriang, S., Lobo, B.A., Koe, G.S., Koe, J.G. and Middaugh, C.R. (2003) Biophysical characterization of PEI/DNA complexes. *Journal of Pharmaceutical Sciences* **92**, 1710-1722
- Choun, A., Cullis, P.R. and Devine, D.V. (1991) The role of surface charge in the activation of the classical and alternative pathways of complement by liposomes. *Journal of Immunology* **146**, 4234-4241
- Chowdhury, N.R., Hays, R.M., Bommineni, V.R., Franki, N., Chowdhury J. R., Wu, C.H. and Wu, G.Y. (1996) Microtubular disruption prolongs the expression of human bilirubin – uridine diphosphoglucouronate-glucuronosyltransferase-1 gene transferred into Gunn rat livers. *Journal of Biological Chemistry* **271**, 2341-2346
- Christophe, D., Christophe-Hobertus, C. and Pichon, B. (2000) Nuclear targeting of proteins: how many different signals? *Cellular Signalling* **12**, 337-341
- Ciechanover, A., Schwartz, A.L. and Lodish, H.F. (1983) Sorting and recycling of cell surface receptors and endocytosed ligands; the asialoglycoprotein and transferrin receptors. *Journal of Cellular Biochemistry* **23**, 107-130
- Ciftci, K. and Levy, R.J. (2001) Enhanced plasmid DNA transfection with lysosomotropic agents in cultured fibroblasts. *International Journal of Pharmaceutics* **218**, 81-92
- Ciolina, C., Byk, G., Blanche, F., Thuillier, V., Scherman, D. and Wils, P. (1999) Coupling of nuclear localization signals to plasmid DNA and specific interaction of the conjugates with importin alpha. *Bioconjugate Chemistry* **10**, 49-55
- Citro, G., Szczylik, C., Ginobbi, P., Zupi, G. and Calabretta, B. (1994) Inhibition of leukaemia cell proliferation by folic acid-polylysine-mediated introduction of c-myc antisense oligodeoxynucleotides into HL-60 cells. *British Journal of Cancer* **69**, 463-467
- Cole, N.B. and Lippincott-Schwartz, J. (1995) Organization of organelles and membrane traffic by microtubules. *Current Opinion in Cell Biology* **7**, 55-64
- Collins, F.S., Morgan, M. and Patrinos, A. (2003) The human genome project: lessons from large-scale biology. *Science* **11**, 286-290
- Console, S., Marty, C., Garcia-Echeverria, C., Schwendener, R. and Ballmer-Hofer, K. (2003) Antennapedia and HIV transactivator of transcription (TAT) protein

- transduction domains' promote endocytosis of high molecular weight cargo upon binding cell surface glycosaminoglycans. *Journal of Biological Chemistry* **278**, 35109-35114
- Cooper, J.A. (1987) Effects of cytochalasin and phalloidin on actin. *Journal of Cell Biology* **105**, 1473-1478
- Cotton, M., Langle-Rouault, F., Kirlappos, H., Wagner, E., Mechtler, K., Zenke, M., Beug, H. and Birnsteil, M.L. (1990) Transferrin-polycation-mediated introduction of DNA into human leukemic cells: Stimulation by agents that affect the survival of transfected DNA or modulate transferrin receptor levels. *Proceedings of the National Academy of Sciences of USA* **87**, 4033-4037
- Coue, M., Brenner, S.L., Spector, I. and Korn, E.D. (1987) Inhibition of actin polymerization by latrunculin-A. *FEBS letters* **213**, 316-318
- Cox, R.A. and Gokcen, M. (1976) Comparison of serum DNA, native DNA binding and deoxyribonuclease levels in ten animal species and man. *Life Science* **19**, 1609-1614
- Cristiano, R.J. and Roth, J.A. (1996) Epidermal growth factor mediated DNA delivery into lung cancer cells via the epidermal growth factor receptor. *Cancer Gene Therapy* **3**, 4-10
- Crothers, D.M., Haran T.E. and Nadeau, M.J.G. (1990) *Journal of Biological Chemistry* **265**, 7093-7096
- Danielsen, S., Vårum, K.M., Stokke, B.T. (2004) Structural analysis of chitosan mediated DNA condensation by AFM: Influence of chitosan molecular parameters. *Biomacromolecules* **5**, 928-936
- Dash, P.R., Toncheva, V., Schacht, E. and Seymour, L.W. (1997) Synthetic polymers for vectorial delivery of DNA: characterisation of polymer – DNA complexes by photon correlation spectroscopy and stability to nuclease degradation and disruption by polyanions in vitro. *Journal of Controlled Release* **48**, 269-276
- Dash, P.R., Read, M.L., Barrett, L.B., Wolfert, M. and Seymour, L.W. (1999) Factors affecting blood clearance and in vivo distribution of polyelectrolyte complexes for gene delivery. *Gene Therapy* **6**, 643–650
- Dash, P.R., Read, M.L., Fisher, K., Howard, K., Wolfert, M., Oupický, D., Subr, V., Strohal, J., Ulbrich, K. and Seymour, L.W. (2000) Decreased binding to proteins and cells of polymeric gene delivery vectors surface modified with a multivalent hydrophilic polymer and retargeting through attachment of transferrin. *Journal of Biological Chemistry* **275**, 3793–3802
- Dautryvarsat, A., Ciechanover, A. and Lodish, H.F. (1983) pH and the recycling of transferrin during receptor-mediated endocytosis. *Proceedings of the National Academy of Sciences of USA* **80**, 2258-2262
- Dautzenberg, H. and Karibyants, N. (1999). Polyelectrolyte complex formation in highly aggregating systems. Effect of salt: response to subsequent addition of NaCl. *Macromolecular Chemistry and Physics* **200**, 118–125
- Davis, S.S., Illum, L., McVie, J.G. and Tomlinson, E. (1984) *Microspheres and Drug Therapy, Pharmaceutical, Immunological and Medical Aspects*. Elsevier, Oxford

- Dean, D.A. (1997). Import of plasmid DNA into the nucleus is sequence specific. *Experimental Cell Research* **230**, 293-302
- Deible, C.R., Beckman, E.J., Russell, A.J. and Wagner, W.R. (1998) Creating molecular barriers to acute platelet deposition on damaged arteries with reactive polyethylene glycol. *Journal of Biomedical Materials Research* **41**, 251-256
- Derossi, D., Chassaing, G. and Prochiantz, A. (1998) Trojan peptides: The penetratin system for intracellular delivery. *Trends in Cell Biology* **8**, 84-87
- Derossi, D., Joliot, A.H., Chassaing, G. and Prochiantz, A. (1994) The third helix of the Antennapedia homeodomain translocates through biological membranes. *Journal of Biological Chemistry* **269**, 10444-10450
- Deshayes, S., Morris, M.C. and Heitz, F. (2005) Cell-penetrating peptides: tools for intracellular delivery of therapeutics. *Cellular and Molecular Life Sciences* **62**, 1839-1849
- Deshpande, M.C. (2002). *Biological and physicochemical studies on polymer-DNA delivery system*. PhD Thesis. The University of Nottingham
- Deshpande, M.C., Davies, M.C., Garnett, M.C., Williams, P.M., Armitage, D., Bailey, L., Vamvakaki, M., Armes, S.P. and Stolnik, S. (2004) The effect of poly(ethylene glycol) molecular architecture on cellular interaction and uptake of DNA complexes. *Journal of Controlled Release* **97**, 143-156
- Dragan, S. and Cristea, M. (2002) Polyelectrolyte complexes. IV. Interpolyelectrolyte complexes between some polycations with *N,N*-dimethyl-2-hydroxypropylammonium chloride units and poly(sodium styrenesulfonate) in dilute aqueous solution. *Polymer* **43**, 55-62.
- Duncan, R. (1992). Polymer-drug conjugates: potential for improved chemotherapy. *Anti-Cancer Drugs* **3**, 175-210
- Duncan, M.J., Shin, J.S. and Abraham, S.N. (2002) Microbial entry through caveolae: variations on a theme. *Cellular Microbiology* **4**, 783-791
- Dunlap, D.D., Maggi, A., Soria, M.R. and Monaco, L. (1997) Nanoscopic structure of DNA condensed for gene delivery. *Nucleic Acid Research* **25**, 3095-3101
- Durrbach, A., Louvard, D. and Courdrier, E. (1996). Actin filaments facilitate two steps of endocytosis. *Journal of Cell Science* **109**, 457-465
- Edelstein, M.L., Abedi, M.R., Wixon, J. and Edelstein, R.M. (2004) Gene therapy clinical trials worldwide 1989-2004 – an overview. *The Journal of Gene Medicine* **6**, 597-602
- Eder, P.S., DeVine, R.J., Dagle, J.M. and Walder, J.A. (1991) Substrate specificity and kinetics of degradation of antisense oligonucleotides by a 3' exonuclease in plasma. *Antisense Research and Development* **1**, 141-151
- Ekrami, H.M. and Shen, W.C. (1995) Carbamylation decreases the cytotoxicity but not the drug-carrier properties of polylysine. *Journal of Drug Targeting* **2**, 469-475
- El-Aneed, A. (2004) Current strategies in cancer gene therapy. *European Journal of Pharmacology* **498**, 1-8

- Elkjaer, M.L., Birn, H., Agre, P., Christensen, E.I. and Nielsen, S. (1995) Effects of microtubule disruption on endocytosis, membrane recycling and polarized distribution of Aquaporin-1 and gp330 in proximal tubule cells. *European Journal of Cell Biology* **67**, 57-72
- Erbacher, P., Roche, A.C., Monsigny, M. and Midoux, P. (1996) Putative role of chloroquine in gene transfer into a human hepatoma cell line by DNA / lactosylated polylysine complexes. *Experimental Cell Research* **225**, 186-194
- Erbacher, P., Bettinger, T., Belguise-Valladier, P., Zou, S., Coll, J.L., Behr, J.P. and Remy, J.S. (1999) Transfection and physical properties of various saccharide, poly(ethylene glycol), and antibody-derivatized polyethylenimines (PEI). *Journal of Gene Medicine* **1**, 210-222
- Erbacher, P., Zou, S., Bettinger, T., Steffan, A.M. and Remy J.S. (1998) Chitosan-based vector / DNA complexes for gene delivery: biophysical characteristics and transfection ability. *Pharmaceutical Research* **15**, 1332-1339
- Fang, Y. and Hoh, J.H. (1999) Cationic silanes stabilize intermediates in DNA condensation. *FEBS Letters* **459**, 173-176
- Farhood, H., Serbina, N. and Huang, L. (1995) The role of dioleoyl phosphatidylethanolamine in cationic liposome mediated gene transfer. *Biochimica et Biophysica Acta* **1235**, 289-295
- Fasbender, A., Zabner, J., Zeiher, B.G. and Welsh, M.J. (1997) A low rate of cell proliferation and reduced DNA uptake limit cationic lipid-mediated gene transfer to primary cultures of ciliated human airway epithelia. *Gene Therapy* **4**, 1173-1180
- Felgner, P.L., Gadek, T.R., Holm, M., Roman, R., Chan, H.W., Wenz, M., Northrop, J.P., Ringold, G.M. and Danielsen, M. (1987) Lipofection: a highly efficient, lipid-mediated DNA transfection procedure. *Proceedings of the National Academy of Sciences of USA* **84**, 7413-7417
- Felgner, P.L. and Ringold, G.M. (1989) Cationic liposomes-mediated transfection. *Nature* **337**, 387-388
- Filion, C. and Phillips, N. (1998) Major limitations in the use of cationic liposomes for DNA delivery. *International Journal of Pharmaceutics* **162**, 159-170
- Fischer, D., Bieber, T., Li, Y., Elsasser, H.P. and Kissel, T. (1999) A novel non-viral vector for DNA delivery based on low molecular weight, branched polyethylenimine: effect of molecular weight on transfection efficiency and cytotoxicity. *Pharmaceutical Research* **16**, 1273-1279
- Fojta, M., Kubišáková, T. and Paleček, E. (1999) Cleavage of supercoiled DNA by deoxyribonuclease I in solution and at the electrode surface. *Electroanalysis* **11**, 10005-1012
- Ford, J.M. and Hait, W.N. (1990). Pharmacology of drugs that alter multidrug resistance in cancer. *Pharmacological Reviews* **42**, 155-199
- Fra, A.M., Willaimson, E., Simons, K. and Parton, R.G. (1995) De novo formation of caveolae in lymphocytes by expression of VIP21-caveolin. *Proceedings of the National Academy of Sciences of USA* **92**, 8655-8659

- Freitas Jr., R. A. (2003) *Nanomedicine, Volume IIA: Biocompatibility*. Landes Bioscience, Georgetown, TX.
- French, A.R., Sudlow, G.P., Wiley, H.S. and Lauffenburger, D.A. (1994) Postendocytic trafficking of epidermal growth factor-receptor complexes is mediated through saturable and specific endosomal interactions. *Journal of Biological Chemistry* **269**, 15749-15755
- French-Anderson, W. (1998) Human gene therapy. *Nature* **392** (Suppl.) 25-30
- Friede, M., Vanregemortel, M.H.V. and Schuber, F. (1993) Lyophilized liposomes as shelf items for the preparation of immunogenic liposome peptide conjugates. *Analytical Biochemistry* **211**, 117-122
- Funhoff, A.M., van Nostrum, C.F., Janssen, A.P.C., Fens, M.H.A.M., Crommelin, D.J.A. and Hennink, W.E. (2004a) Polymer side-chain degradation as a tool to control the destabilization of polyplexes. *Pharmaceutical Research* **21**, 170-176
- Funhoff, A.M., van Nostrum, C.F., Koning, Schuurmans-Nieuwenbroek, N.M.E., Crommelin, D.J.A. and Hennink, W.E. (2004b) Endosomal escape of polymeric gene delivery complexes is not always enhanced by polymers buffering at low pH. *Biomacromolecules* **5**, 32-39
- Funhoff, A.M., Monge, S., Teeuwen, R., Koning, G.A., Schuurmans-Nieuwenbroek, N.M.E., Crommelin, D.J.A., Haddleton, D.M., Hennink, W.E. and van Nostrum, C.F. (2005) PEG shielded polymeric double-layered micelles for gene delivery. *Journal of Controlled Release* **102**, 711-724
- Fynan, E.F., Webster, R.G., Fuller, D.H., Haynes, J.R., Santoro, J.C. and Robinson, H.L. (1993) DNA vaccines – protective immunizations by parenteral, mucosal and gene-gun inoculations. *Proceedings of the National Academy of Sciences of USA* **90**, 11478-11482
- Gabizon, A, Horowitz, A.T., Goren, D., Tzemach, D., Mandelbaum-Shavit, F., Qazen, M.M. and Zalipsky, S. (1999) Targeting folate receptor with folate linked to extremities of poly(ethylene glycol)-grafted liposomes: *in vitro* studies. *Bioconjugate Chemistry* **10**, 289-298
- Gabizon, A., Shmeeda, H., Horowitz, A.T. and Zalipsky, S. (2004) Tumour cell targeting of liposome-entrapped drugs with phospholipid-anchored folic acid – PEG conjugates. *Advanced Drug Delivery Reviews* **56**, 1177-1192
- Gao, X. and Huang, L. (1991). A novel cationic liposome reagent for efficient transfection of mammalian cells. *Biochemical and Biophysical Research Communications* **179**, 280-285
- Gao, X. and Huang, L. (1996) Potentiation of cationic liposome-mediated gene delivery by polycations. *Biochemistry* **35**, 1027-1036
- Gardlík, R., Pálffy, R., Hodosy, J., Lukács, J., Turňa, J. and Celec, P. (2005) Vectors and delivery systems in gene therapy. *Medical Science Monitor* **11**, 110-121
- Gebhart, C.L. and Kabanov, A.V. (2001) Evaluation of polyplexes as gene transfer agents. *Journal of Controlled Release*. **73**, 401-416



- Gessner, A., Waicz, R., Lieske, A., Paulke, B.R., Mäder, K. and Müller, R.H. (2000). Nanoparticles with decreasing surface hydrophobicities: influence on plasma protein adsorption. *International Journal of Pharmaceutics* **196**, 245-249
- Gill, G.N. (1990) Regulation of EGF receptor expression and function. *Molecular Reproduction and Development* **27**, 46-53
- Givan, A.L. (1992) *Flow cytometry: first principles*. Wiley-Liss Press, New York
- Godbey, W.T., Wu, K.K. and Mikos, A.G. (1999) Tracking the intracellular path of poly(ethylenimine)/DNA complexes for gene delivery. *Proceedings of the National Academy of Sciences of USA* **96**, 5177-5181
- Godbey, W.T., Wu, K.K. and Mikos, A.G. (1999a) Poly(ethylenimine) and its role in gene delivery. *Journal of Controlled Release* **60**, 149-160
- Godbey, W.T., Wu, K.K. and Mikos, A.G. (1999b) Size matters: molecular weight affects the efficiency of poly(ethylenimine) as a gene delivery vehicle. *Journal of Biomedical Materials Research* **45**, 268-275
- Godbey, W., Wu, K.K. and Mikos, A.G. (2001) Poly(ethylenimine)-mediated gene delivery affects endothelial cell function and viability. *Biomaterials* **22**, 471-480
- Golan, R., Pietrasanta, L.I., Hsieh, W. and Hansma, H.G. (1999) DNA Toroids: Stages in condensation. *Biochemistry* **38**, 14069-14076
- Golander, C.G. and Pitt, W.G. (1990) Characterization of hydrophobicity gradients prepared by means of radio frequency plasma discharge. *Biomaterials* **11**, 32-35
- Görlich, D. and Mattaj, I. (1996) Nucleocytoplasmic transport. *Science* **271**, 1513-1518
- Gosule, L.C. and Schellman, J.A. (1976) Compact form of DNA induced by spermidine. *Nature* **259**, 333-335
- Gottlieb, T.A., Ivanov, I.E., Adesnik, M. and Sabatini, D.D. (1993) Actin microfilaments play a critical role in endocytosis at the apical but not the basolateral surface of polarized epithelial cells. *Journal of Cell Biology* **120**, 695-710
- Gottschalk, S., Sparrow, J.T., Hauer, J., Mims, M.P., Leland, F.E., Woo, S.L. C. and Smith, L.C. (1996) A novel DNA-peptide complex for efficient gene transfer and expression in mammalian cells. *Gene Therapy* **3**, 448-457
- Gref, R., Minamitake, Y., Peracchia, M.T., Torchilin, V., Trubetskoy, V. and Langer, R. (1994) Biodegradable long-circulating polymeric nanosphere. *Science* **28**, 1600-1603
- Gref, R., Lück, M., Quellec, P., Marchand, M., Dellacherie, E., Harnisch, S., Blunk, T. and Müller, R.H. (2000) 'Stealth' corona-core nanoparticles surface modified by polyethylene glycol (PEG): influence of the corona (PEG chain length and surface density) and of the core composition on phagocytic uptake and plasma protein adsorption. *Colloids and Surfaces B: Biointerfaces* **18**, 301-313
- Groose, S., Aron, Y., Thevenot, G., Trancois, D., Monsigny, M. and Fajac, I. (2005). Potocytosis and cellular exit of complexes as cellular pathways for gene delivery by polycations. *Journal of Gene Medicine* **7**, 1275-1286

- Gruenberg, J. (2001) The endocytic pathway: a mosaic of domains. *Nature Reviews Molecular Cell Biology* **2**, 721-730
- Guo, W, Lee, R.L. (1999) Receptor-targeted gene delivery via folate-conjugated polyethylenimine. *AAPS PharmSci* **1**, E19
- Guo, W. and Lee, R.J. (2001) Efficient gene delivery via non-covalent complexes of folic acid and polyethylenimine. *Journal of Controlled Release* **77**, 131-138
- Gupta, B., Levchenko, T.S. and Torchilin, V.P. (2005). Intracellular delivery of large molecules and small particles by cell-penetrating proteins and peptides. *Advanced Drug Delivery Reviews* **57**, 637-651
- Hacein-Bey-Abina, S., Von Kalle, C., Schmidt, M., McCormack, M.P., Wullfraat, N., Leboulch, P., Lim, A., Osborne, C.S., Pawliuk, R., Morillon, E., Sorensen, R., Forster, A., Fraser, P., Cohen, J.I., de Saint Basile, G., Alexander, I., Wintergerst, U., Frebourg, T., Aurias, A., Stoppa-Lyonnet, D., Romana, S., Radford-Weiss, I., Gross, F., Valensi, F., Delabesse, E., Macintyre, E., Sigaux, F., Soulier, J., Leiva, L.E., Wissler, M., Prinz, C., Rabbitts, T.H., Le Deist, F., Fischer, A. and Cavazzana-Calvo, M. (2003) LMO2-associated clonal T cell proliferation in two patients after gene therapy for SCID-X1. *Science* **302**, 415-419
- Haensler, J. and Szoka, F.C. (1993) Polyamidoamine cascade polymers mediate efficient transfection of cells in culture. *Bioconjugate Chemistry* **4**, 372-379
- Hallbrink, M., Floren, A., Elmquist, A., Pooga, M., Bartfai, T. and Langel, U. (2001) Cargo delivery kinetics of cell-penetrating peptides. *Biochimica et Biophysica Acta* **1515**, 101-109
- Hansen, S.H., Sandvig, K., and van Deurs, B. (1993) Clathrin and HA2 adaptors: effects of potassium depletion, hypertonic medium, and cytosol acidification. *Journal of Cell Biology* **121**, 61-72
- Hansma, H.G., Golan, R., Hsieh, W., Lollo, C.P., Mullen-Ley, P. and Kwok, D. (1998) DNA condensation for gene therapy as monitored by atomic force microscopy. *Nucleic Acid Research* **26**, 2481-2487
- Harada, M., Sakisaka, S., Yoshitake, M., Ohishi, M., Itano, S., Shakado, S., Mimura, Y., Noguchi, K., Sata, M., and Yoshida, H. (1995) Role of cytoskeleton and acidification of endocytic compartment in asialoglycoprotein metabolism in isolated rat hepatocyte couplets. *Hepatology* **21**, 1413-1421
- Harada-Shiba, M., Yamauchi, K., Harada, A., Takamisawa, I., Shimokado, K. and Kataoka, K. (2002) Polyion complex micelles as vectors in gene therapy – pharmacokinetics and in vivo gene transfer. *Gene Therapy* **9**, 407-414
- Hasegawa S., Hirashima, N. and Nakanishi, M. (2001) Microtubule involvement in the intracellular dynamics for gene transfection mediated by cationic liposomes. *Gene Therapy* **8**, 1669-1673
- Hashida, H., Miyamoto, M., Cho, Y., Hida, Y., Kato, K., Kurokawa, T., Okushiba, S., Kondo, S., Dosaka-Akita, H. and Katoh, H. (2004). Fusion of HIV-1 TAT protein transduction domain to poly-lysine as a new DNA delivery tool. *British Journal of Cancer* **90**, 1252-1258

- Hatano, T., Ohkawa, K. and Matsude, M. (1993) Cytotoxic effect of the protein-doxorubicin conjugates on the multidrug-resistant human myelogenous leukaemia-cell line, K562, in vitro. *Tumor Biology* **14**, 288-294
- Hattori, Y. and Maitani, Y. (2004) Enhanced in vitro DNA transfection efficiency by novel folate-linked nanoparticles in human prostate cancer and oral cancer. *Journal of Controlled Release* **97**, 173-183
- Hauser, H., Spitzer, D., Verhoeyen, E., Unsinger, J. and Wirth, D. (2000) New approaches towards ex vivo and in vivo gene therapy. *Cells Tissues Organs* **167**, 75-80
- Hayat, M.A. (1981) *Principles and Techniques of Electron Microscopy: Biological Applications*. Edward Arnold, London.
- Haynes, M., Garrett, R.A. and Gratzer, W.B. (1970) Structure of nucleic acid poly base complexes. *Biochemistry* **9**, 4410-4416
- Herweijer, H. and Wolff, J.A. (2003) Progress and prospects: naked DNA gene transfer and therapy. *Gene Therapy* **10**, 453-458
- Hickman, M.A., Malone, R.W., Lehmann-Bruinsma, K., Sih, T.R., Knoell, D., Szoka, F.C., Walzem, R., Carlson, D.M. and Powell, J.S. (1994) Gene expression following direct injection of DNA into liver. *Human Gene Therapy* **5**, 1477-1483
- Hill, I.R.C., Garnett, M.C., Bignotti, F. and Davis, S.S. (2001) Determination of protection from serum nuclease activity by DNA-polyelectrolyte complexes using an electrophoretic method. *Analytical Biochemistry* **291**, 62-68
- Hirst, J. and Robinson, M.S. (1998) Clathrin and adaptors. *Biochimica et Biophysica Acta* **1404**, 173-193
- Hodel, M.R., Corbett, A.H. and Hodel, A.E. (2001) Dissection of a nuclear localization signal. *Journal of Biological Chemistry* **276**, 1317-1325
- Hofland H.E., Masson, C., Iginla, S., Osetinsky I., Reddy, J.A., Leamon, C.P., Scherman, D., Bessodes, M. and Wils, P. (2002) Folate-targeted gene transfer in vivo. *Molecular Therapy* **5**, 739-744
- Hofland H.E., Shepard, L. and Sullivan, S.M. (1996) Formation of stable cationic lipid / DNA complexes for gene transfer. *Proceedings of the National Academy of Sciences of USA* **93**, 7305-7309
- Hofland, H.E., Nagy, D., Liu, J.J., Spratt, K., Lee, Y.L., Danos, O. and Sullivan, S.M. (1997) In vivo gene transfer by intravenous administration of stable cationic lipid/DNA complexes. *Pharmaceutical Research* **14**, 742-749
- Holmberg, K., Bergstrom, K., Brink, C., Österberg, E., Tiberg, F. and Harris, J.M. (1993) Effects on protein adsorption, bacterial adhesion and contact angle of grafting PEG chains to polystyrene. *Journal of Adhesion Science and Technology* **7**, 503-517
- Hong, K., Zheng, W., Baker, A. and Papahadjopoulos D. (1997) Stabilization of cationic liposome-plasmid DNA complexes by polyamines and poly(ethylene glycol)-phospholipid conjugates for efficient in vivo gene delivery. *FEBS Letter* **400**, 233-237

- Hope, M.J., Mui, B., Ansell, S. and Ahkong, Q.F. (1998) Cationic lipids, phosphatidylethanolamine and the intracellular delivery of polymeric, nucleic acid-based drugs. *Molecular Membrane Biology* **15**, 1-14
- Horwitz, M.A. (1982) Phagocytosis of microorganisms. *Reviews of Infectious Diseases* **3**, 104-123
- Howard, K.A., Dash, P.R., Read, M.L., Ward, K., Tomkins, L.M., Nazaorva, O, Ulbrich, K. and Seymour, L.W. (2000) Influence of hydrophilicity of cationic polymers on the biophysical properties of polyelectrolyte complexes formed by self-assembly with DNA. *Biochimica et Biophysica Acta* **1475**, 245-255
- Hsuan, J.J. (1993) Oncogene regulation by growth factors. *Anticancer Research* **13**, 2521-2522
- Hudde, T., Rayner, S.A., Comer, R.M., Weber, M., Issacs, J.D., Waldmann, H, Larkin, D.P.F. and George, A.J.T. (1999) Activated polyamidoamine dendrimers, as a non-viral vector for gene transfer to the corneal endothelium. *Gene Therapy* **6**, 939-943
- Huebers, H. and Finch, C. (1987) The physiology of transferrin and transferrin receptors. *Physiological Research* **67**, 520-582
- Hunter, S. and Angellini, G.D. (1993) Phosphorylcholine coated chest drainage tubes: improved drainage after heart bypass surgery. *Annals of Thoracic Surgery* **56**, 1339
- Illum, L. and Davis, S.S. (1986) The effect of hydrophilic coatings on the uptake of colloidal particles with mouse peritoneal macrophages. *International Journal of Pharmaceutics* **29**, 53
- Ishihara, K. and Iwasaki, Y. (1998) Reduced protein adsorption on novel phospholipids polymers. *Journal of Biomaterials Applications* **13**, 111-127
- Ishihara, K., Normura, H., Kurita, K., Iwasaki, Y. and Nakabayashi, N. (1998) Why do phospholipids polymers reduce protein adsorption? *Journal of Biomedical Materials Research* **39**, 323-330
- Ista, L.K., Fan, H., Baca, O. and Lopez, G.P. (1996) Attachment of bacteria to model surfaces: oligo(ethylene glycol) surfaces inhibit bacterial attachment. *FEMS Microbiology Letters* **142**, 59-63
- Ivanov, V.A., Stukan, M.R., Vasilevskaya, V.V., Paul, W. and Binder, K. (2000) Structures of stiff macromolecules of finite chain length near the coil-globule transition: A Monte Carlo simulation. *Macromolecular Theory and Simulations* **9**, 488-499
- Jackman, M.R., Shurety, W., Ellis, J.A. and Luzio, J.P. (1994) Inhibition of apical but not basolateral endocytosis of ricin and folate in Caco-2 cells by cytochalasin D. *Journal of Cell Science* **107**, 2547-2556
- Jans, D and Hübner, S (1996). Regulation of protein transport to the nucleus: central role of phosphorylation. *Physiological Reviews* **76**, 651-675
- Jeong, J.H., Kim, S.H., Kim, S.W. and Park, T.G. (2005) In vivo tumor targeting of ODN-PEG-folic acid/PEI polyelectrolyte complex micelles. *Journal of Biomaterials science – polymer edition* **16**, 1409-1419

- Jo, S. and Park, K. (2000). Surface modification using silanated poly(ethylene glycol)s. *Biomaterials* **21**, 605-616
- Jones, R.A., Poniris, M.H. and Wilson, M.R. (2004) pDMAEMA is internalised by endocytosis but does not physically disrupt endosomes. *Journal of Controlled Release* **96**, 3790-391
- Juliano, R.L. and Stamp, D. (1975) Effect of particle – size and charge on clearance rates of liposomes and liposome encapsulated drugs. *Biochemical and Biophysical Research Communications* **63**, 651-658
- Julyan, P.J., Seymour, L.W., Ferry, D.R., Daryani, S., Boivin, C.M., Doran, J., David, M., Anderson, D., Christodoulou, C., Young, A.M., Hesselwood, S. and Kerr, D.J. (1999) Preliminary clinical study of the distribution of HPMA copolymers bearing doxorubicin and galactosamine. *Journal of Controlled Release* **57**, 281-290
- Kabanov, V.A. and Kabanov, A.V. (1995a) DNA complexes with polycations for delivery of genetic material s into cells. *Bioconjugate Chemistry* **6**, 7-20
- Kabanov, A.V., Vinogradov, S.V., Suzdaltseva, Y.G. and Alakhov, V.Y. (1995b) Water soluble block polycations for oligonucleotides delivery. *Bioconjugate Chemistry* **6**, 639-643
- Kabanov, V.A., Zezin, A.B., Izumrudov, V.A., Bronich, T.K. and Bakeev, K.N. (1985) Cooperative interpolyelectrolyte reactions. *Makromolekulare Chemie (Suppl.)* **13**, 137-155
- Kamen, B.A. and Capdevia, A. (1986) Receptor-mediated folate accumulation is regulated by cellular folate content. *Proceedings of the National Academy of Sciences of USA* **83**, 5983-5987
- Katayose, K., Kataoka, K. (1997) Water-soluble polyion complex associates of DNA and poly(ethyleneglycol)-poly(L-lysine) block copolymer. *Bioconjugate Chemistry* **8**, 702-707
- Kawasaki, T. and Ashwell, G. (1976) Chemical and physical properties of an hepatic membrane protein that specifically binds asialoglycoproteins. *Journal of Biological Chemistry* **251**, 1296-1302
- Kawakami, S., Sato, A., Nishikawa, M., Yamashita, F. and Hashida, M. (2000). Mannose receptor-mediated gene transfer into macrophages using novel mannosylated cationic liposomes, *Gene Therapy* **7**, 292–299.
- Ke, C.Y., Mathias, C.J. and Green, M.A. (2004). Folate-receptor-targeted radionuclide imaging agents. *Advanced Drug Delivery Reviews* **56**, 1143-1160
- Kichler, A., Freulon, I., Boutin, V., Mayer, R., Monsigny, M. and Midoux, P. (1999) Glycofection (TM) in the presence of anionic fusogenic peptides: A study of the parameters affecting the peptide-mediated enhancement of the transfection efficiency. *Journal of Gene Medicine* **1**, 134-143
- Kichler, A., Leborgne, C., Coeytaux, E. and Danos, O. (2001) Polyethylenimine-mediated gene delivery: a mechanistic study. *Journal of Gene Medicine* **3**, 135-144

- Kichler, A., Chiilon, M., Leborgne, C., Danos, O and Frisch, B. (2002) Intranasal gene delivery with a polyethylenimine-PEG conjugate. *Journal of Controlled Release* **81**, 379-388
- Kikuchi, A., Sugaya, S., Ueda, H., Tanaka, K., Aramaki, Y., Hara, T., Arima, H., Tsuchiya, S. and Fuwa, T. (1996) Efficient gene transfer to EGF receptor overexpressing cancer cells by means of EGF-labeled cationic liposomes. *Biochemical and Biophysical Research Communications* **227**, 666-671
- Kim, E.M., Jeong, H.J., Park, I.K., Cho, C.S., Moon, H.B., Yu, D.Y., Bom, H.S., Sohn, M.H. and Oh, I.J. (2005) Asialoglycoprotein receptor targeted gene delivery using galactosylated polyethylenimine-graft-poly(ethylene glycol): In vitro and in vivo studies. *Journal of Controlled Release* **108**, 557-567
- Kircheis, R., Kirchlner, A., Wallner, G., Kursa, M., Ogris, M., Felzmann, T., Buchberger, M. and Wagner, E. (1997) Coupling of cell-binding ligands to polyethylenimine for targeted gene delivery. *Gene Therapy* **4**, 409-418
- Kircheis, R., Schuller, S., Brunner, S., Ogris, M., Heider, K.H., Zauner, W. and Wagner, E. (1999) Polycation-based DNA complexes for tumor-targeted gene delivery in vivo. *Journal of Gene Medicine* **1**, 111-120
- Kircheis, R., Wightman, L., Schreiber, A., Robitza, B., Rossler, V. and Wagner, E. (2001) Polyethylenimine/DNA complexes shield by transferrin target gene expression to tumors after systemic application. *Gene Therapy* **8**, 28-40
- Kircheis, R., Wightman, L. and Wagner, E. (2001b) Design and gene delivery of modified polyethylenimines. *Advanced Drug Delivery Reviews* **53**, 341-358
- Kirkham, M. and Parton, R.G. (2005) Clathrin-independent endocytosis: New insights into caveolae and non-caveolar lipid raft carriers. *Biochimica et Biophysica Acta – Molecular Cell Research* **1745**, 273-286
- Klemm, A.R., Young, D. and Lloyd, J.B. (1998) Effects of polyethylenimine on endocytosis and lysosomes stability. *Biochemical Pharmacology* **56**, 41-46
- Klenin, K.V. , Merlitz, H. and Langowski, J. (1998) A Brownian dynamics program for the simulation of linear and circular DNA and other wormlike chain polyelectrolytes. *Biophysical Journal* **74**, 780-788
- Kloeckner, J., Prasmickaite, L., Hogset, A., Berg, K. and Wagner, E. (2004) Photochemically enhanced gene delivery of EGF receptor-targeted DNA polyplexes. *Journal of Drug Targeting* **12**, 205-213
- Konda, S.D., Aref, M., Brechbiel, M. and Wiener, E.C. (2000) Development of a tumor-targeting MR contrast agent using the high affinity folate receptor. *Investigative Radiology* **35**, 50-57
- Konno, T., Kurita, K., Iwasaki, Y., Nakabayashi, N. and Ishihara, K. (2001) Preparation of nanoparticles compared with bioinspired 2-methacryloxyloxyethyl phosphoricholine polymer. *Biomaterial* **22**, 1883-1889
- Kooststra, N.A. and Verma, I.M. (2003) Gene therapy with viral vectors. *Annual Review of Pharmacology and Toxicology* **43**, 413-419

- Kopecek, J., Kopeckova, P., Minko, T. and Lu, Z.R. (2000) HPMA copolymer-anticancer drug conjugates: design, activity, and mechanism of action. *European Journal of Pharmaceutics and Biopharmaceutics* **50**, 61-81
- Koping-Hoggard, M., Tubulekas, I., Guan, H., Edwards, K., Nilsson, M., Varum, K.M. and Artursson, P. (2001) Chitosan as a non-viral gene delivery system. Structure-property relationships and characteristics compared with polyethylenimine in vitro and after lung administration in vivo. *Gene Therapy* **8**, 1108-1121
- Kragh-Hansen, U., le Maire, M. and Moller, J.V. (1998). The mechanism of detergent solubilization of liposomes and protein-containing membranes. *Biophysical Journal* **75**, 2932-2946
- Krieger, M., Acton, S., Ashkenas, J., Pearson, A., Penman, M. and Resnick, D. (1993) Molecular flypaper, host defence, and atherosclerosis – structure, binding-properties, and functions of macrophage scavenger receptors. *Journal of Biological Chemistry* **268**, 4569-4572
- Kukowska-Latallo, J.F., Bielinska, A.U., Johnson, J., Spindler, R., Tomalia, D.A. and Baker, J.R. (1996) Efficient transfer of genetic material into mammalian-cells using starburst polyamidoamine dendrimers. *Proceedings of the National Academy of Sciences of USA* **93**, 4849-4902
- Kurane, S., Krauss, J.C., Watari, E., Kannagi, R., Chang, A.E. and Kudoh, S. (1998) Targeted gene transfer for adenocarcinoma using a combination of tumor-specific antibody and tissue-specific promoter. *Japanese Journal of Cancer Research*. **89**, 1212-1219
- Kuriyama, S., Mitoro, A., Tsujinoue, H., Nakatani, T., Yoshiji, H., Tsujimoto, T., Yamazaki, M. and Fukui, T. (2000). Particle-mediated gene transfer into murine livers using a newly developed gene gun. *Gene Therapy* **7**, 1132-1136
- Kursa, M., Walker, G.F., Roessler, V., Ogris, M., Roedl, W., Kircheis, R. and Wagner, E. (2003) Novel shielded transferrin-polyethylene glycol – polyethylenimine / DNA complexes for systemic tumor-targeted gene transfer. *Bioconjugate Chemistry* **14**, 222-231
- Kwok, Y.K., Adami, R.C., Hester, K.C., Park, Y., Thomas, S. and Rice, K.G. (2000) Strategies for maintaining the particle size of peptide DNA condensates following freeze-drying. *International Journal of Pharmaceutics* **203**, 81-88
- Kwoh, D.Y., Coffin, C.C., Lollo, C.P., Jovenal, J., Banaszeczyk, M.G., Mullen, P., Phillips, A., Amini, A., Fabrycki, J., Bartholomew, R.M., Brostoff, S.W. and Carlo, D.J. (1999) Stabilization of poly-L-lysine/DNA polyplexes for in vivo gene delivery to the liver *Biochimica et Biophysica Acta* **1444**, 171-190
- Lachman, D.S. (2001) Gene delivery and gene therapy with herpes simplex virus-based vectors. *Gene* **264**, 1-9
- Ladino, C.A., Chari, R.V. J., Bourret, L.A., Kedersha, N.L., and Goldmacher, V.S. (1997) Folate-maytansinoids: target-selective drugs of low molecular weight. *International Journal of Cancer* **73**, 859-864
- Laemmli, U.K. (1975) Characterization of DNA condensates induced by poly(ethylene oxide) and polylysine. *Proceedings of the National Academy of Sciences of USA* **72**, 4288-4292

- Lai, B.T., Gao, J.P. and Lanks, K.W. (1997) Mechanism of action and spectrum of cell lines sensitive to a doxorubicin-transferrin conjugate. *Cancer Chemotherapy and Pharmacology* **41**, 155-160
- Lakadamyali, M., Rust, M.J. and Zhuang, X.W. (2004) Endocytosis of influenza viruses. *Microbes and Infection* **6**, 929-936
- Lamaze, C. and Schmid, S.L. (1995) The emergence of clathrin-independent pinocytic pathways. *Current Opinion in Cell Biology* **7**, 573-580
- Lamaze, C., Fujimoto, L.M., Yin, H.L. and Schmid, S.L. (1997) The actin cytoskeleton is required for receptor-mediated endocytosis in mammalian cells. *Journal of Biological Chemistry* **272**, 20332-20335
- Lamaze, C., Dujeancourt, A., Baba, T., Lo, C G, Benmerah, A and Dautry-Varsat A (2001). Interleukin 2 receptors and detergent-resistant membrane domains define a clathrin-independent endocytic pathway. *Molecular Cell* **7**, 661-671
- Lasic, D.D. and Peralman, R. (1996) Liposomes and lipidic particles in gene therapy. In: *Vesicle*, pp. 477-489 (Ed Rosoff, M.) Marcel Dekker, Brooklyn, New York
- Le Pecaq, J.B. and Paoletti, C. (1967) A fluorescent complex between ethidium bromide and nucleic acids. Physical-chemical characterisation. *Journal of Molecular Biology* **27**, 87-106
- Leamon, C.P. and Low, P.S. (1991) Delivery of macromolecules into living cells: a method that exploits folate receptor endocytosis. *Proceedings of the National Academy of Sciences of USA* **88** 5572-5576
- Leamon, C.P. and Low, P. (1992) Cytotoxicity of momordin-folate conjugates in cultured human cells. *Journal of Biological Chemistry* **267**, 24966-24971
- Leamon, C.P. and Low, P.S. (1993) Cytotoxicity of folate-pseudomonas exotoxin conjugates toward tumor cells. *Journal of Biological Chemistry* **268**, 24847-24854
- Leamon, C.P., Weigl, D. and Hendren, R.W. (1999) Folate copolymer-mediated transfection of cultured cells. *Bioconjugate Chemistry* **10**, 947-957
- Leamon, C.P. and Reddy, J.A. (2004) Folate-targeted chemotherapy. *Advanced Drug Delivery Reviews* **56**, 1127-1141
- Lechardeur, D., Verkman, A.S. and Lukacs, G.L. (2005) Intracellular routing of plasmid DNA during non-viral gene transfer. *Advanced Drug Delivery Reviews* **57**, 755-767
- Leclercq, L., Boustta, M. and Vert, M. (2003) A physicochemical approach of polyanion-polycation interactions aimed at better understanding the in vivo behavior of polyelectrolyte-based drug delivery and gene transfection. *Journal of Drug Targeting* **11**, 129-138.
- Lecocq, M., Andrianaivo, F., Warnier, M.T., Wattiaux-De Coninck, S., Wattiaux, R. and Jadot, M. (2003) Uptake by mouse liver and intracellular fate of plasmid DNA after a rapid tail vein injection of a small or a large volume. *Journal of Gene Medicine* **5**, 142-156



- Lee, R.J. and Low, P.S. (1994). Delivery of liposomes into culture KB cells via folate receptor-mediated endocytosis. *Journal of Biological Chemistry* **269**, 3198, 3204
- Lee, R.J. and Huang, L. (1996) Folate-targeted, anionic liposome-entrapped polylysine-condensed DNA for tumor cell-specific gene transfer. *Journal of Biological Chemistry* **271**, 8481-8487
- Lee, H., Jeong, J.H. and Park, T.G. (2001) A new gene delivery formulation of polyethylenimine / DNA complexes coated with PEG conjugated fosugenic peptide. *Journal of Controlled Release* **76**, 183-192
- Lee, J.W., Lu, J.Y., Low, P.S., and Fuchs, P.L. (2002) Synthesis and evaluation of taxol-folic acid conjugates as targeted antineoplastics (dagger). *Bioorganic Medical Chemistry* **10**, 2397-2414
- Lee, K.M., Kim, I.S., Lee, Y.B., Shin, S.C., Lee, K.C. and Oh, I.J. (2005) Evaluation of transferrin-polyethylenimine conjugate for targeted gene delivery. *Archives of Pharmacal Research* **28**, 722-729
- Lee, M. and Kim, S.W. (2005) Polyethylene glycol-conjugated copolymers for plasmid DNA delivery. *Pharmaceutical Research* **22**, 1-10
- Lehrman, S. (1999) Virus treatment questioned after gene therapy death. *Nature* **401**, 517-518
- Lentz, B.R. (1989). Membrane 'fluidity' as detected by diphenylhexatriene probes. *Chemistry and Physics of Lipids*. **50**, 171-190
- Letoha, T., Gaal, S., Somlai, C., Czajlik, A., Perczel, A. and Penke, B. (2003) Membrane translocation of penetratin and its derivatives in different cell lines. *Journal of Molecular Recognition* **16**, 272-279
- Lewis, A.L. (2000). Phosphorylcholine-based polymers and their use in the prevention of biofouling. *Colloid and Surf B: Biointerfaces* **18**, 261-275
- Lewis, A.L., Hughes, P.D., Kirkwood, L.C., Leppard, S.W., Redman, R.P., Tolhurst, L.A. and Stratford, P.W. (2000) Synthesis and characterisation of phosphorylcholine-based polymers useful for coating blood filtration devices. *Biomaterials* **21**, 1847-1859
- Lewis, A.L., Cumming, Z.L., Goreish, H.H., Kirkwood, L.C., Tolhurst, L.A. and Stratford, P.W. (2001a) Crosslinkable coatings from phosphorylcholine-based polymers. *Biomaterials* **22**, 99-111
- Lewis, A.L., Vick, T.A., Collias, A.C.M., Hughes, L.G., Palmer, R.R., Leppard, S.W., Furze, J.D., Taylor, A.S. and Stratford, P.W. (2001b) Phosphorylcholine-based polymer coatings for stent drug delivery. *Journal of Materials Science* **12**, 865-870
- Lewis, A.L. and Stratford, P. (2002) Phosphorylcholine-coated stents. *Journal of Long Terms Effects of Medical Implants* **12**, 231-250
- Lewis, A.L., Tolhurst, L.A. and Stratford, P.W. (2002) Analysis of a phosphorylcholine-based polymer coating on a coronary stent pre- and post-implantation. *Biomaterials* **23**, 1697-1706
- Li, S., Deshmukh, H.M. and Huang, L. (1998) Folate-mediated targeting of antisense oligonucleotides to ovarian cancer cells. *Pharmaceutical Research* **15**, 1540-1545

- Li, B., Li, S., Tan, T., Stolz, D.B., Watkins, S.C., Block, L.H. and Huang, L. (2000) Lyophilization of cationic lipid-protamine-DNA (LPD) complexes. *Journal of Pharmaceutical Sciences* **89**, 355-364
- Li, H., and Qian, Z.M. (2002) Transferrin/transferrin receptor mediated drug delivery. *Medicinal Research Reviews* **22**, 225-250
- Licciardi, M., Tang, Y., Billingham, N.C. and Armes, S.P. (2005). Synthesis of novel folic acid-functionalized biocompatible block copolymers by atom transfer radical polymerization for gene delivery and encapsulation of hydrophobic drugs. *Biomacromolecules* **6**, 1085-1096
- Lindberg, J., Fernandez, M.A.M., Ropp, J.D. and Hamm-Alvarez, S.F. (2001) Nocodazole treatment of CV-1 cells enhances nuclear/perinuclear accumulation of lipid-DNA complexes and increases gene expression. *Pharmaceutical Research* **18**, 246-249
- Lindgren, M., Hällbrink, M., Prochiantz, A. and Langel, Ü. (2000) Cell-penetrating peptides. *Trends in Pharmacological Science* **21**, 99-103
- Liu, D., Wang, C., Lin, Z., Li, J., Xu, B., Wei, Z., Wang, Z. and Bai, C. (2001) Visualization of the intermediates in a uniform DNA condensation system by tapping mode atomic force microscopy. *Surface and Interface Analysis* **32**, 15-19
- Liu, X., Tian, P., Yu, Y., Yao, M., Cao, X. and Gu, J. (2002) Enhanced antitumor effect of EGF R-targeted p21WAF-1 and GM-CSF gene transfer in the established murine hepatoma by peritumoral injection. *Cancer Gene Therapy* **9**, 100-108
- Lokowicz, J. (1999) *Principles of fluorescence spectroscopy*. Kluwer Academic, New York
- Low, P.S. (2004) Folate receptor-targeted drugs for cancer and inflammatory diseases. *Advanced Drug Delivery Reviews* **56**, 1055-1058
- Lu, Y.J. and Low, P.S. (2002) Folate-mediated delivery of macromolecular anticancer therapeutic agents. *Advanced Drug Delivery Reviews* **54**, 675-693
- Lu, Y.J., Weers, B. and Stellwagen, N.C. (2002) DNA persistence length revisited. *Biopolymers* **61**, 261-275
- Lu, Y., Sega, E., Leamon, C.P. and Low, P. (2004) Folate receptor-targeted immunotherapy of cancer: mechanism and therapeutic potential. *Advanced Drug Delivery Reviews* **56**, 1161-1176
- Ludtke, J.J., Zhang, G., Sebestyen, M.G. and Wolff, J.A. (1999) A nuclear localization signal can enhance both the nuclear transport and expression of 1kb DNA. *Journal of Cell Science* **112**, 2033-2041
- Luthman, H. and Magnusson, G. (1983) High efficiency polyoma DNA transfection of chloroquine treated cells. *Nucleic Acids Research* **11**, 1295-1308
- Lyklema, J. (2000) *Fundamentals of interface and colloidal science: Volume 1 (fundamentals)*, Academic Press, UK

- Lyubartsev, A P and Nordenskiöld, L (1995). Monte Carlo simulation study of ion distribution and osmotic pressure in hexagonally oriented DNA. *Journal of Physical Chemistry* **99**, 10373-10382
- Ma, T., Tang, T., Billingham, N.C. and Armes, S.P. (2003) Well-defined biocompatible block copolymers via atom transfer radical polymerization of 2-methacryloyloxyethyl phosphorylcholine in protic media. *Macromolecules* **36**, 3475-3484
- MacLaughlin, F.C., Mumper, R.J., Wang, J., Tagliaferri, J.M., Gill, I., Hinchcliffe, M. and Rolland, A.P. (1998) Chitosan and depolymerised chitosan oligomers as condensing carriers for *in vivo* plasmid delivery. *Journal of Controlled Release* **56**, 259-272
- Mahato, R., Rolland, A. and Tomlinson, E. (1997) Cationic lipid-based gene delivery system: pharmaceutical perspectives. *Pharmaceutical Research* **14**, 853-859
- Mahato, R.I., Furgeson, D.Y., Maheshwari, A., Han, S.O. and Kim, S.W.. (2000) Polymeric gene delivery for cancer treatment. In: *Biomaterials and Drug Delivery Towards New Millennium*, pp. 249–280 (Eds. Park, K., Kwon, I., Yui, N., Jeong, S., Park, K) Han Rim Wonn Publishing, Seoul, Korea
- Mannisto, M., Ronkko, S., Matto, M., Honkakoski, P., Hyttinen, M., Pelkonen, J. and Urtti, A. (2005) The role of cell cycle on polyplex-mediated gene transfer into a retinal pigment epithelial cell line. *Journal of Gene Medicine* **7**, 466-476
- Mao, H.A., Roy, K., Troung-Le, V.L., Janes, K.A., Lin, K.Y., Wang, Y., August, J.T. and Leong, K.W. (2001) Chitosan-DNA nanoparticles as gene carriers: synthesis, characterization and transfection efficiency. *Journal of Controlled Release* **70**, 399-421
- Marcucci, F. and Lefoulon, F. (2004) Active targeting with particulate drug carriers in tumor therapy: fundamentals and recent progress. *Drug Discovery Today* **9**, 219-228
- Margolis, R.L., Rauch, C.T. and Wilson, L. (1980) Mechanism of colchicine-dimer addition to microtubule ends – implications for the microtubule polymerization mechanism. *Biochemistry* **19**, 5550-5557
- Marquet, R, Houssier, C (1991). Thermodynamics of cation-induced DNA condensation. *Journal of Biomolecular Structure Dynamics* **9**, 159-167
- Marshall, E. (1999) Gene therapy death prompts review of adenovirus vector. *Science* **286**, 2244-2245
- Martin, F. and Boulikas, T. (1998) The challenge of liposomes in gene therapy. *Gene Therapy and Molecular Biology* **1**, 173-214
- Martin, A.L., Davies, M.C., Rackstraw, B.J., Roberts, C.J., Stolnik, S., Tendler, S.J.B. and Williams, P.M. (2000) Observation of DNA-polymer condensate formation in real time at a molecular level. *FEBS Letters* **480**, 106-112
- Marx, K.A. and Ruben, G.C. (1983) Evidence for hydrated spermidine-calf thymus DNA toruses organized by circumferential DNA wrapping. *Nucleic Acids Research* **11**, 1839-1854
- Mattaj, I.W. and Englmeier, L. (1998) Nucleocytoplasmic transport: The soluble phase. *Annual Review of Biochemistry* **67**, 265-306

- Maurstad, G., Danielsen, S. and Stokke, B.T. (2003) Analysis of compacted semiflexible polyanions visualized by atomic force microscopy: influence of chain stiffness on the morphologies of polyelectrolyte complexes. *Journal of Physical Chemistry B* **107**, 8172-8180.
- Maurstad, G. and Stokke, B.T. (2005) Toroids of stiff polyelectrolytes. *Current Opinion in Colloid and Interface Science* **10**, 16-21
- McConnell, M.J. and Imperiale, M.J. (2004) Biology of adenovirus and its use as a vector for gene therapy. *Human Gene Therapy* **15**, 1022-1033
- McLachlan, G., Davidson, H., Davidson, D., Dickinson, P., Dorin, J. and Porteous, D. (1994) DOTAP as a vehicle for efficient gene delivery in vitro and in vivo. *Biochemistry* **11**, 19-21
- Mellman, I. (1996). Endocytosis and molecular sorting. *Annual Review of Cell Biology* **12**, 575-625
- Merdan, T., Kunath, K., Petersen, H., Bakowsky, U., Voigt, K.H., Kopecek, J. and Kissel, T. (2005) PEGylation of poly(ethylene imine) affects stability of complexes with plasmid DNA under *in vivo* conditions in dose-dependent manner after intravenous injection into mice. *Bioconjugate Chemistry* **16**, 785-792
- Middaugh, C.R., Evans, R.K., Montgomery, D.L. and Casimiro, D.R. (1998) Analysis of plasmid DNA from a pharmaceutical perspective. *Journal of Pharmaceutical Science* **87**, 130-146
- Mislick, K.A., Baldeschwieler, J.D., Kayyem, J.F. and Meade, T.J. (1995) Transfection of folate-polylysine DNA complexes: evidence for lysosomal delivery. *Bioconjugate Chemistry* **6**, 512-515
- Molina, M.D.C., Allison, S.D. and Anchordoquy, T.J. (2001). Maintenance of nonviral vector particle size during the freezing step of the lyophilization process is insufficient for preservation of activity: insight from other structural indicators. *Journal of Pharmaceutical Science* **90**, 1445-1455
- Moret, I., Peris, J.E., Guillem, V.M., Benet, M., Revert, F., Dasi, F., Crespo, A. and Aliño, S.F. (2001) Stability of PEI-DNA and DOTAP-DNA complexes: effect of alkaline pH, heparin and serum. *Journal of Controlled Release* **76**, 169-181
- Morgan, S.M., Subr, V., Ulbrich, K., Woodley, J.F. and Duncan, R. (1996) Evaluation of N-(2-hydroxypropyl)methacrylamide copolymer-peptide conjugates as potential oral vaccines. Studies on their degradation by isolated rat small intestinal peptidases and their uptake by adult rat small intestinal tissue in vitro. *International Journal of Pharmaceutics* **128**, 99-111
- Moroianu, J. (1999). Nuclear import and export pathways. *Journal of Cellular Biochemistry (Suppl.)* **32-33**, 76-83
- Mortimer, I., Tam, P., MacLachlan I., Graham, R.W., Saravolac, E.G. and Joshi, P.B. (1999) Cationic lipid-mediated transfection of cells in culture requires mitotic activity. *Gene Therapy* **6**, 403-411
- Morton, W.M., Ayscough, K.R., and McLaughlin, P.J. (2000). Latrunculin alters the actin-monomer subunit interface to prevent polymerization. *Nature Cell Biology* **2**, 376-378

- Mousavi, S.L., Malerød, L., Berg, T. and Kjekken, R. (2004) Clathrin-dependent endocytosis. *Biochemical Journal* **377**, 1-16
- Mulders, F., Vanlangen, H., Vanginkel, G. and Levine, Y.K. (1986). The static and dynamic behaviour of fluorescent probe molecules in lipid bilayers. *Biochimica et Biophysica Acta* **859**, 209-218
- Mullen, C.A. (1994). Metabolic suicide genes in gene therapy. *Pharmacology Therapeutics* **63**, 199-207
- Müller, R.H., Ruhl, D., Luck, M. and Paulke, B.R. (1997) Influence of fluorescent labelling of polystyrene particles on phagocytic uptake, surface hydrophobicity, and plasma protein adsorption. *Pharmaceutical Research* **14**, 18-24
- Mundy, D.I., Machleidt, T., Ying, Y-S., Anderson, R.G.W. and Bloom, G.S. (2002) Dual control of caveolar membrane traffic by microtubules and the actin cytoskeleton. *Journal of Cell Science* **115**, 4327-4339
- Murai, M, Seki, K, Sakurada, J, Usui, A and Masuda, S (1993). Effects of cytochalasins B and D on *Staphylococcus aureus* adherence to and ingestion by mouse renal cells from primary culture. *Microbiology and Immunology* **37**, 69-73
- Murphy, J.E., Uno, T., Hamer, J.D., Cohen, F.E., Dwarki, V. and Zuckermann, R.N. (1998) A combinatorial approach to the discovery of efficient cationic peptoid reagents for gene delivery. *Proceedings of the National Academy of Sciences of USA* **95**, 1517-1522
- Murphy, E.F. and Lu, J.R. (2000) Characterization of protein adsorption at the phosphorylcholine incorporated polymer – water interface. *Macromolecules* **33**, 4545-4554
- Murray, J.W. and Wolkoff, A.W. (2003) Roles of the cytoskeleton and motor proteins in endocytic sorting. *Advanced Drug Delivery Reviews* **55**, 1385-1403
- Nabel, G.J., Chang, A., Nabel, E.G., Plautz, G., Fox, B.A., Huang, L. and Su, S. (1992) Immunotherapy of malignancy by *in vivo* gene transfer into tumors. *Human Gene Therapy* **3**, 399-410
- Nabel, G.J., Nabel, E.G., Yang, Z.Y., Fox, B.A., Plautz, G.E., Gao, A., Huang, L., Shu, S., Gordan, D. and Chang, A.E. (1993) Direct gene transfer with DNA-liposome complexes in melanomas: expression, biologic activity, and lack of toxicity in humans *Proceedings of the National Academy of Sciences of USA* **90**, 11307-11311
- Nabi, I.R. and Le, P.U. (2003) Caveolae / raft dependent endocytosis. *Journal of Cell Biology* **161**, 673-677
- Nair, R.R., Rodgers, J.R. and Schwarz, L.A. (2002) Enhancement of transgene expression by combining glucocorticoids and anti-mitotic agents during transient transfection using DNA-cationic liposomes. *Molecular Therapy* **5**, 455-462
- Nagy, I.B., Hudecz, F., Alsina, M.A. and Reig, F. (2003) Physicochemical characterization of branched chain polymeric polypeptide carriers based on a poly-lysine backbone *Biopolymers* **70**, 323-335

- Nettelbeck, D.M., Jerome, V., Muller, R. (2000) Gene therapy: designer promoters for tumour targeting. *Trends Genetics* **16**, 174-181
- Neu, J.C. (1999). Wall-mediated forces between like-charged bodies in an electrolyte. *Physical Review Letters* **82**, 1072-1074
- Neu, M., Fischer, D. and Kissel, T. (2005) Recent advances in rational gene transfer vector design based on poly(ethylene imine) and its derivatives. *Journal of Gene Medicine* **7**, 992-1009
- Neves, C., Byk, G., Scherman, D. and Wils, P. (1999). Coupling of a targeting peptide to plasmid DNA by covalent triple helix formation. *FEBS letters* **453**, 41-45
- Nguyen, H-K., Lemieux, P., Vinogradov, S.V., Gebhart, C.L., Guerin, N., Paradis, G., Bronich, T.K., Alakhov, V.Y. and Kabonov, A.V. (2000) Evaluation of polyether-polyethylenimine graft copolymers as gene transfer agents. *Gene Therapy* **7**, 126-138
- Nichols, B.J., Kenworthy, A.K., Polishchuk, R.S., Lodge, R., Roberts, T.H., Hirschberg, K., Phair, R.D. and Lippincott-Schwartz, J. (2001) Rapid cycling of lipid raft markers between the cell surface and Golgi complex. *Journal of Cell Biology* **153**, 529-541
- Nicolau, C., Le Pape, A., Soriano, P., Fargette, F. and Juhel, N.F. (1983) In vivo expression of rat insulin after intravenous administration of the liposome entrapped gene for rat insulin I. *Proceedings of the National Academy of Sciences of USA* **75** 1068-1072
- Nicolau, C., and Cudd, A. (1989) Liposomes as carriers of DNA. *Critical Review in Therapeutic Drug Carrier Systems* **6**, 239-271
- Nishikawa, M., Takemura, S., Takakura, Y. and Hashida, M. (1998) Targeted delivery of plasmid DNA to hepatocytes *in vivo*: optimization of the pharmacokinetics of plasmid DNA/galactosylated poly(L-lysine) complexes by controlling their physicochemical properties. *Journal of Pharmacology and Experimental Therapeutics* **287**, 408-415
- Nishitani, M.A., Sakai, T., Kanayama, H.O., Himeno, K. and Kagawa, S. (2000) Cytokine gene therapy for cancer with naked DNA. *Molecular Urology* **4**, 47-50
- Noguchi, H., and Yoshikawa, K.J. (1998). Morphological variation in a collapsed single homopolymer chain. *Journal of Chemical Physics*. **109**, 5070-5077
- Ogris, M., Brunner, S., Schuller, S., Kircheis, R. and Wagner, E. (1999) Pegylated DNA/transferrin-PEI complexes: reduced interaction with blood components, extended circulation in blood and potential for systemic gene delivery. *Gene Therapy* **6**, 595-605
- Ogris, M., Wagner, E. and Steinlein, P. (2000) A versatile assay to study cellular uptake of gene transfer complexes by flow cytometry. *Biochimica et Biophysica Acta* **1474**. 237-243
- Oku, N., Tokudome, Y., Namba, Y., Saito, N., Endo, M., Hasegawa, Y., Kawai, M., Tsukada, H. and Okada, S. (1996) Effect of serum protein binding on real-time trafficking of liposomes with different charges analyzed by positron emission tomography. *Biochimica et Biophysica Acta* **1280**, 149-154
- Orkin, S.H., Daddona, P.E., Shewach, D.S., Markham, A.F., Bruns, G.A., Goff, S.C. and Kelley, W.N. (1983). Molecular cloning of human adenosine deaminase gene sequences. *Journal of Biological Chemistry* **258**, 12753-12756

- Orkin, S.H. (1986) Molecular genetics and potential gene therapy. *Clinical Immunology Immunopathology* **40**, 151-156
- Orlandi, P.A. and Fishman, P.H. (1998). Filipin-dependent inhibition of cholera toxin: evidence for toxin internalisation and activation through caveolae-like domains. *Journal of Cell Biology*. **141**, 905-915
- Otsuka, H., Nagasaki, Y., and Kataoka, K. (2001) Self-assembly of poly(ethylene glycol)-based block copolymers for biomedical applications. *Current Opinion in Colloid Interface Science* **6**, 3-10
- Otsuka, H., Nagasaki, Y. and Kataoka, K. (2003) PEGylated nanoparticles for biological and pharmaceutical applications. *Advanced Drug Delivery Reviews* **55**, 403-419
- Oupický, D., Koňák, Č. and Ulbrich, K. (1999) DNA complexes with block and graft copolymers of *N*-(2-hydroxypropyl)methacrylamide and 2-(trimethylammonio)ethyl methacrylate. *Journal of Biomaterials Science Polymer Edition* **10**, 573-590
- Oupický, D., Howard, K.A., Konak, C., Dash, P.R., Ulbrich, K. and Seymour, L.W. (2000a). Steric stabilization of poly-L-lysine / DNA complexes by the covalent attachment of semitelechelic poly[*N*-(2-hydroxypropyl)methacrylamide]. *Bioconjugate Chemistry* **11**, 492-501
- Oupický, D., Koňák, Č., Ulbrich, K., Wolfert, M.A. and Seymour, L.W. (2000b) DNA delivery systems based on complexes of DNA with synthetic polycations and their copolymers. *Journal of Controlled Release* **65**, 149-171
- Oupický, D., Ogris, M., Howard, K.A., Dash, P.R., Ulbrich, K. and Seymour, L.W. (2002). Importance of lateral and steric stabilization of polyelectrolyte gene delivery vectors for extended systemic circulation. *Molecular Therapy* **5**, 463-472
- Pan, C.Q., Ulmer, J.S., Herzka, A. and Lazarus, R.A. (1998) Mutational analysis of human DNase I at the DNA binding interface: implications for DNA recognition, catalysis and metal ion dependence. *Protein Science* **7**, 628-636
- Parent, J.L., Labrecque, P., Driss Rochdi, M. and Benovic, J.L. (2001) Role of the differentially spliced carboxyl terminus in thromboxane a<sub>2</sub> receptor trafficking: identification of a distinct motif for tonic internalization. *Journal of Biological Chemistry* **276**, 7079-7085
- Parente, R.A., Nir, S., Szoka, F.C. (1990) Mechanism of leakage of phospholipid vesicle contents induced by the peptide GALA. *Biochemistry* **29**, 8720-8728
- Park, S.Y., Harries, D. and Gelbart, W. (1998) Topological defects and the optimum size of DNA condensates. *Biophysical Journal* **75**, 714-720
- Park, Y.K., Park, Y.H., Shin, B.A., Choi, E.S., Park, Y.R., Akaike, T. and Cho, C.S. (2000) Galactosylated chitosan – graft- dextran as hepatocyte-targeting DNA carrier. *Journal of Controlled Release* **69**, 97-108
- Park, M.R., Han, K.I., Han, I.K., Cho, M.H., Nah, J.W., Choi, Y.J. and Cho, C.S. (2005). Degradable polyethylenimine-alt-poly(ethylene glycol) copolymers as novel gene carriers. *Journal of Controlled Release* **105**, 367-380

- Parker, A.L., Collins, L., Zhang, X.H. and Fabre, J.W. (2005) Exploration of peptide motifs for potent non-viral gene delivery highly selective for dividing cells. *Journal of Gene Medicine* **7**, 1545-1554
- Parton, R.G., Joggerst, B., and Simons, K. (1994) Regulated internalization of caveolae. *Journal of Cell Biology* **127**, 1199-1215
- Parton, R.G. and Richards, A.A. (2003) Lipid rafts and caveolae as portals for endocytosis: new insights and common mechanisms. *Traffic* **4**, 724-738
- Patel, K.R., Li, M.P. and Baldeschwieler, J.D. (1983) Suppression of liver uptake of liposomes by dextran sulphate 500. *Proceedings of the National Academy of Sciences of USA* **80** 6518– 6522
- Patel, H.M. (1992) Serum opsonins and liposomes – their interaction and opsonophagocytosis. *Critical Reviews in Therapeutic Drug Carrier Systems* **7**, 12875-12883
- Pattnaik, P. (2005) Surface plasmon resonance - Applications in understanding receptor-ligand interaction. *Applied Biochemistry and Biotechnology* **126**, 79-92
- Paulos, C.M., Turk, M.J., Breur, G.J. and Low, P.S. (2004) Folate receptor-mediated targeting of therapeutic and imaging agents to activated macrophages in rheumatoid arthritis. *Advanced Drug Delivery Reviews* **56**, 1205-1217
- Pector, V., Backmann, J., Maes, D., Vandenbranden, M. and Ruyschaert J. (2000) Biophysical and structural properties of DNA-diC(14)-amidine complexes. *Journal of Biological Chemistry* **275**, 29533-29538
- Pelkmans, L., Kartenbeck, J. and Helenius, A. (2001) Caveolar endocytosis of simian virus 40 reveals a new two-step vesicular-transport pathway to the ER. *Nature Cell Biology* **3**, 473-483
- Pelkmans, L. and Helenius, A. (2002) Endocytosis via caveolae. *Traffic* **3**, 311-320
- Pelkmans, L. and Helenius, A. (2003) Insider information: what viruses tell us about endocytosis. *Current Opinion in Cell Biology* **15**, 414-422
- Peng, Z.H. (2005) Current status of gendicine in China: Recombinant human Ad-p53 agent for treatment of cancers. *Human Gene Therapy* **16**, 1016-1027
- Petersen, H., Frchner, P.M., Martin, A.L., Kunath, K., Stolnik, S., Roberts, C.J., Fischer, D., Davies, M.C. and Kissel, T. (2002) Polyethylenimine-graft-poly(ethylene glycol) copolymers: influence of copolymer block structure on DNA complexation and biological activities as gene delivery system. *Bioconjugate Chemistry* **13**, 845-854
- Pooga, M., Hallbrink, M., Zorko, M. and Langel, U. (1998) Cell penetration by transportan. *FASEB Journal* **12**, 67-77
- Pope, L.H., Davies, M.C., Laughton, C.A., Roberts, C.J., Tendler, C.J.B., Williams, P.M. (1999) Interaction-induced changes in DNA supercoiling observed in real-time by atomic force microscopy. *Analytica Chimica Acta* **400**, 27-32
- Pouton, C. (1998) Nuclear transport of polypeptides, polynucleotides and supramolecular complexes. *Advanced Drug Delivery Reviews* **34**, 41-64



- Pouton, C.W., Lucas, P., Thomas, B.J., Uduehi, A.N., Milroy, D.A. and Moss, S.H. (1998) Polycation-DNA complexes for gene delivery: a comparison of the biopharmaceutical properties of cationic polypeptides and cationic lipids. *Journal of Controlled Release* **53**, 289-299
- Qian, Z.M. and Tang, P. (1995) Mechanisms of iron uptake by mammalian-cells. *Biochimica et Biophysica Acta* **1269**, 205-214
- Qiu, P., Ziegelhoffer, P., Sun, J. and Yang, N.S. (1996) Gene gun delivery of mRNA *in situ* results in efficient transgene expression and genetic immunization. *Gene Therapy* **3**, 262-268
- Qualmann, B., Kessels, M.M. and Kelly, R.B. (2000) Molecular links between endocytosis and the actin cytoskeleton. *Journal of Cell Biology* **150**, 111-116
- Rao, U.S., Fine, R.L. and Scarborough, G.A. (1994) Antiestrogens and steroid hormones: substrates of the human P-glycoprotein. *Biochemical Pharmacology* **48**, 287-292
- Read M.L., Bremner, K.H., Oupick, D., Green, N.K., Searle P.F. and Seymour, L.W. (2003) Vector based on reducible polycations facilitate intracellular release of nucleic acids. *Journal of Gene Medicine* **5**, 232-245
- Reddy, J.A. and Low, P.S. (1998) Folate-mediated targeting of therapeutic and imaging agents to cancers. *Critical Review in Therapeutic Drug Carrier Systems* **15**, 587-627
- Reddy, J.A., Westrick, E., Vlahov, I., Howard, S.J., Santhapuram, H.K. and Leamon, C.P. (2006) Folate receptor specific anti-tumor activity of folate-mitomycin conjugates. *Cancer Chemotherapy and Pharmacology* **58**, 229-236
- Rejman, J., Oberle, V., Zuhorn, I.S. and Hoekstra, D. (2004) Size-dependent internalization of particles via the pathways of clathrin- and caveolae-mediated endocytosis. *Biochemical Journal* **377**, 159-169
- Rejman, J., Bragonzi, A. and Conese, M. (2005) Role of clathrin- and caveolae-mediated endocytosis in gene transfer mediated by lipo- and polyplexes. *Molecular Therapy* **12**, 468-474
- Relph, K., Harrington, K. and Pandha, H. (2004) Recent development and current status of gene therapy using viral vectors in the United Kingdom. *British Medical Journal* **329**, 839-842
- Remy-Kristensen, A., Clamme, J.P., Vuilleumier, C., Kuhry, J.G. and Mely, Y. (2000) Role of endocytosis in the transfection of L929 fibroblasts by polyethylenimine / DNA complexes. *Biochimica et Biophysica Acta* **1514**, 21-32
- Richardson, D.R. and Ponka, P. (1997) The molecular mechanisms of the metabolism and transport of iron in normal and neoplastic cells. *Biochimica et Biophysica Acta* **1333**, 1-40
- Richardson, S.C.W., Kolbe, H.V.J. and Duncan, R. (1999). Potential of low molecular mass chitosan as a DNA delivery system: biocompatibility, body distribution and ability to complex and protect DNA. *International Journal of Pharmaceutics* **178**, 231-243

- Richardson, S.C.W., Patrick, N.G., Man, S., Ferruti, P. and Duncan, R. (2001). Poly(Amidoamine)s as potential nonviral vectors: ability to form interpolyelectrolyte complexes and to mediate transfection *in vitro*. *Biomacromolecules* **2**, 1023-1028
- Rijnbouts, S., Jansen, G., Posthuma, G., Hynes, J.B., Schornagel, J.H. and Strous, G.J. (1996) Endocytosis of GPI-linked membrane folate receptor-alpha. *Journal of Cell Biology* **132**, 35-47
- Riordan, J.R., Rommens, J.M., Kerem, B.S., Alon, N., Rozmahel, R., Grzelczak, Z., Zielenski, J., Lok, S., Plavsic, N., Chou, J.L., Drumm, M.L., Iannuzzi, M.C., Collins, F.S. and Tsui, L.C. (1989) Identification of the cystic fibrosis gene: cloning and characterization of the complementary DNA. *Science* **245**, 1066-1073
- Rizzuto, G., Cappelletti, M., Maione, D., Savino, R., Lazzaro, D., Costa, P., Mathiesen, I., Cortese, R., Ciliberto, G., Laufer, R., La Monica, N. and Fattori, E. (1999) Efficient and regulated erythropoietin production by naked DNA injection and muscle electroporation. *Proceedings of the National Academy of Sciences of USA* **96**, 6417-6422
- Robinowitz, J.E. and Samulski, J. (1998) Adeno-associated virus expression systems for gene transfer. *Current Opinion in Biotechnology* **9**, 470-475
- Rols, M.P., Delteil, C., Golzio, M., Dumond, P., Cros, S. and Teissie, J. (1998) In vivo electrically mediated protein and gene transfer in murine melanoma. *Nature Biotechnology* **16**, 168-171
- Rosenberg, S.A., Aebersold, P., Cornetta, K., Kasid, A., Morgan, R.A., Moen, R., Karson, E.M.; Lotze, M.T., Yang, J.C., Topalian, S.L., Merino, M.J., Culver, K., Miller, A.D., Blaese, M.D., and Anderson, W.F. (1990) Gene transfer into humans-immunotherapy of patients with advanced melanoma, using tumor-infiltrating lymphocytes modified by retroviral gene transduction. *New England Journal of Medicine* **323**, 570-578
- Ross, J.F., Chaudhuri, P.K. and Ratnam, M. (1994) Differential regulation of folate receptor isoforms in normal and malignant tissues *in vivo* and in established cell lines. Physiologic and clinical implications. *Cancer* **73**, 2432-2443
- Rothbard, J.B., Jessop, T.C., Lewis, R.S., Murray, B.A. and Wender, P.A. (2004) Role of membrane potential and hydrogen bonding in the mechanism of translocation of guanidinium-rich peptides into cells. *Journal of American Chemical Society* **126**, 9506-9507
- Rothberg, K.G., Ying, Y.S., Kolhouse, J.F., Kamen, B.A. and Anderson, R.G. (1990) The glycopospholipid-linked folate receptor internalizes folate without entering the clathrin-coated pit endocytic pathway. *Journal of Cell Biology* **110**, 637-649
- Rothberg, K.G., Heuser, J.E., Donzell, W.C., Ying, Y.S., Glenney, J.R. and Anderson, R.G. (1992). Caveolin, a protein component of caveolae membrane coats. *Cell* **68**, 673-682
- Rungsardthong, U., Deshpande, M., Bailey, L., Vamvakaki, M., Armes, S.P., Garnett, M.C. and Stolnik, S. (2001) Copolymers of amine methacrylate with poly(ethylene glycol) as vectors for gene therapy. *Journal of Controlled Release* **73**, 350-380
- Rungsardthong, U (2002). *Physicochemical evaluation of polymer-DNA complexes for DNA delivery*. PhD Thesis. The University of Nottingham.

- Rungsardthong, U., Ehtezazi, T., Bailey, L., Armes, S.P., Garnett, M.C. and Stolnik, S. (2003) Effect of polymer ionization on the interaction with DNA in nonviral gene delivery systems. *Biomacromolecules* **4**, 683-690
- Ruonen, M., Ylä-Herttuala, S. and Urtti, A. (1999) Interactions of polymeric and liposomal gene delivery systems with extracellular glycosaminoglycans: physicochemical and transfection studies. *Biochimica et Biophysica Acta* **1415**, 331-341
- Ryan, K.J. and Wenthe, S.R. (2000) The nuclear pore complex: A protein machine bridging the nucleus and cytoplasm. *Current Opinion in Cell Biology* **12**, 361-371
- Saalik, P., Elmquist, A., Hansen, M., Padari, K., Saar, K., Viht, K., Langel, V. and Pooga, M. (2004) Protein cargo delivery properties of cell-penetrating peptides. A comparative study. *Bioconjugate Chemistry* **15**, 1246-1253
- Sader, J.E. and Chan, D.Y.C. (1999) Long-range electrostatic attractions between identically charged particles in confined geometries: an unresolved problem. *Journal of Colloid Interface Science* **213**, 268-269
- Salas, P.J.I., Misek, D.E., Vega-Salas, D.E., Gundersen, D., Cereijido, M. and Rodriguez-Boulan, E. (1986) Microtubules and actin filaments are not critically involved in the biogenesis of epithelial cell surface polarity. *Journal of Cell Biology* **102**, 1853-1867
- Salomon, D.S., Brandt, R., Ciardiello, and Normanno, N. (1995) Epidermal growth factor – related peptides and their receptors in human malignancies. *Critical Reviews in Oncology Hematology* **19**, 183-232
- Salvage, J.P., Rose, S.F., Phillips, G.J., Hanlon, G.W., Lloyd, A.W., Ma, I.Y., Armes, S.P., Billingham, N.C. and Lewis, A.L. (2005) Novel biocompatible phosphorylcholine-based self-assembled nanoparticles for drug delivery. *Journal of Controlled Release* **104**, 259-270
- Sampath, P. and Pollard, T.D. (1991) Effects of cytochalasin, phalloidin, and pH on the elongation of actin filaments. *Biochemistry* **30**, 1973-1980
- Sarraguça, J.M.G. and Pais, A.A.C.C. (2004) Simulation of polyelectrolyte solutions. The density of bound ions. *Chemical Physics Letters* **398**, 140-145
- Sato, T., Ishii, T. and Okhata (2001). In vitro gene delivery mediated by chitosan. Effect of pH, serum, and molecular mass of chitosan on the transfection efficiency. *Biomaterials* **22**, 2075-2080
- Saul, J.M., Annapragada, A., Natarajan, J.V. and Bellamkonda, R.V. (2003) Controlled targeting of liposomal doxorubicin via the folate receptor in vitro. *Journal of Controlled Release* **92**, 49-67
- Schaffer, D.V., Fidelman, N.A., Dan, N. and Lauffenburger, D.A. (2000) Vector unpacking as a potential barrier for receptor-mediated polyplex gene delivery. *Biotechnology and Bioengineering* **67**, 598-606
- Schätzlein, A.G. (2001) Non-viral vectors in cancer gene therapy: principles and progress. *Anticancer Drugs* **12**, 275-304

- Schätzlein, A.G. (2003) Targeting of synthetic gene delivery systems. *Journal of Biomedicine and Biotechnology* **2**, 149-158
- Schinitzer, J.E., Oh, P., Pinney, E. and Allard, J. (1994) Filipin-sensitive caveolae-mediated transport in endothelium: reduced transcytosis, scavenger endocytosis, and capillary permeability of select macromolecules. *Journal of Cell Biology* **127**, 1217-1233
- Schleissinger, J. (1986) Allosteric regulation of the epidermal growth factor receptor kinase. *Journal of Cell Biology* **103**, 2067-2072
- Schwarze, S.R. and Dowdy, S.F. (2000) *In vivo* protein transduction: intracellular delivery of biological active proteins, compounds and DNA. *Trends in Pharmacological Science* **21**, 45-48
- Sebestyen, M.G., Ludtke, J.J., Bassik, M.C., Zhang, G., Budker, V., Lukhtanov, E.A., Hagstrom, J.E. and Wolff, J.A. (1998) DNA vector chemistry: the covalent attachment of signal peptides to plasmid DNA. *Nature Biotechnology* **16**, 80-85
- Semple, S.C., Chonn, A. and Cullis, P.R. (1998) Interactions of liposomes and lipid-based carrier systems with blood proteins: Relation to clearance behaviour *in vivo*. *Advanced Drug Delivery Reviews* **32**, 3-17
- Senior, J., Trimble, K.R. and Maskiewicz, R. (1991) Interaction of positively-charged liposomes with blood: Implications for their application *in vivo*. *Biochimica et Biophysica Acta* **1070**, 173-179
- Seville, P.C., Kellaway, I.W. and Birchall, J.C. (2002) Preparation of dry powder dispersions for non-viral gene delivery by freeze-drying and spray-drying. *Journal of Gene Medicine* **4**, 428-437
- Shen, H., Mai, J.C., Qiu, L., Cao, S., Robbins, P.D. and Cheng, R.T. (2004) Evaluation of peptide-mediated transduction in human CD34<sup>+</sup> cells. *Human Gene Therapy* **15**, 415-419
- Shen, W.C. and Ryser, H.J.P. (1981) Poly(L-lysine) has different membrane transport and drug-carrier properties when complexed with heparin. *Proceedings of the National Academy of Sciences of USA* **78**, 7589-7593
- Shi, N., Zhang, Y., Zhu, C., Boado, R.J., and Pardridge, W.M. (2001) Brain-specific expression of an exogenous gene after i.v. administration. *Proceedings of the National Academy of Sciences of USA* **98**, 12754-12759
- Shin, J.S. and Abraham, S.N. (2001). Caveolae as portals of entry for microbes. *Microbes and Infection* **3**, 755-761
- Shinitzkym, M. and Barenholz, Y. (1978) *Biochimica et Biophysica Acta* **515**, 367-394
- Sieczkarski, S.B. and Whittaker, G.R. (2002) Dissecting virus entry via endocytosis. *Journal of General Virology* **83**, 1535-1545
- Simoës, S., Slepushkin, V., Gaspar, R., Pedroso, M.C. and Düzgünes, N. (1998) Gene delivery by negatively charged ternary complexes of DNA, cationic liposomes, and transferrin or fusigenic peptides. *Gene Therapy* **5**, 955-964

- Simoes, S., Slepushkin, V., Pires, P., Gaspar, R., de Lima, M.P. and Duzgunes, N. (1999) Mechanisms of gene transfer mediated by lipoplexes associated with targeting ligands or pH-sensitive peptides. *Gene Therapy* **6**, 1798-1807
- Singh, A.K., Kasinath, B.S. and Lewis, E.J. (1992) Interaction of polycations with cell-surface negative charges of epithelial cells. *Biochimica et Biophysica Acta* **1120**, 337-342
- Singh, M. and Ariatti, M. (2003) Targeted gene delivery into HepG2 cells using complexes containing DNA, cationized asialoorosomucoid and activated cationic liposomes. *Journal of Controlled Release* **92**, 383-394
- Sirotnak, F.M. and Tolner, B. (1999) Carrier-mediated membrane transport of folates in mammalian cells. *Annual Review of Nutrition* **19**, 91-122
- Smith, B.F., Baker, H.J., Curiel, D.T., Jiang, W. and Conry, R.M. (1998) Humoral and cellular immune responses of dogs immunized with a nucleic acid vaccine encoding human carcinoembryonic antigen. *Gene Therapy* **5**, 865-868
- Smith, J., Yu, R. and Hinkle, P.M. (2001) Activation of MAPK by TRH requires clathrin-dependent endocytosis and PKC but not receptor interaction with  $\beta$ -arrestin or receptor endocytosis. *Molecular Endocrinology* **15**, 1539-1548
- Snyder, E.L. and Dowdy, S.F. (2004) Cell penetrating peptides in drug delivery. *Pharmaceutical Research* **21**, 389-393
- Sottas, P.E., Larquet, E., Stasiak, A. and Dubochet, J. (1999) Brownian dynamics simulation of DNA condensation. *Biophysical Journal* **77**, 1858-1870
- Spector, I., Shochet, N.R., Kashman, Y. and Groweiss, A. (1983) Latrunculins – Novel marine toxins that disrupt microfilaments organization in cultured-cells. *Science* **219**, 493-495
- Stankovics, J., Crane, A.M., Andres, E., Wu, C.H., Wu, G.Y. and Ledley, F. D. (1994). Overexpression of human methylmalonyl CoA mutase in mice after *in vivo* gene transfer with asialoglycoprotein/polylysine/DNA complexes. *Human Gene Therapy* **5**, 1095-1104
- Stein, C.A. and Cheng, Y.C. (1993) Antisense oligonucleotides as therapeutic agents – is the bullet really magical? *Science* **261**, 1004-1012
- Stevens, M.J. (2001) Simple simulation of DNA condensation. *Biophysical Journal* **80**, 130-139
- Stockert, R.J. (1995) The asialoglycoprotein receptor: relationships between structure, function and expression. *Physiological Reviews* **75**, 591-609
- Stolnik, S., Illum, L. and Davis, S.S. (1995) Long circulating microparticulate drug carriers. *Advanced Drug Delivery Reviews* **16**, 195-214
- Su, J., Kim, C.J. and Ciftci, K. (2002) Characterization of poly((N-trimethylammonium) ethyl methacrylate)-based gene delivery systems. *Gene Therapy* **9**, 1031-1036
- Sudimack, J.J. and Lee, R.J. (2000) Targeted drug delivery via the folate receptor. *Advanced Drug Delivery Reviews* **41**, 147-162

- Suhr, S.T. and Gage, F.H. (1993) Gene therapy for neurologic disease. *Archives of Neurology* **50**, 1252-1268
- Surman, D.R., Irvine, K.R., Shulman, E.P., Allweis, T.M., Rosenberg, S.A. and Restifo, N.P. (1998) Generation of polyclonal rabbit antisera to mouse melanoma associated antigens using gene gun immunization. *Journal of Immunological Methods* **214**, 51-62
- Swann, M.J., Peel, L.L., Carrington, S. and Freeman, N.J. (2004) Dual-polarization interferometry: an analytical technique to measure changes in protein structure in real time, to determine the stoichiometry of binding events, and to differentiate between specific and nonspecific interactions. *Analytical Biochemistry* **329**, 190-198
- Tait, A.S., Brown, C.J., Galbraith, D.J., Hines, M.J., Hoare, M., Birch, J.R. and James, D.C. (2004) Transient production of recombinant proteins by Chinese hamster ovary cells using polyethylenimine/DNA complexes in combination with microtubule disrupting anti-mitotic agents. *Biotechnology and Bioengineering* **88**, 707-721
- Tajmir-Riahi, H.A., Naoui, M. and Miamantoglou, S. (1994) DNA-carbohydrate interaction. The effects of mono- and disaccharides on the solution structure of calf-thymus DNA. *Journal of Biomolecular Structure Dynamics* **12**, 217-234
- Takei, K. and Haucke, V. (2001) Clathrin-mediated endocytosis: membrane factors pull the trigger. *Trends in Cell Biology* **11**, 385-391
- Talsma, H., Cherng, J.Y., Lehrmann, H., Kurs, M., Ogris, M., Hennink, W. E., Cotton, M. and Wagner, E. (1997) Stabilization of gene delivery systems by freeze-drying. *International Journal of Pharmaceutics* **157**, 233-238
- Tang, M.X., Redemann, C.T. and Szoka Jr. F.C. (1996) *In vitro* gene delivery by degraded polyamidoamine dendrimers. *Bioconjugate Chemistry* **7**, 703-714
- Tang, M.X. and Szoka, F.C. (1997) The influence of polymer structure on the interactions of cationic polymers with DNA and morphology of the resulting complexes. *Gene Therapy* **4**, 823-832
- Tang, G.P., Zeng, J.M., Gao, S.J., Ma, Y.X., Shi, L., Li, Y., Too, H.P. and Wang, S. (2003) Polyethylene glycol modified polyethylenimine for improved CNS gene transfer: effects of PEGylation extent. *Biomaterials* **24**, 2351-2362
- Thomas, C.E., Ehrhardt, A. and Kay, M.A. (2003) Progress and problems with the use of viral vectors for gene therapy. *Nature Reviews Genetics* **4**, 346-358
- Thomsen, P., Roespstorff, K., Stahlhut, M. and van Deurs, B. (2002). Caveolae are highly immobile plasma membrane microdomains, which are not involved in constitutive endocytic trafficking. *Molecular Biology of the Cell* **13**, 238-250
- Tiyaboonchai, W., Woiszwill, J. and Middaugh, C.R. (2003) Formulation and characterization of DNA-polyethylenimine-dextran sulphate nanoparticles. *European Journal of Pharmaceutical Sciences* **19**, 191-202
- Toffoli, G., Cernigoi, C., Russo, A., Gallo, A., Bagnoli, M., and Boiocchi, M. (1997) Overexpression of folate binding protein in ovarian cancers. *International Journal of Cancer* **74**, 193-198
- Toncheva, V., Wolfert, M. A., Dash, P. R., Oupicky, D., Ulbrich, K., Seymour, L. W. and Schacht, E. H. (1998). Novel vectors for gene delivery formed by self-assembly of DNA

---

with poly(L-lysine) grafted with hydrophilic polymers. *Biochimica et Biophysica Acta* **1380**, 354-368

Torchilin, V.P. and Trubetskoy, V.S. (1995) Which polymers can make nanoparticulate drug carriers long-circulating? *Advanced Drug Delivery Reviews* **16**, 141-155

Tousignant, J.D., Gates, A.L., Ingram, L.A., Johnson, C.L., Nietupski, J.B., Cheng, S.H., Eastman, S.J. and Scheule, R.K. (2000) Comprehensive analysis of the acute toxicities induced by systemic administration of cationic-lipid:plasmid DNA complexes in mice. *Human Gene Therapy* **11**, 2493-2513

Tran, D., Carpentier, J.L., Sawano, F., Gorden, P. and Orci, L. (1987) Ligands internalized through coated or noncoated invaginations follow a common intracellular pathway. *Proceedings of the National Academy of Sciences of USA* **84**, 7957-7961

Tseng, W.C., Haselton, F.R. and Giorgio, T.D. (1999) Mitosis enhances transgene expression of plasmid delivered by cationic liposomes. *Biochimica et Biophysica Acta*. **1445**, 53-64

Tseng, W.C. and Jong, C.M. (2003) Improved stability of polycationic vector by dextran-grafted branched polyethylenimine. *Biomacromolecules* **4**, 1277-1284

Tseng, W.C., Tang, C.H. and Fang, T.Y. (2004) The role of dextran conjugation in transfection mediated by dextran-grafted polyethylenimine. *Journal of Gene Medicine* **6**, 895-905

Tupin, E., Poirier, B., Bureau, M.F., Khallou-Laschet, J., Vranckx, R., Caligiuri, G., Gaston, A.T., Van Huyen, J.P.D., Scherman, D., Bariety, J., Michel, J.B. and Nicoletti, A. (2003) Non-viral gene transfer of murine spleen cells achieved by *in vivo* electroporation. *Gene Therapy* **10**, 569-579

Turek, J.J., Leamon, C.P. and Low, P.S. (1993) Endocytosis of folate-protein conjugates: ultrastructural localization in KB cells. *Journal of Cell Science* **106**, 423-430

Turk, M.J., Reddy, J.A., Chmielewski, J.A. and Low, P.S. (2002) Characterisation of a novel pH-sensitive peptide that enhances drug release from folate-targeted liposomes at endosomal pHs. *Biochimica et Biophysica Acta* **1559**, 56-58

Ulmer, J.B., Donnelly, J.J., Parker, S.E., Rhodes, G.H., Gromkowski, S.H., Deck, R.R., Dewitt, C.M., Friedman, A., Hawe, L.A., Leander, K.R., Marninez, D., Perry, H.C., Shiver, J.W., Montgomery, D.L. and Liu, M.A. (1993). Heterologous protection against influenza by injection of DNA encoding a viral protein. *Science* **259**, 1745-1749

van de Walle, G.R., Favoreel, H.W., Nauwynck, H.J., van Oostveldt, P. and Pensaert, M.B. (2001) Involvement of cellular cytoskeleton components in antibody-induced internalization of viral glycoproteins in pseudorabies virus-infected monocytes. *Virology* **288**, 129-138

van de Wetering, P., Cherng, J.Y., Talsma, H. and Hennink, W.E. (1997) Relation between transfection efficiency and cytotoxicity of poly(2-(dimethylamino)ethyl methacrylate)/plasmid complexes. *Journal of Controlled Release* **49**, 59-69

van de Wetering, P., Cherng, J.Y., Talsma, H., Crommelin, D.J.A. and Hennink, W.E. (1998) 2-(dimethylamino)ethyl methacrylate based (co)polymers as gene transfer agents. *Journal of Controlled Release* **53**, 145-153

- van de Wetering, P., Moret, E.E., Schuurmans-Nieuwenbroek, N.M.E., van Steenbergen, M.J. and Hennink, W.E. (1999) Structure-activity relationships of water-soluble cationic methacrylate/methacrylamide polymers for nonviral gene delivery. *Bioconjugated Chemistry* **10**, 587-597
- van der Aa, M.A.E.M., Huth, U., Koning, G.A., Häfele, S., Peschka-Süss, Oosting, R.S. and Hennink, W.E. (2005) Cellular uptake and intracellular routing of a cationic polymer-based gene delivery system. *Controlled Release Society 32<sup>nd</sup> Annual Meeting and Exposition*, abstract 151
- van Steenis, J.H., van Maarseveen, E.M., Verbaan, F.J., Verrijck, R., Crommelin, D.J.A., Storm, G. and Hennink, W.E. (2003) Preparation and characterization of folate-targeted pEG-coated pDMAEMA-based polyplexes. *Journal of Controlled Release* **87**, 167-176
- Verbaan, F., van Dam, I., Takakura, Y., Hashida, M., Hennink W.E., Storm, G. and Oussoren, C. (2003) Intravenous fate of poly(2-(dimethylamino)ethyl methacrylate)-based polyplexes. *European Journal of Pharmaceutical Sciences* **20**, 419-427
- Varda-Bloom, N., Shaish, A., Gonen, A., Levanon, K., Greenbereger, S., Ferber, S., Levkovitz, H., Castel, D., Goldberg, I., Afek, A., Kopolovitch, Y. and Harats, D. (2001) Tissue-specific gene therapy directed to tumor angiogenesis. *Gene Therapy* **8**, 819-827
- Varga, C.M., Wickham, T.J. and Lauffenburger, D.A. (2000) Receptor-mediated targeting of gene delivery vectors: insights from molecular mechanisms for improved vehicle design. *Biotechnology and Bioengineering* **70**, 593-605
- Vasey, P.A., Kaye, S.B., Morrison, R., Twelves, C., Wilson, P., Duncan, R., Thompson, A.H., Murray, L.S., Hilditch, T.E., Murray, T., Burtles, S., Fraier, D., Frigerio, E. and Cassidy, J. (1999) Phase I clinical and pharmacokinetic study of PK1 [N-(2-hydroxypropyl)methacrylamine copolymer doxorubicin]: first member of a new class of chemotherapeutic agents-drug-polymer conjugates. *Clinical Cancer Research* **5**, 83-94
- Verbaan, F.J., Oussoren, C., Snel, C.J., Crommelin, D.J.A., Hennink, W.E. and Storm, G. (2004) Steric stabilization of poly(2-(dimethylamino)ethyl methacrylate)-based polyplexes mediates prolonged circulation and tumor targeting in mice. *Journal of Gene Medicine* **6**, 64-75
- Vives, E., Brodin, P., and Lebleu, B. (1997) A truncated HIV-1 TAT protein basic domain rapidly translocates through the plasma membrane and accumulates in the cell nucleus. *Journal of Biological Chemistry* **272**, 16010-16017
- Voldborg, B.R., Damstrup, L., Spang-Thomsen, M. and Poulsen, H.S. (1997) Epidermal growth factor receptor (EGFR) and EGFR mutations, function and possible role in clinical trials. *Annals of Oncology* **8**, 1197-1206
- Von Gersdorff, K., Ogris, M. and Wagner, E. (2005) Cryoconserved shielded and EGF receptor targeted DNA polyplexes: cellular mechanisms. *European Journal of Pharmaceutics and Biopharmaceutics* **60**, 279-285
- Wadia, J.S., Stan, R.V. and Dowdy, S.F. (2004) Transducible TAT-HA fusogenic peptide enhances escape of TAT-fusion proteins after lipid raft macropinocytosis. *Nature Medicine* **10**, 310-315



- 
- Wagner, E., Zenke, M., Cotton, M., Beug, H., and Birnstiel, M.L. (1990) Transferrin-polycation conjugates as carriers for DNA uptake into cells. *Proceedings of the National Academy of Sciences of USA* **87**, 3410-3414
- Wagner, E., Curiel, D. and Cotton, M. (1994) Delivery of drugs, proteins and genes into cells using transferrin as a ligand for receptor-mediated endocytosis. *Advanced Drug Delivery Reviews* **14**, 113-136
- Wagner, E. (1998). Effects of membrane-active agents in gene delivery. *Journal of Controlled Release* **53**, 155-158
- Walter, P. (1999) The transport of molecules into and out of the nucleus. In: *Molecular Biology of the Cell*, pp. 561-568 (Eds. Lberts, B., Bray, D., Lewis, J., Raff, M., Roberts, K., Watson, J.D.) Garland Publishing, New York
- Walther, W. and Stein, U. (1996) Cell type specific and inducible promoters for vectors in gene therapy as an approach for cell targeting. *Journal of Molecular Medicine* **74**, 379-392
- Walther, S., and Stein, U. (2000) Viral vectors for gene transfer: a review of their use in the treatment of human diseases. *Drugs* **60**, 249-71
- Wang, S., Beechem, J.M., Gratton, E. and Glasser, M. (1991). Orientational distribution of 1,6-diphenyl-1,3,5-hexatriene in phospholipid vesicles as determined by global analysis of frequency domain fluorimetry data. *Biochemistry* **30**, 5565-5572
- Wang, L.H., Rothberg, K.G. and Anderson, G.W. (1993) Mis-assembly of clathrin lattices on endosomes reveals a regulatory switch for coated pit formation. *Journal of Cell Biology* **123**, 1107-1117
- Wang, W., Lee, R.J., Mathias, C.J., Green, M.A. and Low, P.S. (1996) Synthesis, purification and tumor cell uptake of <sup>67</sup>Gadeferoxamine-folate, a potential radiopharmaceutical for tumor imaging. *Bionconjugate Chemistry* **7**, 56-62
- Wang, S. and Low, P.S. (1998) Folate-mediated targeting of anti-neoplastic drugs, imaging agents, and nucleic acids to cancer cells. *Journal of Controlled Release* **53**, 39-48
- Wang, W. (2000) Lyophilization and development of solid protein pharmaceuticals. *International Journal of Phamarceutics* **203**, 1-60
- Wang, F., Jiang, X.P., Yang, D.C., Elliott, R.L. and Head, J.F. (2000) Doxorubicin-gallium-transferrin conjugate overcomes multidrug resistance: Evidence for drug accumulation in the nucleus of drug resistant MCF-7/ADR cells. *Anticancer Research* **20**, 799-808
- Wang, L. and MacDonald, R.C. (2004) Effects of microtubule-depolymerizing agents on the transfection of cultured vascular smooth muscle cells: enhanced expression with free drug and especially with drug-gene lipoplexes. *Molecular Therapy* **9**, 729-737
- Ward, C.M., Acheson, N. and Seymour, L.M. (2000) Folic acid targeting of protein conjugates into ascites tumor cells from ovarian cancer patients. *Journal of Drug Targeting* **8**, 119-123
- Ward, C.M., Pechar, M., Oupicky, D., Ulbrich, K. and Seymour, L.W. (2002) Modification of pLL/DNA complexes with a multivalent hydrophilic polymer permits
-

- 
- folate-mediated targeting *in vitro* and prolonged plasma circulation *in vivo*. *Journal of Gene Medicine* **4**, 536-547
- Washington, C. (1992) *Particle size analysis in pharmaceutical and other industries: theory and practice*. : Ellis Horwood, New York
- Waterman, H. and Yarden, Y. (2001) Molecular mechanisms underlying endocytosis and sorting of ErbB receptor tyrosine kinases. *FEBS Letters* **490**, 142-152
- Watson, J.D. and Crick, F.H.C. (1953) Molecular structure of nucleic acids: a structure for deoxyribose nucleic acid. *Nature*, **171**, 737-738
- Wattiaux, R., Laurent, N., Wattiaux-de Crinck, S. and Jadot, M. (2000) Endosomes, lysosomes: their implication in gene transfer. *Advanced Drug Delivery Reviews* **41**, 201-208
- Weber, E., Anderson, W.F. and Kasahara, N. (2001) Recent advances in retrovirus vector-mediated gene therapy: teaching an old vector new tricks. *Current Opinion in Molecular Therapeutics* **3**, 439-453
- Weigel, P.H. (1994) Galactosyl and N-acetylgalactosaminyl homeostasis: a function for mammalian asialoglycoprotein receptors. *BioEssays* **16**, 519-524
- Weigel, P.H. and Yik, J.H.N. (2002) Glycans as endocytosis signals: the cases of the asialoglycoprotein and hyaluronan.chondroitin sulphate receptors. *Biochimica et Biophysica Acta* **1572**, 341-363
- Weitman, S.D., Frazier, K.M., and Kamen, B.A. (1994) The folate receptor in central nervous system malignancies of childhood. *Journal of Neuro Oncology* **21**, 107-112
- Wells, C.L., van de Westerlo, E.M.A., Jechorek, R.P., Haines, H.M. and Erlandsen, S.L. (1998) Cytochalasin-induced actin disruption of polarized enterocytes can augment internalisation of bacteria. *Infection and Immunity* **66**, 2410-2419
- Wells, A. (2000) The epidermal growth factor receptor (EGFR)- a new target in cancer therapy. *Signal* **1**, 4-11
- Wells, J.M., Li, L.H., Sen, A., Jahreis, G.P. and Hui, S.W. (2000) Electroporation-enhanced gene delivery in mammary tumors. *Gene Therapy* **7**, 541-547
- Whiteman, K.R., Subr, V., Ulbrich, K. and Torchilin, V.P. (2001) Poly(HPMA)-coated liposomes demonstrate prolonged circulation in mice. *Journal of Liposome Research* **11**, 153-164
- Wickstrom, E. (1986) Oligodeoxynucleotide stability in subcellular extracts and tissue culture media. *Journal of Biochemical and Biophysical Methods* **13**, 97-102
- Wilke, M., Fortunati, E., van den Broek, M., Hoogeveen, A.T. and Scholte, B.J. (1996) Efficacy of a peptide based gene delivery system depends on mitotic activity. *Gene Therapy* **3**, 1133-1142
- Wilson, R.W. and Bloomfield, V.A. (1979) Counter-ion-induced condensation of deoxyribonucleic acid – light scattering study. *Biochemistry* **18**, 2192-2196
- Wilson, J.M. (2005) The first commercial gene therapy product. *Human Gene Therapy* **16**, 1014
-

- 
- Wiseman, J.W., Goddard, C.A., McLelland, D. and Colledge, W.H. (2003) A comparison of linear and branched polyethylenimine (PEI) with DCChol/DOPE liposomes for gene delivery to epithelial cells in vitro and in vivo. *Gene Therapy* **10**, 1652-1662
- Wolfert, M.A. and Seymour, L.W. (1996) Atomic force microscopic analysis of the influence of the molecular weight of poly(L)lysine on the size of polyelectrolyte complexes formed with DNA. *Gene Therapy* **3**, 269-273
- Wolfert, M.A., Schacht, E.H., Toncheva, V., Ulbrich, K., Nazarova, O. and Seymour, L.W. (1996b) Characterization of vectors for gene therapy formed by self-assembly of DNA with synthetic block copolymers. *Human Gene Therapy* **7**, 2123-2133
- Wolff, J.A., Malone, R.W., Williams, P., Chong, W., Aacadi, G., Jani, A. and Felgner, P.L. (1990) Direct gene transfer into mouse muscle in vivo. *Science* **247**, 1465-1468
- Wong, T.K. and Neumann, E. (1982) Electric field mediated gene transfer. *Biochemical and Biophysical Research Communications* **107**, 584-587
- Woodburn, J.R. (1999) The epidermal growth factor receptor and its inhibition in cancer therapy. *Pharmacology and Therapeutics* **82**, 241-250
- Woodle, M.C. and Lasic, D.D. (1992) Sterically stabilized liposomes. *Biochimica et Biophysica Acta* **1113**, 171-199
- Wu, G.Y. and Wu, C.H. (1987) Receptor-mediated *in vitro* gene transformation by a soluble DNA carrier system. *Journal of Biological Chemistry* **262**, 4429-4432
- Wu, G.Y. and Wu, C.H. (1988). Evidence for targeted gene delivery to HepG2 hepatoma cells in vitro. *Biochemistry* **27**, 887-892
- Wu, G.Y. and Wu, C.H. (1988b) Receptor-mediated gene delivery and expression in vivo. *Journal of Biological Chemistry* **29**, 14621-14624
- Wu, J., Nantz, M.H. and Zern, M.A. (2002) Targeting hepatocytes for drug and gene delivery: emerging novel approaches and applications. *Frontiers in Bioscience* **7**, 717-725
- Xu, B., Wiehle, S., Roth, J.A., Cristiano, R.J. (1998) The contribution of poly-L-lysine, epidermal growth factor and streptavidin to EGF/PLL/DNA polyplex formation. *Gene Therapy* **5**, 1235-1243
- Yang, J.P. and Huang, L. (1996) Direct gene transfer to mouse melanoma by intratumor injection of free DNA. *Gene Therapy* **3**, 542-548
- Yla-Herttuala, S. and Martin, J.F. (2000) Cardiovascular gene therapy. *Lancet* **355**, 212-222
- Yoo, H.S. and Park, T.G. (2004) Folate-receptor-targeted delivery of doxorubicin nano-aggregates stabilized by doxorubicin-PEG-folate conjugate. *Journal of Controlled Release* **100**, 247-256
- Young, B.R., Pitt, W.G. and Cooper, S.L. (1998) Protein adsorption on polymeric biomaterials I. Adsorption isotherms. *Journal of Colloid and Interface Science* **124**, 29-38

- Youssef, S., Wildbaum, G., Maor, G., Lanir, N., Gour-Lavie, A., Gracie, N. and Karin, N. (1998) Long-lasting protective immunity to experimental autoimmune encephalomyelitis following vaccination with naked DNA encoding C-C chemokines. *Journal of Immunology* **161**, 3870-3879
- Yu, W.H., Kashani-Sabet, M., Liggitt, D., Moore, D., Heath, T.D. and Debs, R.J. (1999) Topical gene delivery to murine skin. *Journal of Investigative Dermatology* **112**, 370-375
- Zabner, J., Fasbender, A.J., Moninger, T., Poellinger, K.A. and Welsh, M.J. (1995) Cellular and molecular barriers to gene transfer by a cationic lipid. *Journal of Biological Chemistry* **270**, 18997-19007
- Zanta, M.A., Belguise-Valladier, P. and Behr, J-P. (1999) Gene delivery: A single nuclear localization signal peptide is sufficient to carry DNA to the cell nucleus. *Proceedings of the National Academy of Sciences of USA* **96**, 91-96
- Zauner, W., Ogris, M. and Wagner, E. (1998) Polylysine-based transfection systems utilizing receptor-mediated delivery. *Advanced Drug Delivery Reviews* **30**, 97-113
- Zegers, M.M.P., Zaal, K.J.M., van Ijzendoorn, S.C.D., Klappe, K. and Hoekstra, D. (1998) Actin filaments and microtubules are involved in different membrane traffic pathways that transport sphingolipids to the apical surface of polarized HepG2 cells. *Molecular Biology* **9**, 1939-1949
- Zelphati, O., Nguyen, C., Ferrari, M., Felgner, J., Tsai, Y. and Felgner, P.L. (1998) Stable and monodisperse lipoplex formulations for gene delivery. *Gene Therapy* **5**, 1272-1282
- Zhang, G., Vargo, D., Budker, V., Armstrong, N., Knechtle, S. and Wolff, J.A. (1997) Expression of naked plasmid DNA injected into the afferent and efferent vessels of rodent and dog livers. *Human Gene Therapy* **8**, 1763-1772
- Zhou, W., Yuan, X., Wilson, A., Yang, L., Mokotoff, M., Pitt, B. and Li, S. (2002) Efficient intracellular delivery of oligonucleotides formulated in folate receptor-targeted lipid vesicles. *Bioconjugate Chemistry* **13**, 1220-1225
- Zinselmeyer, B., Schatzlein, A.G., Mackay, S.P. and Uchegbu, I.F. (2002) The lower generation polypropylenimine dendrimers are effective gene transfer agents. *Pharmaceutical Research* **19**, 960,967
- Zintchenko, A., Rother, G. and Dautzenberg, H. (2003) Transition highly aggregated complexes-soluble complexes via polyelectrolyte exchange reactions: kinetics, structural changes, and mechanism, *Langmuir* **19**, 2507-2513
- Zndanov, R., Podobed, O. and Vlassov, V. (2002) Cationic lipid-DNA complexes-liposomes for gene transfer and therapy. *Bioelectrochemistry* **58**, 53-64
- Zuidam, N.J. and Barenholz, Y. (1998) Electrostatic and structural properties of complexes involving plasmid DNA and cationic lipids commonly used for gene delivery. *Biochimica et Biophysica Acta* **1368**, 115-128
- Zuidam, N.J., Posthuma, G., de Vries, E.T., Crommelin, D.J., Hennink, W.E. and Storm, G. (2000). Effects of physicochemical characteristics of poly(2-(dimethylamino)ethyl methacrylate)-based polyplexes on cellular association and internalization. *Journal of Drug Targeting* **8**, 51-66